



TECHNISCHE  
UNIVERSITÄT  
WIEN  
Vienna | Austria

# DIPLOMA THESIS

## Biocompatible Photoinitiators based on Poly- $\alpha$ -ketoesters

Institute of Applied Synthetic Chemistry

TU Wien



under the supervision of

Univ. Prof. Dipl.-Ing. Dr. techn. Robert Liska

and

Senior Scientist Dipl.-Ing Dr.techn. Patrick Knaack

by

Roland TASCHNER, BSc

Matr. No.: 1328810

Vienna, 20.02.2019

## TABLE OF CONTENTS

ABSTRACT .....	5	
INTRODUCTION .....	7	
Photopolymerizable Formulations .....	7	
Alternative Photoinitiators .....	16	
OBJECTIVE.....	20	
STATE OF THE ART.....	21	
Polymeric Photoinitiators.....	21	
Polymerizable Photoinitiators.....	22	
GENERAL PART .....	24	
EXPERIMENTAL PART .....	110	
		<u>Gen. Exp.</u>
1. Optimization of the Esterification .....	26	110
1.1. Synthesis of $\alpha$ -Ketoglutaric Acid Di(m)ethylester [KGADi(m)et].....	26	110
1.1.1. $\alpha$ -Ketoglutaric Acid Diethylester [KGADiet] .....	-	110
1.1.2. $\alpha$ -Ketoglutaric Acid Dimethylester [KGADimet].....	-	111
1.2. Synthesis of $\alpha$ -Ketoglutaric Acid Dibenzylester [KGADibenz] .....	26	111
1.3. Synthesis of $\alpha$ -Ketoglutaric Acid Di-2-Hydroxypropylester [KGADihydroxyprop].....	27	-
1.3.1. Acidic Esterification .....	27	-
1.3.2. Addition of Propylene Oxide .....	28	-
2. Synthesis of Polymerizable Photoinitiators [KGA2HEMA] .....	29	113
3. Synthesis of Macromolecular Photoinitiators.....	31	114
3.1. Synthesis of Glutaric Acid-based Polyesters [Poly(HD/ISO)GA] .....	31	114
3.2. Synthesis of $\alpha$ -Ketoglutaric Acid-based Polyesters [Poly(HD/ISO)KGA].....	32	116
3.3. Molecular Weight Determination of the Polyesters .....	36	120
3.3.1. Acid Value Determination .....	36	120
3.3.2. Hydroxyl Value Determination.....	37	121
3.3.2.1. Reaction with Acetic Anhydride and Titration .....	38	122
3.3.2.2. Reaction with Acetic Acid and Titration .....	39	122
3.3.3. Gel Permeation Chromatography .....	40	122
3.3.4. $^1\text{H-NMR}$ Determination .....	42	122

3.3.5.	<sup>31</sup> P-NMR Determination .....	45	123
3.3.6.	Reaction with Phenyl Isocyanate and Titration .....	47	123
3.4.	Selecting the Set of Macromolecular Photoinitiators .....	49	-
4.	Synthesis of Macromolecular, Polymerizable Photoinitiators.....	51	125
4.1.	$\alpha$ -Ketoglutaric Acid Hexanediol Polyester with 2-IEM Endgroup [PolyHDKGA-m].....	51	125
4.2.	Synthesis of Polyesters with the IPDI-HEMA Endgroup .....	52	126
4.2.1.	Synthesis of the IPDI-HEMA Endgroup [IPDI-HEMA] .....	52	126
4.2.2.	Synthesis of the Polyesters .....	53	128
4.2.2.1.	Glutaric Acid-based Polyesters with IPDI-HEMA Endgroup [Poly(HD/ISO)GA-M] .....	53	128
4.2.2.2.	$\alpha$ -Ketoglutaric Acid-based Polyesters with IPDI-HEMA Endgroup [Poly(HD/ISO)KGA-M] .....	56	130
5.	Analytics .....	59	132
5.1.	UV-VIS Absorption .....	59	132
5.2.	Reactivity Tests .....	60	132
5.2.1.	Photo Differential Scanning Calorimetry .....	64	135
5.2.2.	Photorheometer Measurements .....	73	136
5.3.	Photorheometer Measurements of selected Initiators.....	78	136
5.4.	Mechanical Tests .....	83	137
5.4.1.	Dynamic Mechanical Thermal Analysis.....	89	137
5.4.2.	Tensile Tests .....	95	138
5.4.3.	Charpy Impact Tests .....	99	138
5.5.	Leaching Tests.....	100	138
CONCLUSION .....			139
MATERIALS AND METHODS .....			141
ABBREVIATIONS.....			144
SUPPLEMENTING INFORMATION.....			146
REFERENCES .....			158

## Danksagung

Zuerst möchte ich mich bei meinem Professor, Robert Liska, für die Möglichkeit der Durchführung meiner Diplomarbeit in seiner Arbeitsgruppe und für all die wissenschaftliche Unterstützung, bedanken. Auch meinem Betreuer Patrick Knaack gilt großer Dank, da er mich während der praktischen Arbeit und dem Schreiben der Diplomarbeit immer unterstützt hat.

Des Weiteren möchte ich mich bei der ganzen Arbeitsgruppe FBMC bedanken, da die Arbeitsatmosphäre stets locker und angenehm für mich war. Besonderer Dank gilt hierbei meiner Freundin Betti, die regelmäßig an meinem Platz vorbeischaute um mit mir über ihre neuesten Syntheseprobleme zu tratschen, und mich daher von meinen eigenen ablenkte. Und natürlich auch ein großes Danke an meinem Labornachbarn Chris, ohne den es nur halb so lustig im Labor gewesen wäre. Außerdem danke ich Flo, meinem Bachelorstudent, für die unzähligen Synthesen und vor allem für die ausdauernde Schleifarbeit der über 100 Proben für mechanische Tests.

Meinen Eltern, Großeltern und meinen Verwandten möchte ich für die tolle und nie endende Unterstützung meiner Entscheidung, Technische Chemie zu studieren, danken!

## ABSTRACT

### English

Photopolymerization of (meth)acrylate-based formulations has become a widespread method for many industry sectors due to the high energy efficiency and low curing times of this technology. Various products, from simple coatings to more complex applications are based on this method. Common industrial radical photoinitiators are generally based on aromatic ketones with the benzoyl-chromophore as the key constituent. In medical or food packaging applications, residual photoinitiator or photoproducts migrating into the packaged product have to be avoided, particularly of toxicological reasons. The benzoyl-chromophores of cleavable photoinitiators are generally problematic as well as various photoproducts, which are generated during the curing reaction. Especially volatile and odorous compounds such as benzaldehyde can be problematic at the production site or when it comes to food packaging.<sup>1</sup> Degradation and recombination products of aromatic initiators are potentially mutagenic or toxic to the human body.<sup>2</sup> Therefore, even safe initiators can lead to substances migrating out of the resulting polymer network and becoming hazardous. So non-aromatic, non-migrating photoinitiators are of high interest for industrial applications. Therefore a new generation of initiator systems, based on  $\alpha$ -ketoesters, was developed.  $\alpha$ -Ketoglutaric acid is a metabolite in the human body and therefore a highly biocompatible. It serves as non-volatile photoinitiator based on the  $\alpha$ -ketoester concept. Additionally there are approaches to limit the migration of those initiators after curing, by synthesizing macromolecular and polymerizable photoinitiators. Compared to the classical benzophenone-amine photoinitiator systems, the small  $\alpha$ -ketoesters show increased reactivity and higher curing speed. As expected, the macromolecular, polyester-based photoinitiators show lower reactivity due to the limited diffusion of the radicals in a (meth)acrylate-based formulation. With a low amount of migratable components out of the cured material, the aim of the thesis has been successfully reached. Furthermore, there were improved mechanical properties measurable, in terms of higher glass transition temperature, raised storage modulus at elevated temperatures and enhanced tensile strength in an (meth)acrylate-based monomer system.

## Deutsch

Die Photopolymerisation von (Meth)acrylat-basierten Formulierungen hat sich aufgrund der hohen Energieeffizienz und niedrigen Aushärtungszeiten dieser Technologie für viele Branchen zu einer weit verbreiteten Methode entwickelt. Verschiedene Produkte, von einfachen Beschichtungen bis zu komplexeren Anwendungen, basieren auf dieser Methode. Konventionelle radikalische Photoinitiatoren für die Industrie basieren im Allgemeinen auf aromatischen Ketonen mit dem Benzoylchromophor als Schlüsselbestandteil. Im medizinischen Sektor oder in Verpackungen für Lebensmitteln müssen Rückstände von Photoinitiatoren oder Photoprodukten, die in das verpackte Produkt wandern, insbesondere aus toxikologischen Gründen vermieden werden. Im Allgemeinen sind Photoinitiatoren, welche das Benzoylchromophor enthalten, ebenso problematisch wie verschiedene Photoprodukte, die während der Aushärtung mit UV-Licht erzeugt werden. Besonders flüchtige und geruchsintensive Verbindungen wie Benzaldehyd können am Produktionsstandort oder bei Lebensmittelverpackungen problematisch sein. Abbau- und Rekombinationsprodukte von aromatischen Initiatoren sind möglicherweise mutagen oder toxisch für den menschlichen Körper. Daher können selbst sichere Initiatoren dazu führen, dass Substanzen aus dem resultierenden Polymernetzwerk migrieren und gefährlich werden. Nichtaromatische, nicht migrierende Photoinitiatoren sind daher für industrielle Anwendungen von großem Interesse. Daher wurde eine neue Generation von Initiatorsystemen auf Basis von  $\alpha$ -Ketoestern entwickelt.  $\alpha$ -Ketoglutar säure ist ein Metabolit im menschlichen Körper und daher sehr biokompatibel. Es war daher Ziel dieser Arbeit, Photoinitiatoren mit guter Migrationsstabilität zu entwickeln. Dies soll durch Synthese makromolekularer und polymerisierbarer Photoinitiatoren erreicht werden. Im Vergleich zu klassischen Photoinitatorsystemen, wie Benzophenon-Amin, zeigen die kleinen  $\alpha$ -Ketoester eine erhöhte Reaktivität und eine höhere Härtungsgeschwindigkeit. Wie zu erwarten war, zeigen makromolekulare Photoinitiatoren auf Polyesterbasis eine geringere Reaktivität aufgrund der begrenzten Diffusion der Radikale in einer Formulierung auf (Meth)acrylatbasis. Mit einer deutlich verringerten Menge migrierbarer Komponenten aus dem ausgehärteten Material wurde das Ziel der Arbeit erfolgreich erreicht. Des Weiteren wurden verbesserte mechanische Eigenschaften gemessen. Dies inkludierte eine höhere Glasübergangstemperatur, einen erhöhten Speichermodul bei erhöhten Temperaturen und eine verbesserte Zugfestigkeit in einem Monomersystem auf (Meth)acrylatbasis.

## INTRODUCTION

### Photopolymerizable Formulations

Today, a huge amount of everyday used items, like transparent food packages, thin foils, paints and different car part finishes, are manufactured via curing of resin containing formulations.<sup>3-5</sup> Also the curing techniques transited from environmental harmful, resource and cost inefficient solvent evaporations to more advanced solutions. To cure a formulation, water-based solvent evaporations, thermal treating or radical polymerization of polymerizable groups, are common. In coatings polymerizable groups, like a double bonds, are most widespread cured via electron beam (EBC)<sup>6, 7</sup> or UV-light irradiation.<sup>7</sup> Both beam-based methods have their advantages and drawbacks, but the lower energy input and operational cost of a UV-based curing device, are more interesting for industrial scale production.

Radical photopolymerization is the fastest growing curing method,<sup>8</sup> with a wide range of applications. Photocuring even outperforms the disadvantages, like a higher cost of the formulations due to the more complex mixture for the curing process, expensive lamp equipment, eye and skin protection for safety reasons while handling. A high curing speed, a resulting increased throughput and better mechanical properties of the materials after irradiation are the advantages of this method. There is no need for any solvents during photocuring.

Radical photopolymerization is commonly used in countless applications due to its convenience for many branches:

- The coating industry relies on a variety of resins to provide thin, glossy coatings for decorative applications, such as covers of magazines or books, posters or wood finishes. A protective coating needs specific properties to serve its purpose, for example heat or abrasion resistant coatings for a wide range of materials or corrosion protection of metals.<sup>9</sup>
- Printing-ink manufacturing and even water-based inks for posters or Braille printing of characters uses photo polymerizable source materials.<sup>9</sup>
- In dentistry, formulations based on different methacrylates with inorganic filler and a photoinitiator, are used to fill the dental hole and irradiated via a LED to achieve curing of the formulation, resulting in a permanent bond with the tooth.<sup>9, 10</sup>
- Optic and electronic industry take advantage of photocuring for optical fiber coatings, cable coatings, protective coatings for discs, optical lenses or even contact lenses for everyday use. Further applications are photoresists for the semiconductor industry, solder resists, and insulation or conductive layers for printed circuits.<sup>9</sup>
- Primer and adhesive branches uses primers for metal and glass coatings, adhesive layers for safety glass, coating for composite materials and release and seal coatings.<sup>9</sup>

- Further applications are traffic markings, 3D printing, leak repairing or floor finishing.<sup>9, 11, 12</sup>

To fulfill the needs of such applications, a photopolymerizable formulation has to be prepared. This mixture of many different components is usually tailor-made for every application, to serve with the aimed properties after curing.

To achieve a finished photopolymerizable formulation for a given application, two basic ingredients are necessary, the monomer and the photoinitiator. However, every formulation used in industry, consists usually out of two more major classes, a reactive diluent and many additives with different purposes (Figure 1)

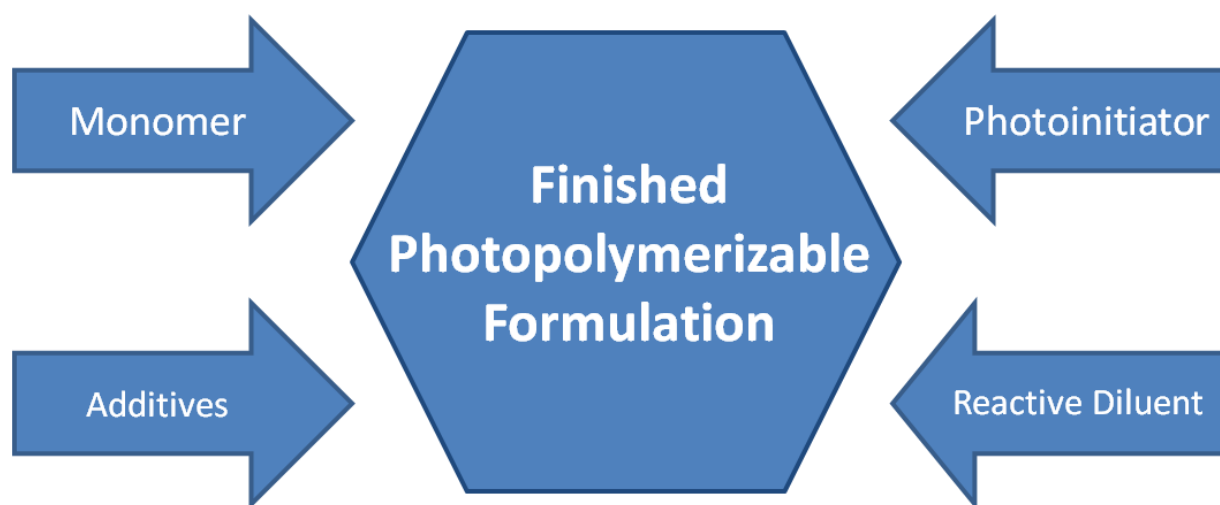


Figure 1: Ready to use photopolymerizable formulation

Beside the monomer and the photoinitiator, various additives are present in formulations for radical polymerization, usually in 1-3 wt% with the exception of fillers and softeners, which are used in much higher percentages. Typical are antioxidants, metal deactivators, light protection agents, softener, plasticizer, surfactants, filler, pigments, flame retardants, nucleating and brightening agents.<sup>13</sup> The focus stays on the monomer and reactive diluent, due to their importance in this whole system.

Monomers for photopolymerization are network building blocks, which are usually at least difunctional in terms of reactive groups, to form a crosslinked material after UV-exposure. These components are often high molecular weight and therefore very viscous.

On a global view, a huge demand of polymerizable monomers is present, and therefore much effort is spent, to find suitable monomer mixtures for every application. These monomers make up the majority of a polymerizable formulation, and define the mechanical properties of the resulting polymer. These formulations are usually a mixture of many components, to serve the requirements of an application by fine tuning the polymer network architecture.<sup>14, 15</sup>

Properties of a good monomer are fast curing speed, high conversion and high propagation rate, as well as abrasion resistance, low toxicity, neutral odor, low shrinkage stress and low



oxygen inhibition during polymerization.<sup>9</sup> To fulfill these demands, a variety of monomers can be used, depending on the application. In Figure 2 different, difunctional monomers are shown. The spacer R between the reactive endgroups can be based for example on polyethers, polyesters, polyurethanes, aromatic moieties or aliphatic chains in various molecular weights. Acrylates are more reactive compared to methacrylates in general, therefore more commonly used in industry. They achieve higher conversions and are more viscous than methacrylates.

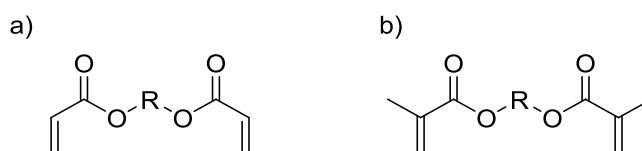


Figure 2: Common monomers for radical photopolymerization; a: diacrylate; b: dimethacrylate

The reactive diluent serves the role of thinner and viscosity adjuster to ensure a good processability. It is usually multifunctional, low molecular weight and therefore act as crosslinker. The number of functional groups manipulates the mechanical properties of the resulting material (Figure 3).

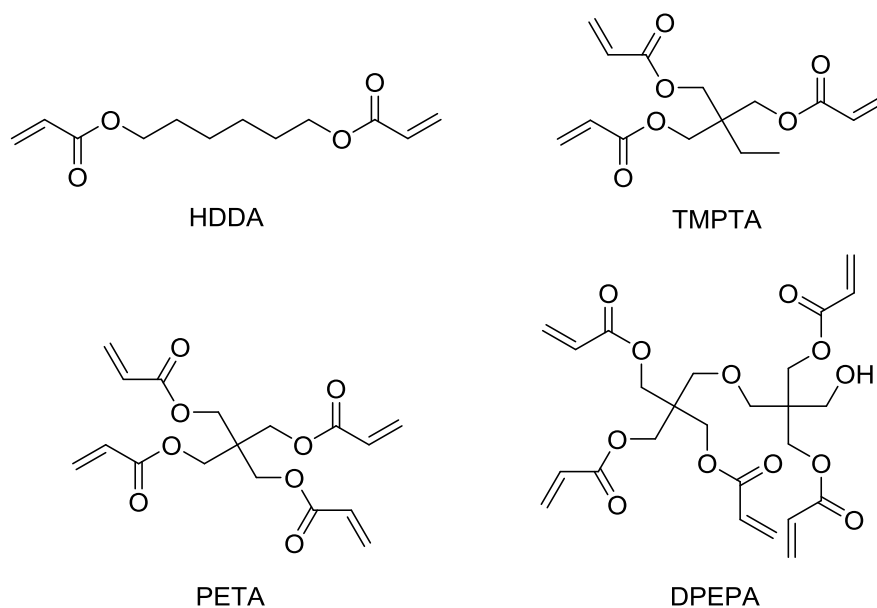


Figure 3: Common reactive diluents; HDDA - 1,6-hexanediol diacrylate; TMPTA - trimethylolpropane triacrylate; PETA - pentaerythritol tetraacrylate; DPEPA - dipentaerythritol pentaacrylate

To form a polymer chain or a network out of the monomer and reactive diluent building blocks, an initiator is necessary to start the polymerization of those compounds.

To polymerize the monomers via exposure to UV-light, a photoinitiator is necessary to absorb the irradiation. The light energy is absorbed by the photoinitiator in form of a photon and converted into useful chemical energy to initiate the polymerization. These photons can be emitted from different sources, such as traditional mercury lamps or more modern lasers or LED's in all different wavelength, reaching from highly energetic UV light to visible light.

Properties of a good photoinitiator are a high initiation efficiency, low toxicity, low odor, no yellowing effect of the resulting polymer, storage stable within the formulation and of course a low price.<sup>9</sup>

The photoinitiation process can be divided into five general steps:<sup>9, 14</sup>

1. Light absorption or energy transfer: From a photon directly to the photoinitiator, resulting in an excited state or indirectly from a photosensitizer (Figure 4).

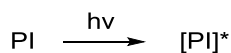


Figure 4: Light absorption and transition to an excited state

2. Formation of radicals: Via  $\alpha$ - or  $\beta$ -photofragmentation<sup>16</sup>, hydrogen abstraction<sup>17</sup> or electron/proton transfer,<sup>18</sup> illustrated in Figure 5.



Figure 5: Radical formation

Depending on the radical stability generated by the photoinitiator, it can initiate a chain growth reaction, recombine with other radicals, terminate or transfer polymer chains.<sup>19</sup>

3. Start of the propagation reaction: The photoinitiator radical attacks the double bond of the monomer, therefore starting the polymerization reaction (Figure 6).

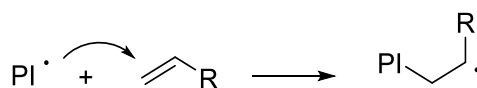


Figure 6: Start of the propagation reaction

The formed monomer radical is now able to propagate, by attacking further monomer molecules.

4. Propagation: Polymer chain growth and chain transfer.

The propagation reaction of a growing chain radically adds more and more monomer molecules to the forming polymer chain, favoring the 1,3-addition (head-to-tail) over the 1,2-addition (head-to-head) illustrated in Figure 7.<sup>20</sup>

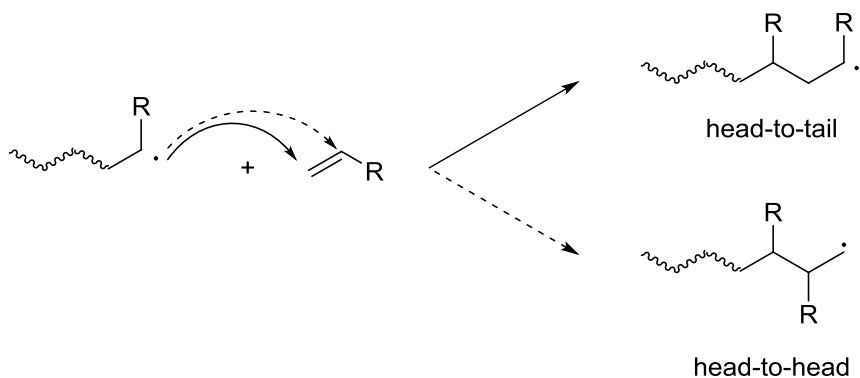


Figure 7: Head-to-tail or head-to-head propagation reaction

The chain transfer mechanism of a polymer chain can result in longer or shorter polymer branches, depending if the transfer occurs inter- or intra-molecular, shown in Figure 8.<sup>20</sup>

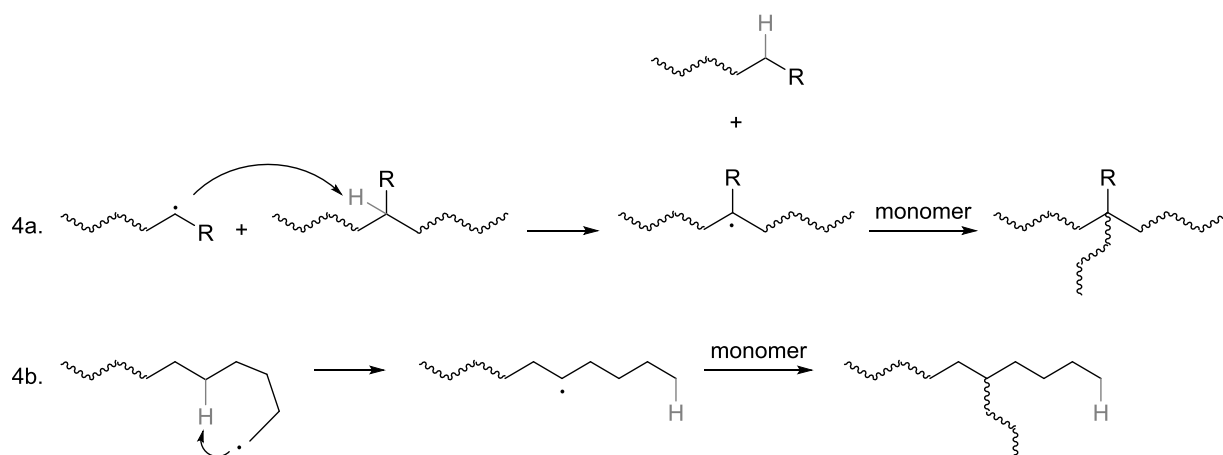


Figure 8: 4a: intermolecular chain transfer; 4b: intramolecular chain transfer

##### 5. Termination: Via recombination of radicals or disproportionation.

The termination step consist either of a recombination of two radicals or of a disproportionation of the growing polymer chain. This step is also depending on reaction conditions, like temperature. Increased temperature promotes disproportionation reactions, while a lower temperature lead to more recombination reaction and therefore a resulting higher molecular weight. The mechanism is illustrated in Figure 9.<sup>20</sup>

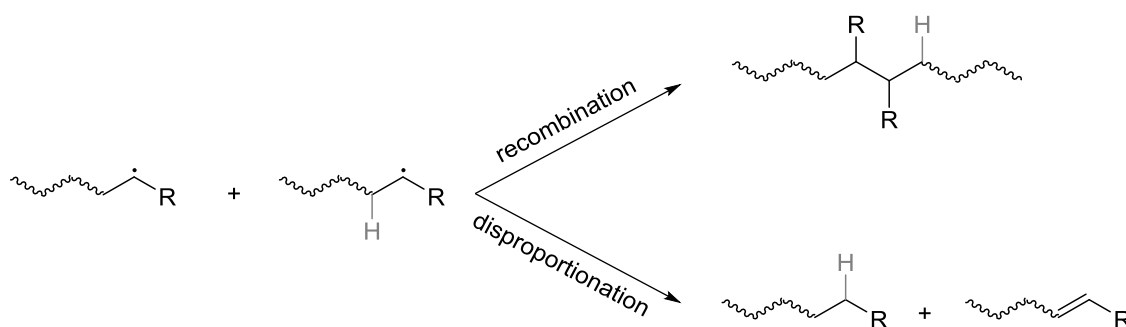


Figure 9: Termination reaction via recombination or disproportionation [22]

The photoinitiator is the key component in a polymerizable formulation. It absorbs the radiation and creates radicals, which are capable of starting the polymerization reaction. As already explained, photoinitiators can directly absorb the irradiation energy in form of a photon (Type I), or via triplet-triplet transfer from a photosensitizer (Type II). Is the absorption maximum of the photoinitiator within the wavelength spectrum of the irradiation source, usually an UV-emitting device, the chromophore absorbs the photon and induces an electron transition from  $\pi$  or  $n$  to  $\pi^*$  orbitals.<sup>21</sup> This transition wavelength can be found in Table 1 for common chromophores.

Table 1: Absorption maxima of different chromophores<sup>21</sup>

Chromophore	$\lambda_{\max}$ [nm] $\pi$ - $\pi^*$	$\lambda_{\max}$ [nm] n- $\pi^*$
C=C	170	-
C=O	166	280
C=N	190	300
N=N	-	350
C=S	-	500

The absorption spectrum<sup>21</sup> of benzophenone, an industrial Type II photoinitiator, is illustrated in Figure 10. Its n- $\pi^*$  transition is at 347 nm and the  $\pi$ - $\pi^*$  transition is at 204 and 248 nm.<sup>22</sup>

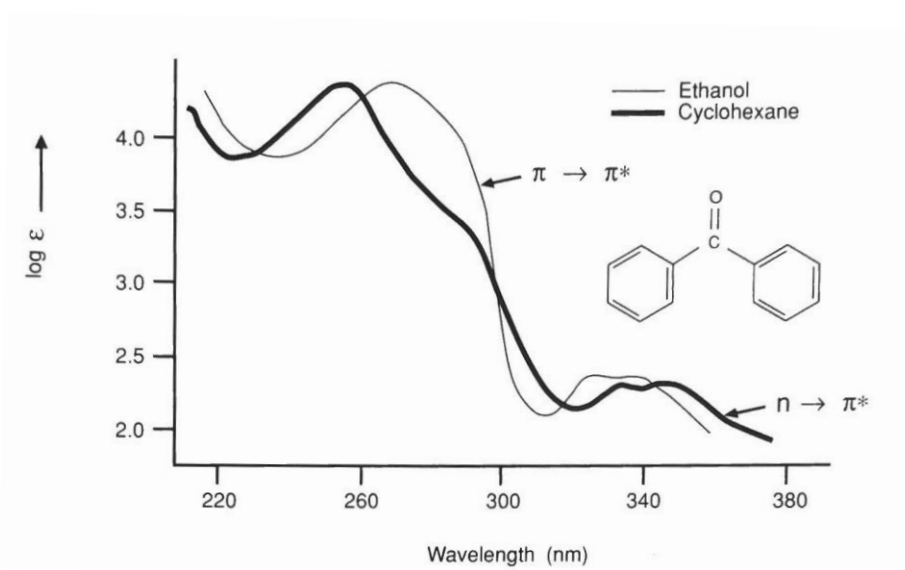


Figure 10: UV spectrum of benzophenone in ethanol and cyclohexane<sup>21</sup>

Initiation via absorption of a light particle by a photoinitiator is described in the Jabłoński Scheme, which describes the radical formation after reaching the excited state of an initiator (Figure 11).

At first, an electron is raised from its ground state  $S_0$  via photon absorption to its excited singlet state  $S_1^*$ . This absorbed energy can be released via fluorescence or via an internal conversion followed by an intersystem crossing, where the spin of an electron gets reversed, convert into an excited triplet state  $T_2^*$ . After a second internal conversion, the triplet state  $T_1$  is achieved. The internal conversions and intersystem crossings are energy level transitions without any radiation released. There is also a third possibility, vibration relaxation, when excited molecules interact with their non-excited surrounding molecules. Most likely the energy is released via vibration relaxation ( $< 10^{-12}$  s) followed by fluorescence from the singlet state ( $\sim 10^{-9}$  s), due to the short lifetimes of the excited states. Triplet states have much longer lifetimes, approximately 3 magnitudes higher than the singlet states ( $\sim 10^{-6}$  s). As soon as a triplet state is achieved, a radical formation can occur, but phosphorescence and transitions

without the release of radiation can counteract this radical formation. This process of radical decay is more likely to happen, the more stable the radicals triplet state is.<sup>23, 24</sup>

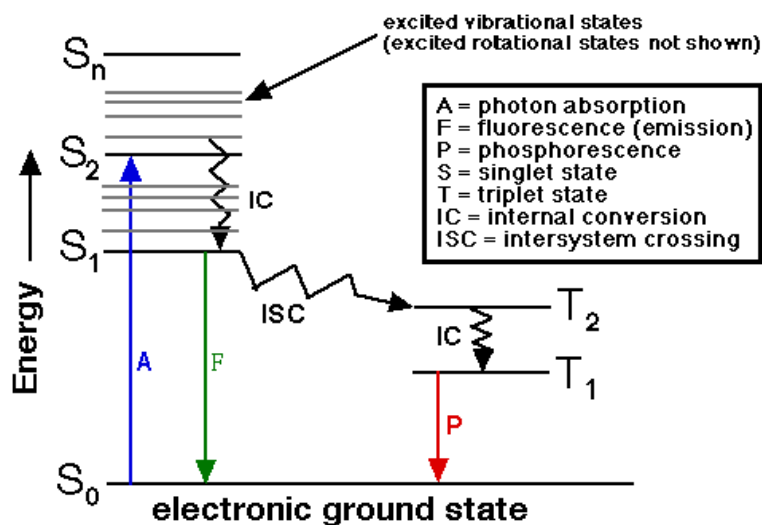


Figure 11: Jablonski Scheme illustration<sup>23</sup>

Photoinitiators are the key component for every photopolymerizable formulation. After exposure to UV-light of specific wavelengths, this molecule can either react mono- or bi-molecular depending on its structure. Monomolecular reaction mechanisms are called Type I and absorb the photon directly with the resulting cleavage of the molecule. If the mechanism is bimolecular, therefore depending on the initiator and the photosensitizer, the system reacts according to Type II. Electron/proton transfer from the co-initiator to the photoinitiator occurs.

Photoinitiators can be cleaved directly, via  $\alpha$ -cleavage (Figure 12). The reactivity of these so called Type I initiators depends only on the molecule itself, therefore is monomolecular in terms of rate-limiting steps.<sup>15</sup>

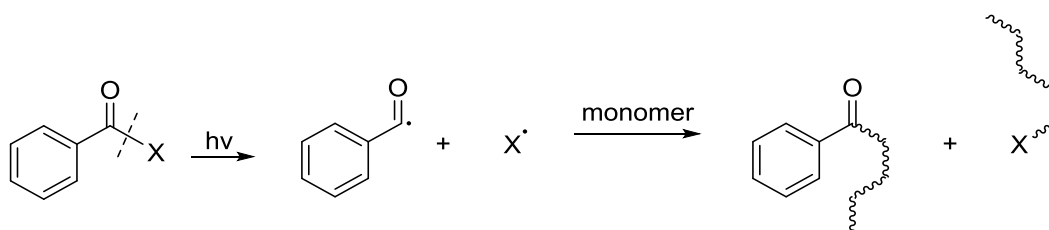


Figure 12: Type I  $\alpha$ -cleavage mechanism

Examples for  $\alpha$ -cleavable photoinitiators, like benzoin ethers, metal-based initiators and benzoylphosphineoxides are shown in Figure 13. All of them share the benzoyl chromophore moiety, due to its good UV absorption in the range of 200-400 nm and high reactivity.

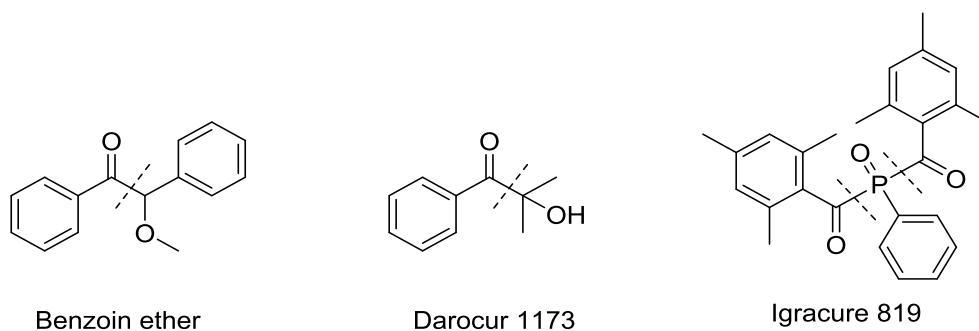


Figure 13: Different Type I  $\alpha$ -cleavable photoinitiators

If such a Type I photoinitiator undergoes  $\alpha$ -cleavage next to the carbonyl group, the result is a benzoyl radical and a radical leaving group. This homolytic cleavage is present due to the electron donating  $\beta$ -substituents. This substituents are oxygen containing groups, like in the examples above.<sup>25</sup>

Photoinitiators can also be cleaved at the  $\beta$ -position to the carbonyl group. This special mechanism is possible for  $\alpha$ -halogenated ketones, shown in Figure 14

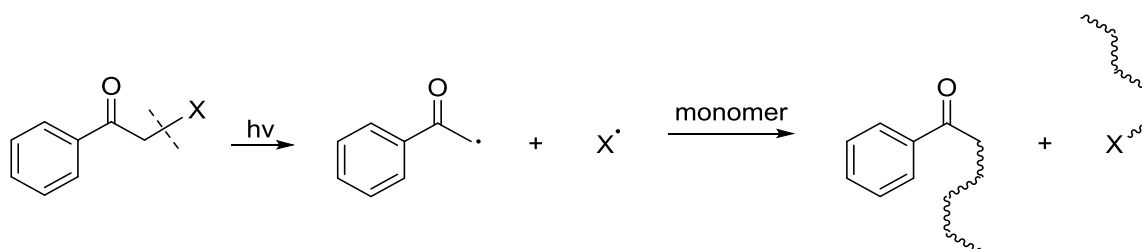


Figure 14: Type I  $\beta$ -cleavage mechanism

A Type II photoinitiator reaction is bimolecular, which means the reactivity and therefore the rate-limiting step is depending on two molecules, an initiator and a co-initiator. One molecule abstracts a hydrogen atom from a hydrogen donating molecule or an electron/proton transfer takes place, in the presence of an amine.<sup>15</sup>

To form a stable radical, which can start the polymerization chain reaction, alcohols or ethers are needed, to generate such starting intermediates via hydrogen abstraction (Figure 15a). In the more commonly used case first on electron/proton transfer from a co-initiator (Figure 15b), which usually is an tertiary amine<sup>26</sup>, this leads to the formation of two ionic radicals subsequently abstracting hydrogen in  $\alpha$ -position of the amine. The hydrogen donor finally initiates the polymerization.<sup>27, 28</sup> In a last step, the two complementary radicals to the already propagating amine radicals, form an unreactive species via recombination.

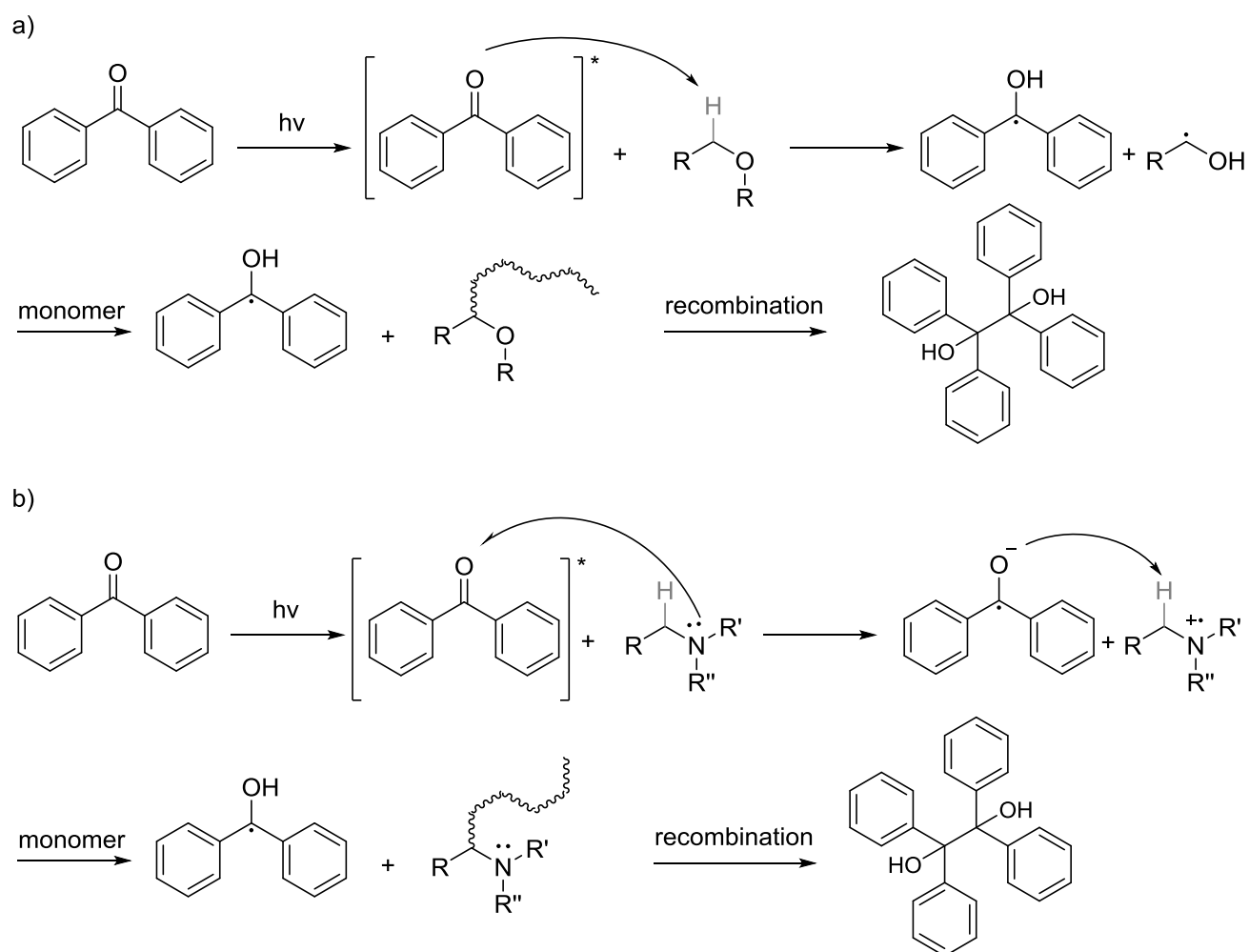


Figure 15: Type II photo initiation mechanisms; a: hydrogen abstraction from ether; b: electron/proton transfer via tertiary amine

Such compounds<sup>25</sup> are, analogous to the Type I photoinitiators, equipped with the benzoyl moiety, to efficiently absorb UV-light in the range of 200-400 nm, are shown in Figure 16.

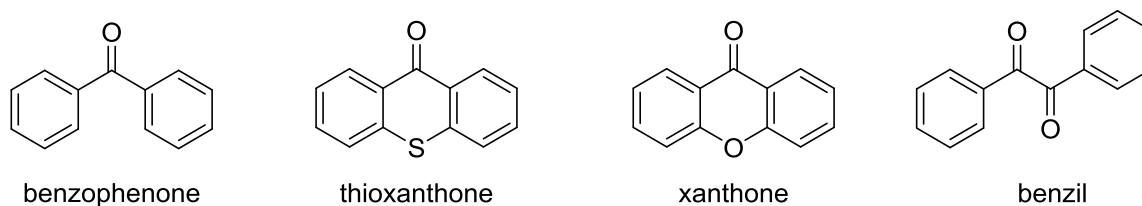


Figure 16: Different Type II photoinitiators

The benzoyl moiety is a key constituent of most commercial Type I and Type II photoinitiators. All resulting photoproducts, generated during the UV-exposure, are able to migrate out of the cured material. Therefore an alternative to this benzoyl moiety is of interest.

## Alternative Photoinitiators

During the irradiation process of a photopolymerizable formulation, the photoinitiators generate radicals via Type I or Type II initiation. A major drawback of this method is, that in the cured polymer material is still the majority of the photoinitiator in its unreacted state present.<sup>9, 29, 30</sup> Due to the high conversion rates in a very short time, only a few initiator molecules are able to covalently bind to the growing polymer network. This could be solved by irradiating for a very long period of time or using small amounts of initiator. For industrial scale applications, short exposure times to UV-light to ensure high throughput are necessary. To still provide a reasonable conversion, and due to the fact, that most photoinitiators are very cheap, an increased percentage of those molecules is used.

This leads, combined with exposure to radiation sources, for example the UV-light used for the initiation process or sunlight, to photoproducts. They cause odor, volatile compounds such as benzaldehyde, yellowing of the material and migration of all these byproducts out of the polymer matrix over time.<sup>1, 9, 29-31</sup>

Especially problematic is, that the photopolymer industry is focused on protective and decorative coatings, including food packaging and other all day use items, which can come in contact with humans, causing a general hazard, due to the photoproducts and unreacted photoinitiators migrating out of the cured polymers.<sup>1, 32</sup> Recent studies showed, that benzophenone and its photoproducts are carcinogenic.<sup>33</sup> Nevertheless a major part of the industry uses benzophenone as a photoinitiator due to its low price, availability of many derivatives and its good performance as a Type II photoinitiator. The photoproducts of a commercial benzophenone-amine system are shown in Figure 17.

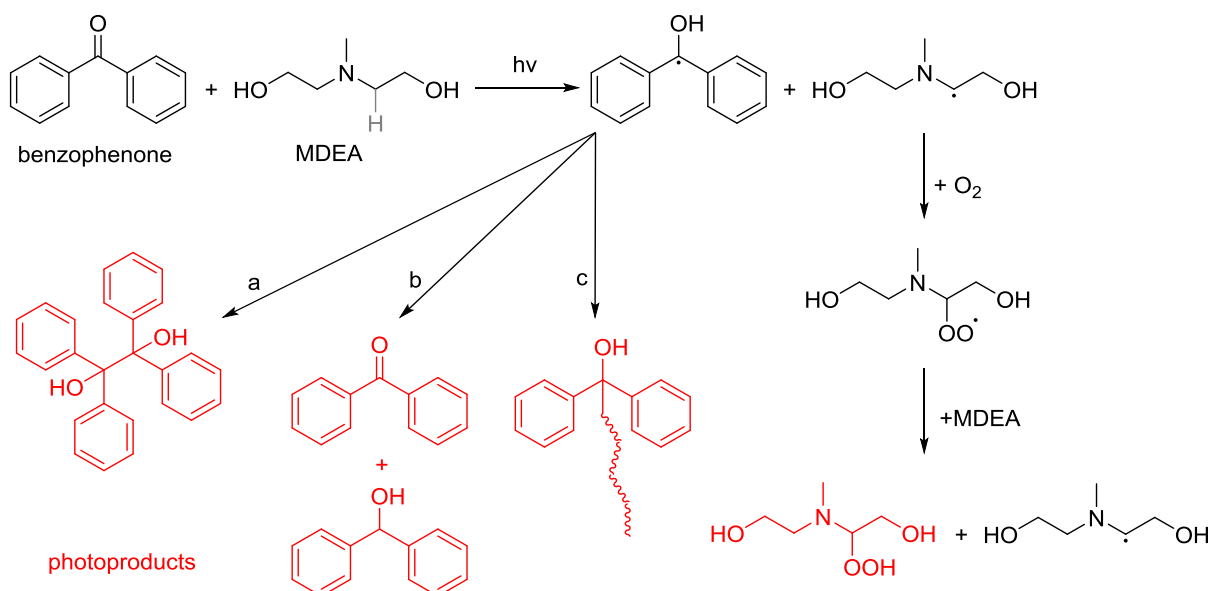


Figure 17: Photoproducts of benzophenone and methyl-diethanolamine (MDEA); a: recombination, b: disproportionation, c: termination of a growing polymer chain<sup>34</sup>



If Type I photoinitiators, based on benzoyl chromophores, are exposed to UV-light, photoproducts like benzil, di-ketones, benzaldehyde and their derivatives are formed and cause yellowing, bad odor and also a hazard to the human body.<sup>1, 34</sup>

Therefore non-aromatic, non-migrating, non-mutagenic initiators are of high interest for the coating and packaging industry. The first aim was to replace the aromatic moiety with aliphatic ones. If schematically one aromatic ring of benzophenone is exchanged with aliphatic structures, this leads to already known phenyl glyoxylates<sup>35, 36</sup> or acetophenones<sup>37</sup> (Figure 18). By combining these two theoretical concepts, a non-aromatic photoinitiator, the aliphatic  $\alpha$ -ketoester was investigated<sup>38</sup>.

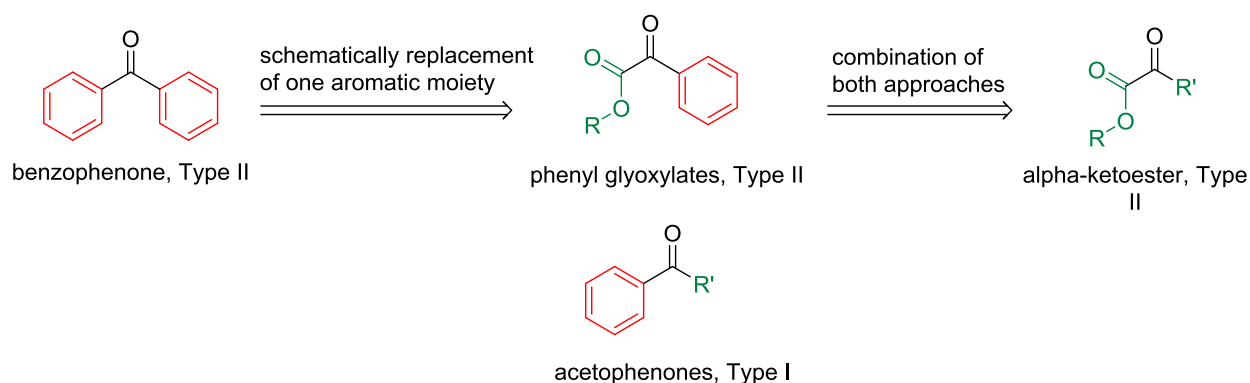


Figure 18: Pathway of aromatic ring exchange in the molecule to achieve  $\alpha$ -ketoester structure

It is already known, that  $\alpha$ -ketoesters, such as ethyl pyruvate for example, are sensitive to UV-light with an absorption maximum at around 330 nm ( $n-\pi^*$ ).<sup>38, 39</sup> The triplet energies of ketoesters are insignificantly lower than of benzophenone (272 compared to 287 kJ/mol<sup>40</sup>). Therefore, they might be used as conventional Type II photoinitiators, like benzophenone, to radically polymerize monomers. This process is possible without the use of a co-initiator, due to the pretty efficient hydrogen abstraction from itself, other initiators or monomer molecules (Figure 19a). There is no recombination of the initiator radicals like in benzophenone systems, due to the high reactivity of the tertiary radical next to the ester and the hydroxyl group. Nevertheless, a conventional co-initiator, for example an amine, can be used as well for  $\alpha$ -ketoesters, to increase the reactivity of the propagating radical (Figure 19b).

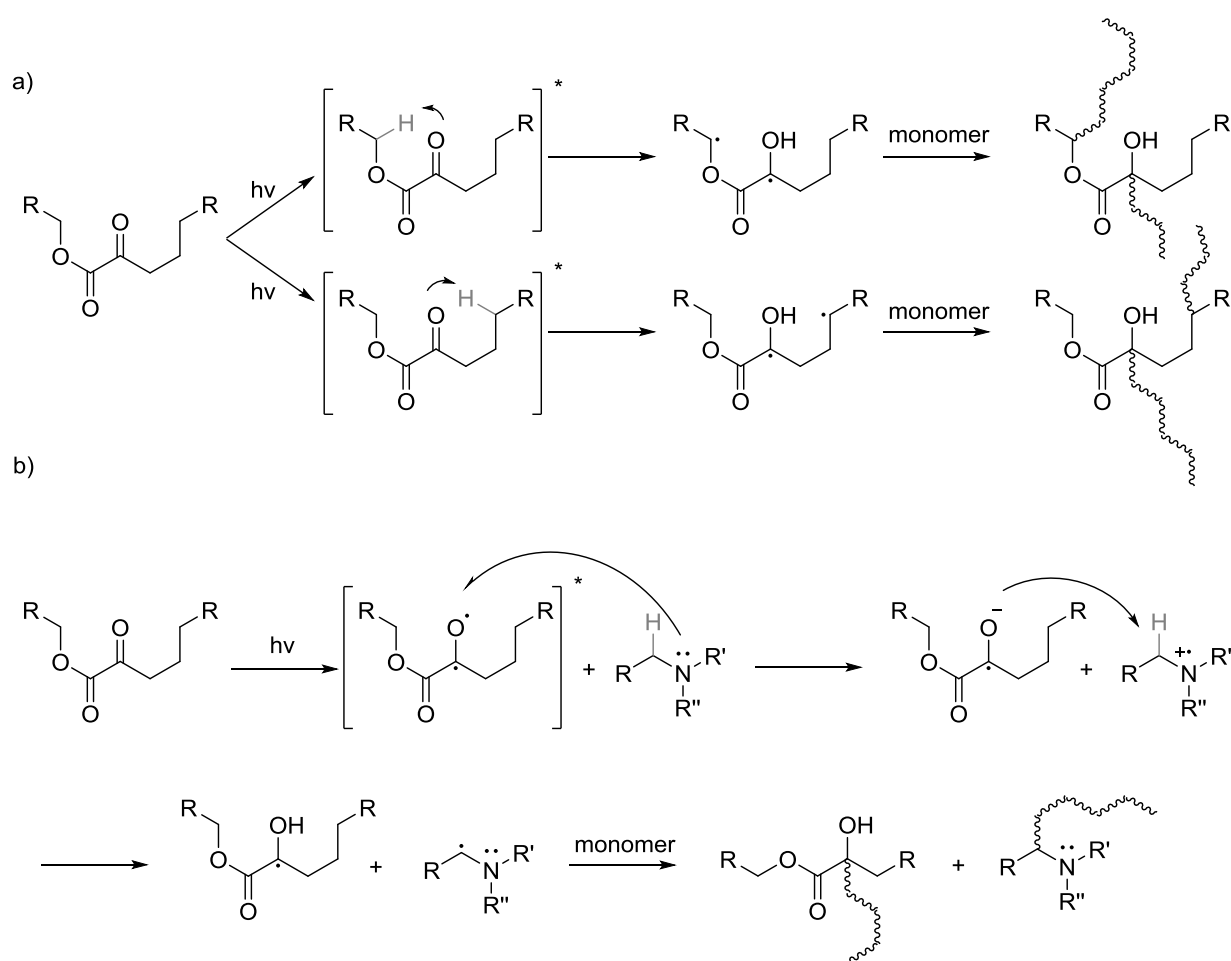


Figure 19: Type II photo initiation of  $\alpha$ -ketoesters; a: hydrogen abstraction from the ester or the alkyl end of itself; b: electron/proton transfer via amine

The photoproducts of  $\alpha$ -ketoesters underwent toxicological tests and were considered as harmless to humans.<sup>41</sup> The decomposition mechanism after irradiation and photoproducts are illustrated in Figure 20.<sup>39</sup>

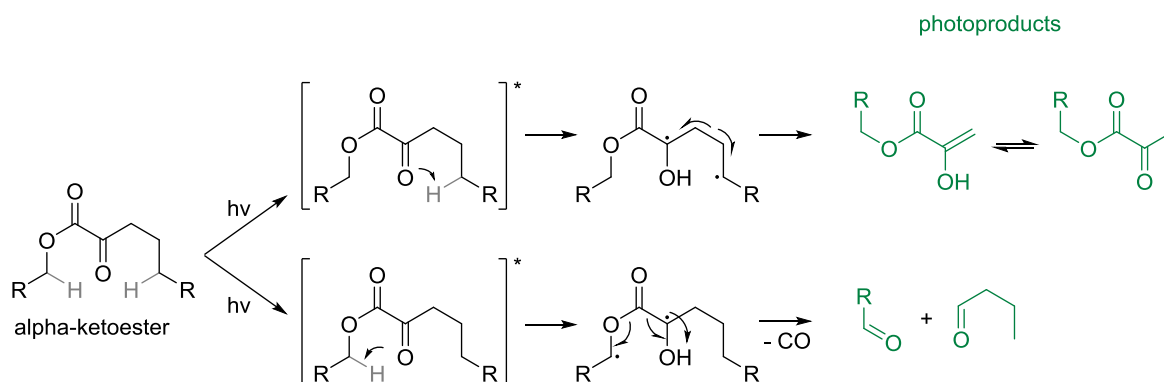


Figure 20: Photoproducts of  $\alpha$ -ketoesters ( $R \neq$  aromatic moiety)

It could be shown, that the bi-radical case followed by CO release is favored over the hydrogen abstraction.<sup>39</sup>

Recent studies in our group have shown, that  $\alpha$ -ketoesters have a high potential as non-aromatic UV-photoinitiators, without the risk of contaminating food or the environment with toxic or even carcinogenic photoproducts migrating out of the cured polymer network. They also have equal or increased performance, compared to Type II photoinitiators, like benzophenone, BMS or phenyl glyoxylates. Different  $\alpha$ -ketoesters (Figure 22) were tested in terms of reactivity (Figure 21), efficiency, UV-aging (yellowing), toxicological impact and absorption behavior, compared to commercial Type II initiators.<sup>38</sup>

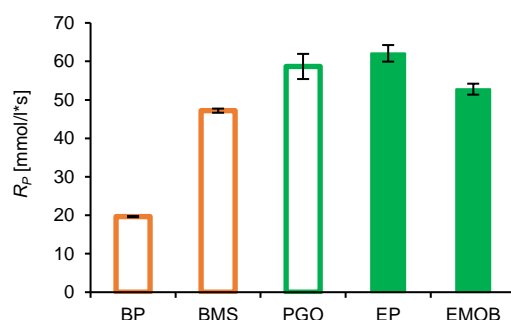


Figure 21: Rate of polymerization determined via Photo-DSC measurements: industrial initiators (□) and  $\alpha$ -ketoesters (■), with co-initiator MDEA ■ (orange) and without co-initiator ■ (green)<sup>38</sup>

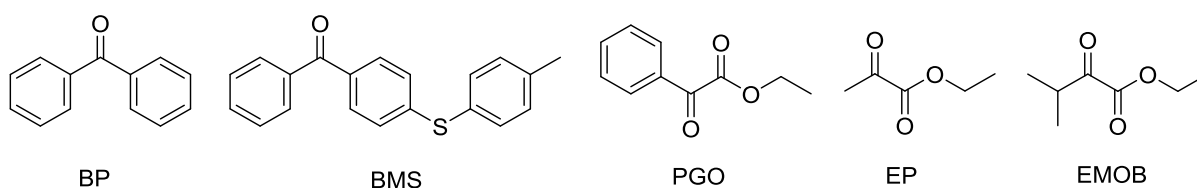


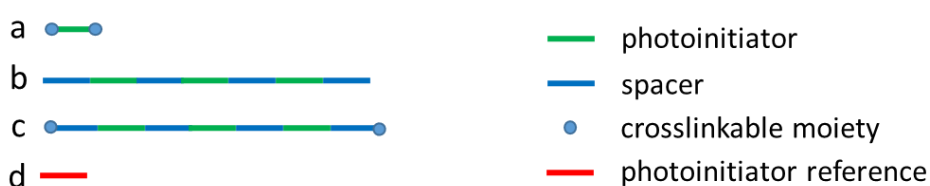
Figure 22: Commercial Type II photoinitiators: BP: benzophenone, BMS: 4-benzoyl-4'-methylthiophenyl sulphide;  $\alpha$ -ketoesters: PGO: ethyl phenylglyoxylate, EP: ethyl pyruvate, EMOB: ethyl 3-methyl-2-oxobutyrate

Overall, the toxic and possibly mutagenic photoproducts, generated by commercial benzoyl-based photoinitiators can be avoided with the introduction of the  $\alpha$ -ketoester. Although they still lead, exactly like benzophenone for example, to high amounts of unreacted photoinitiator leftover in the cured material<sup>9, 29, 30</sup>, the  $\alpha$ -ketoesters themselves and their photoproducts are harmless to humans. This advantage is significant and a step forward to biocompatible photoinitiators in packaging and coating industry.

Nevertheless the photoinitiator and the  $\alpha$ -ketoesters photoproducts are still migrating out of a material. For some applications, where it is unintended to contaminate the product with low molecular weight compounds, even non-toxic migrating substances have to be avoided. For such applications, macromolecular or polymerizable initiators are the initiator of choice. They are either to huge for migrating out of the cured network or covalently bond into the material during polymerization.

## OBJECTIVE

The focus on this thesis is to synthesize biocompatible and non-migratable  $\alpha$ -ketoester-based photoinitiators. Therefore,  $\alpha$ -ketoglutaric acid should be selected as the main molecule for all further products. The limitation of their migratability is planned to be achieved via three concepts. A simple approach are small, polymerizable molecules (a) based on the  $\alpha$ -ketoglutaric acid, which should co-polymerize into the polymer network. Another approach is to synthesize a polyester, which should have the photoinitiating group in its backbone (b), to immobilize the macromolecule due to its own molecular weight. Thirdly, a combination of the polymeric and the polymerizable photoinitiator (c) should be tried to synthesize, to achieve low migration after curing.



To introduce a reference polyester to the  $\alpha$ -ketoglutaric acid-based one, a photo-unreactive molecule should be chosen. Therefore glutaric acid-based polyesters have to be synthesized too, to better compare the influence of the photoinitiator in the polymer backbone on the mechanical properties. Also a low molecular reference initiator system (d) was necessary to compare the reactivity of the  $\alpha$ -ketoglutaric acid-based photoinitiators and the resulting mechanical properties of the materials.

After the synthesis of all target materials, various measurements considering the reactivity of the photoinitiators should to be carried out. Photo-DSC and photorheometry for an instance, are revealing techniques to determine the kinetics of a polymerization reaction. In terms of mechanical properties and network architecture, different analysis methods, like DMTA, impact and tensile testes, should also aimed to proceed. The last step should be a leaching test of cured samples, to quantify the migrating photoproducts and remaining initiator molecules. These methods combined should give a detailed insight into the properties of the final polymer materials, and will be compared with a cured material, containing a commercial photoinitiator.

## STATE OF THE ART

### Polymeric Photoinitiators

There are two concepts in industry, to immobilize photoinitiators, therefore preventing them from migrating or leaching out of the polymer matrix. The first, much more common system, depends on high molecular weight initiators, which are immobilized due to their own size. No diffusion or mobility in the cured network is apparent for molecules above the 1000 g/mol threshold (Figure 23). This study was performed in an diacrylate system, using polymeric photoinitiators.<sup>34</sup>

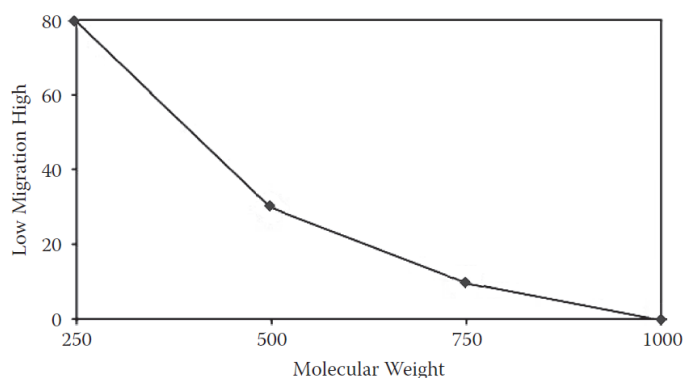


Figure 23: Migration vs. molecular weight<sup>34</sup>

The macromolecular photoinitiators gets even more trapped physically in the polymer network, by increasing its size. Type I photoinitiators (e.g. Omnipol® 910; Figure 24) will always lead to low molecular weight photoproducts, due to the scission process of the molecule, while Type II photoinitiators are more likely to completely stay in the cured material. Therefore the majority of polymeric initiators is Type II (e.g. Omnipol® 2702 and Igracure® 754). Those Type II initiators can perform hydrogen abstraction only, or the electron/proton transfer, which depends on a co-initiator. This co-initiator (e.g. Omnipol® ASA) should also be polymeric, otherwise this component will migrate out of the material afterwards.

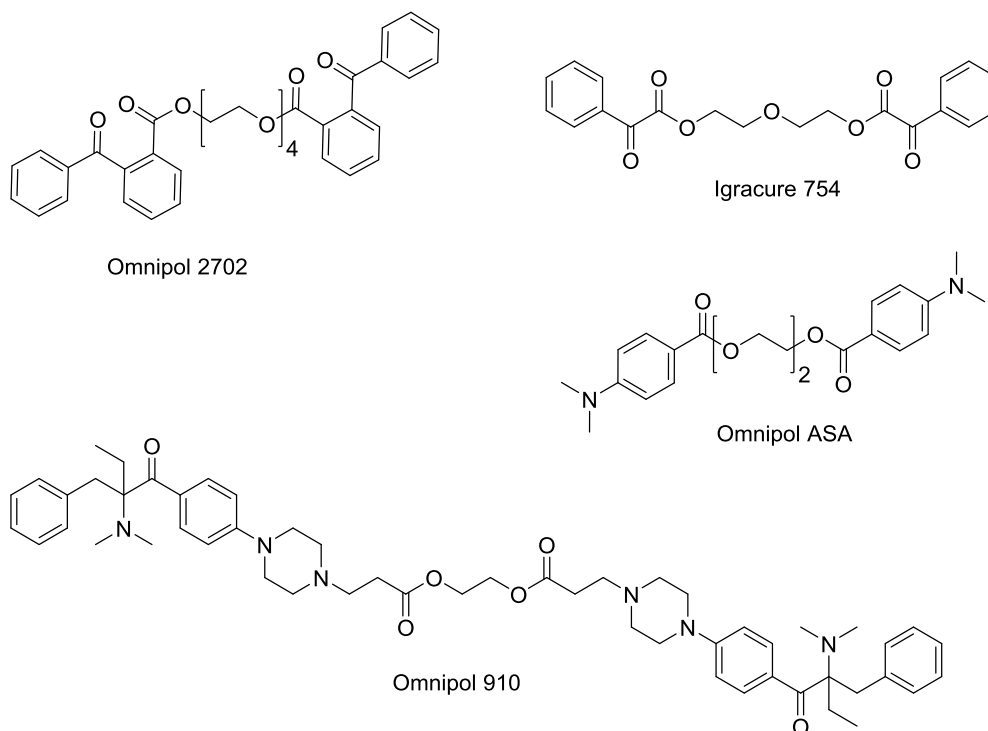


Figure 24: Type II polymeric initiators Omnipol® 2702 and Igracure® 754; sensitizer Omnipol® ASA; Type I polymeric initiator Omnipol® 910

The reactivity of such polymeric initiators is usually lower, compared to their low molecular equivalent due to diffusion restrictions. However, good cure speeds can be achieved by increasing the photoinitiator concentration up to 50% compared to the standard system. They also affect the viscosity of the formulation, particularly if they are used in high stoichiometric ratios, because those polymeric initiators are very viscous liquids or even solids.<sup>34, 42</sup>

### Polymerizable Photoinitiators

The second concept to limit migration of a photoinitiator is the introduction of polymerizable moieties, therefore covalently crosslink it into the network via co-polymerization. This immobilization is, in contrast to the first approach, chemical instead of physical nature. The copolymerizable initiators were in a variety on the market available, but they are disappearing gradually. Industry focused more on polymeric photoinitiators, therefore shifting the demand away from polymerizable initiators.

Representing the Type II initiators, benzophenones equipped with (meth)acrylates (e.g. Uvecryl® P-36) and Type I initiators (e.g. Esacure® ONE) were on the market (Figure 25). These compounds copolymerize into the growing polymer network with their (meth)acrylic groups, but in the case of the Type I initiators, there are still photoproducts with a low molecular weight generated during cleavage, which are able to migrate.

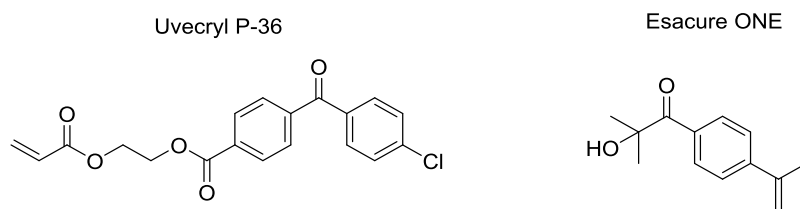


Figure 25: Type II polymerizable Initiator Uvecryl® P-36; Type I polymerizable initiator Esacure® ONE

The disadvantage of polymerizable photoinitiators are the rather low reactivity after co-polymerizing their (meth)acrylate moieties. A growing polymer chain with immobile initiator molecules in the backbone is not able to initiate as efficient as their non-polymerizable counterpart due to diffusion restrictions of the formed radicals. The second drawback is the final conversion of 70 to 80%<sup>34</sup> for most (meth)acrylate formulations, resulting in leftover, unreacted monomer molecules. They provide additional toxicity due to the acrylate moiety, as they migrate out of the cured material. This could be solved with the introduction of a second polymerizable group to increase the probability of co-polymerizing, but simultaneously more immobilization and therefore lowered reactivity is achieved.

## GENERAL PART

According to recent research on this topic,  $\alpha$ -ketoesters are a promising, non-aromatic alternative for the coating industry. Especially when it comes to requirements in biocompatibility or non-toxic byproducts during the manufacturing,  $\alpha$ -ketoglutaric acid was chosen to be the main compound focused on. This di-acid is an important biological molecule and present in every humans body as the anion,  $\alpha$ -ketoglutarate, further processed in the vitric acid cycle (Krebs Cycle), so its biocompatibility is granted.<sup>43</sup> Even though, photoproducts of  $\alpha$ -ketoglutaric acid derivatives are not harmful to humans, the aim was to minimize the migration via three basic concepts (Figure 26). Focusing a small, polymerizable molecule (a), an  $\alpha$ -ketoglutaric acid containing hydroxyl-terminated polyester (b) and a polymeric, polymerizable polyester with methacrylate endgroups (c).

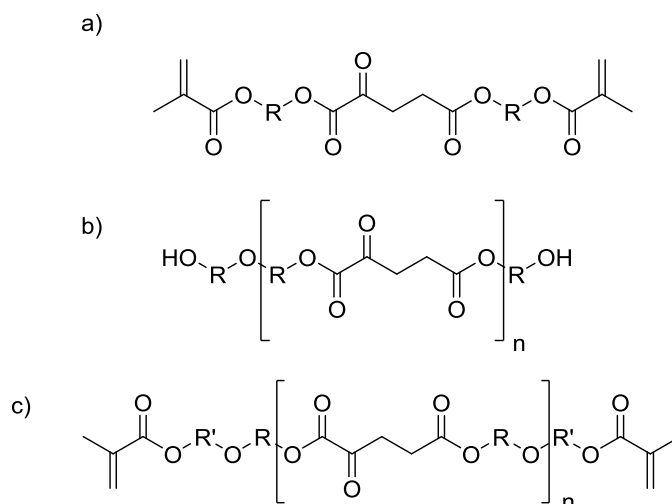


Figure 26: three concepts for low migration photoinitiators

The polymerizable,  $\alpha$ -ketoglutaric acid-based photoinitiator was the first target to synthesize. Beforehand, the reaction conditions for  $\alpha$ -ketoglutaric acid had to be tested, to achieve nearly complete conversion during the esterification. The Carothers equation demands very high conversions to achieve the aimed molecular weights for polycondensation reactions. In Figure 27 the average degree of polymerization is shown, affected tremendously by the conversion achieved.



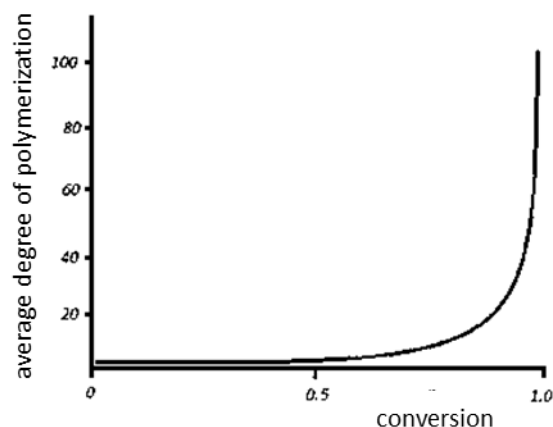


Figure 27: Average degree of polymerization plotted against the conversion<sup>44</sup>

With the Carothers equation (Equation 1), the stoichiometric ratios for the polycondensation reactions with an aimed molecular weight were calculated.

Equation 1: Carothers equation for AA-BB step growth reactions<sup>45</sup>

$$\bar{X}_n = \frac{1 + r}{1 + r - 2 * r * p}$$

$\bar{X}_n$  ... average degree of polymerization [ ]

r ... stoichiometric ration of difunctional monomer A to difunctional monomer B [ ]

p ... conversion [ ]

Various esterification reactions with the  $\alpha$ -ketoglutaric acid were performed to gain experience and apply those results for the polycondensation approach, which was carried out afterwards. As an advantageous side effect of these test reactions, those di-esters could also be used as photoinitiators and compared among themselves.

## 1. Optimization of the Esterification

### 1.1. Synthesis of $\alpha$ -Ketoglutaric Acid Di(m)ethylester [KGADi(m)et]

Before trying to synthesize high molecular weight polyesters, the first reactions done were diesterifications to proof the concept of acidic esterification of  $\alpha$ -ketoglutaric acid. The diethylester was the first compound synthesized to achieve a photoinitiator, which is soluble in organic solvents and polar monomers. The synthesis was based on the book Polymer Synthesis<sup>46</sup> (Figure 28).

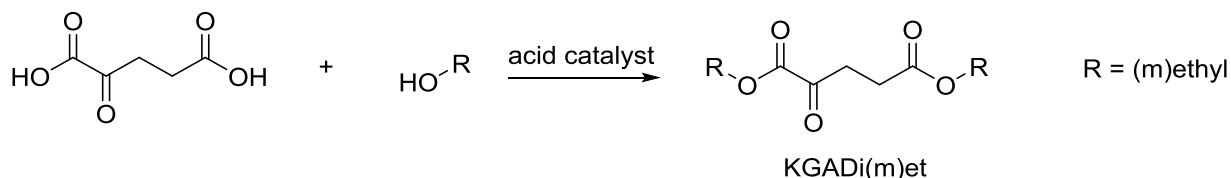


Figure 28: Acidic esterification of  $\alpha$ -ketoglutaric acid with (m)ethanol

To synthesize the KGADi(m)et, 1 eq. of  $\alpha$ -ketoglutaric acid was diluted in (m)ethanol. Then 0.3 eq. of sulfuric acid for the diethylester, and 0.01 eq. of para-toluolsulfonic acid for the dimethylester, were added as the catalyst and the whole mixture was stirred and heated up. Reaction progress was controlled via TLC. After aqueous workup, the diethylester was flushed through a silica gel column via MPLC. The yield of  $\alpha$ -ketoglutaric acid diethylester was 35% as a clear colorless oil. The dimethylester yielded 81% after distillation in vacuum as a transparent, colorless oil.

### 1.2. Synthesis of $\alpha$ -Ketoglutaric Acid Dibenzylester [KGADibenz]

$\alpha$ -Ketoglutaric acid dibenzylester was synthesized to further test, if there was a difference between aliphatic and aromatic substituents in reactivity. The synthesis of this compound referred to the book Polymer Synthesis<sup>46</sup> and the work of Roscales S.<sup>47</sup> (Figure 29).

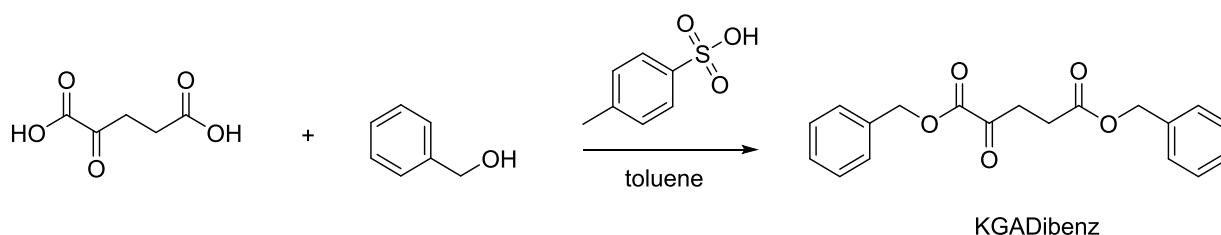


Figure 29: Acidic esterification of  $\alpha$ -ketoglutaric acid with benzyl alcohol

To achieve the compound KGADibenz, 1 eq. of  $\alpha$ -ketoglutaric acid, 2 eq. of benzyl alcohol and 0.045 eq. of para-toluolsulfonic acid were refluxed for 18 h. After aqueous workup, the product was flushed through a silica gel column via MPLC and yielded 65% as a clear colorless oil.

### 1.3. Synthesis of $\alpha$ -Ketoglutaric Acid Di-2-Hydroxypropylester [KGADihydroxyprop]

The  $\alpha$ -ketoglutaric acid di-2-hydroxypropylester was synthesized to obtain a product, which can further be modified on its hydroxyl endgroups with isocyanates for example. It is also a proof of concept to convert the acid endgroups of a polyester to hydroxyl groups.

#### 1.3.1. Acidic Esterification

The first approach was to synthesize the  $\alpha$ -ketoglutaric acid di-2-hydroxypropylester by acid catalyzed esterification based on the book Polymer Synthesis<sup>46</sup> (Figure 30).

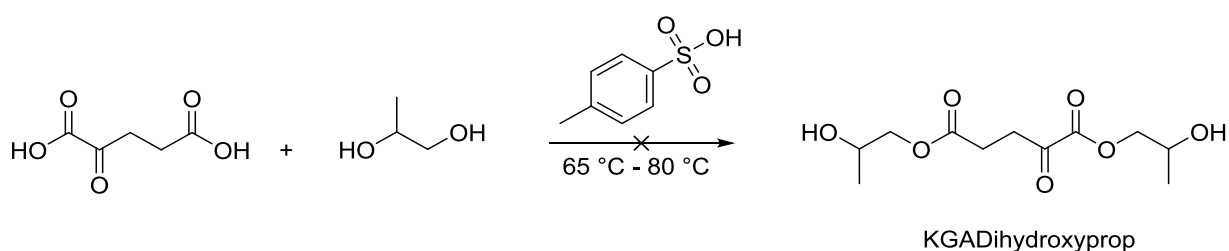


Figure 30: Acidic esterification of  $\alpha$ -Ketoglutaric acid and propylene glycol

To synthesize KGADihydroxyprop, 1 eq. of the  $\alpha$ -ketoglutaric acid was dissolved in dry THF in a beaker and later transferred into a dropping funnel. 20 eq. of the propylene glycol and 0.005 eq. of para-toluolsulfonic acid were added into a flask, which was attached to a Dean-Stark apparatus and heated. After the addition of the di-acid had finished and the temperature was raised. After a total reaction time of 43 h, the mixture was distilled in a Kugel-Rohr apparatus and purified afterwards by MPLC and characterized by NMR. Unfortunately the aimed product was not achieved via this reaction.

The problem during this synthesis was, that the resulting products were oligomers with two or more  $\alpha$ -ketoglutaric acid repeating units connected by the diols, according to NMR measurements. Even the excess of diol in this reaction was not enough to force the equilibrium to the only di-substituted  $\alpha$ -ketoglutaric acid. Also the acidic conditions lead to transesterification reactions and acetal forming (Figure 31).

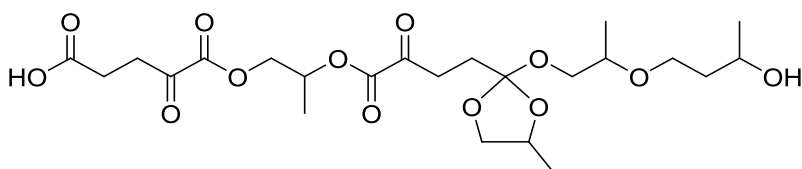


Figure 31: Oligomer and acetalized product

May a shorter reaction time can overcome this problem, but a different approach, with the addition of an epoxide and therefore expected less side reactions possible, was focused onto.

### 1.3.2. Addition of Propylene Oxide

Based on the work of Guoliang C.<sup>48</sup> with reactions of epoxides and acids in pressurized reactors (Figure 32), molecular sieve was used as a catalyst.

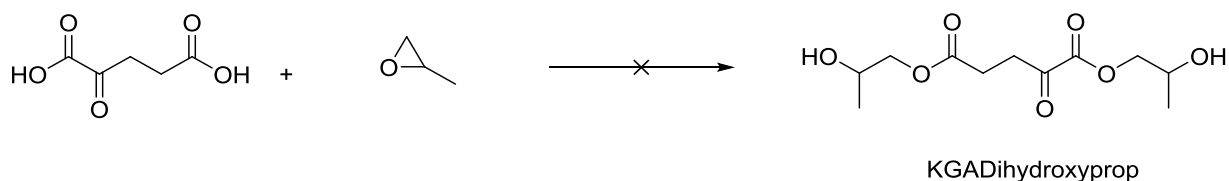


Figure 32: Addition of propylene oxide to  $\alpha$ -ketoglutaric acid

To achieve the KGADihydroxyprop, 1 eq. of the  $\alpha$ -ketoglutaric acid and 4 wt% of molecular sieve, were weighed into a Teflon reaction flask. Then absolute THF and 2.06 eq. of the propylene oxide were added. The pressure was set to 5 bar using nitrogen gas. The autoclave was programmed to run at 45 °C for 120 minutes. The reaction mixture was purified via MPLC chromatography, resulting in a clear, colorless and viscous liquid. Also this time no hydroxyl peaks were visible after performing a deuterium exchange and comparing the spectra to one, measured in DMSO.

The reaction conditions with the least side products, analyzed via TLC and NMR, were tried to achieve. An increase of reaction time or temperature for example lead to more side products (60 °C, 200 min, 5 bar and 45 °C, 200 min, 5 bar). NMR analysis show that many characteristic peaks are present in the spectrum, but also some other peaks, which cannot be explained, including the missing of a hydroxyl peak. This was confirmed via deuterium exchange of all acidic hydrogens. In a 2D TLC experiment was further confirmed, that the product decomposes during interaction with silica gel a bit.

In the next approach, a similar reaction route was selected, but this time with triphenyl phosphine as a catalyst referred to the work of Joly G. D.<sup>49</sup>

The same procedure as before was used, but the autoclave was programmed to run at 80 °C for 600 minutes. TLC was used to monitor the reaction progress and the reaction mixture was purified with silica gel via MPLC column chromatography. Again, a transparent, colorless and viscous product was achieved.

Interestingly the NMR of the three products, obtained by adding propylene oxide with different catalysts and various conditions, after MPLC chromatography were exactly the same. Also this time no hydroxyl peaks were present and therefore not the aimed product synthesized.

## 2. Synthesis of Polymerizable Photoinitiators [KGA2HEMA]

To achieve a polymerizable photoinitiator based on  $\alpha$ -ketoglutaric acid, (meth)acrylate moieties had to be attached to the di-acid. Their purpose was to covalently bond the molecule to a growing polymer network, therefore immobilizing the photoinitiator and preventing it from migrating out of the material.

$\alpha$ -Ketoglutaric acid di-2-hydroxymethylmethacrylate ester was synthesized to form a photoinitiator, which can crosslink itself into the polymer network during curing. There were different synthesis routes to achieve this compound. Acidic and basic esterification, but also enzymatic esterification as a modern approach of polyester synthesis.

### Acidic Esterification

At first the KGA2HEMA was tried to be synthesized, following the same reaction route as the dibenzyl- and diethyl ester of the acid.<sup>46</sup> Additionally an aerobic inhibitor BHT was added to prevent the methacrylates from polymerizing during the reaction (Figure 33).

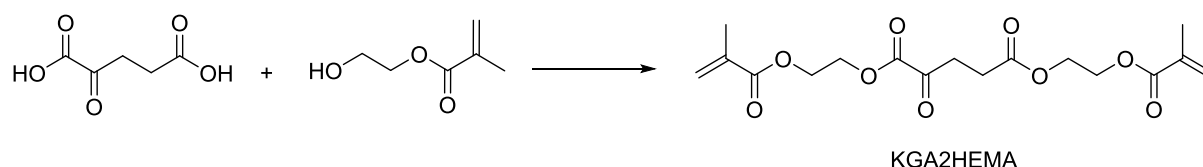


Figure 33: Acidic esterification of  $\alpha$ -ketoglutaric acid with 2-hydroxyethylmethacrylate (HEMA)

To synthesize KGA2HEMA, 1 eq. of  $\alpha$ -ketoglutaric acid, 2 eq. of 2-hydroxyethylmethacrylate, 100 ppm of BHT and 0.046 eq. of para-toluolsulfonic acid were put in dry toluene in a Dean Stark apparatus. The reaction was carried out for 21 h and the heating unit set to 150 °C. Some insoluble crosslinked polymer was formed during this. After aqueous workup, the product was flushed through a silica gel column via MPLC. NMR results of all fractions had shown no sign of the expected product (no double bonds present).

Acidic esterification with BHT and para-toluolsulfonic acid in toluene or benzene (to decrease the reaction temperature) lead to a crosslinked, insoluble polymer. Even without a catalyst the crosslinking kept a problem under these conditions. The acidic esterification in bulk also did not work and ended up with a crosslinked polymer too.

The second approach, after the unsuccessful acidic esterification in this case, to achieve a di-substituted  $\alpha$ -ketoglutaric acid with HEMA was via the Steglich Esterification.<sup>50</sup>

### Basic Esterification

The next reaction pathway to achieve KGA2HEMA was performed. 2.2 eq. of DCC were dissolved in dichloromethane. Then 1 eq. of  $\alpha$ -ketoglutaric acid, 2 eq. of 2-hydroxymethylmethacrylate, 0.5 mol% of N,N'-dimethylpyridin-4-amine (EDB) and dichloromethane were added into the flask. Now the DCC solution was added dropwise over

20 min and the result was a red colored solution, which was further stirred at room temperature over night for a total of 20 h. After aqueous workup, the residue was analyzed via NMR, but no sign of the expected product was present.

Basic esterification with N,N'-dicyclohexylcarbodiimide (DCC) and N,N-dimethylpyridin-4-amine (EDB) as a catalyst lead to an orange/red substance, which was not the expected product, because there were no methacrylate signals any more (NMR).

### Enzymatic Esterification

Acidic and basic esterifications did not work for this reaction. Now an enzymatic approach was focused. An immobilized lipase enzyme was used to form at very mild conditions, and without the presence of a strong acid catalyst, the ester bonds. This synthesis route was referred to the work of Douka A.<sup>51</sup> and Kumar A.<sup>52</sup>.

To synthesize KGA2HEMA, 1 eq. of  $\alpha$ -ketoglutaric acid, 2 eq. of 2-hydroxymethylmethacrylate and 1 wt% of Lipase acrylic resin from *Candida Antarctica* were added into a flask. The reaction mixture was stirred under inert atmosphere and the oil bath was set to 60 °C and vacuum was applied. The reaction progress was checked via NMR. After a total reaction time of 306 h the mixture was purified by MPLC. The product yielded 31% as a colorless, transparent oil.

Enzymatic esterification also lead to many problems before it worked. Temperature set equal or above 70 °C or vacuum below 800 mbar for an extended period of time (more than several minutes) lead to crosslinking of HEMA and the product. Event inhibitors, which are made to perform under vacuum conditions did not work. The way it finally worked, was an enzymatic esterification of the  $\alpha$ -ketoglutaric acid by Lipase CALB with 2-hydroxymethylmethacrylate (HEMA) and butylated hydroxytoluene (BHT) as an inhibitor under very mild conditions.

Finally the polymerizable photoinitiator KGA2HEMA was synthesized with 31% yield as a colorless, transparent oil. Therefore the next step, preparation of a macromolecular, polyester-based, initiator was conducted.

### 3. Synthesis of Macromolecular Photoinitiators

The aim of this synthesis was, to achieve different molecular weight polyesters containing diverse building blocks. The targeted molecular weights were approximately 3000, 5000 and 10000 g/mol. All polyesters should be therefore immobilized through their own size, and should not leach out of a cured material. To compare the influence of different molecular weight polyesters on the mechanical properties, like storage and loss modulus, as well as elongation at break or toughness, different polyesters were synthesized. The concept of acidic esterification, performed in chapter "Optimization of the Esterification" was also planned to be used for the polymeric initiators. First, a test reaction with the non-photoinitiating glutaric acid was performed to achieve a reference polyester, and later on the  $\alpha$ -ketoglutaric acid was used to synthesize photoinitiating polyesters. The diol building block was exchanged from 1,6-hexanediol to the sugar-based monomer, isosorbide to hopefully improve the rigidity of the molecule.

#### 3.1. Synthesis of Glutaric Acid-based Polyesters [Poly(HD/ISO)GA]

This glutaric acid-based polyesters were synthesized as a reference to the photoinitiating polyester with  $\alpha$ -ketoglutaric acid as a building block, and to gather information about the reaction conditions with a less complex system. Based on the book Polymer Synthesis,<sup>46</sup> polyesters were synthesized via acidic esterification (Figure 34).

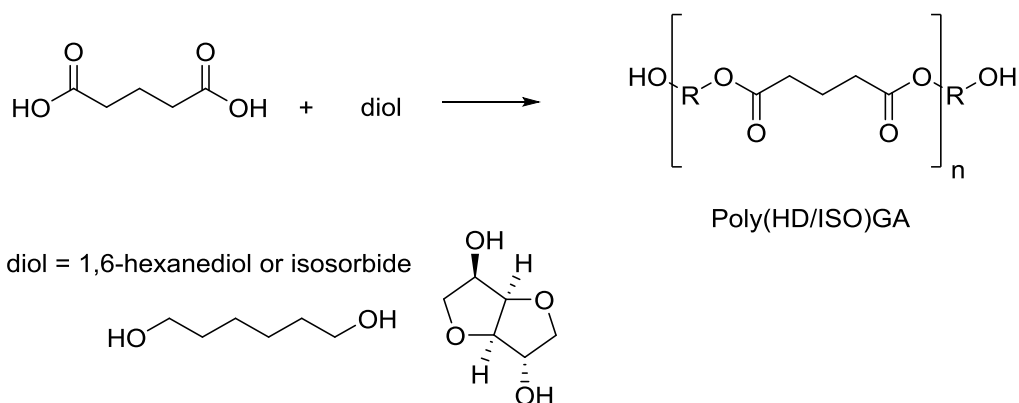


Figure 34: Acidic esterification of glutaric acid with 1,6-hexanediol or isosorbide

#### Glutaric Acid Hexanediol Polyester [PolyHDGA]

To synthesize the PolyHDGA, 1 eq. of the glutaric acid, a suitable amount of hexanediol for the aimed molecular weight (Table 2), and 0.0025 eq. of para-toluolsulfonic acid were added into a flask, which was attached to a Dean-Stark Apparatus. Then dry toluene was added. The oil bath was set to 125 °C and the reaction progress was checked via acid value and NMR. After a total reaction time of 50 h, the product was precipitated in diethyl ether and further dried in vacuum. Yields between 64% and 83% were achieved (Table 2).

Table 2: Molar ratios, expected molecular weights, solvent amounts and yields of the different products

Product	Expected $M_n$ [g/mol]	Eq. of di-acid	Eq. of diol	Yield [%]
<b>POLYESTER-1</b>	15000	1	1.01	77
<b>POLYESTER-2</b>	3000	1	1.10	77
<b>POLYESTER-3</b>	5000	1	1.05	83
<b>POLYESTER-4</b>	10000	1	1.02	64

For these polyester, the acid value determination encountered no problems. After 50 h of reaction time the acid value was around 0 mgKOH/g and did not change any more.

#### Glutaric Acid Isosorbide Polyester [PolyISOGA]

To synthesize a reference polyester containing isosorbide as a building block, the glutaric acid-based polymer was established. It was also predicted to result in a more rigid polymer, due to the missing of a flexible aliphatic chain. The synthesis route was carried out, according to the work of Noordover B. R. J.<sup>53</sup>

To achieve the PolyISOGA, 1 eq. of the  $\alpha$ -ketoglutaric acid, a suitable amount of isosorbide for the aimed molecular weight (Table 3), and 0.006 eq. of para-toluolsulfonic acid were added into a flask. The oil bath was set to 150 °C and the reaction progress was checked via acid value and NMR. Later, vacuum was applied. After a total of 47 h the acid value had shown full conversion and therefore the reaction was stopped. Acetonitrile was added to dissolve the viscous polyester in the flask. The polymer was then precipitated, and further dried in vacuum, yielding 80% as a brownish polyester.

Table 3: Molar ratios, expected molecular weights, solvent amounts and yields of the different products

Product	Expected $M_n$ [g/mol]	Eq. of di-acid	Eq. of diol	Yield [%]
<b>POLYESTER-5</b>	10000	1	1.05	78
<b>POLYESTER-6</b>	5000	1	1.10	80
<b>POLYESTER-7</b>	3000	1	1.21	69

This non-initiating polyester was synthesized under the same conditions, as the  $\alpha$ -ketoglutaric one. With the exception of reaction time, due to the lower reactivity of the glutaric acid and the diol. The glutaric acid and isosorbide-based polyesters were achieving the theoretically calculated molecular weight very accurately.

### 3.2. Synthesis of $\alpha$ -Ketoglutaric Acid-based Polyesters [Poly(HD/ISO)KGA]

Analogous to the synthesis of the glutaric acid-based polyesters, the same molecular weight polymers were prepared with  $\alpha$ -ketoglutaric as a photoinitiating system for all further measurements. So the influence of the keto group, and therefore a photo initiating polymer backbone, on the cured polymer network can be compared to the non-photoactive species. The polyester was synthesized via acidic esterification in solvent according to the book Polymer Synthesis<sup>46</sup> (Figure 35).



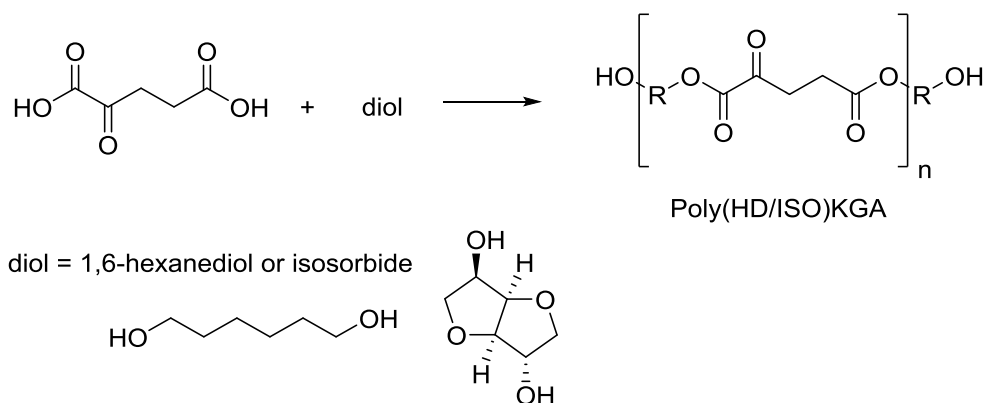


Figure 35: Acidic esterification of  $\alpha$ -ketoglutaric acid with 1,6-hexanediol and isosorbide

### $\alpha$ -Ketoglutaric Acid Hexanediol Polyester [PolyHDKGA]

The same procedure as for the glutaric acid-polyesters was carried out. The reaction progress was checked via NMR and the total reaction time was 24 h. Yields between 50% and 82% were achieved, depending on the molecular weight of the polyester (Table 4).

Table 4: Molar ratios, expected molecular weights, solvent amounts and yields of the different products

Product	Expected $M_n$ [g/mol]	Eq. of di-acid	Eq. of diol	Yield [%]
POLYESTER-8	15000	1	1.01	62
POLYESTER-9	3000	1	1.10	82
POLYESTER-11	5000	1	1.05	53
POLYESTER-12	5000	1	1.04	59

All synthesis were performed under the same conditions. The yields are very comparable in the cases of the lower molecular weight polyesters, which are in the range of 50-60%. The high molecular weight polyester could be obtained with a yield of 82%, due to its lower solubility and better agglomeration in the precipitation solvents.

Approximately 20 wt% of POLYESTER-8 were crosslinked and could not be dissolved in hot toluene or THF. To remove the crosslinked fraction in the product, the polyester was melted and then dissolved in 60 mL of THF. After filtration it was reprecipitated in cold diethyl ether and the result was a white polyester, which was further dried in vacuum.

A problem was the slow crosslinking of the polyester chains during the reaction. If the reaction time does not exceeded 30 h, the crosslinked part in the flask is minor. In one test reaction, after 48 h of stirring, the magnetic stir bar got stuck due to the huge amount of crosslinked, insoluble polymer inside of the reaction flask. So 24 h were chosen as a reasonable reaction time, due to no further reaction progress in the NMR spectra.

### $\alpha$ -Ketoglutaric Acid Isosorbide Polyester [PolyISOKGA]

To synthesize a photoinitiating polyester, which is non-migratable and biocompatible, a sugar-based monomer was used to achieve this compound. Isosorbide and  $\alpha$ -ketoglutaric acid build up the backbone of the polymer, hopefully improving the rigidity and toughness of the cured

polymer matrix, due to the inflexible isosorbide compared to the hexanediol. A possible drawback of the isosorbide in the polyester is the sterically hindrance. This could decrease the reactivity of this initiator. The synthesis was performed as an acid catalyzed bulk polycondensation according to the work of Noorder B. A. J.<sup>53</sup>, where they produced isosorbide and terephthalic acid-based polyesters.

The same procedure as for the glutaric acid-based polyesters was carried out. After a total reaction time of 25 h, the yield was 12% to 51% of yellowish polyesters (Table 5).

*Table 5: Molar ratios, expected molecular weights, solvent amounts and yields of the different products*

<b>Product</b>	<b>Expected M<sub>n</sub> [g/mol]</b>	<b>Eq. of di-acid</b>	<b>Eq. of diol</b>	<b>Yield [%]</b>
<b>POLYESTER-14</b>	5000	1	1.05	27
<b>POLYESTER-15</b>	3000	1	1.10	51
<b>POLYESTER-16</b>	10000	1	1.01	45
<b>POLYESTER-14A</b>	5000	1	1.05	30
<b>POLYESTER-17</b>	10000	1	1.02	14
<b>POLYESTER-16A</b>	10000	1	1.01	12

During this synthesis many problems occurred. At first a solvent polymerization approach was tried, under the same conditions like the hexanediol polyesters, using toluene as a solvent,<sup>46</sup> resulting in phase separation after a few hours of reaction time. Then acetonitrile was tried to increase polarity and keep everything in solution, but the conversion of this synthesis route was really low. Acetonitrile and water mixed, unlike toluene and water, resulted in a continuous discard of the distilled azeotrope. Due to the removal of the acetonitrile water mixture, new, absolute acetonitrile had to be added continuously to the flask. This was very time consuming and after 72 h the reaction was stopped, resulting in dimers, trimers and other smaller oligomers only.

Then the bulk polymerization route was performed, to remove the formed water more efficient. The molecular weight achieved via these polyester synthesis after 25 h was not exceeding 2500 g/mol for POLYESTER-14, POLYESTER-15 and POLYESTER-16, no matter which molar ratio was selected. By increasing the reaction time, an uncontrolled crosslinking of the polyester chains was observed. After approximately 26 h, this process started and the polyester expanded in the flask until the mechanical stirrer got stuck and the whole flask was full of polyester foam. This residue was insoluble in chloroform, acetonitrile, acetone, dimethyl sulfoxide and dimethylformamide. So a reaction time of maximum 25 h was chosen.

Next, an increase of acidic catalyst was tried to achieve more conversion in less time. So the equivalents of para-toluolsulfonic acid was raised to 0.006. The polyesters POLYESTER-14A, POLYESTER-17 and POLYESTER-16A were carried out under these adjusted conditions, obtaining the same result as before.

Due to no success of getting high molecular weight products, the polyester based on  $\alpha$ -ketoglutaric acid and isosorbide with a molecular weight of approximately 2500 g/mol was used in further reactivity and mechanical tests.

#### $\alpha$ -Ketoglutaric Acid Hexanediol Polyester by Transesterification [PolyHDKGA]

Next the transesterification concept with methanol as a condensate and therefore mild reaction conditions was tried. Therefore  $\alpha$ -ketoglutaric acid dimethylester and hexanediol were taken as educts. The transesterification was performed according to the book Polymer Synthesis.<sup>46</sup>

The reaction was carried out analogous to the direct esterification with  $\alpha$ -ketoglutaric acid. After a total reaction time of 118 h the product was precipitated. The product was a white sticky polymer. 39% of the polyester were achieved (Table 6).

Table 6: Molar ratios, expected molecular weight, solvent amount and yield

Product	Expected $M_n$ [g/mol]	Eq. of di-acid	Eq. of diol	Yield [%]
POLYESTER-13	5000	1	1.05	39

There occurred no major problems during the synthesis of  $\alpha$ -ketoglutaric acid hexanediol polyester. The precipitation in diethyl ether may could be skipped, because hexanediol is non-soluble in diethyl ether, but instead miscible with deionized water.

To summarize, a few problems during all polyester synthesis occurred regularly. One problem during the synthesis of the  $\alpha$ -ketoglutaric acid-based polyesters was the acid value determination. A final acid value of the polyester with around 100 mgKOH/g was found. This effect could be reproduced by titration of the pure dimethylester of the  $\alpha$ -ketoglutaric acid, which had shown even higher acid values. The potassium hydroxide, used for titration, can cleave especially activated ester bonds, like the one on the keto side of the (poly)-esters, very fast, resulting in much higher acid values. So NMR was chosen to determine the conversion instead.

Also the resulting molecular weights of the  $\alpha$ -ketoglutaric acid-based polyesters at the beginning of the experiments were a major problem. They were calculated via Carothers's equation to get the accurate molar amounts of the di-acid and the diol. For the polyesters the theoretically calculated molecular weight always exceeded the real value after precipitation and determining the molecular weight via GPC and NMR. This experience lead to approaches with a higher theoretical molecular weight than expected after the synthesis. So the molar ratios of the di-acid and diol were selected intentionally non-correlating to the Carothers's equation for all following experiments. The same effect was visible during the synthesis of the glutaric acid-based polyesters, but there it was not as tremendous.

After the successful synthesis of the polymeric photoinitiator and the corresponding reference polyesters, the last category of photoinitiators could be synthesized. The crosslinkable, macromolecular initiators.

### 3.3. Molecular Weight Determination of the Polyesters

To determine or calculate the molecular weight of the synthesized polyesters, many different approaches were carried out. Indeed the very exact molecular weight was not necessary for the modifications of the polyesters with isocyanate endgroups, due to an excess of these isocyanates during the synthesis, but a close range of the molecular weight provided more precise calculations and less error.

#### 3.3.1. Acid Value Determination

Usually the molecular weight of a polyester is determined with the acid value in combination with the hydroxyl value. Therefore these standard methods were performed.

The acid value was determined to monitor the reaction progress during synthesis of the polyesters. So the unreacted acid groups in the reaction mixture could be specified in mgKOH/g with a titration of the samples, by a base. To indicate the progress of titration, phenolphthalein was used to determine the neutralization point. Also a blank value was determined to avoid inaccuracy during acid value calculation. This blank value was later subtracted from the measured value of the sample. At first the titer concentration was determined to further calculate the acid values. The titer was a 0.1 N potassium hydroxide solution in methanol and the acid used, to evaluate the real concentration of the titer, was potassium hydrogen phthalate.

The sample masses, the consumption of base, the resulting acid value (AV) and the conversion are shown over time in Table 7 exemplary for one glutaric acid-based polyester and in Table 8 for an  $\alpha$ -ketoglutaric acid-based polyester.

*Table 7: Acid value determination for POLYESTER-1 (1 mL aliquot) in toluene; blank value of 0.008 ml (0.1649 mol/l KOH)*

reaction time [h]	KOH [ml]	m <sub>sample</sub> [mg]	AV [mgKOH/g]	conversion [%]
<b>1</b>	2.934	335.1	80.8	81.9
<b>2</b>	1.614	335.1	44.3	90.1
<b>23</b>	0.140	335.1	3.6	99.2
<b>26</b>	0.104	335.1	2.7	99.4
<b>44</b>	0.042	335.1	0.9	99.8
<b>46</b>	0.032	335.1	0.7	99.9

Table 8: Acid value determination for POLYESTER-12 in toluene and a blank value of 0.008 ml (0.16488 mol/l KOH)

reaction time [h]	KOH [ml]	m <sub>sample</sub> [mg]	AV [mgKOH/g]	conversion [%]
<b>0.5</b>	0.288	11.8	191.3	54.8
<b>2</b>	3.432	342.3	91.6	78.4
<b>20</b>	2.348	342.3	62.3	85.3
<b>23</b>	2.364	260.5	83.7	80.2

Also the distilled and pure dimethylester of the  $\alpha$ -ketoglutaric acid was tested. The data of the di-esters acid value is listed in Table 9. Therefore the acid value was not meaningful, due to the fast cleavage of ester bonds by KOH.

Table 9:  $\alpha$ -Ketoglutaric acid dimethylester AV in toluene and a blank value of 0.008 ml (0.16488 mol/l KOH)

KOH [ml]	m <sub>sample</sub> [mg]	AV [mgKOH/g]
<b>5.534</b>	349.9	146.1
<b>4.902</b>	306.1	147.9

The acid value evaluation worked well for glutaric acid-based polyesters and the conversion could be monitored over the reaction time, but for the  $\alpha$ -ketoglutaric acid ones this approach did not work at all. Values around 100mgKOH/g per sample were determined, even though the polyester synthesis was completed and the molecular weight achieved according to NMR and GPC analysis. The reason was the highly activated keto-acid ester bond, which could be cleaved by the basic titer easily. This change resulted in an increase of titer consumption by the additional acid groups and therefore in a higher acid value. Hence for all  $\alpha$ -ketoglutaric acid-based polyesters the determination of the acid value via titration did not work. The proof of concept delivered a titration of the distilled  $\alpha$ -ketoglutaric acid dimethylester, which also achieved acid values even higher than the polyester products, due to the basic hydrolysis of the ester bond.

### 3.3.2. Hydroxyl Value Determination

To determine the hydroxyl value, and therefore in combination with the acid value the absolute molecular weight  $M_n$ , of the synthesized polyesters, different methods were approached. The hydroxyl value and the acid value were determined at the same time, therefore the knowledge about the very rapid cleavage of the activated keto esters, under alkaline conditions, was not yet present.

### 3.3.2.1. Reaction with Acetic Anhydride and Titration

At first, the classical method for hydroxyl value evaluation, based on the work of Ogg C. L.<sup>54</sup>, was selected (Figure 36). In the first step an acetylation reagent, containing 30 wt% of acetic anhydride and 70 wt% of pyridine, was prepared. Then approximately 1 g of the sample were weighed into a penicillin vial and dissolved in pyridine and the acetylation reagent was added. This mixture was now stirred at 110 °C for 70 min and then quenched with deionized water. Now a phenolphthalein solution was added and the mixture was titrated with 1 N potassium hydroxide solution in methanol from colorless to pink. Two blanks were treated equally and titrated the same way to get the blank value for the hydroxyl value calculations.

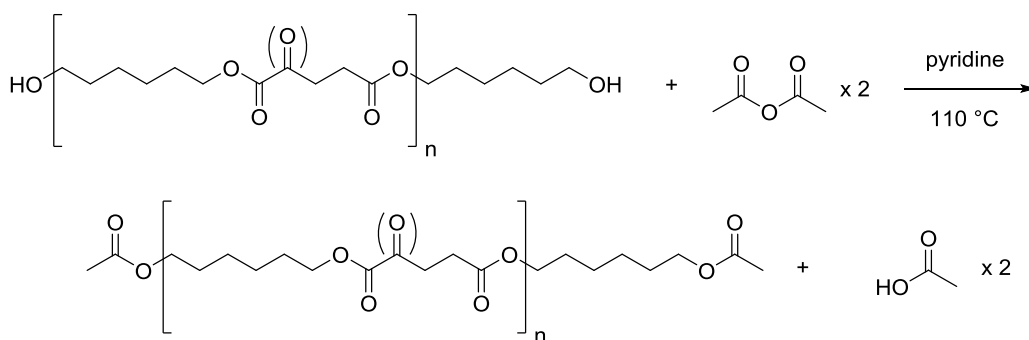


Figure 36: Reaction of a hydroxyl-terminated polyester with acetic anhydride

An example for one  $\alpha$ -ketoglutaric acid and one glutaric acid polyester (Table 10).

Table 10: OHV and corr. OHV value determination of polyesters with a blank value of 20.949 ml (0.8997 mol/l KOH)

sample	KOH [mL]	m <sub>sample</sub> [g]	OHV [mgKOH/g]	AV [mgKOH/g]	corr.OHV [mgKOH/g]
POLYESTER-12_1	-	1.0245	-	-	-
POLYESTER-12_2	-	1.0073	-	-	-
POLYESTER-1_1	20.51	1.0290	21.7	0.7	22.4
POLYESTER-1_2	20.52	1.0080	21.4	0.7	22.1

The main problem during this procedure was a black precipitate forming during the 70 min reaction in pyridine. This problem occurred only in the samples, containing  $\alpha$ -ketoglutaric acid, the other polyester without the keto group was still clear with no solid precipitating. With a black, disperse sample, the titration and the evaluation of the equivalence point were especially hard. Pyridine as a solvent was most likely the main problem of this reaction, due to the experiences during the synthesis of the  $\alpha$ -ketoglutaric acid-based polyesters with amines or other bases, resulting in unwanted side reactions only. Also after calculations were done, the resulting hydroxyl values were all negative, due to the high acid value of the  $\alpha$ -ketoglutaric acid-based polyesters and therefore not usable for the evaluation of the molecular weight.

### 3.3.2.2. Reaction with Acetic Acid and Titration

The second method to determine the hydroxyl value of the polyesters was the acid catalyzed esterification of the terminal hydroxyl groups with acetic acid (Figure 37). This procedure renounced amines like pyridine during the reaction process and was therefore considered as a better method for the  $\alpha$ -ketoglutaric acid-based polyesters based on the book Polymer Synthesis<sup>46</sup>. Basically 1 g of sample was weight into a penicillin vial and dissolved in distilled acetone, following with the addition of a 1.14% solution of para-toluolsulfonic acid in a mixture of 10 vol% acetic acid and 90 vol% ethyl acetate. This mixture was stirred at 50 °C for 45 min and quenched with a mixture of 60 vol% pyridine and 40 vol% deionized water. The sample was titrated with the 1 N potassium hydroxide solution in methanol from colorless to pink, using phenolphthalein solution as an indicator. A blank was treated equally and after the procedure titrated too.

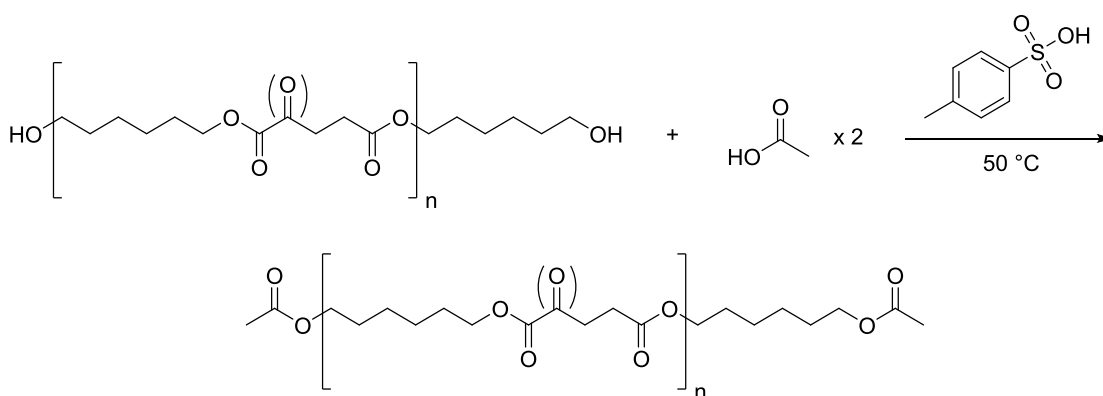


Figure 37: Acid catalyzed reaction of a hydroxyl-terminated polyester with acetic acid

An example for an  $\alpha$ -ketoglutaric acid-based polyester is shown in Table 11.

Table 11: OHV and corr. OHV value determination of one polyester with a blank value of 20.584 ml (0.8997 mol/l KOH)

sample	KOH [mL]	m <sub>sample</sub> [g]	OHV [mgKOH/g]	AV [mgKOH/g]	corr.OHV [mgKOH/g]
POLYESTER-12_1	24.02	1.0062	-172.5	-	-
POLYESTER-12_2	22.43	0.6075	-153.0	-	-

This method of hydroxyl value determination used pyridine only to quench the solution after the reaction had taken place in the vial. So this time no black precipitate formed during the heating of the polyester in the solvent, which seem to be an improvement for titration. But the volume of potassium hydroxide solution was greater for the blank as it was for the sample containing the  $\alpha$ -ketoglutaric acid-based polyester, which meant this method lead to other problems occurring, because it should be the other way round, due to the consumption of acetic acid by the terminal hydroxyl groups of the sample and therefore a lower volume of titer needed. This effect can be explained again via the fact, that the base cleaves the ester bonds next to the keto-acid, resulting in more acidic behavior of the sample. The moderate temperature of this reaction should not allow many transesterification reactions, but still there is para-toluolsulfonic acid and a polyester present and transesterifications cannot be

avoided completely, leading also to an increased consumption of titer. Overall, this method also did not work for the  $\alpha$ -ketoglutaric acid polyesters.

### 3.3.3. Gel Permeation Chromatography

The usually low error and straight forward to use methods, like the acid and hydroxyl value determination, did not work the  $\alpha$ -ketoglutaric acid based polyesters. Therefore GPC was focused next. To get an approximate value of the molecular weight of each polyester, a size exclusion chromatography was performed. The expected molecular weights could now be compared to the absolute values of  $M_n$ . The molecular weights of the synthesized polyesters were firstly determined by gel permeation chromatography (GPC). Two different methods were used to characterize the polymers. At first the conventional method was used. It used a refraction index detector to compare the polymers molecular weight compared to a flow marker and a set of already known molecular weight styrene polymers as standards, therefore was a relative method only. The second method used triple detection (refractive, viscosity and light scattering detector) to determine the absolute molecular weight of the polymer. Both methods delivered an  $M_w$  value and with the poly dispersity index (PDI),  $M_n$  was calculated. In Table 12 to Table 15 all results for the different types of polyesters can be found.

For the  $\alpha$ -ketoglutaric acid and hexanediol-based polyesters (Table 12) the GPC measurement provided an absolute  $M_w$  value via triple detection, which correlates not too bad to the relative value, resulted by the conventional calibration method. If the PDI was included to calculate the molecular weight, the values of the two different methods fit even better together, represented in the  $M_n$  value. Overall the conventional methods tended to higher molecular weights for this polymers.

Table 12: GPC measurement data for the conventional and triple detection method for  $\alpha$ -ketoglutaric acid hexanediol-based polyesters

Sample	Method	$M_n$ [g/mol]	$M_w$ [g/mol]	PDI
<b>POLYESTER-13</b>	conventional	5400	12700	2.37
	triple detection	2500	8100	3.20
<b>POLYESTER-9</b>	conventional	4800	11000	2.28
	triple detection	3200	9400	2.96
<b>POLYESTER-10</b>	conventional	7600	18100	2.38
	triple detection	5700	13800	2.41
<b>POLYESTER-8</b>	conventional	9900	23200	2.34
	triple detection	9900	29200	2.96
<b>POLYESTER-11</b>	conventional	6500	14600	2.24
	triple detection	6600	12200	1.84
<b>POLYESTER-12</b>	conventional	5300	11300	2.11
	triple detection	4700	10900	2.31

The glutaric acid and hexanediol-based polyesters (Table 13) were analyzed via both methods too. In this case the difference between conventional and triple detection method increased



in terms of the  $M_w$  value. After considering the PDI, the  $M_n$  values approach each other of both different evaluations. The same effect as for the  $\alpha$ -ketoglutaric acid was present, the conventional method resulted in higher molecular weight values.

Table 13: GPC measurement data for the conventional and triple detection method for glutaric acid hexanediol-based polyesters

Sample	Method	$M_n$ [g/mol]	$M_w$ [g/mol]	PDI
<b>POLYESTER-1</b>	conventional	14600	30000	2.05
	triple detection	8100	16500	2.03
<b>POLYESTER-2</b>	conventional	4600	8700	1.89
	triple detection	3000	5900	1.96
<b>POLYESTER-3</b>	conventional	7200	16000	2.23
	triple detection	5100	9500	1.88
<b>POLYESTER-4</b>	conventional	13600	28400	2.09
	triple detection	9500	19500	2.05

Triple detection did not work as a determination of the molecular weight for the  $\alpha$ -ketoglutaric acid and isosorbide-based polyesters (Table 14). The molecular weight and therefore the signal of the light scattering unit was too low for this evaluation method, due to the too low  $\frac{dn}{dc}$ . This value is unique for every polymer, and that explains why all isosorbide-based polyesters could not be evaluated with the triple detection method. So the conventional method only could be considered for these polymers.

Table 14: GPC measurement data for the conventional method for  $\alpha$ -ketoglutaric acid isosorbide-based polyesters

Sample	Method	$M_n$ [g/mol]	$M_w$ [g/mol]	PDI
<b>POLYESTER-14</b>	conventional	1200	1700	1.40
<b>POLYESTER-15</b>	conventional	1200	1600	1.44
<b>POLYESTER-16</b>	conventional	1000	1400	1.43
<b>POLYESTER-14A</b>	conventional	1100	1600	1.48
<b>POLYESTER-17</b>	conventional	1000	1400	1.42
<b>POLYESTER-16A</b>	conventional	1100	1500	1.40

Table 15 includes the glutaric acid and isosorbide-based polyesters. The same evaluation problem, as with the  $\alpha$ -ketoglutaric acid ones, occurred. Due to the low  $\frac{dn}{dc}$ , only the conventional method could be used for molecular weight calculation.

Table 15: GPC measurement data for the conventional method for glutaric acid isosorbide-based polyesters

Sample	Method	$M_n$ [g/mol]	$M_w$ [g/mol]	PDI
<b>POLYESTER-5</b>	conventional	6500	13100	2.02
<b>POLYESTER-6</b>	conventional	5300	10600	1.99
<b>POLYESTER-7</b>	conventional	2200	4300	2.00

Overall, the GPC results alone were not able to determine the molecular weight of the various products. The expected molecular weights differed clearly from the measured ones, therefore another method is necessary to evaluate the  $M_n$ . The expected molecular weight can be found in 3.1 and 3.2.

### 3.3.4. $^1\text{H-NMR}$ Determination

The GPC evaluation had shown molecular weights of the different polyesters as relative and absolute values. To support these results, NMR of all polymers was measured. Every synthesized polyester had a defined endgroup or repeating unit in the NMR spectra. For example this could be a double bond. After integration of these specific endgroup signals, the ratio between the endgroups integral value and the value of integrals of the residual peaks in the spectrum was an indicator for the average degree of polymerization and molecular weight of the polyester.

For the polyesters with hydroxyl endgroups, there was a significant shift in the NMR spectrum of the  $\text{CH}_2$  next to the hydroxyl group. By integration of this signal and referring it to the other  $\text{CH}_2$  signals without the nearby OH-group an average molecular weight and degree of polymerization could be calculated.

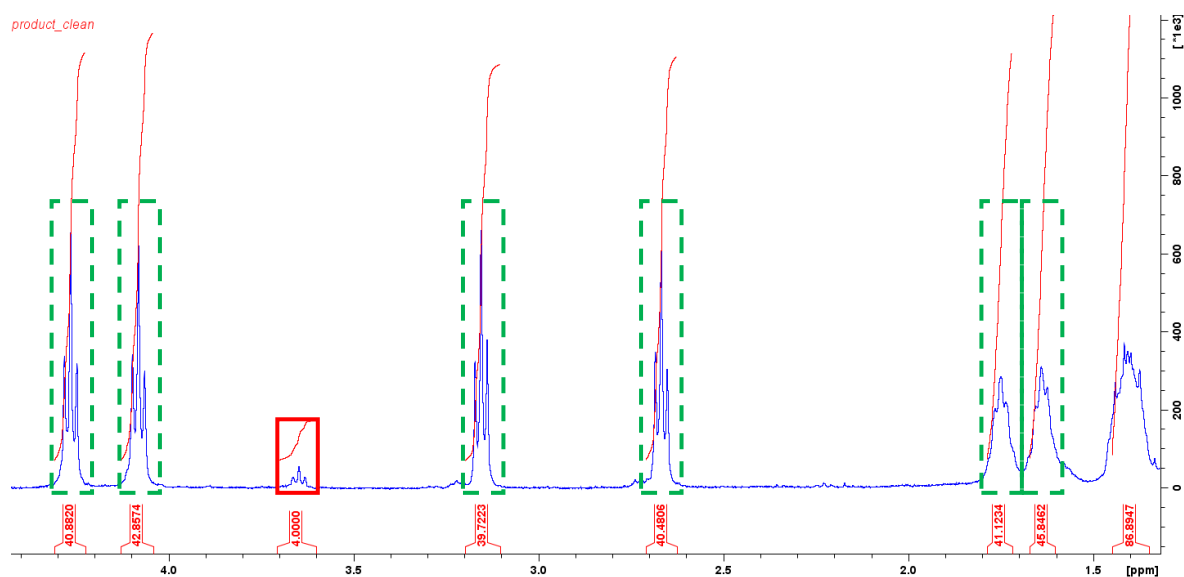


Figure 38: Integration of the signals in the 400 MHz NMR spectrum of product POLYESTER-12 ( $\alpha$ -ketoglutaric acid hexanediol polyester) (solid, red frame:  $\text{CH}_2$  with nearby OH-group; dashed, green frame:  $\text{CH}_2$ 's of the polyester without OH-group nearby)

In Figure 38 the ratio between the signals ( $\text{CH}_2$  groups without and with nearby hydroxyl endgroup) was 41:4. Therefore, the average  $\alpha$ -ketoglutaric acid hexanediol polyester molecule had 20.5 repeating units with hydroxyl groups on both ends.

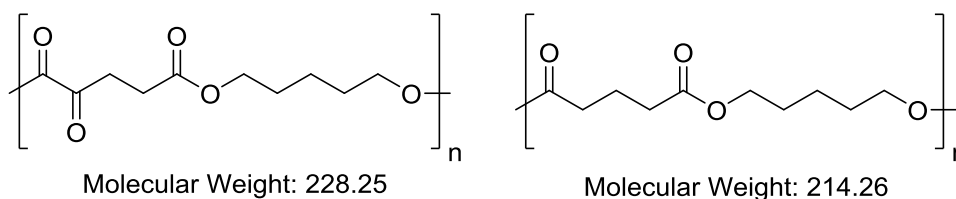


Figure 39: Repeating units' molecular weight for the 2 types of polyesters with hexanediol

The average degree of polymerization was 20.5, and therefore for an  $\alpha$ -ketoglutaric acid hexanediol polyester, with a repeating unit molecular weight, which can be taken from Figure 39, the calculated  $M_n$  would be 4700 g/mol, which actually fit very well to the molecular weight, the GPC analysis evaluated. The error of this method by choosing the average value of all CH<sub>2</sub> integrals was less than 5%. Calculated with the lowest value alone the result was 4530 g/mol and for the highest integral value 4890 g/mol. Similar errors were achieved with the 14000 g/mol polyesters.

The analogous procedure was done for all hexanediol-based polyesters (Figure 40), and their molecular weights are shown in Table 16.

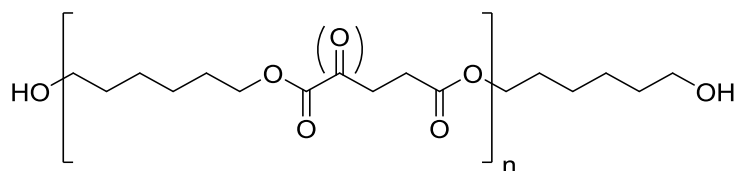


Figure 40: ( $\alpha$ -Keto)glutaric acid and hexanediol polyester

Table 16:  $M_n$ , determined via NMR

Polyester	Sample	$M_n$ [g/mol] via NMR
<b><math>\alpha</math>-Ketoglutaric Acid</b>	POLYESTER-13	3500
	POLYESTER-9	3000
	POLYESTER-10	6500
	POLYESTER-8	13800
	POLYESTER-11	4600
	POLYESTER-12	5000
<b>Glutaric Acid</b>	POLYESTER-1	7000
	POLYESTER-2	3200
	POLYESTER-3	6400
	POLYESTER-4	14000

The same determination was carried out with the  $\alpha$ -ketoglutaric acid isosorbide-based polyesters, due to the different chemical shift of the CH next to a terminal hydroxyl group in the spectrum. It was not as accurate, as for the hexanediol-based polymers, due to the absence of more than one CH<sub>2</sub>, which was baseline separated and none overlapping with other peaks.

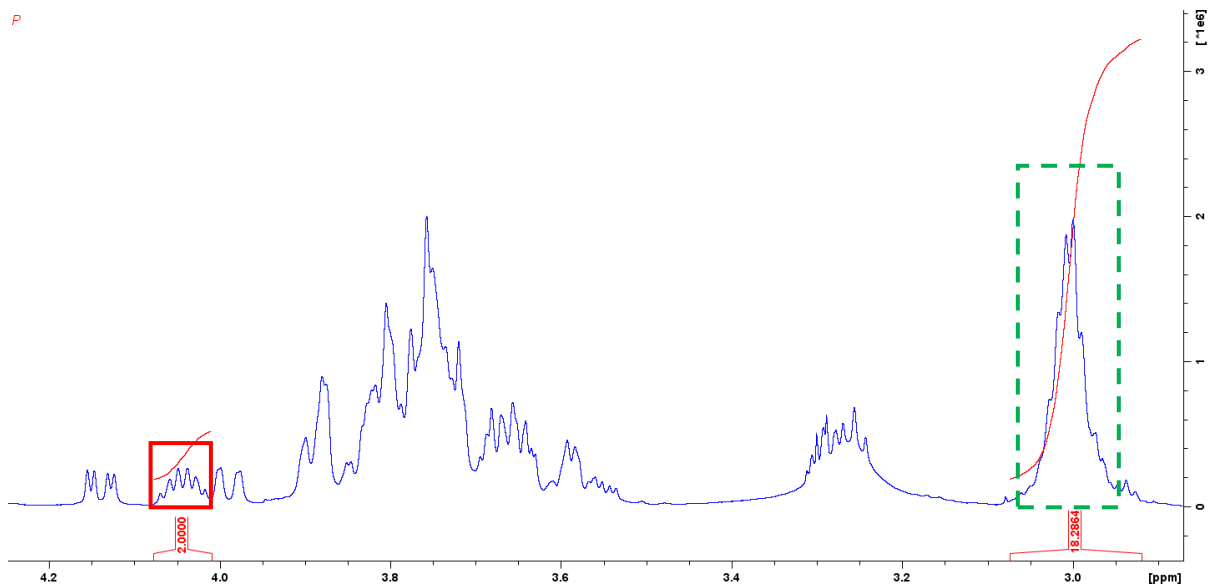


Figure 41: Integration of the signals in the 600 MHz NMR spectrum of product POLYESTER-14 ( $\alpha$ -ketoglutaric acid isosorbide polyester) (solid, red line: CH with nearby OH-group; dashed, green line: CH<sub>2</sub>'s of the polyester without OH-group nearby)

In Figure 41 the ratio between the signals (CH<sub>2</sub> groups without a nearby hydroxyl group and the CH next to the hydroxyl endgroup) is 18:2. So the average degree of polymerization is 9 units.

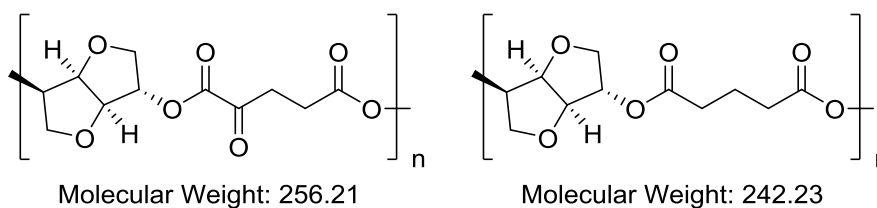


Figure 42: Repeating units' molecular weight for the 4 types of polyesters

The average degree of polymerization was 9 and therefore for an  $\alpha$ -ketoglutaric acid isosorbide polyester, with a repeating unit molecular weight, which could be taken from Figure 42, the calculated  $M_n$  would be 2300 g/mol, which did not fit to the molecular weight, the GPC analysis resulted.

The analogous procedure was done for all isosorbide-based polyesters (Figure 43) illustrated in Table 17.

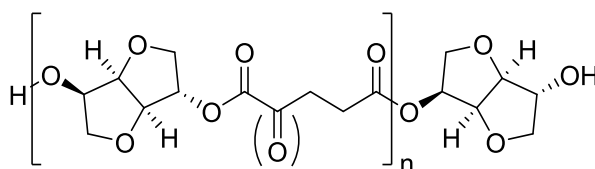


Figure 43: ( $\alpha$ -Keto)glutaric acid and isosorbide polyester

Table 17:  $M_n$ , determined via NMR

Polyester	Sample	$M_n$ [g/mol] via NMR
$\alpha$ -Ketoglutaric Acid	POLYESTER-14	2500
	POLYESTER-15	2300
	POLYESTER-16	2100
	POLYESTER-14A	2200
	POLYESTER-17	2100
	POLYESTER-16A	2200
Glutaric Acid	POLYESTER-5	7000
	POLYESTER-6	5000
	POLYESTER-7	2700

### 3.3.5. $^{31}\text{P}$ -NMR Determination

According to the research work of Pu Y. Q.<sup>55</sup>, a new method of determining the hydroxyl values for lignin-based molecules was established. In the paper they used an additional relaxation reagent based on chromium, which increased the relaxation speed of the molecules during the measurement. Due to the complexity of Lignin compared to the polyester systems in this case, it was assumed no additional reagent was necessary. Therefore a quantitatively  $^{31}\text{P}$ -NMR analysis was tried without the use of chromium(III)-acetylacetonate. For this determination of the hydroxyl value only 30-50 mg of sample are required, which were dissolved in absolute DMF. Then 1/10 of the samples weight as an internal standard (N-hydroxy-5-norbornene-2,3-dicarboximide) were added, to quantitatively evaluate the hydroxyl portion in the NMR spectrum, and the reactant, 2-chloro-1,3,2-dioxaphospholane, were added. In the end, deuterated chloroform and absolute pyridine, to neutralize the formed HCl, were added and the mixture was stirred for 10 minutes at room temperature, followed by an immediate NMR measurement. The reaction equation is shown in Figure 44.

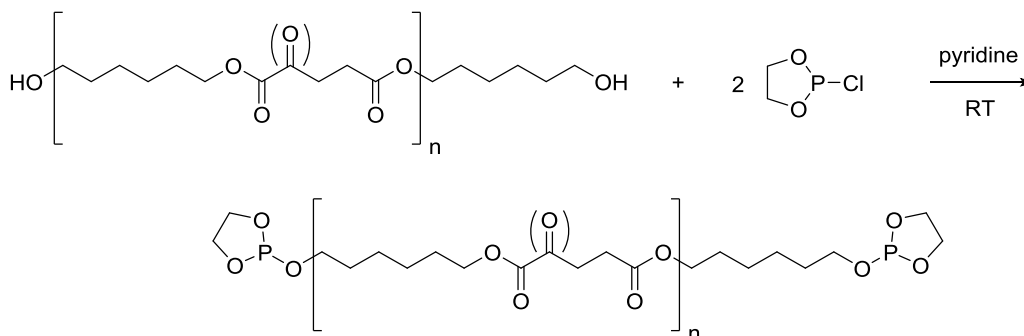


Figure 44: Reaction of a hydroxyl-terminated polyester with 2-Chloro-1,3,2-dioxaphospholane

This hydroxyl value determination was also not successful for  $\alpha$ -ketoglutaric acid-based polyesters, the reference system, poly-THF, with a known  $M_n$  of 2900 g/mol and other smaller molecules like hexanediol or  $\alpha$ -ketoglutaric acid. Advantageous for this method is the reaction of the phosphorous reactant with carboxylic groups in the polyester. Therefore capable of

determine the absolute number of endgroups like the isocyanate approach. As illustrated in Figure 45, the aliphatic hydroxyl groups were integrated and compared to the integral of the internal standard, resulting in the  $J_{\text{sample}}$  value for further calculations.

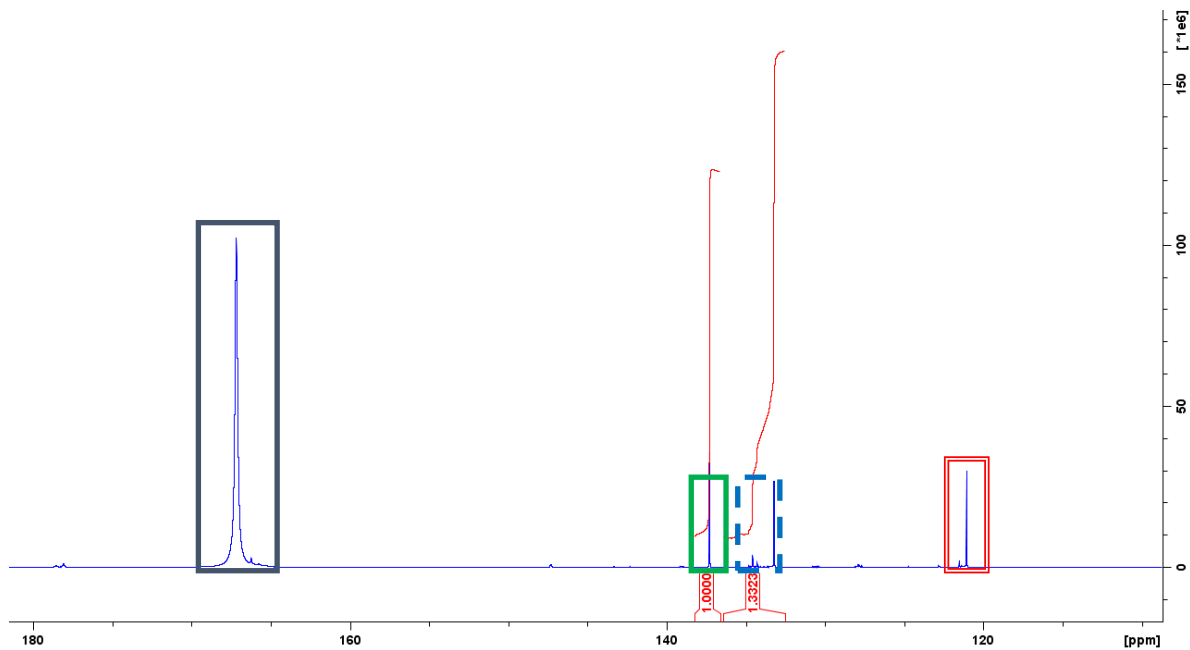


Figure 45: Evaluation of the integrals ( $J_{\text{sample}}$ ) of poly-THF-2900 in the  $^{31}\text{P}$ -NMR; huge, grey edged peak on the left is unreacted 2-Chloro-1,3,2-dioxaphospholane; green edged peak is the internal standard, N-Hydroxy-5-norbornene-2,3-dicarboximide; blue edged and dashed peak are aliphatic hydroxyl groups of the poly-THF-2900; red double edged peak on the right is hydrolyzed 2-Chloro-1,3,2-dioxaphospholane

The hydroxyl values were calculated via Equation 2.

Equation 2: Calculation of the hydroxyl value<sup>55</sup>

$$OHV \left[ \frac{\text{mmol}}{\text{g}} \right] = \frac{m_{IS} * J_{\text{sample}}}{M_{IS} * m_{\text{sample}}}$$

$m_{IS}$  ... mass of the internal standard [g]

$J_{\text{sample}}$  ... sum of the hydroxyl group correlating integrals in the  $^{31}\text{P}$ -NMR spectrum [ ]

$M_{IS}$  ... molecular weight of the internal standard [g/mol]

$m_{\text{sample}}$  ... mass of the sample [g]

The hydroxyl value was further used to evaluate the molecular weight of the tested substances in Equation 3.

Equation 3: Calculation of the molecular weight

$$M_n \left[ \frac{\text{g}}{\text{mol}} \right] = \frac{z * 1000}{OHV}$$

$z$  ... number of hydroxyl endgroups in the molecule [ ]

OHV ... hydroxyl value [mmol/g]

The method worked for the smaller molecules surprisingly better, due to the tremendously increased number of groups which have to be reacted, than for the  $\alpha$ -ketoglutaric acid-based

polyesters, but still with a deviation of 4-28%. For the polyester-based samples, the molecular weight was off with the factor of 3, which was worse than the accuracy of NMR, GPC or isocyanate endgroup determination. With glutaric acid an experiment was executed, to obtain the influence of waiting time until the sample was measured. For glutaric acid, the deviation increased over time. Results are shown in Table 18.

Table 18: Theoretical molecular weights of small molecules and one polyester compared to the measured molecular weight including deviations

Sample	M <sub>n</sub> theory [g/mol]	M <sub>n</sub> measured [g/mol]	Deviation [%]
<b>α-Ketoglutaric acid</b>	146.11	158.02	7
<b>1,6-Hexanediol</b>	118.18	151.3	28
<b>Isosorbide</b>	146.14	118.57	19
<b>Poly-THF-2900</b>	2900	2683	8
<b>Glutaric acid 0min</b>	132.12	127.02	4
<b>Glutaric acid 30min</b>	132.12	113.14	14
<b>POLYESTER-12</b>	4900 (NMR)	1830	268

Later studies had shown, that the missing of the relaxation agent, chromium(III)-acetylacetonate, leads to significant increases of the deviation. And the higher the molecular weight and more complex the molecules were, the more a relaxation agent was needed. Eventually the phosphorous NMR evaluations of the molecular weight were not further improved for the polyesters, due to three other accurate methods established for them. Also the immediate measurements of these samples and an increased inaccuracy, if 30 min or more were waited till the NMR spectrum was recorded.

### 3.3.6. Reaction with Phenyl Isocyanate and Titration

To support the GPC and NMR values for the molecular weight, a last method to determine the hydroxyl value via titration was the conversion of terminal hydroxyl groups with an isocyanate, followed by titration (Figure 46). At first the titer, a 0.1 N hydrochloric acid solution in deionized water, was established and the real concentration determined titrating a known concentration sodium carbonate solution.

This concept was based on the work of Reed D. H.,<sup>56</sup> who reacted polyoxyalkylenes with isocyanates, by weighing in approximately 0.3 g of sample into a penicillin vial and dissolving it in DMF. Then a 1 N solution of phenyl isocyanate and dibutyltin dilaurate, as a catalyst for isocyanate additions to hydroxyl groups, were added. The reaction time was set to 40 minutes at 98 °C and after that, a 2 N solution of dibutylamine was added to quench the reaction and being able to titrate it. After 15 minutes of waiting time, isopropanol was added to ensure solubility of the formed salts during titration with 0.1 N hydrochloric acid, from blue to green to a yellow end point, using bromocresol green as an indicator. Two blanks were treated equally.

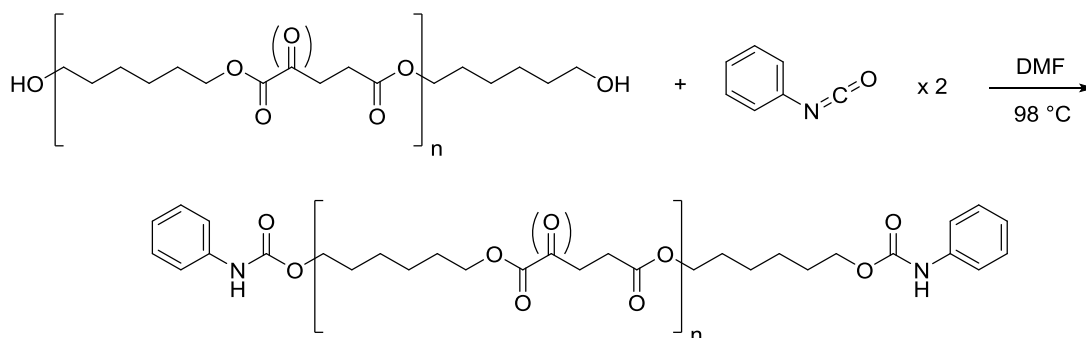


Figure 46: Reaction of a hydroxyl-terminated polyester with phenyl isocyanate

This time the  $\alpha$ -ketoglutaric acid-based polyesters and a sample with a known molecular weight, poly-THF with a  $M_n$  of 2900 g/mol, were used to test, if this method works for our system. The advantage of this endgroup determination was, that there was no need for an acid value for the molecular weight calculation, due to the reaction of isocyanates with terminal acid groups too.<sup>57</sup> So the total amount of endgroups in the polyester could be calculated via Equation 4.

Equation 4: Calculation of the NCO value for endgroup determination<sup>56</sup>

$$NCO [\%] = \frac{(V_{acid} - V_{blank}) * C_{titer} * M_{NCO}}{m_{sample}} * 100$$

$V_{acid}$  ... volume used of hydrochloric acid solution in deionized water for the sample [L]

$V_{blank}$  ... volume used of hydrochloric acid solution in deionized water for the blank value [L]

$C_{titer}$  ... concentration of the titer [mol/L]

$M_{NCO}$  ... molecular weight of one isocyanate group [g/mol]

$m_{sample}$  ... mass of sample used [mg]

This value evaluated the percentage of isocyanate groups in the polymer, based on the molecular weight. So the molecular weight was determined via Equation 5.

Equation 5: Calculation of the molecular weight of the polymers

$$M_n \left[ \frac{g}{mol} \right] = \frac{M_{NCO} * z * 100}{NCO}$$

$M_{NCO}$  ... molecular weight of one isocyanate group [g/mol]

$z$  ... number of isocyanate endgroups in the molecule [ ]

$NCO$  ... isocyanate value [%]

Overall this method delivered accurate results, fit well together with the determination of the molecular weight via NMR and was also not too far away from the GPC measurements, for our purpose. So this evaluation was proven to work for polyesters too. Due to the simplicity of proton NMR and the well matching data (Table 19) with the isocyanate endgroup determination, NMR was selected to be the main analysis tool for our molecular weight determinations, in combination with GPC.



Table 19:  $M_n$ , determined via NMR and  $M_n$ , calculated via GPC triple detection for comparison (calculated average molecular weight for POLYESTER-12: 4850 g/mol (GPC and NMR); theoretical molecular weight for polyTHF2900: 2900 g/mol)

Sample	$M_n$ [g/mol] via GPC	$M_n$ [g/mol] via NMR	$M_n$ [g/mol] via Phenyl isocyanate
POLYESTER-12	4700	4900	5000
Poly-THF 2900	-	2900	2800

### 3.4. Selecting the Set of Macromolecular Photoinitiators

To get a set of comparable polyesters based on ( $\alpha$ -keto)glutaric acid and hexanediol, similar molecular weights had to be selected. After the various molecular weight determinations, only GPC and NMR analysis were reasonable. Therefore the sets could be compiled. Underlined products were taken for further modification of the hydroxyl endgroups (Table 20).

Table 20:  $M_n$ , determined via NMR and  $M_n$ , calculated via GPC triple detection for comparison of the hexanediol polyesters

Polyester	Sample	$M_n$ [g/mol] via GPC	$M_n$ [g/mol] via NMR
$\alpha$ -Ketoglutaric Acid	POLYESTER-13	2500	3500
	<u>POLYESTER-9</u>	<u>3200</u>	<u>3000</u>
	POLYESTER-10	5700	6500
	<u>POLYESTER-8</u>	<u>9900</u>	<u>13800</u>
	POLYESTER-11	6600	4600
	<u>POLYESTER-12</u>	<u>4700</u>	<u>5000</u>
Glutaric Acid	POLYESTER-1	8100	7000
	<u>POLYESTER-2</u>	<u>3000</u>	<u>3200</u>
	<u>POLYESTER-3</u>	<u>5100</u>	<u>6400</u>
	<u>POLYESTER-4</u>	<u>13600</u>	<u>14000</u>

The analogous procedure was done for all ( $\alpha$ -keto)glutaric acid and isosorbide-based polyesters. Underlined products were taken for further modification (Table 21).

Table 21:  $M_n$ , determined via NMR and  $M_n$ , calculated via GPC conventional method for comparison of the isosorbide polyesters

Polyester	Sample	$M_n$ [g/mol] via GPC	$M_n$ [g/mol] via NMR
$\alpha$ -Ketoglutaric Acid	POLYESTER-14	1200	2500
	<u>POLYESTER-15</u>	<u>1200</u>	<u>2300</u>
	POLYESTER-16	1000	2100
	POLYESTER-14A	1100	2200
	POLYESTER-17	1000	2100
	POLYESTER-16A	1100	2200
Glutaric Acid	POLYESTER-5	6500	7000
	POLYESTER-6	5300	5000
	<u>POLYESTER-7</u>	<u>2200</u>	<u>2700</u>

Now the sequential numbers of the selected polyester products were transformed into more reasonable names for further reactivity and mechanical tests. Also the endgroup modified polyesters were named equally to their starting polyesters, with the exception of an additional “M” at the end of the description. The average molecular weight was calculated with the GPC and NMR data. Started with the ( $\alpha$ -keto)glutaric acid and hexanediol-based polymers (Figure 56), shown in Table 22.

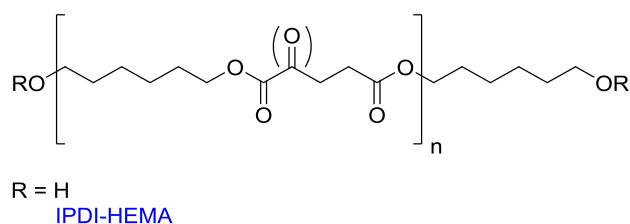


Figure 47: ( $\alpha$ -Keto)glutaric acid and hexanediol polyester with hydroxyl endgroups (with IPDI-HEMA endgroups)

Table 22: Transformation of the sequential, numeric names of the ( $\alpha$ -Keto)glutaric acid and hexanediol polyesters; *M* is the IPDI-HEMA endgroup modified version

Sequential Name	Average $M_n$ [g/mol]	New Description
POLYESTER-9	3100	PolyHDKGA_3000M
POLYESTER-12	4850	PolyHDKGA_5000M
POLYESTER-8	11850	PolyHDKGA_14000M
POLYESTER-2	3100	PolyHDGA_3000M
POLYESTER-3	5750	PolyHDGA_5000M
POLYESTER-4	13800	PolyHDGA_14000M

Analogous, the sequential numbers and their resulting names for later analysis of the selected polyester products, based on ( $\alpha$ -keto)glutaric acid and isosorbide (Figure 57), are listed in Table 29.

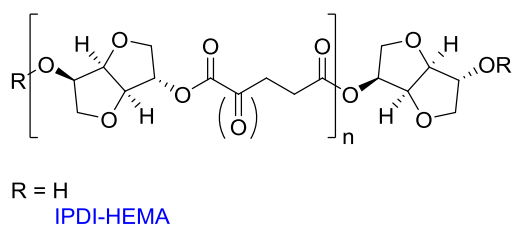


Figure 48: ( $\alpha$ -Keto)glutaric acid and isosorbide polyester with hydroxyl endgroups (with IPDI-HEMA endgroups)

Table 23: Transformation of the sequential, numeric names of the ( $\alpha$ -Keto)glutaric acid and isosorbide polyesters; *M* is the IPDI-HEMA endgroup modified version

Sequential Name	Average $M_n$ [g/mol]	New Description
POLYESTER-15	1750	PolyISOKGAM
POLYESTER-7	2450	PolyISOGAM

## 4. Synthesis of Macromolecular, Polymerizable Photoinitiators

Hydroxyl-terminated polyesters, synthesized in three different molecular weights, were used as starting material for the modifications with crosslinkable moieties. The (meth)acrylates on both ends of the polyester chain could be covalently integrated into the polymer network during UV-curing. Although the starting polyester is prevented from migrating, due to its molecular weight, the functionalization of the endgroups should achieve even better results in further leaching tests, compared to polyesters without these (meth)acrylates. Furthermore the mechanical properties should be improved compared to the reference system with the glutaric acid building blocks. And no softening effect should be obtained with the  $\alpha$ -ketoglutaric acid-based and modified polyesters.

### 4.1. $\alpha$ -Ketoglutaric Acid Hexanediol Polyester with 2-IEM Endgroup [PolyHDKGA-m]

To achieve a polyester with crosslinkable moieties, a test reaction with a commercially available isocyanate and a hydroxyl-terminated polyester was performed. Such a macromolecular compound is illustrated in Figure 49. The idea of using the dibutyltin dilaurate catalyst at room temperature was based on the work of Muller I. A.<sup>58</sup> The resulting polyester can copolymerize into the polymer network during curing with the methacrylate groups. Therefore it is a non migratable, self-initiating macro monomer.

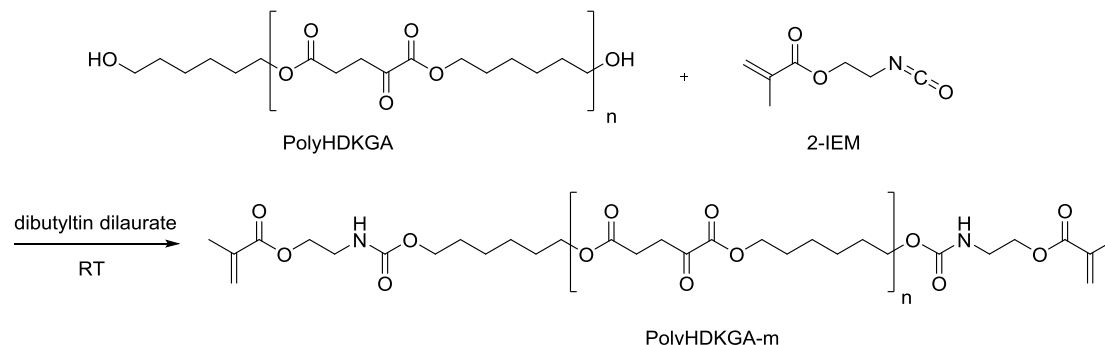


Figure 49: Catalyzed reaction of a primary isocyanate and a primary alcohol

At first the polyesters molecular weight was determined by GPC and hydroxyl group determination via NMR. A  $M_n$  of 4900 g/mol was taken to further calculate the amount of 2-isocyanatoethyl methacrylate (2-IEM).

To achieve the PolyHDKGA-m, 1 eq. of the polyester, 2 drops of dibutyltin dilaurate and absolute toluene were added. Then 2.05 eq. of the 2-isocyanatoethyl methacrylate were added dropwise to the reaction mixture. The mixture was stirred for 14 h and then quenched with methanol. Distilled acetone was added and the polyester was precipitated in cold diethyl ether. The white polymer product was dried in vacuum with a resulting yield 34%.

Endgroup modification of the hexanediol and  $\alpha$ -ketoglutaric acid polyester with 2-isocyanatoethyl methacrylate was a success, analyzed by NMR.

This 2-isocyanatomethyl methacrylate reactant is very expensive and therefore the polyester synthesis would not be economically profitable. Nevertheless, for the first modification test of the hydroxyl endgroups it was a proof of concept. For further modifications a new, more scalable endgroup had to be designed.

## 4.2. Synthesis of Polyesters with the IPDI-HEMA Endgroup

### 4.2.1. Synthesis of the IPDI-HEMA Endgroup [IPDI-HEMA]

To covalently bind the polymer chains into the cured network via crosslinking, polymerizable endgroups had to be attached to the polyester endgroups. All previous polyester synthesis were aimed to have hydroxyl endgroups, which could be easily modified via addition of an isocyanate. The commercially available educts, 2-hydroxyethylmethacrylate and isophorone diisocyanate, were combined to form a polymerizable endgroup (Figure 50). The synthesis was carried out according to the book *Chemistry and Technology*<sup>59</sup>. The resulting product can be linked to a polyesters hydroxyl groups.

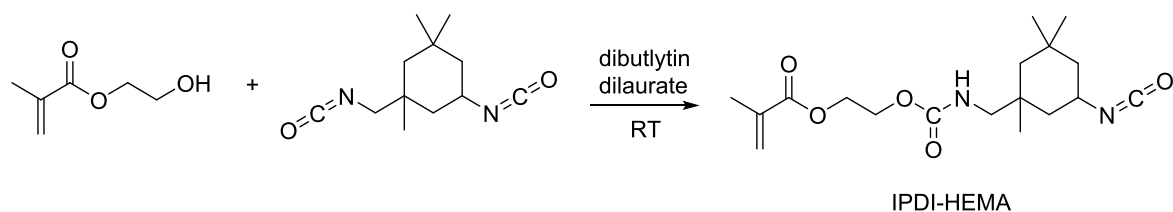


Figure 50: Addition of 2-Hydroxyethylmethacrylate (HEMA) to isophorone diisocyanate (IPDI) using a tin catalyst

To synthesize the IPDI-HEMA endgroup, 1 eq. of isophorone diisocyanate and 1 eq. of 2-hydroxyethyl methacrylate were weighed into a flask and heated. Reaction progress was monitored via ATR-IR spectroscopy and isocyanate value. After 24 h two drops of dibutyltin dilaurate were added to the mixture to access full conversion. The reaction was stirred overnight, while cooling down to room temperature. NCO-value titration indicated 98.3% conversion and a yield of 99% was achieved.

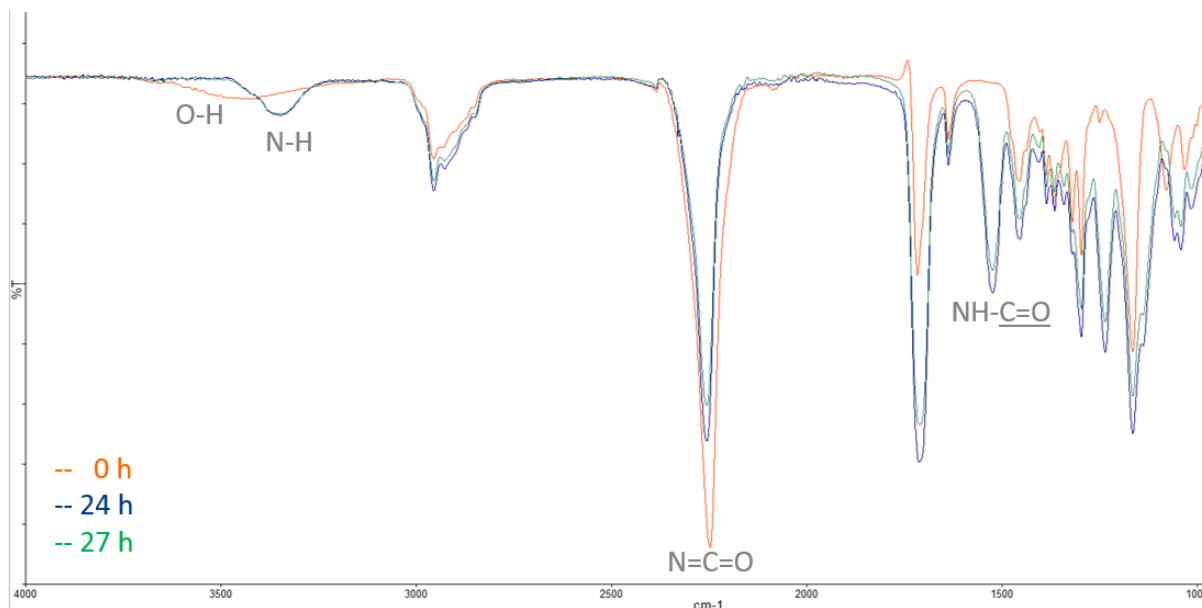


Figure 51: monitoring the IPDI-HEMA synthesis via ATR-IR

During this synthesis no problems occurred and the established product was used to further modify the polyesters. In the ATR-IT spectrum (Figure 51) one can see the conversion of all hydroxyl groups and the increase of the urethane band. Also the N-H band is new formed and the isocyanate band decreases significant.

To evaluate the conversion of the isocyanates during the synthesis of the IPDI-HEMA endgroup, a titration method was used according to the standard method for isocyanate groups in urethane materials or prepolymers<sup>60</sup>. As soon as the conversion hit about 99%, the synthesis was finished and the aimed product can be characterized.

#### 4.2.2. Synthesis of the Polyesters

##### 4.2.2.1. Glutaric Acid-based Polyesters with IPDI-HEMA Endgroup [Poly(HD/ISO)GA-M]

The first modifications were done with the glutaric acid and hexanediol-based polyesters, to access crosslinkable moieties at the ends of the macromolecule. This synthesis was performed based on the work of Muller I. A.<sup>58</sup>, by addition of a secondary isocyanate to a hydroxyl group, forming a urethane structure (Figure 51).

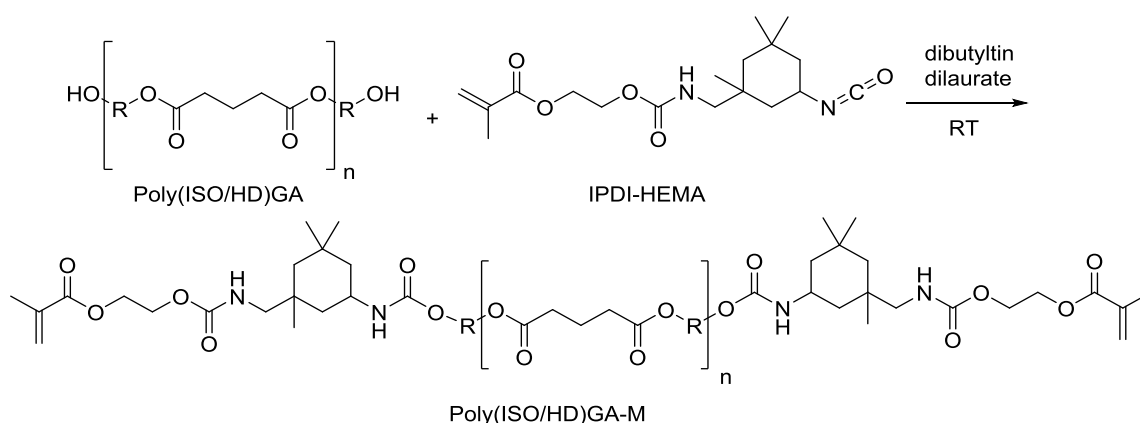


Figure 52: Linking of the IPDI-HEMA endgroup to the glutaric acid hexanediol polyester; R = hexanediol or isosorbide

### Glutaric Acid Hexanediol Polyester with IPDI-HEMA Endgroup [PolyHDGA-M]

At first the polyesters molecular weight was determined by GPC and hydroxyl group determination via NMR, and according to that result, the amount of IPDI-HEMA endgroup was calculated.

To synthesize the PolyHDGA-M, 1 eq. of the polyester and 2.20 eq. of the isocyanate endgroup, dibutyltin dilaurate and absolute dichloromethane were added into a flask with a magnetic stir bar. NMR and ATR-IR was selected to determine complete conversion of the IPDI-HEMA endgroup. The mixture was stirred for 24 h at room temperature under argon and finally the solvent was evaporated at the rotary evaporator. Then the residue was stirred overnight in petrol ether to remove the excess of the isocyanate endgroup and the tin catalyst. Afterwards the petrol ether was removed via decantation and the white polymer products were dried in vacuum with resulting yields of 81% to 99% of white, viscous or solid, depending on the molecular weight, polyesters.

Table 24:  $M_n$  of all products, determined via NMR and GPC and resulting yields

Product	$M_n$ [g/mol] GPC of educt polyester	$M_n$ [g/mol] NMR of educt polyester	Yield [%]
<b>POLYESTER-2-1</b>	3000	3200	81 (viscous)
<b>POLYESTER-3-1</b>	5100	6400	90 (viscous)
<b>POLYESTER-4-1</b>	9500	14000	99 (solid)

The deviation of the two different molecular weight determinations of the educt polyesters is significant. The GPC had shown lower molecular weight than the NMR predicted. To be on the safe side, the lower value of the two results was taken to calculate the amount of isocyanate endgroup needed. Also a 10 mol% excess per hydroxyl group of the IPDI-HEMA endgroup was taken to provide a complete conversion.

After the 24 h of reaction time, a proton NMR of the product was measured and the increase of both NH peaks from the initial value of one, to two was observed and therefore the reaction stopped. Also the ATR-IR had shown complete conversion, due the isocyanate peak decreased in intensity. The spectra are shown in Figure 53.

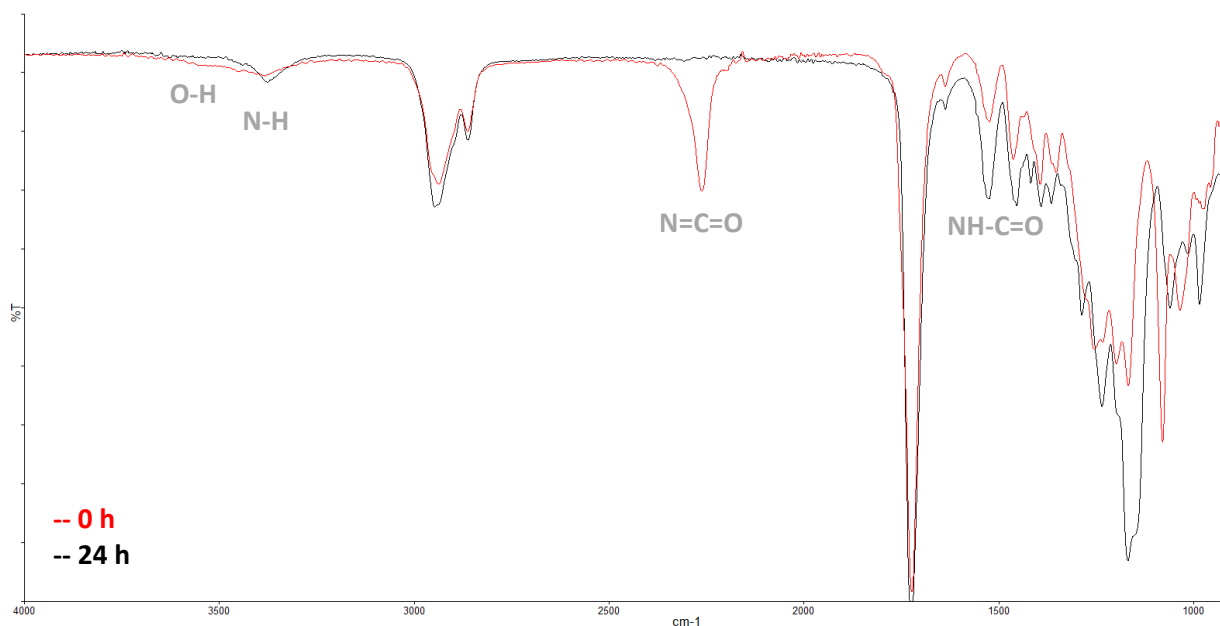


Figure 53: ATR-IR spectrum of the polyester POLYESTER-2-1 before and after the reaction took place

Finally NMR (Figure 54) was selected to determine the conversions, due to the more accurate and especially quantitatively values. ATR-IR was handled as a qualitative co-method, if necessary for a polyester modification reaction, because it was decisive, how much of the urethane bonds did form until a certain time and not just if some of the isocyanates reacted. After attaching the IPDI-HEMA endgroup ( $M_w = 352.43$  g/mol) to polyesters, a molecular weight increase of around 700 g/mol was expected. Considering the nearly complete conversion of this method, the new molecular weight was now 3800 instead of 3100 g/mol.

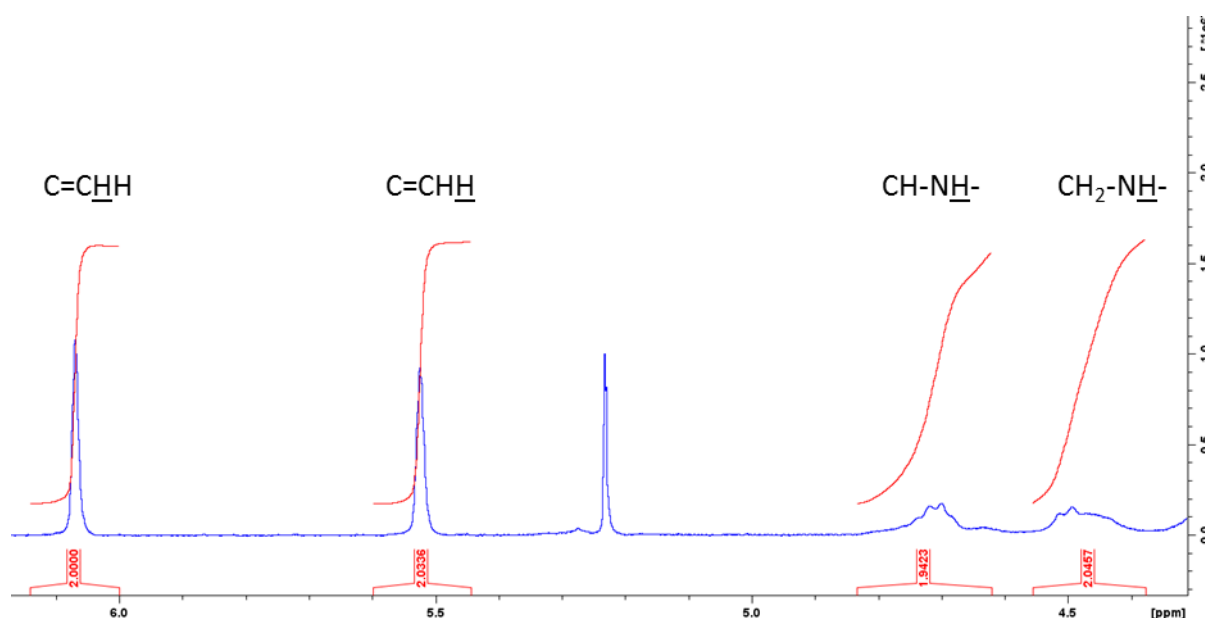


Figure 54:  $^1\text{H-NMR}$  of the IPDI-HEMA endgroup attached to the glutaric acid and hexanediol-based polyester POLYESTER-2 resulting in POLYESTER-2-1; two peaks on the left – hydrogens of the methacrylate double bond; two peaks on the right – secondary and primary NH signal of the urethane bonds; undescribed peak is residual dichloro methane

### Glutaric Acid Hexanediol Polyester with IPDI-HEMA Endgroup [PolyISOGA-M]

The isosorbide glutaric acid-based polyester was also endfunctionalized with the IPDI-HEMA endgroup according to the work of Muller I. A.<sup>58</sup> Due to the problem of achieving higher molecular weights than 2500 g/mol in the  $\alpha$ -ketoglutaric acid-based polyesters, only one of three glutaric acid-based polyester products was modified.

The modification procedure was equal to the glutaric acid and hexanediol-based polyester, but only 2.05 eq. of the isocyanate endgroup were used. After the mixture was stirred for 28 h at room temperature, the brownish polymer product was dried in vacuum with a resulting yield of 88%.

Table 25:  $M_n$  of educt, determined via NMR and GPC and resulting yield

Product	$M_n$ [g/mol] GPC of educt polyester	$M_n$ [g/mol] NMR of educt polyester	Yield [%]
POLYESTER-7-1	no result	2700	88

During this modification of the glutaric acid and isosorbide-based polyester, no problems occurred.

#### 4.2.2.2. $\alpha$ -Ketoglutaric Acid-based Polyesters with IPDI-HEMA Endgroup [Poly(HD/ISO)KGA-M]

Next the  $\alpha$ -ketoglutaric acid polyesters were modified (Figure 55), undergoing the same conditions as the glutaric ones, based on the work of Muller I. A.<sup>58</sup>

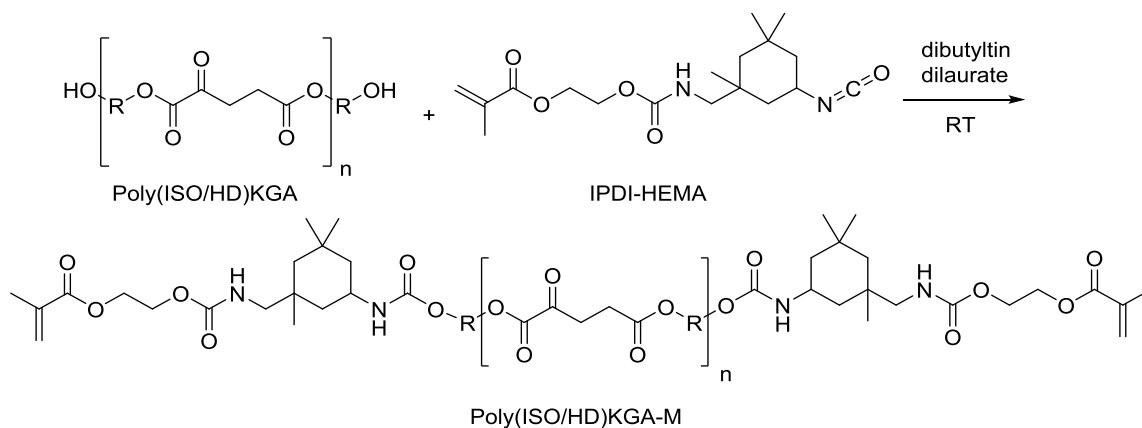


Figure 55: Linking of the IPDI-HEMA endgroup to the  $\alpha$ -ketoglutaric acid hexanediol polyester; R = hexanediol or isosorbide

### $\alpha$ -Ketoglutaric Acid Hexanediol Polyester with IPDI-HEMA Endgroup [PolyHDKGA-M]

Reaction route was analogous to the glutaric acid-based polyester modifications. The resulting white polymer products were dried in vacuum with resulting yields of 37% to 96% (Table26).



Table 26:  $M_n$  of all educts, determined via NMR and GPC and resulting yields

Product	$M_n$ [g/mol] GPC of educt polyester	$M_n$ [g/mol] NMR of educt polyester	Yield [%]
<b>POLYESTER-12-0</b>	4700	5000	37
<b>POLYESTER-9-1</b>	3200	3000	86
<b>POLYESTER-12-1</b>	4700	5000	93
<b>POLYESTER-8-1</b>	9900	13800	88

The POLYESTER-12-0 had shown significant lower yield, due to the different workup at the end. In this case, the reaction mixture was precipitated in petrol ether and only the polymer product at the bottom of the beaker was further dried. The slightly cloudy petrol ether, which unfortunately was thrown away, may contained the rest of the polyester. So for the workup of all future polyesters, the dichloro methane was removed via evaporation and the residual polymer was washed with petrol ether, instead of precipitating in it.

A huge problem, occurred during the drying process in the desiccator. After one day of drying the NMR spectra were measured and the products were completely soluble. Two days later none of the  $\alpha$ -ketoglutaric acid-based polyesters were soluble or meltable anymore. All polyesters crosslinked during the drying process. The most likely reason is, that the crosslinking started already in the flask at the rotary evaporator, due to the accidental, short exposure of a 40 °C water bath, before switching to room temperature.

So a second batch of these modified polyesters (Table 27) was prepared the same way as described above, for one exception, this time only 2.5% instead of 10% IPDI-HEMA endgroup excess were used, due to the accurately fitting molecular weight of the polymer before and after modification, determined via NMR. So less unreacted isocyanate endgroup has to be washed out of the polyester during the workup.

Table 27: Second Batch -  $M_n$  of all educts, determined via NMR and GPC and resulting yields

Product	$M_n$ [g/mol] GPC of educt polyester	$M_n$ [g/mol] NMR of educt polyester	Yield [%]
<b>POLYESTER-9-2</b>	3200	3000	96
<b>POLYESTER-12-2</b>	4700	5000	93
<b>POLYESTER-8-2</b>	9900	13800	94

Unlike in the first batch, this time the removal of the solvent at the rotary evaporator was all the time at room temperature and the drying procedure were carried out for only one day. Then the polyesters were dissolved in acetone and an anaerobe inhibitor, phenothiazine, was added to the solution. This solution was divided by three, to avoid the crosslinking of the whole solution at once, and kept separately in closed penicillin vials at -20 °C in the dark. For all further analysis these solution, with known concentrations, were taken.

For the second batch of polyester modification, a more sensitive method than NMR, the ATR-IR analysis, was selected, to monitor the conversion of the isocyanate.

#### $\alpha$ -Ketoglutaric Acid Isosorbide Polyester with IPDI-HEMA Endgroup [PolyISOKGA-M]

Now the  $\alpha$ -ketoglutaric acid and isosorbide-based polyester was endfunctionalized with the IPDI-HEMA endgroup, also based on the work of Muller I. A.<sup>58</sup> The highest molecular weight achieved with all of these polyesters was around 2500 g/mol, so only one of them was modified.

The procedure was analogous to the glutaric acid-based polyester modification and a yellowish polymer product was achieved, further dried in vacuum with a resulting yield of 81% (Table 28).

Table 28:  $M_n$  of all products, determined via NMR and GPC and resulting yields

<b>Product</b>	<b><math>M_n</math> [g/mol] GPC of educt polyester</b>	<b><math>M_n</math> [g/mol] NMR of educt polyester</b>	<b>Yield [%]</b>
<b>POLYESTER-15-1</b>	no result	2500	81

During the synthesis of this polyester, no problems were noticed. Considering the problem with the crosslinking of the modified  $\alpha$ -ketoglutaric acid and hexanediol polyesters during the drying procedure, the polymer was also only dried for one day, and afterwards three solutions in acetone with known concentration were prepared in closed penicillin vials. The solutions were also stored in the dark at -20 °C to minimize risk of crosslinking during storage.

## 5. Analytics

### 5.1. UV-VIS Absorption

For further reactivity and mechanical tests the samples had to be irradiated with UV light, which induces the radical polymerization. As a reference system, benzophenone (BP) was used. Compounds based on the  $\alpha$ -ketoglutaric acid were selected for this analysis (Figure 56). The di-acid itself, the dimethylester and the polyesters based on hexanediol and isosorbide. Concentrations of approximately  $10^{-3}$  mol/L were aimed. To determine which light source and wavelength filter is used to conduct these experiments, a UV-VIS light absorption test was carried out with a few in acetonitrile dissolved samples based on  $\alpha$ -ketoglutaric acid. The absorption maxima and extinction coefficients are listed in Table 29.

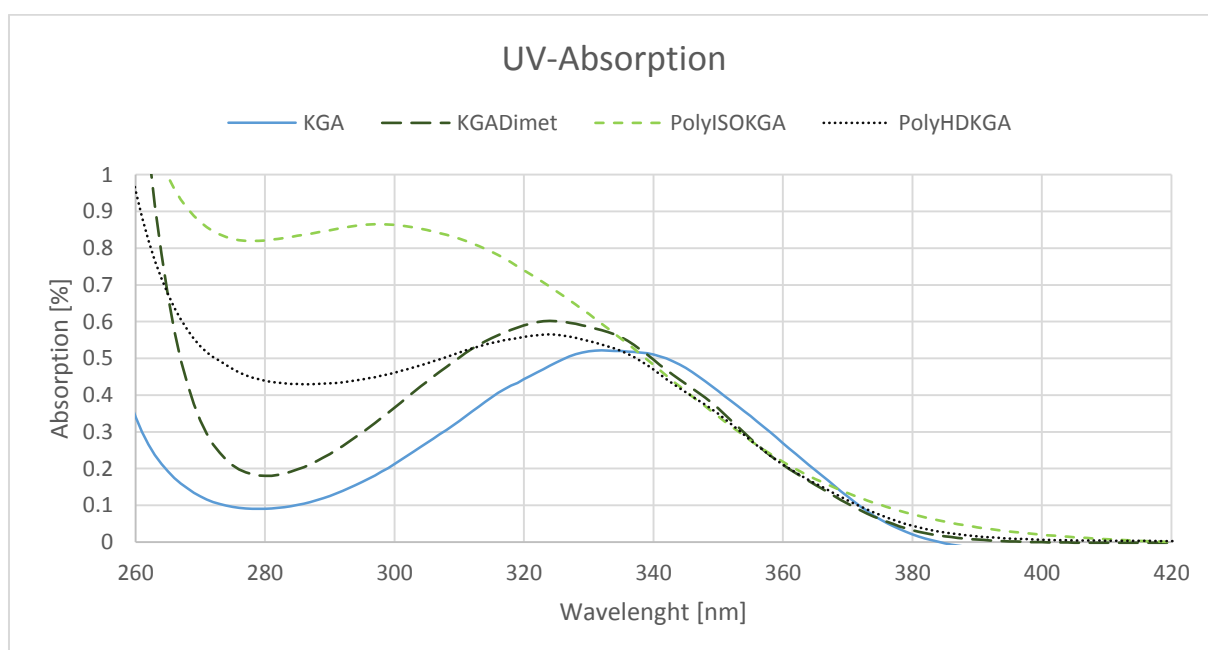


Figure 56: UV light absorption of  $\alpha$ -ketoglutaric acid (KGA),  $\alpha$ -ketoglutaric acid dimethylester (KGADimet),  $\alpha$ -ketoglutaric acid isosorbide polyester (PolyISOKGA\_2500) and  $\alpha$ -ketoglutaric acid hexanediol polyester (PolyHDKGA\_5000)

Table 29: maxima of the samples between 260 and 420 nm and extinction coefficient  $\epsilon$ ; for the polymeric initiators the extinction coefficients were calculated for the repeating unit

	KGA	KGADimet	PolyISOKGA	PolyHDKGA	BP
<b>Maximum [nm]:</b>	332	324	298	324	338
<b><math>\epsilon</math> [L/mol*cm]</b>	16	20	36	24	140

Three of the four components tested had their maxima in the range of 324 to 332 nm. Only the polyester containing isosorbide and the  $\alpha$ -ketoglutaric acid absorbed the UV light at 298 nm the most, slightly shifted to shorter wavelength compared to the other samples measured. This may can be explained due to the rigidity of the isosorbide-based polyester compared to the flexible hexanediol spacer. These experiments lead to the usage of a 320 to 500 nm filter for a mercury lamp, as the UV source, for further studies. The extinction coefficient of the

polymeric photoinitiators is significantly higher, compared to the small molecules based on  $\alpha$ -ketoglutaric acid. The reason for this behavior is the multiple photoinitiating building blocks in the polymer chain, therefore the polyester achieve increased extinction coefficients. Benzophenone, as a small molecule, measured a significantly higher extinction coefficients compared to the KGADimet and the KGA.

## 5.2. Reactivity Tests

To determine the reactivity of the synthesized  $\alpha$ -ketoglutaric acid-based initiators, including the polymerizable and macromolecular derivatives of the  $\alpha$ -ketoglutaric acid, were used in different concentrations. This should result in information about the reactivity of the generated radicals, the kinetics of the polymerization over time, the ability for the photoproducts to migrate out of the cured polymer network and storage stability of the “ready to use” formulations. The monomer used for these tests was the commercially available Miramer® UA5216 (Figure 57) from MIWON, an aliphatic di-functional acrylate formulation with high elongation at break, excellent adhesion, good flexibility and low yellowing. One compound, with 40 wt% appearance, of this monomer mixture was a high molecular weight (30000 g/mol) aliphatic di-functional acrylate and the second, main component was isobornylacrylate (IBA) as the reactive diluent with 60 wt% as a mono-functional acrylate, which was able to raise the glass transition temperature of the final material due to its bulky structure.

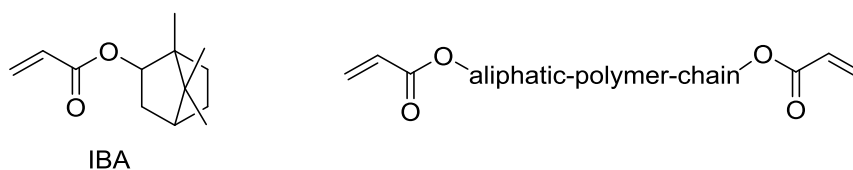


Figure 57: Components of Miramer® UA5216

Due to the moderate compatibility of this highly apolar monomer with the rather polar hexanediol-based polyester and the immiscibility of the Miramer and the polar isosorbide-based polyester, a second, polar monomer was tried. With tetraethyleneglycol dimethacrylate (TEGDMA), the miscibility problems were overcome, but the mechanical properties were expected to be bad, due to the resulting highly crosslinked network and therefore a very brittle material. So TEGDMA (Figure 58) was used only in the reactivity tests for illustration of the concept, using a polar monomer.

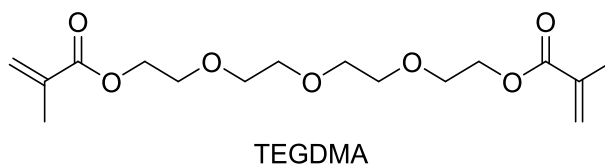


Figure 58: Tetraethyleneglycol dimethacrylate

As a reference, the Type II photoinitiator system, benzophenone (BP) with the co-initiator methyldiethanolamine (MDEA) were selected in the concentrations 2 wt% and 5 wt%, shown in Figure 59.



Figure 59: Reference system BP-MDEA

According to these weight percentages, the molar ratios (mol%) of all used  $\alpha$ -ketoglutaric acid-based photoinitiators were calculated for the formulations. This was done to ensure the same molar amount of photoinitiator in the formulation, therefore providing a fair comparison. For the macromolecular photoinitiators, the molar ratio was based on the reactive repeating unit of the polyester (Figure 39 and Figure 42). All  $\alpha$ -ketoesters were used without co-initiator in this experiment (Figure 60).

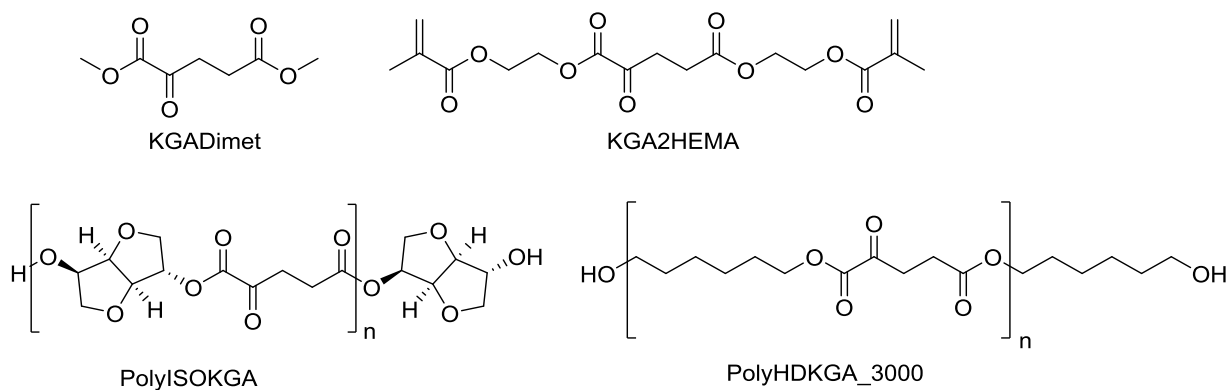


Figure 60: KGADimet:  $\alpha$ -ketoglutaric acid dimethylester; KGA2HEMA:  $\alpha$ -ketoglutaric acid di-2-hydroxyethyl methacrylate; PolyISOKGA: Polyester based on isosorbide and  $\alpha$ -ketoglutaric acid (POLYESTER-15); PolyHDKGA: Polyester based on 1,6-hexanediol and  $\alpha$ -ketoglutaric acid (POLYESTER-9)

To compare the reactivity in apolar di(meth)acrylate systems, another set of formulations was prepared. Three different types of monomers were used to make the two formulations for the measurement. The first one was only HDDA and the second one was a mixture of the monomers D<sub>3</sub>MA and UDMA, in a molar ratio of 1:1, called 2M (Figure 61).

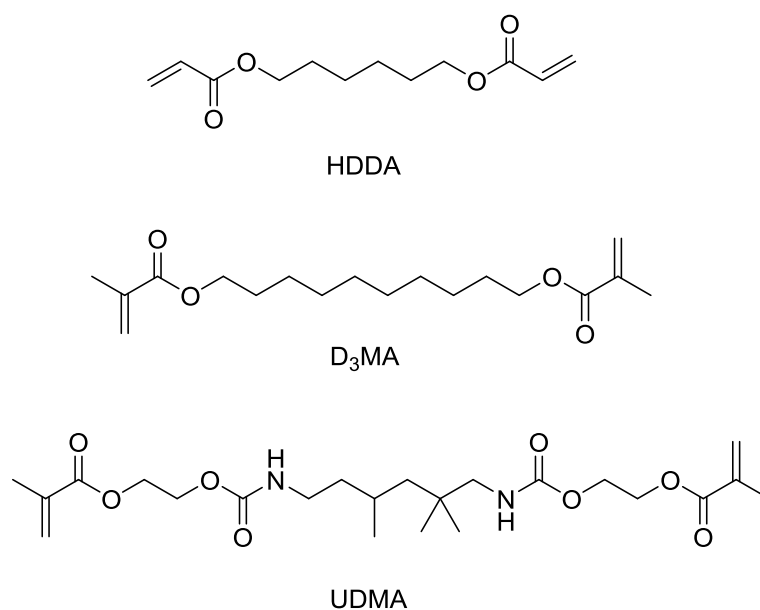


Figure 61: HDDA (1,6-hexanediol dimethacrylate), D<sub>3</sub>MA (decane-1,10-diyl bis(2-methylacrylate)) and UDMA (7,7,9-trimethyl-4,13-dioxo-3,14-dioxo-5,12-diazahexadecane-1,16-diyl bis(2-methylacrylate))

As a photoinitiator for these formulations the synthesized  $\alpha$ -ketoglutaric acid-based (poly)-esters were used. Also ethyl pyruvate was measured to compare the reactivity with an already known  $\alpha$ -keto ester. The formulations were prepared with 1 wt% ethyl pyruvate and based on the molar amount of ethyl pyruvate, the amount of the other initiators was calculated. The different type II photoinitiators are illustrated in Figure 62.

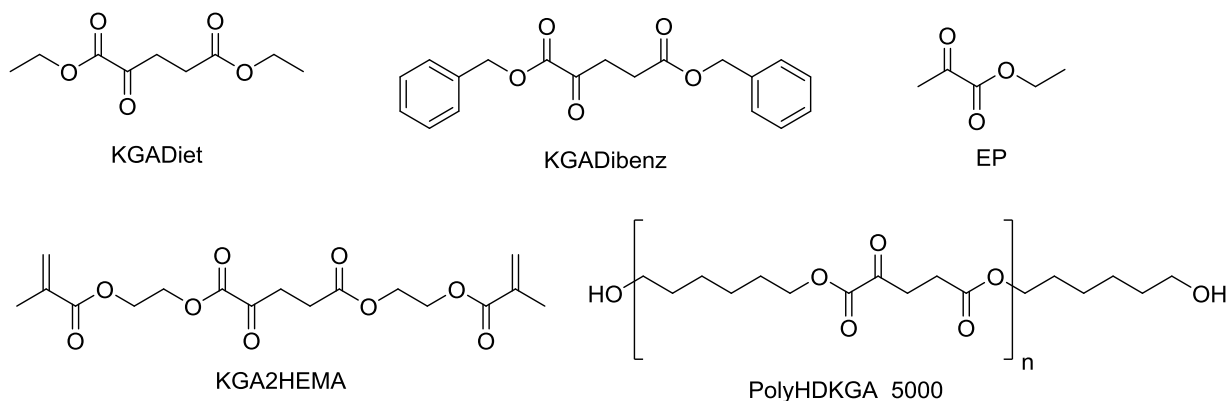


Figure 62: KGADiet ( $\alpha$ -ketoglutaric acid diethylester), KGADibenz ( $\alpha$ -ketoglutaric acid dibenzylester), KGA2HEMA ( $\alpha$ -ketoglutaric acid di-2-hydroxyethylmethacrylate), EP (ethyl pyruvate) and PolyHDKGA ( $\alpha$ -ketoglutaric acid hexanediol polyester – POLYESTER-12)

Also two industrial type II photoinitiators (BP and Speedcure<sup>®</sup> BMS) were measured to compare existing aromatic photoinitiators with the  $\alpha$ -ketoglutaric acid-based ones. As co-initiator EDB was used (Figure 63). The amount of initiator and co-initiator used, was also based on the molar amount of 1 wt% ethyl pyruvate.

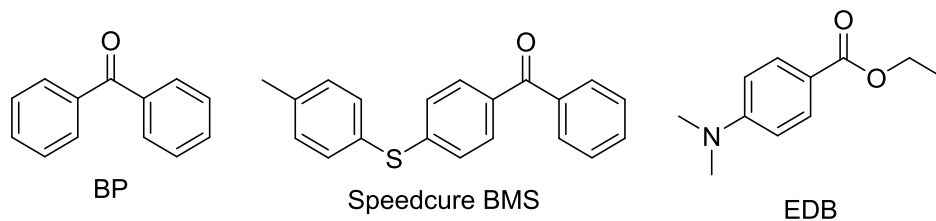


Figure 63: BP (benzophenone), Speedcure BMS (4-benzoyl-4'-methylphenyl sulphide), Speedcure 73 (2-hydroxy-2-methyl-1-phenylpropan-1-one) and EDB (ethyl-4-dimethylaminobenzoate)

### Storage Stability Tests

Storage stability tests of formulations based on Miramer were conducted. To determine the time, after which a finished photopolymerizable formulation could still be cured without significant reactivity loss. This tests were performed at the photorheometer with already measured formulations from the “mechanical tests”, which are measured again after a certain amount of time. Two and four weeks are shown in Figure 64. All tested samples were stored at -18 °C in the dark.



Figure 64: Comparison of the 0, 2 and 4 week data

Results after two weeks are unchanged. The insignificant differences are presented in Table 30 including percentage they changed. With a maximum change at 7% for the time to reach the gel point, all other dimensions were basically unchanged. Therefore the formulations are completely stable over 2 weeks.

Table 30: Important dimensions after 2 weeks compared to the initial data

Sample	$t_g$ [s]	DBC at $t_g$ [%]	DBC [%]	$t_{95\%}$ [s]	$G'$ [kPa]
<b>PolyHDKGA_3000M</b>					
<b>0 weeks</b>	79	70	92.4	257.7	842.5
<b>2 weeks</b>	85	68	94.2	252	821.3
<b>Change</b>	7%	3%	2%	2%	3%

After four weeks of storage the change of the reactivity is shown in Table 31. The results did not change significant too. The most important values like  $t_g$ , DBC and  $t_{95\%}$  were the same with a maximum deviation of 5%. Only the DBC at the gel point and the final storage modulus changed 12%.

Table 31: Important dimensions after 4 weeks compared to the initial data

Sample	$t_g$ [s]	DBC at $t_g$ [%]	DBC [%]	$t_{95\%}$ [s]	$G'$ [kPa]
<b>PolyHDKGA_5000M</b>					
<b>0 weeks</b>	73.5	67.5	93.5	259.5	758.2
<b>4 weeks</b>	76	60.0	95.7	246	857.2
<b>Change</b>	3%	12%	2%	5%	12%

### 5.2.1. Photo Differential Scanning Calorimetry

#### Miramer Formulations

The reference system BP\_MDEA was selected and compared to a variety of  $\alpha$ -ketoglutaric acid based small molecules, polymeric and polymerizable photoinitiators. In the following part, the characteristics of a photo-DSC measurement in the monomer Miramer are presented. Homogeneous formulations were achieved with all compounds tested, but the solid macro-initiator PolyISOKGA did only disperse in the liquid monomer, due to high polarity differences.

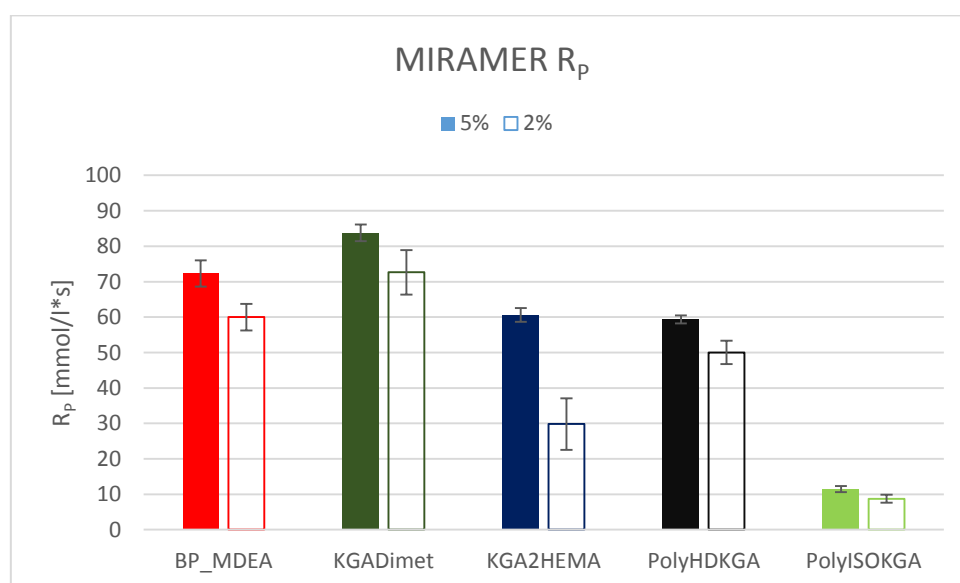


Figure 65: Rate of polymerization in Miramer



In terms of reactivity (Figure 65), the KGADimet significantly outperforms all tested initiators in this series with a  $R_p$  of over 80 mmol/l\*s for the 5 mol% formulation, followed by the commercial BP\_MDEA system. Lower reactivity shown the macromolecular (PolyHDKGA) and polymerizable (KGA2HEMA) initiators. A major increase of the  $R_p$  in the KGA2HEMA formulation was present, when changing the initiator concentration from 2 to 5 mol%. The second, much more polar macromolecular initiator, PolyISOKGA, was just dispersed in the formulation and did not mix well with the Miramer. Due to that compatibility issue, this initiator achieved the lowest  $R_p$  value, around 10 mmol/l\*s, in this experiment so far.

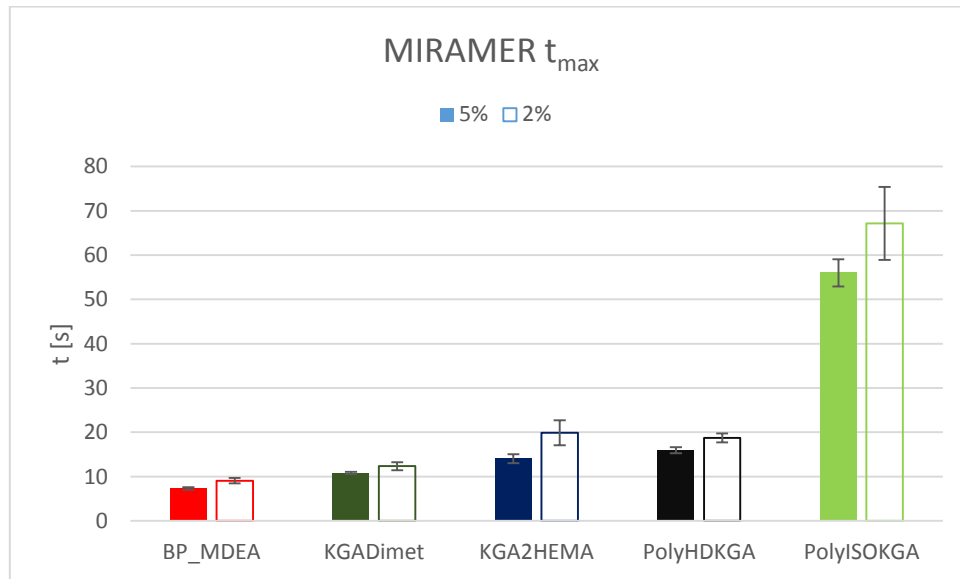


Figure 66: Time to reach peak maximum in Miramer

The  $t_{max}$  (Figure 66) was reached by the formulation, containing BP and MDEA at first in under 10 s, followed by the KGADimet at 10 s, the polymerizable KGA2HEMA and nearly equal values for PolyHDKGA. The same trend occurs for the 2 mol% formulations, just slightly shifted to longer  $t_{max}$ . Again, the polymeric PolyISOKGA initiator could not develop its full potential in the Miramer system, therefore resulting in very high  $t_{max}$  values.

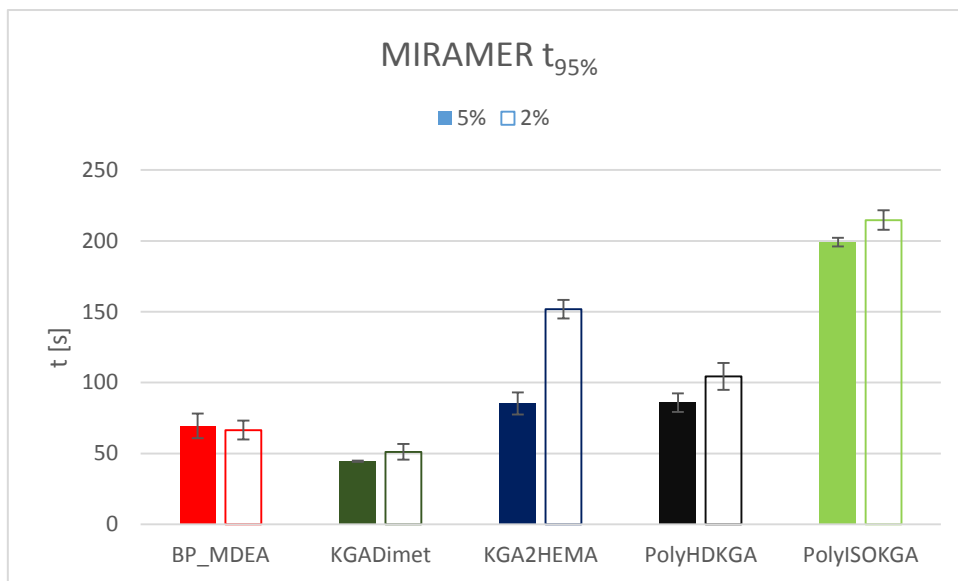


Figure 67: Time to reach 95% conversion in Miramer

To reach 95% of the total conversion (Figure 67), KGADimet was the fastest initiator system, even outperforming at only 2 mol% compared to the 5 wt% BP\_MDEA. Next, the polymeric PolyHDKGA (5 mol%) and the polymerizable KGA2HEMA (5 mol%) finish the majority of the polymerization after approximately the same time. The PolyISOKGA finishes 95% of its conversion in over 200 s, which is very slow. Basically there is a trend to increased  $t_{95\%}$ , if switching from 5 to 2mol%.

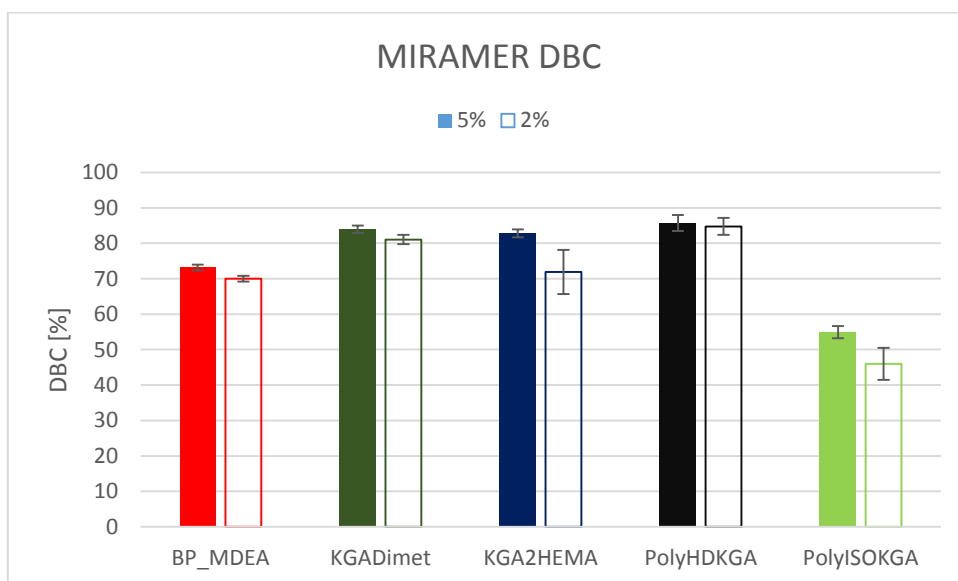


Figure 68: Double bond conversion in Miramer

Compared to the BP\_MDEA reference system, conversion increased for all other tested initiators up to 12%, with the exception of PolyISOKGA, which performed the worse in the Miramer-based photo-DSC experiments. The highest double bond conversion achieved PolyHDKGA followed by KGADimet and KGA2HEMA, shown in Figure 68.

## TEGDMA Formulations

Due to the compatibility issue of the polymeric PolyISOKGA and Miramer, a second and more polar monomer was tested. So the experiments at the photo-DSC were repeated for the macro-initiators and the reference system in TEGDMA.

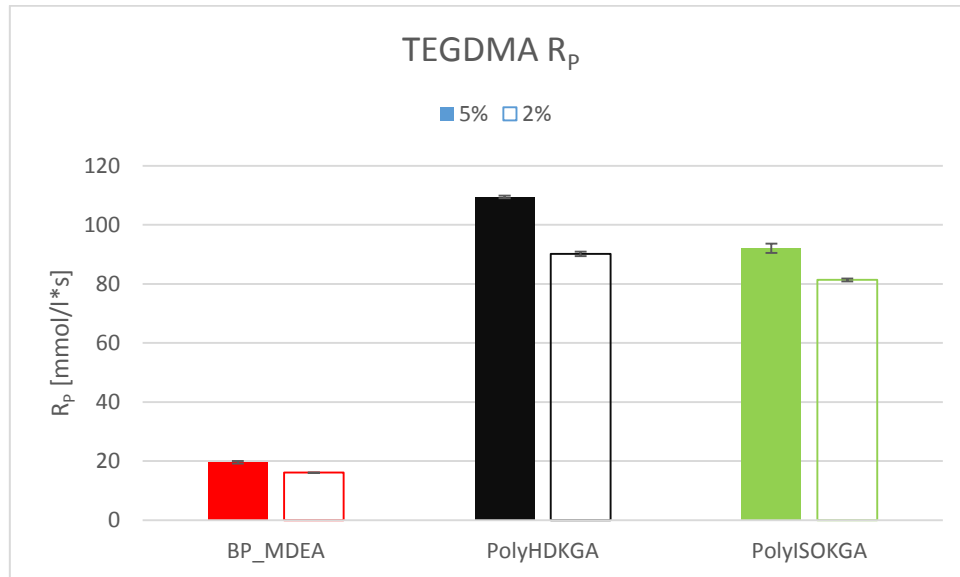


Figure 69: Rate of polymerization in TEGDMA

In this matrix, the macromolecular initiators outperform the BP\_MDEA system totally by the factor of four to five. Now the two polymeric initiators, PolyHDKGA and PolyISOKGA, achieved values above 90 mmol/l\*s, while benzophenone and the amine are below 20 mmol/l\*s, shown in Figure 69.

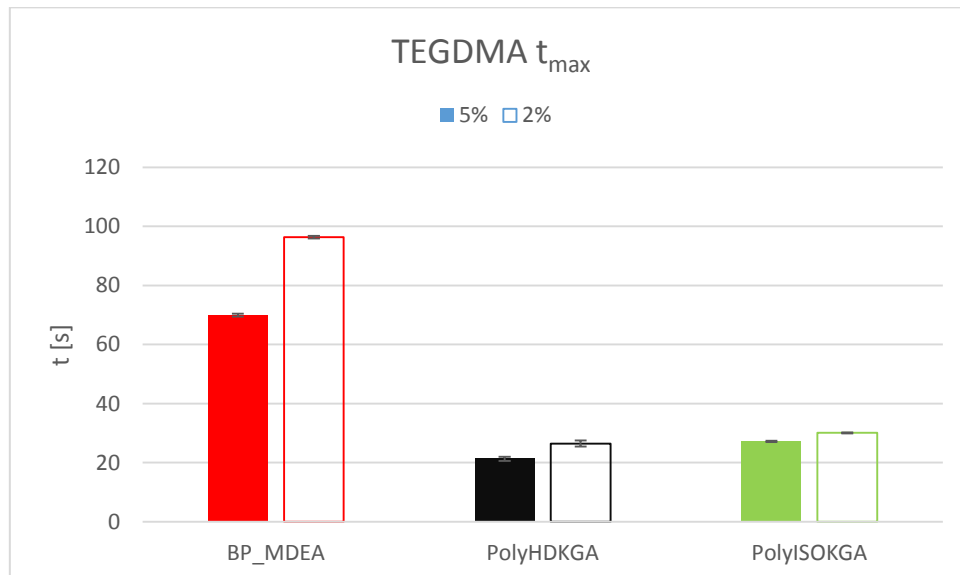


Figure 70: Time to reach peak maximum in TEGDMA

As illustrated in Figure 70, the fastest time to achieve the peak maximum, was provided by PolyHDKGA, followed by PolyISOKGA. The reference system took it approximately three times as long in TEGDMA. They are therefore much more reactive in this monomer matrix.

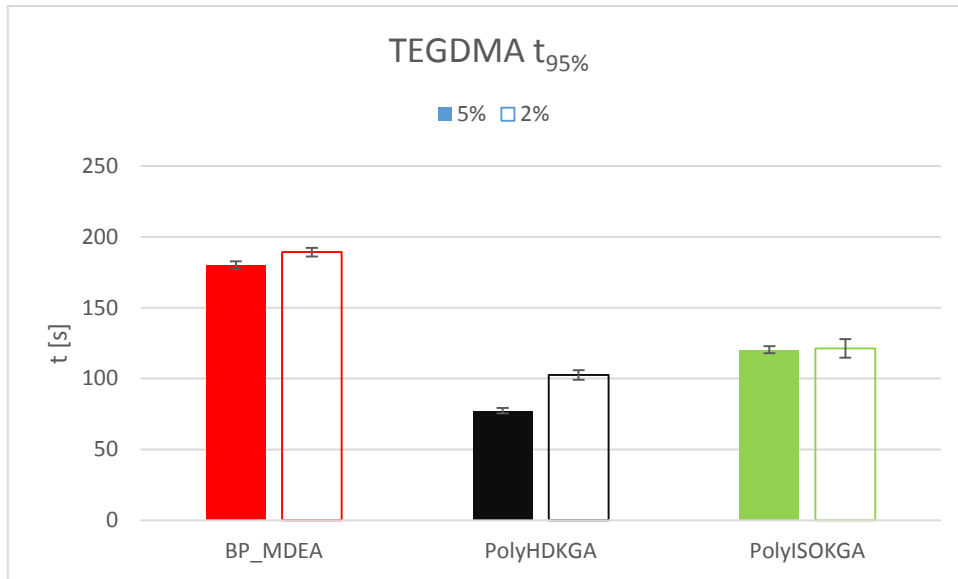


Figure 71: Time to reach 95% conversion in TEGDMA

The curing speed to reach 95% of the total conversion (Figure 71), was halved for the PolyHDKGA system compared to BP\_MDEA. PolyISOKGA delivered in this experiment also a significant decrease of the  $t_{95\%}$  value. The total irradiation time is therefore lower for the polymeric,  $\alpha$ -ketoglutaric acid-based initiators.

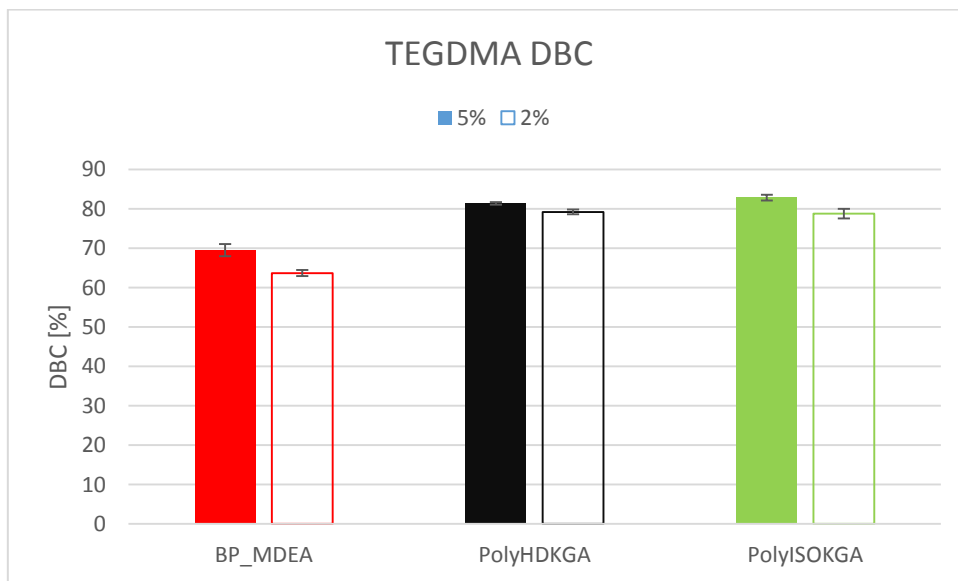


Figure 72: Double bond conversion in TEGDMA

Over 10% more conversion was achieved by the macromolecular initiators in TEGDMA compared to BP\_MDEA with around 70% for the 5 wt% formulation and 64% for the 2 wt% system (Figure 72). The increased DBC's for the polymeric initiators probably result from the more efficient, intermolecular hydrogen abstraction from the TEGDMA molecules.

## HDDA and 2M Formulations

After those experiments, the last series of photo-DSC measurements was performed. This time with the formulations based on the monomers HDDA and 2M. The rates of polymerization of the different samples are illustrated for HDDA in Figure 73 and for 2M in Figure 74. Two series of measurements were carried out to compare the influence of the co-initiator EDB. Initiator systems with aromatic molecules inside are indicated with a diagonal pattern. To compare the systems and the effect of the co-initiator better, EDB was also used with the non-aromatic  $\alpha$ -ketoesters.

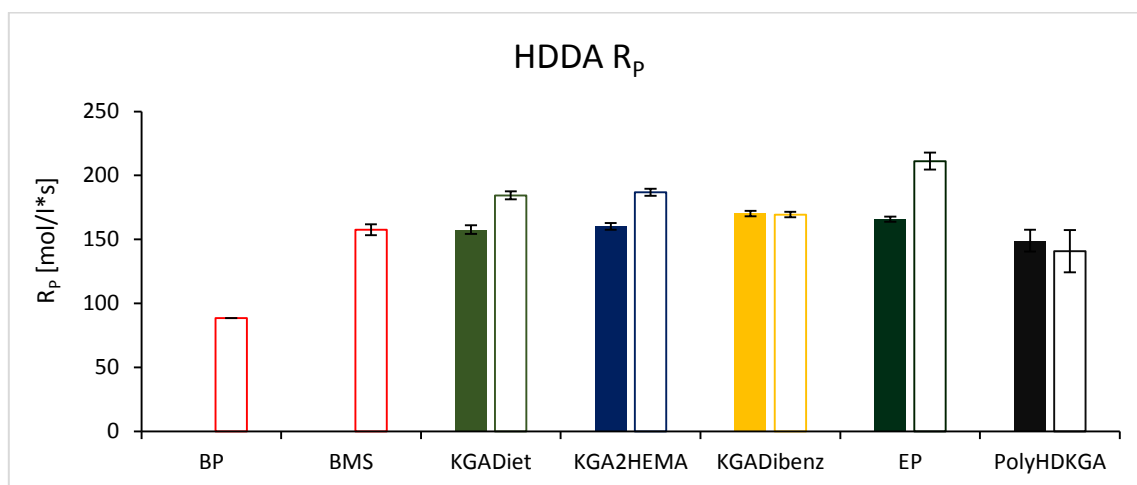


Figure 73: Rate of polymerization in the monomer HDDA of the different initiators. In the first series (solid fill) there was no co-initiator used in the formulations and in the second series (no fill) EDB was used as the co-initiator

KGADiet, KGA2HEMA, KGADibenz and EP had shown without the use of a co-initiator higher reactivity than an industrial used type II photoinitiator like BMS or BP. Only the polymeric PolyHDKGA had a lower rate of polymerization compared to the industrial initiators. If there was EDB in the formulations the KGADiet, the polymerizable KGA2HEMA and EP performed even better and got a significant boost in reactivity. There was no change in reactivity for the formulation with KGADibenz with co-initiator.

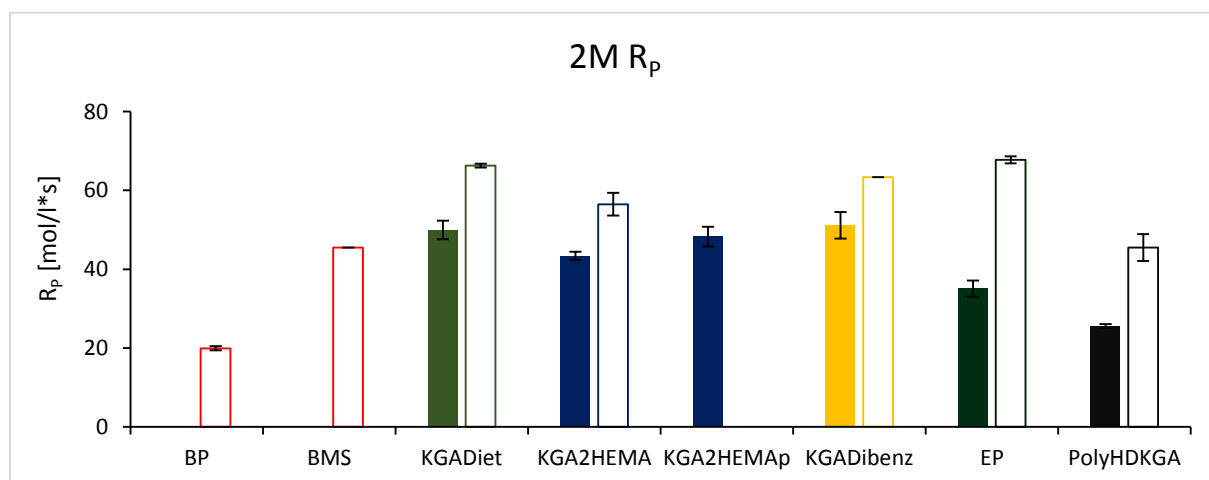


Figure 74: Rate of polymerization in the monomer 2M of the different initiators. In the first series (solid fill) there was no co-initiator used in the formulations and in the second series (no fill) EDB was used as the co-initiator

In the monomer system with 2M the results were similar to them in HDDA. KGADiet, KGADibenz and EP outperforms the commercial initiator system with BP and also BMS. Even the KGA2HEMA\_pure was more reactive, but the formulation with KGA2HEMA had shown less reactivity. The addition of EDB as co-initiator resulted in a reactivity increase for the system. In contrast to HDDA, in the experiment with formulations based on 2M, PolyHDKGA's reactivity was increased significant with the use of a co-initiator.

The  $t_{max}$  values are shown graphically in Figure 75 for HDDA and in Figure 76 for 2M.

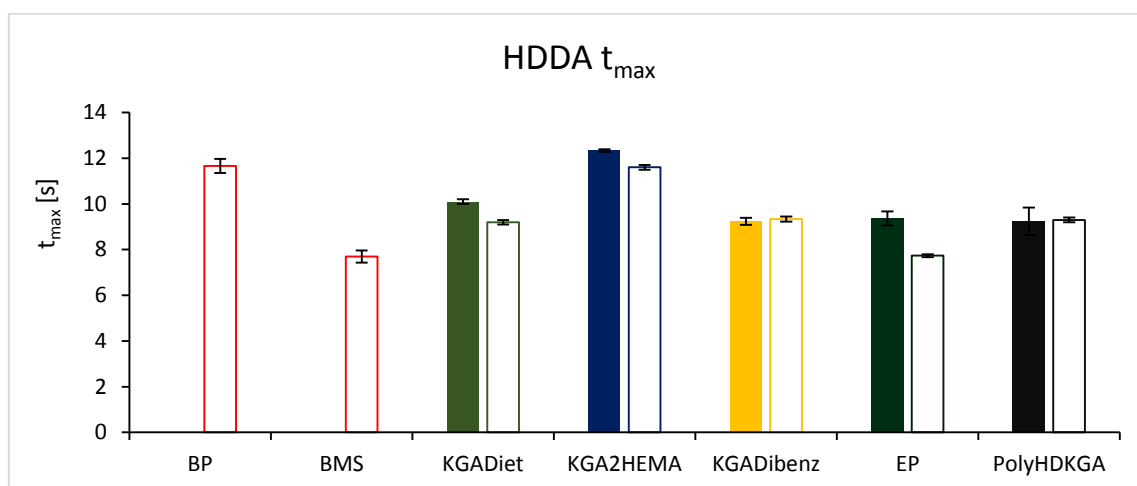


Figure 75:  $t_{max}$  in the monomer HDDA of the different initiators. In the first series (solid fill) there was no co-initiator used in the formulations and in the second series (no fill) EDB was used as the co-initiator

The shortest time to the highest exothermic was achieved by BMS, followed by EP with EDB and KGADiet/PolyHDKGA/KGADibenz also with co-initiator. Then the formulations without the use of EDB were next, like KGADiet, KGADibenz, EP and PolyHDKGA. KGA2HEMA and BP reached their maximum after 12 s and were the worst performing initiators in this experiment.

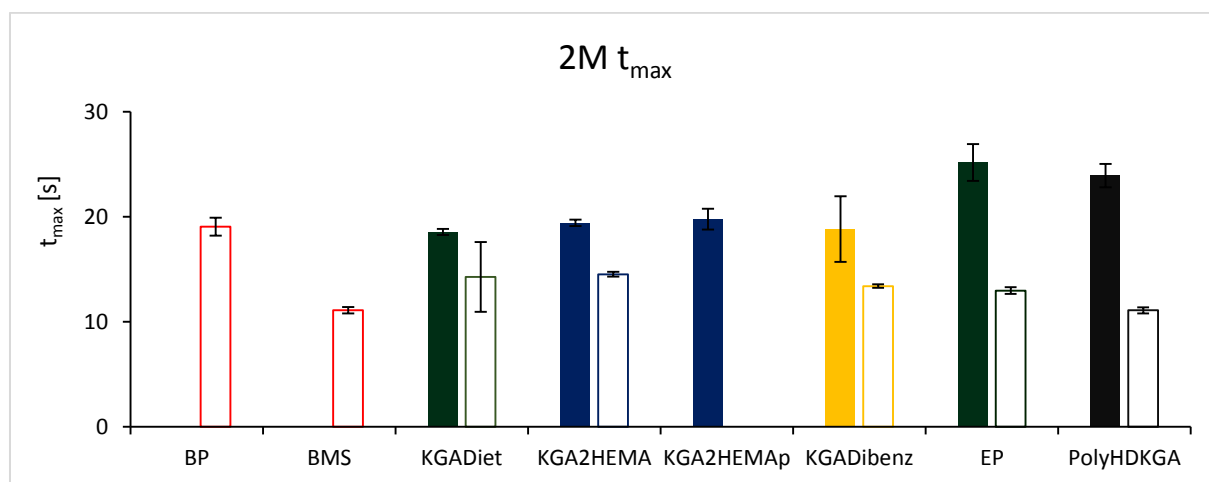


Figure 76:  $t_{max}$  in the monomer 2M of the different initiators. In the first series (solid fill) there was no co-initiator used in the formulations and in the second series (no fill) EDB was used as the co-initiator

In the experiment with 2M the shortest time to the highest exothermic was achieved also by BMS, followed by the polymeric PolyHDKGA with EDB and KGADibenz, the polymerizable KGA2HEMA with co-initiator. BP was only as good as KGADiet, KGA2HEMA, KGADibenz and

KGA2HEMA\_pure without EDB. The lowest performance was achieved by the formulations containing EP and PolyHDKGA without co-initiator.

The  $t_{95\%}$  values are shown in for HDDA and in for 2M are shown in Figure 77 and Figure 78.

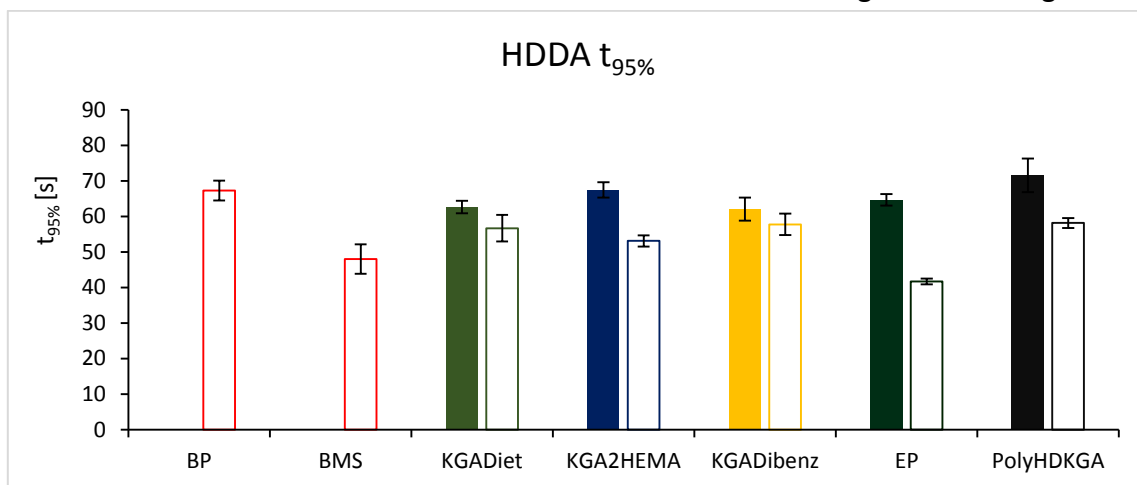


Figure 77:  $t_{95\%}$  in the monomer HDDA of the different initiators. In the first series (solid fill) there was no co-initiator used in the formulations and in the second series (no fill) EDB was used as the co-initiator

The fastest  $t_{95\%}$  was reached by EP with EDB followed by BMS and KGA2HEMA with co-initiator. KGADiet and KGADibenz (both with EDB) performed equally well. BP, KGA2HEMA and PolyHDKGA needed the longest time to reach  $t_{95\%}$ . Slightly better than BP are KGADiet and EP.

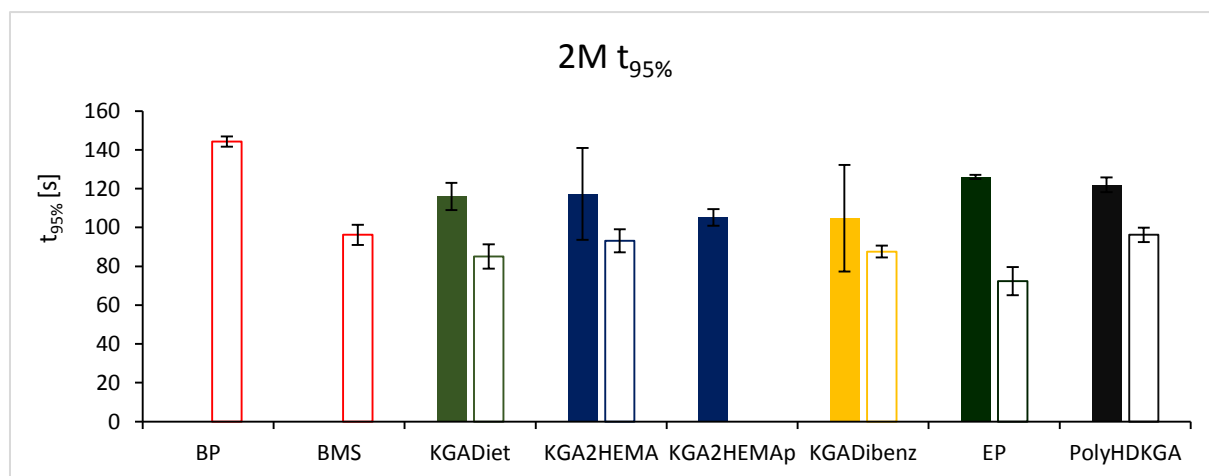


Figure 78:  $t_{95\%}$  in the monomer 2M of the different initiators. In the first series (solid fill) there was no co-initiator used in the formulations and in the second series (no fill) EDB was used as the co-initiator

In the 2M system EP performed the best, followed by KGADiet, KGADibenz, KGA2HEMA, BMS and KGADibenz6 (all formulations with EDB). The shortest time to cover 95% of the total DBC without EDB was achieved by KGA2HEMA\_pure followed by KGADiet, KGADibenz, KGA2HEMA, PolyHDKGA and EP. All samples tested were faster in reaching  $t_{95\%}$  than BP, but not BMS.

The double bound conversion (DBC) is illustrated in Figure 79 for HDDA and in Figure 80 for 2M.

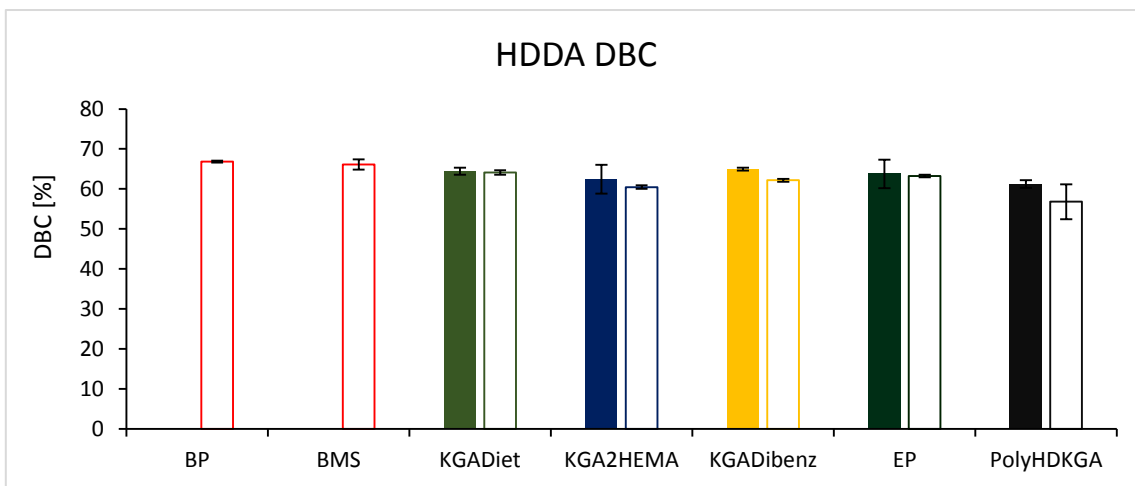


Figure 79: DBC in the monomer HDDA of the different initiators. In the first series (solid fill) there was no co-initiator used in the formulations and in the second series (no fill) EDB was used as the co-initiator

The DBC of all samples in HDDA was  $63.0 \pm 2.7\%$ . So it is approximately the same conversion for all initiator systems.

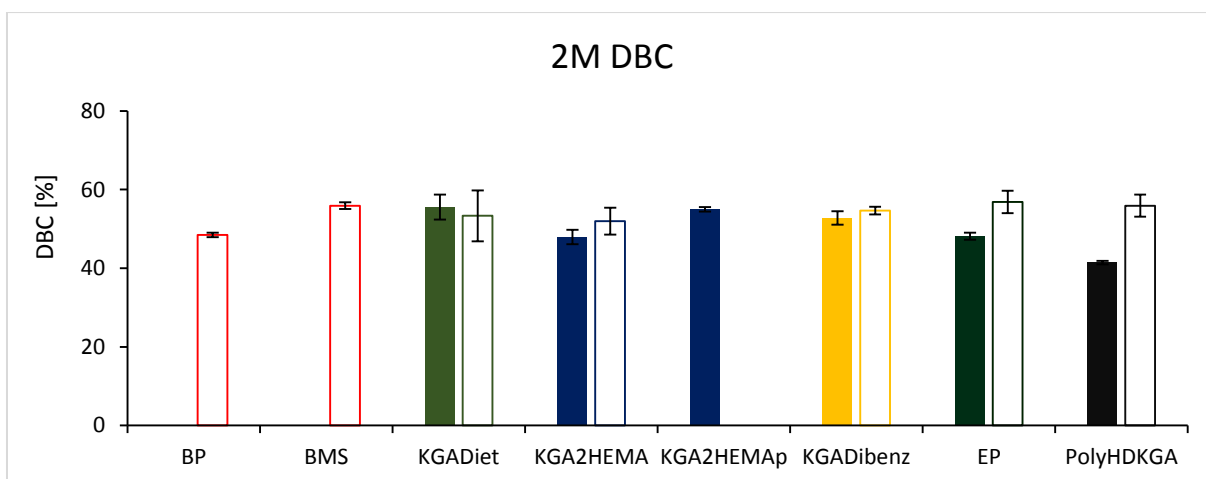


Figure 80: DBC in the monomer 2M of the different initiators. In the first series (solid fill) there was no co-initiator used in the formulations and in the second series (no fill) EDB was used as the co-initiator

The DBC of all samples in 2M was  $52.2 \pm 4.5\%$ . So it is approximately the same conversion for all initiator systems. Only the sample with PolyHDKGA as photoinitiator without EDB reached significantly less DBC than the other formulations.

Overall the reactivity of the KGADimet was increased in terms of rate of polymerizing, faster curing speed ( $t_{95\%}$ ) and total conversion, compared to the reference system BP\_MDEA in Miramer. In monomers like HDDA and 2M, basically all  $\alpha$ -ketoester-based initiators performed better than BP\_EDB. KGADiet and the polymerizable KGA2HEMA reached slightly increased or similar values for  $R_p$  as the BMS\_EDB system, but higher  $t_{95\%}$  values.



### 5.2.2. Photorheometer Measurements

To characterize the kinetics of the polymerization, photorheometry experiments were carried out with many different formulations, containing the synthesized initiators, measuring at least triplicates. Approximately 150  $\mu\text{L}$  of the formulations based on Miramer and TEGDMA were transferred via a pipette onto the glass plate of the photorheometer. There a stamp was lowered down towards the glass plate, finally forming a gap with a size of 200  $\mu\text{m}$ . Before and during the UV-light exposure, the stamp was oscillating at a rate of 1 Hz at an amplitude of 1%. The samples were cured isothermally at room temperature via irradiation for 250 s for the TEGDMA formulations and 400 s for the Miramer-based ones, using a 320-500 nm UV-light source. During the photopolymerization, the double bond conversion was monitored in real time with an FT-IR spectrometer (NIR) and the normal force, exerted by the solidifying sample,  $F_N$  is recorded, shown in Figure 81. To calculate the double bond conversion, the band from 6240 to 6100  $\text{cm}^{-1}$  (characteristic methacrylate/acrylate double bond) was integrated and the change of the area recorded over time. After the polymerization, the solid sample films were saved for further leaching tests.

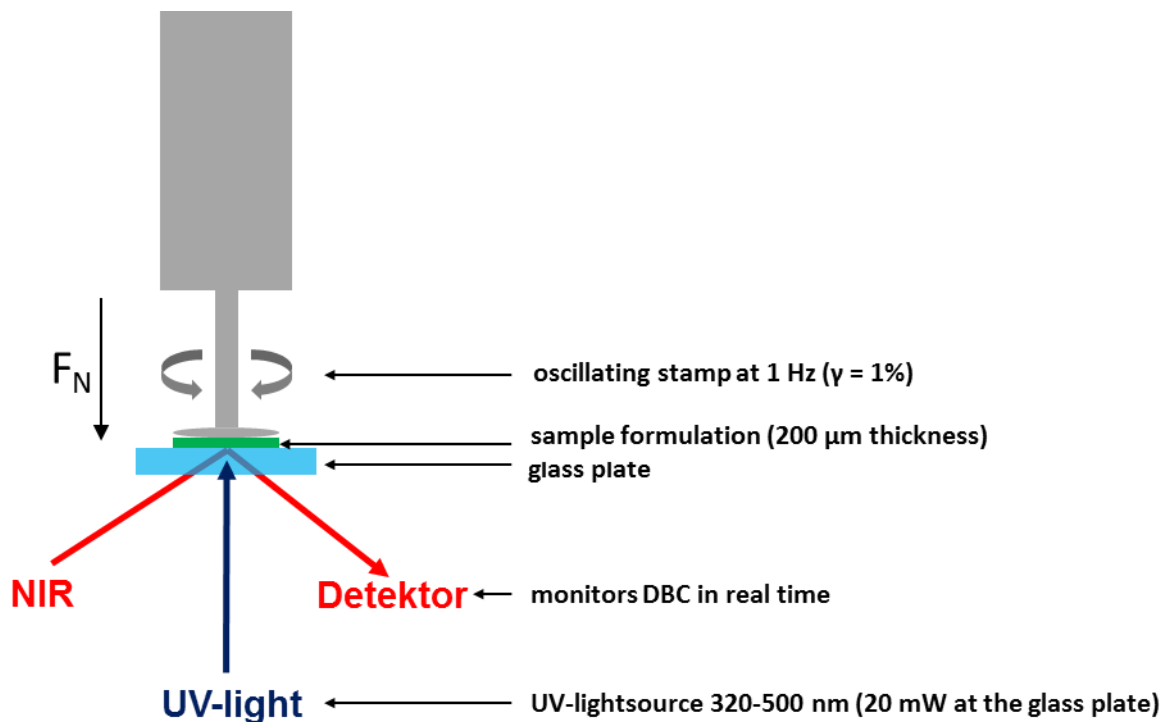


Figure 81: Schematic illustration of the photorheometer

The transition from the liquid formulation to a solid material is called gel point. The more conversion at this point in time is achieved, the higher is usually the resulting normal force, exerted by the polymerizing sample due to shrinkage. At the gel point also the storage and the loss modulus intersected. To cover 95% of the total double bond conversion (DBC), a certain time was needed ( $t_{95\%}$ ). Short  $t_{95\%}$  were aimed, to limit the exposure time and energy requirement for the curing of a sample. One exemplary measurement curve is shown per monomer in Figure 82 for Miramer and in Figure 83 for TEGDMA.

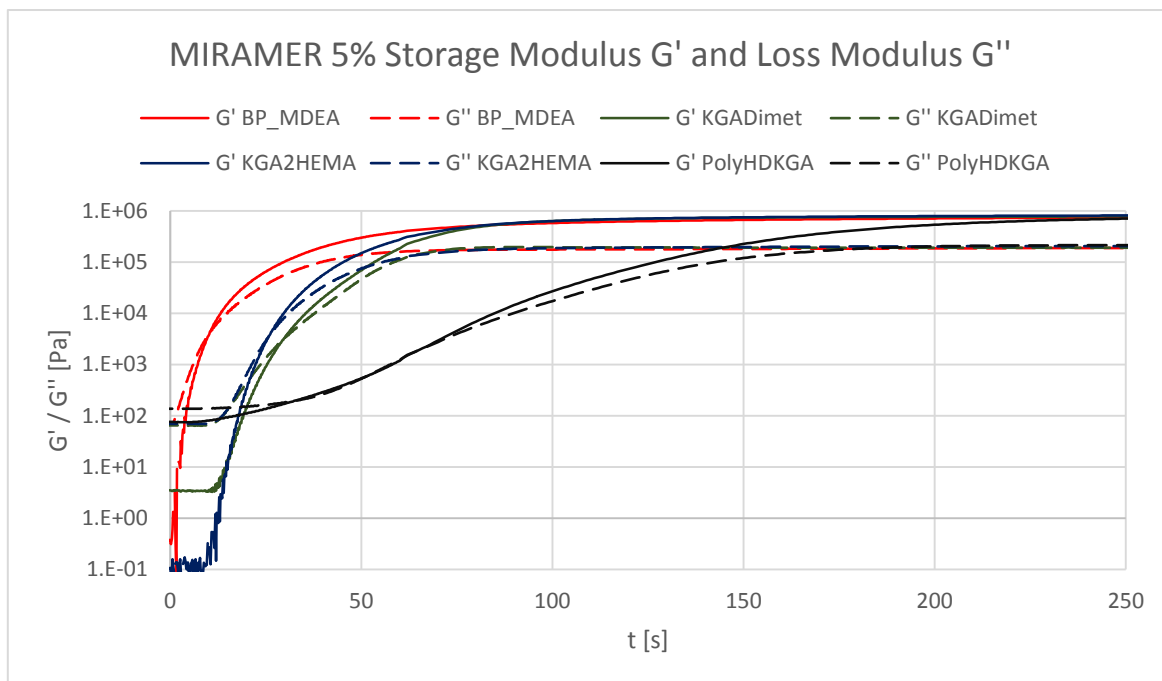


Figure 82: Photorheometer data in the monomer Miramer

In this time resolved graph, the first noticeable difference were the kinetics of the PolyHDKGA sample. The  $G'$  and  $G''$  values intersect significantly later in time, compared to the other three samples measured, due to the size of the polyester. There was less mobility and practical no diffusion in the liquid formulation possible for these long polyester chain, unlike the smaller molecules' behavior. Also the gradient was changing much slower at the beginning of irradiation. PolyISOKGA could not be cured in Miramer irradiating with  $20 \text{ mW/cm}^2$  light intensity.

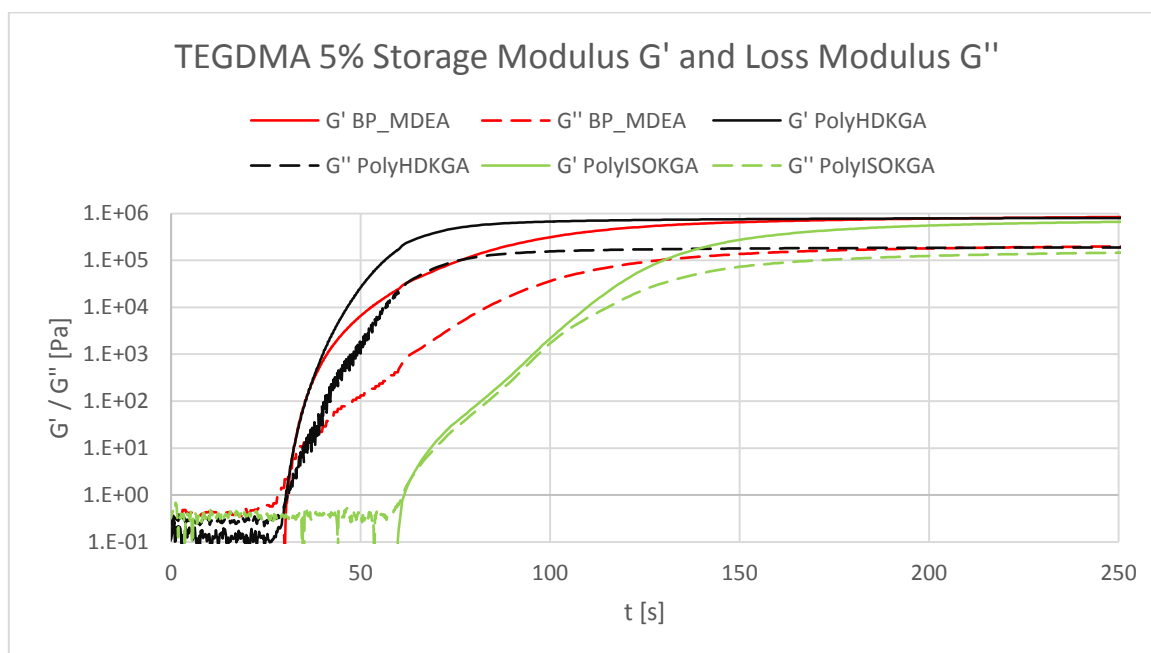


Figure 83: Photorheometer data in the monomer TEGDMA

This problem was solved with the change of the monomer. Switching to TEGDMA, the kinetics of the polymerizations changed for the polymeric PolyHDKGA completely. Decreasing from a gel point at 72 s in Miramer to 32 s in TEGDMA. Also the polymeric PolyISOKGA could now react with the more polar monomer.

### Miramer Formulations

The first series of tests was performed with the formulations based on Miramer.

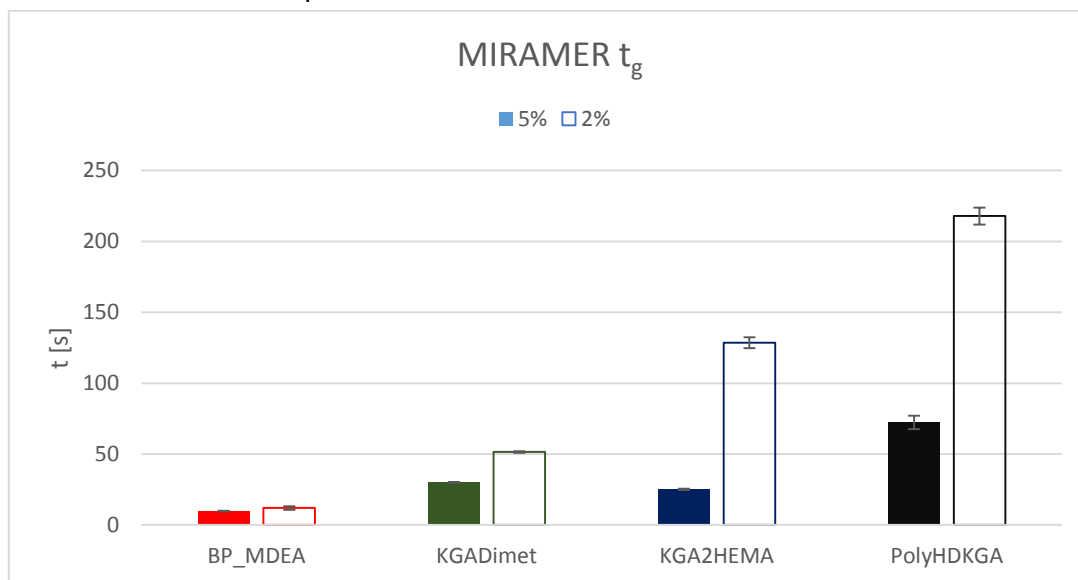


Figure 84: Time to reach the gel point in Miramer

The reference system BP\_MDEA reaches the gel point  $t_g$  (Figure 84) the fastest, within under 10 s, followed by the KGA2HEMA and KGADimet formulations. With more than 70 s. PolyHDKGA reached the gel point the slowest in this comparison, due to the decreased amount of crosslinking moieties. Interestingly the 2% formulation of KGA2HEMA reached its gel point after the double amount of time compared to KGADimet. The lower initiator concentration seems to shift the influence of reaching the liquid to solid transfer, from the more crosslinking KGA2HEMA to the more reactive and sterically unhindered KGADimet initiator, as previous photo-DSC measurements had shown. Therefore the KGADimet reacted faster, and formed a solid polymer network more efficient than the KGA2HEMA could do with its two additional crosslinkable moieties. At 5% concentration this effect was inverse.

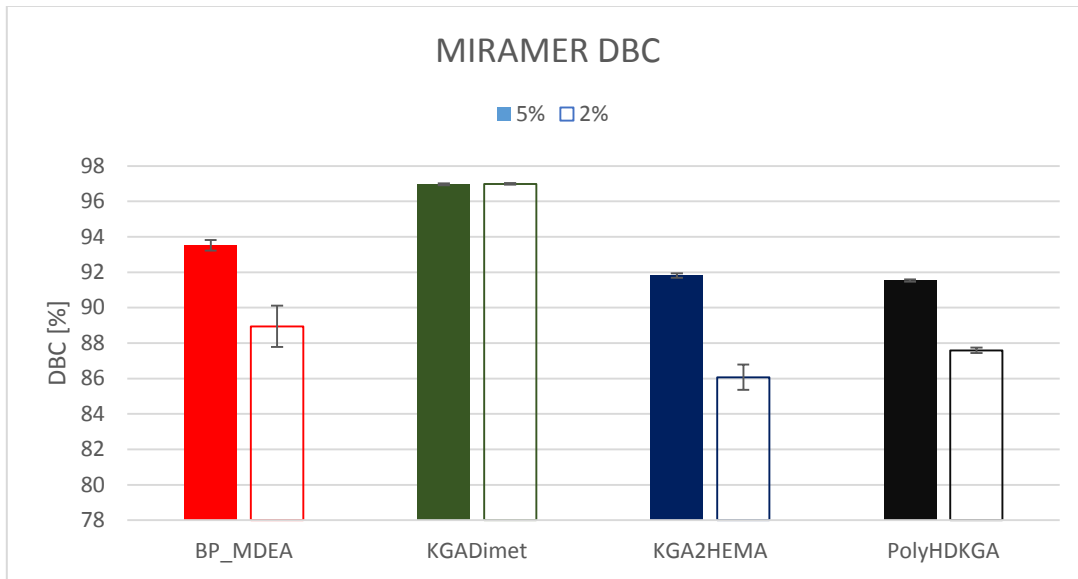


Figure 85: Total double bond conversion in Miramer

Interestingly a total double bond conversions of 97% was achieved by the KGADimet system in and 5 mol%, outperforming the reference system and the other two  $\alpha$ -ketoglutaric acid-based photoinitiators. For the other three samples, conversions between 92 and 94% were reached, with a trend to lower conversions for the 2% formulations. This can be explained due to the increased crosslinkable points in the KGADimet initiator molecule, resulting in increased DBC's.

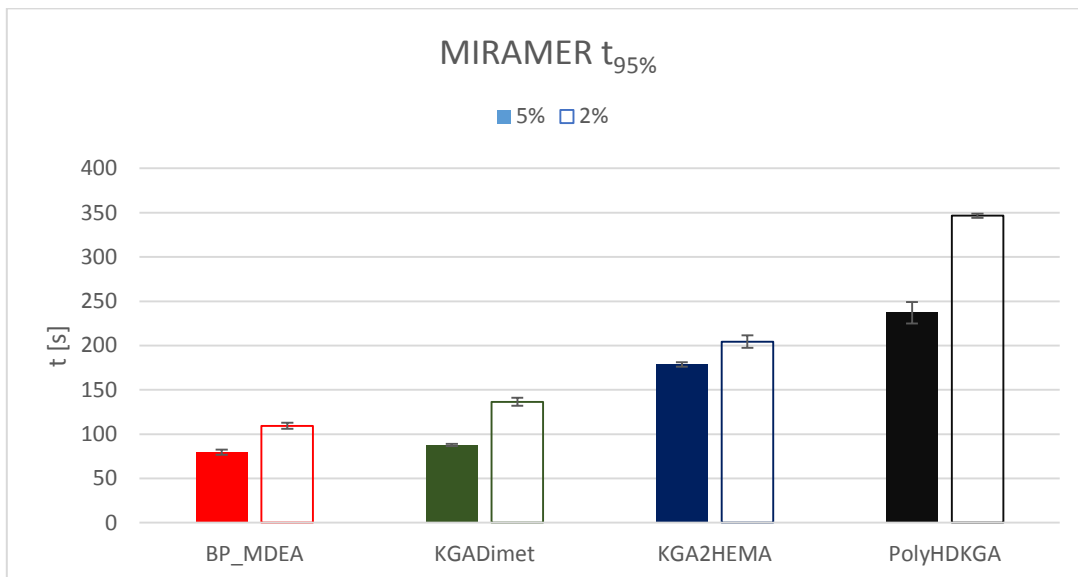


Figure 86: Time to cover 95% of the total conversion in Miramer

The time to cover 95% of the total achieved conversion, in other words the time to finish the majority of the photopolymerization, is shown for all samples in Figure 86. KGADimet was only slightly slower in reaching this dimension compared to the reference system, followed by the KGA2HEMA and PolyHDKGA. All 2% formulations had shown the same trend.

## TEGDMA Formulations

Due to the compatibility issue of PolyISOKGA and Miramer, a second, more polar monomer was tested. So the photorheometer experiments were repeated for the macro-initiators and the reference system in TEGDMA.

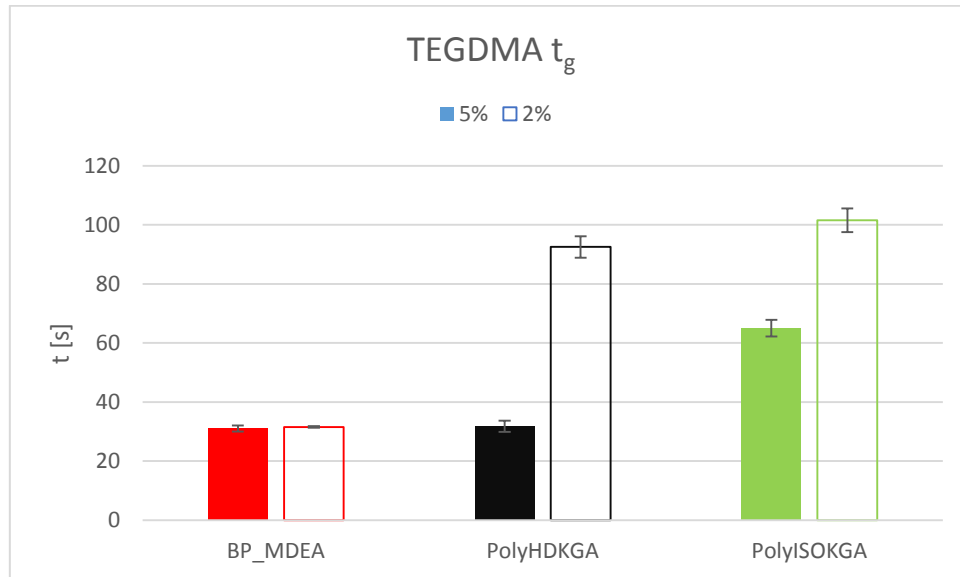


Figure 87: Time to reach the gel point in TEGDMA

In the TEGDMA system (Figure 87), the time to reach the gel point is now comparable for the reference system and the initiator PolyHDKGA. Only the isosorbide-based macromolecular initiator had shown approximately double the amount of time to reach the gel point.

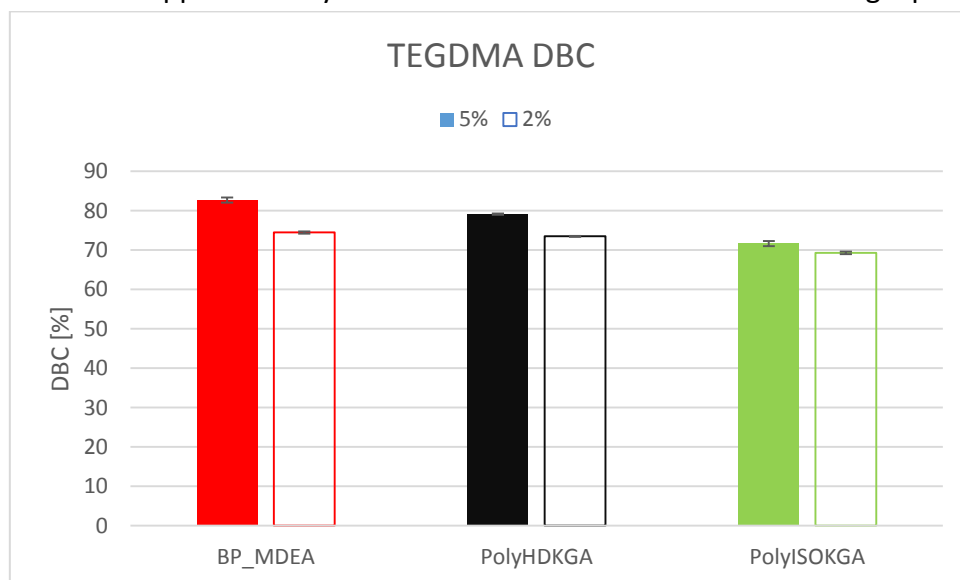


Figure 88: Total double bond conversion in TEGDMA

Overall, the total DBC's, shown in Figure 88, were the highest for BP\_MDEA, followed by PolyHDKGA and PolyISOKGA. Same trend occurred for the 2% formulations. This can be explained due to the high compatibility of the polymeric initiators and TEGDMA.

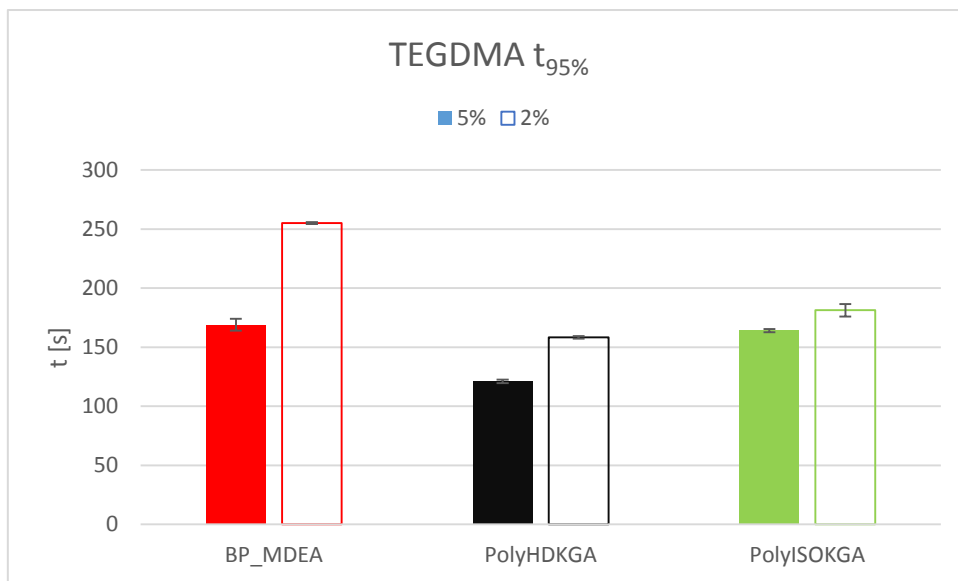


Figure 89: Time to cover 95% of the total conversion in TEGDMA

To cover 95% of the total conversion, the macromolecular PolyHDKGA and PolyISOKGA initiators outperformed the reference system in TEGDMA considering polymerization speed, illustrated in Figure 89. Even the 2% samples achieved faster  $t_{95\%}$  values than the BP\_MDEA in 5% did.

Noticeable was the increased total DBC of the KGADimet formulation at above 97% in Miramer compared to BP\_MDEA.

### 5.3. Photometer Measurements of selected Initiators

A second photometer study was performed. The samples were based on the methacrylate-terminated, polymerizable, polymeric photoinitiators based on  $\alpha$ -ketoglutaric acid and glutaric acid. The selection of these compounds was done in 3.4.

The monomer used for photometry and later mechanical tests was like in the reactivity tests, Miramer® UA5216 from MIWON. Consisting of 40 wt% high molecular weight aliphatic diacrylate (30000 g/mol) and 60 wt% isobornylacrylate (IBA) as reactive diluent. Those two compounds are shown in Figure 90.

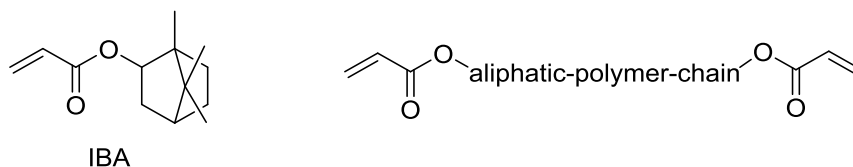


Figure 90: Components of Miramer® UA5216

As a reference, the Type II photoinitiator system, benzophenone (BP) with the co-initiator methyldiethanolamine (MDEA) was selected in a 5 wt% concentration. Due to the fact, that some oligomeric initiators based on  $\alpha$ -ketoglutaric acid need anaerobe inhibitor to prevent polymerization before its usage, 500 ppm of phenothiazine were added. All components of the reference formulation are shown in Figure 91.

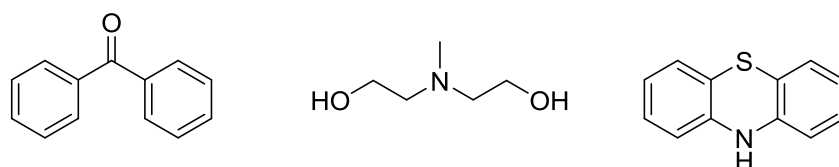


Figure 91: Reference system BP-MDEA with 500 ppm of phenothiazine

According to these weight percentages, the molar ratios (mol%) of all used  $\alpha$ -ketoglutaric acid-based photoinitiators were calculated for the formulations. This was done to ensure the same molar amount of photoinitiator in the formulation, therefore providing a fair comparison. For the macromolecular photoinitiators, the molar ratio was based on the reactive repeating unit of the polyester (Figure 39). All  $\alpha$ -ketoesters were used without co-initiator in this experiment, but with a total of 500 ppm phenothiazine in the finished formulation (Figure 92).

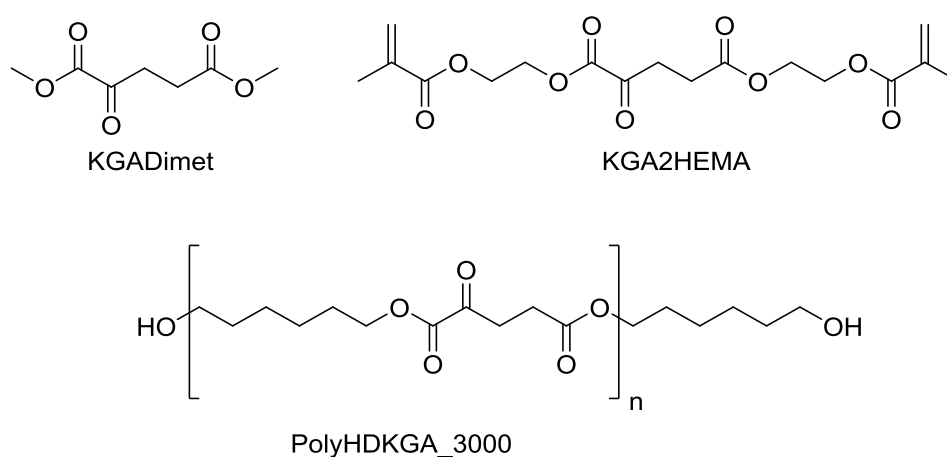
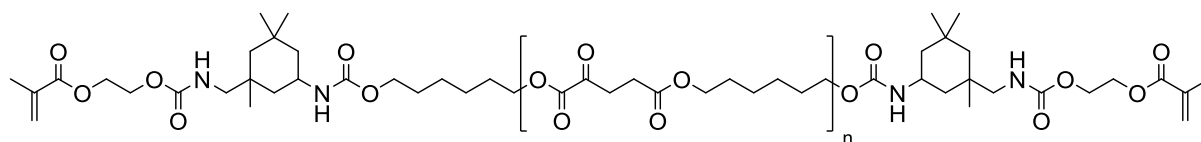


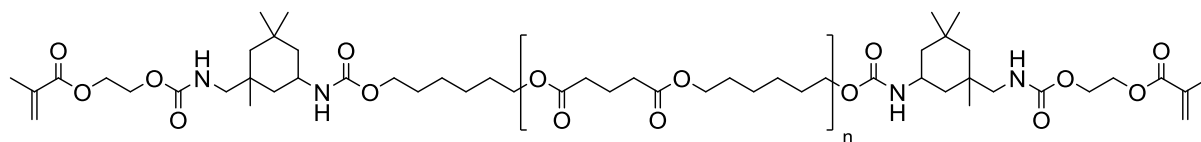
Figure 92: KGADimet:  $\alpha$ -ketoglutaric acid dimethylester; KGA2HEMA:  $\alpha$ -ketoglutaric acid di-2-hydroxyethyl methacrylate; PolyHDKGA: Polyester based on 1,6-hexanediol and  $\alpha$ -ketoglutaric acid (POLYESTER-9)

Also the polyesters with the IPDI-HEMA endgroup attached were considered as test samples for the mechanical properties evaluation and comparison. The modified  $\alpha$ -ketoglutaric acid and hexanediol-based polyesters in all three different molecular weights (3200, 4700 and 9900 g/mol) and the equally modified reference polyester chains based on glutaric acid and hexanediol (3000, 5100 and 13600 g/mol) were tested to compare the mechanical differences and network architectures of initiating polyesters and non-initiating polyester chains. The glutaric acid-based polyesters were only considered as an additive in 5 mol% (calculated with the repeating unit: Figure 39) ratio based on the photoinitiator, which were benzophenone (5 wt%) and MDEA (5 mol%) in this case.

Even though the molecular weights of those endgroup functionalized polyesters (Figure 93) were not exactly 3000, 5000 and 14000 g/mol, it was assumed for better comparability in one diagram. The exact values can be found in the GPC/NMR comparison section (3.4), where the molecular weights were evaluated.



PolyHDKGA-M



PolyHDGA-M

Figure 93: PolyHDKGA-M: Polyester based on 1,6-hexanediol and  $\alpha$ -ketoglutaric acid with the IPDI-HEMA endgroup attached to both ends (POLYESTER-9-2/POLYESTER-12-2/POLYESTER-8-2); PolyHDGA-M: Polyester based on 1,6-hexanediol and glutaric acid with the IPDI-HEMA endgroup attached to both ends (POLYESTER-2-1/POLYESTER-3-1/POLYESTER-4-1);

The photorheometry was performed on the same device and with the same parameters, as described in chapter 5.2.2. As in previous photorheometry experiments in the reactivity test section had shown, the gel point of the PolyHDKGA samples is shifted to an increased time to reach the gel point, due to the immobility of the macromolecule.

#### Small molecules, polymerizable and polymeric Photoinitiators

Firstly, the formulations containing the reference system, the dimethylester, the di-2-hydroxyethyl methacrylate and the macromolecular polyester of  $\alpha$ -ketoglutaric acid were measured and compared.

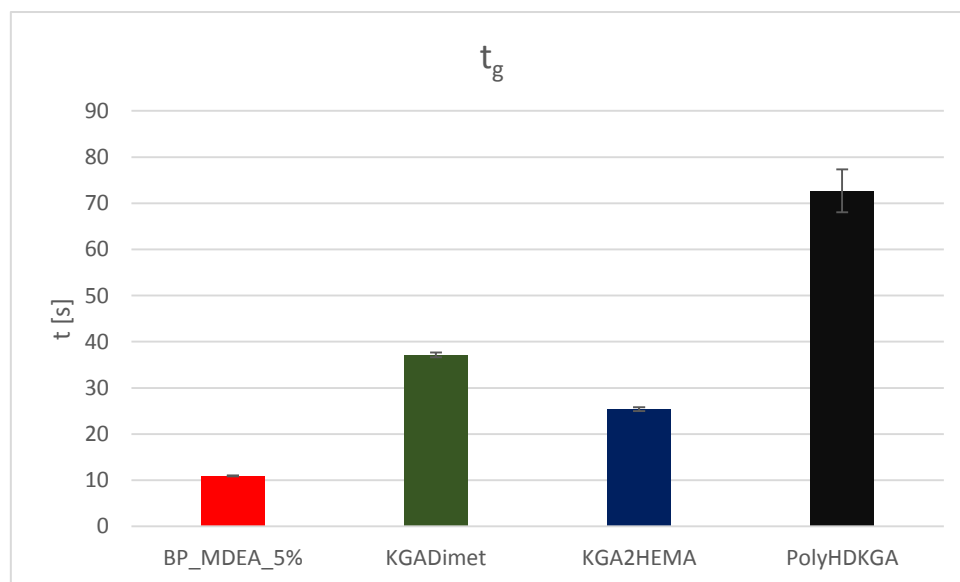


Figure 94: Time to reach the gel point

The time to reach the gel point of the formulations (Figure 94). Like in the previous reactivity study, the results are the same, but with slightly shifted results to increased values, due to the 500 ppm inhibitor added to the system. BM\_MDEA reaches the gel point the fastest, followed



by the highly crosslinkable KGA2HEMA, the KGADimet and at last for the macromolecular PolyHDKGA.

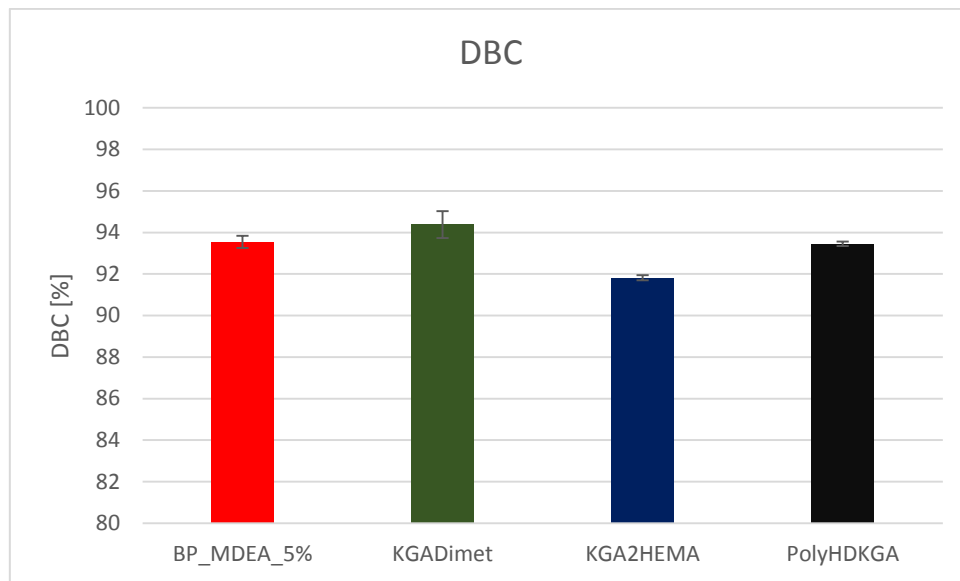


Figure 95: Total double bond conversion

The total DBC (Figure 95) was similar to the previous photorheometer experiments, the highest for the KGADimet at above 94%, followed by the reference system and the PolyHDKGA and at around 92% the KGA2HEMA initiator. Overall, the conversions do not differ in a significant manner, the averaged conversion of all 4 samples was  $93.3 \pm 0.9\%$ .

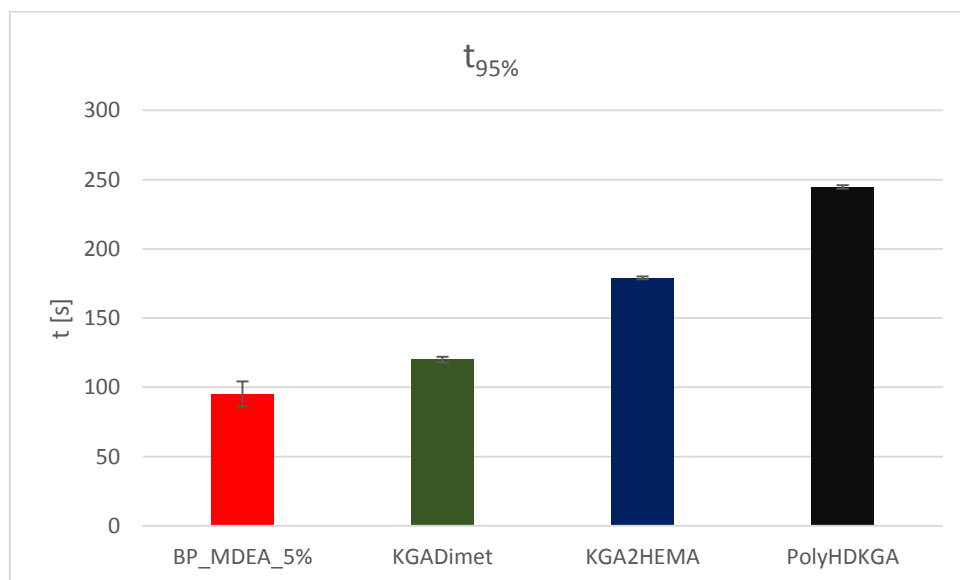


Figure 96: Time to cover 95% of the total DBC

To cover 95% of the total conversion, the reference system was the fastest, which achieved below 100 s, followed by KGADimet, KGA2HEMA and with approximately 250 s the macromolecular PolyHDKGA. The  $t_{95\%}$  values are slightly increased compared to the reactivity study, due to the lack of inhibitor compared to the data (Figure 96).

## Polymerizable, polymeric Photoinitiators

The second measuring series was conducted with the macromolecular, polymerizable initiators based on  $\alpha$ -ketoglutaric acid and glutaric acid.

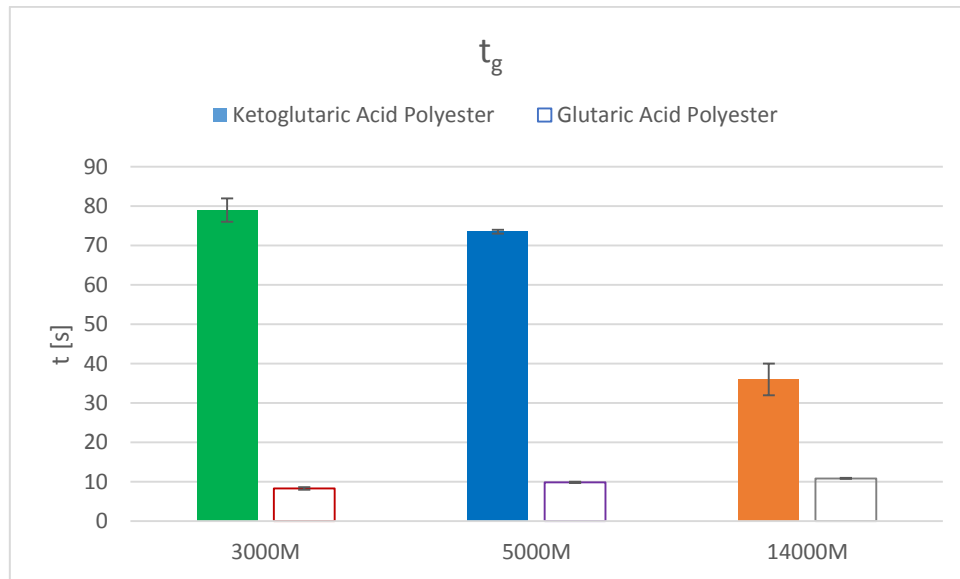


Figure 97: Time to reach the gel point for PolyHD(K)GA products

The formulations, containing the glutaric acid-based polyester and benzophenone-MDEA as photoinitiator system, reached the gel point (Figure 97) after around 10 s, with a trend to shorter times, the lower the molecular weight of the polyesters were, therefore increasing the crosslinking density of this network faster. For the  $\alpha$ -ketoglutaric acid-based polyesters, there was a trend visible, the higher the molecular weight of the polyesters are, the faster they reach the gel point. This totally made sense, due to the fast increase of the viscosity, if an already huge polyester chain crosslinks or starts radical polymerization from its initiators in the backbone.

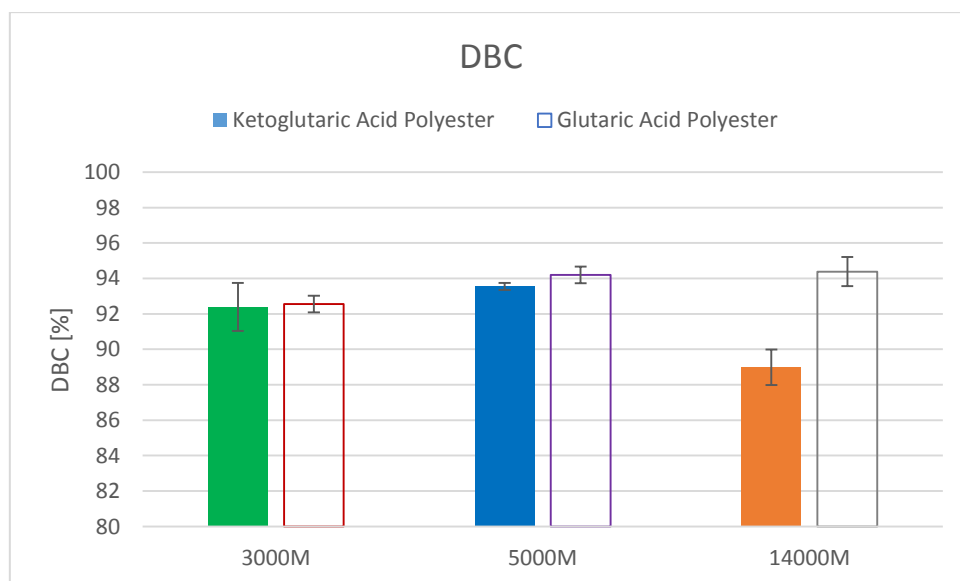


Figure 98: Total DBC for PolyHD(K)GA products

The total double bond conversion of these samples ranged from 92 to 94%, with the exception of the 14000 g/mol  $\alpha$ -ketoglutaric acid-based polyester, which only reached 89% (Figure 98). This can be explained due to the huge polyester chain, which could form coils and therefore masking some of its initiating parts. Also the diffusion in the liquid formulation of such a high molecular weight photoinitiator is very limited.

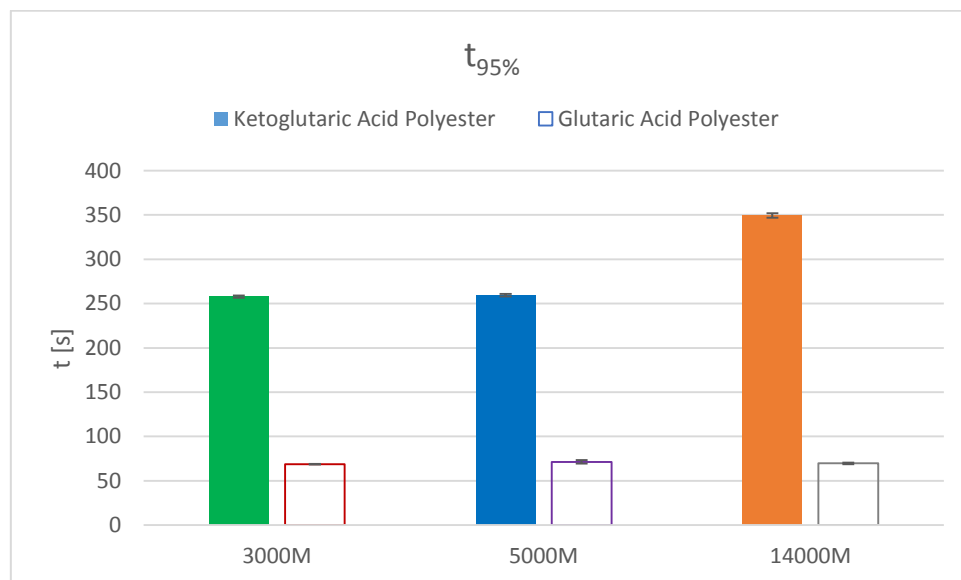


Figure 99: Time to cover 95% of the total DBC for PolyHD(K)GA products

In terms of speed, the polymerization was at 95% of the total DBC at first for the benzophenone-MDEA systems with the additive glutaric acid polyesters at approximately 70 s. The  $\alpha$ -ketoglutaric acid-based polyesters had shown a trend in Figure 99 to increased  $t_{95\%}$  values by increasing the molecular weight and therefore the mobility and ability to diffuse, resulting in a less reactive initiator.

Similar to the reactivity study, KGADimet achieved the highest total conversion during the measurements. Also the shift of the gel points to shorter times, by increasing the molecular weights of the modified polyesters, was visible. The  $t_{95\%}$  values and accordingly the curing speed, was the faster, the lower the molecular weight of the polymeric, polymerizable photoinitiators.

#### 5.4. Mechanical Tests

To determine the mechanical properties of the synthesized  $\alpha$ -ketoglutaric acid-based initiators, including the polymerizable initiators, macromolecular initiators, the combination of both approaches (polymerizable, macromolecular initiators) and derivatives of the di-acid, were used in different concentrations in a monomer formulation for radical photopolymerization. The selection of compounds was done in chapter 5.3. Therefore these measurements should result in information about the glass transition, the storage modulus at elevated temperatures, tensile strength, elongation at break and impact resistance.

The first approach (Figure 100) focused on small molecules, equipped with polymerizable endgroups (a). This concept depends on self-initiating molecules, which are able to covalently bind themselves to the network via crosslinking.

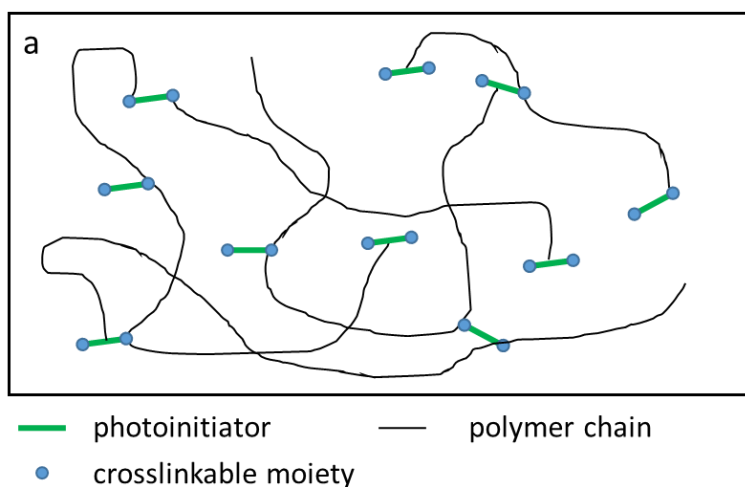


Figure 100: Immobilization via crosslinking

The second concept of non-migratable  $\alpha$ -ketoglutaric acid-based photoinitiators was, to synthesize long polyester chains. The initiators stay in the polyester backbone (b), while growing branches from the alternating photoinitiator building blocks. Therefore the initiator is immobilizing itself due to its molecular weight, even if there is no initiation at a chain (Figure 101).

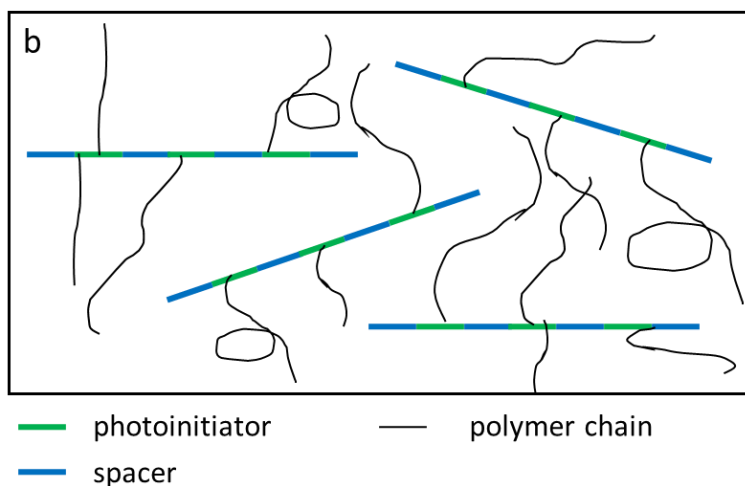


Figure 101: Immobilization via molecular weight

It is also possible to combine both concepts to achieve immobilization due to the high molecular weight and covalent binding to the polymer network via polymerizable endgroups (c) (Figure 102).

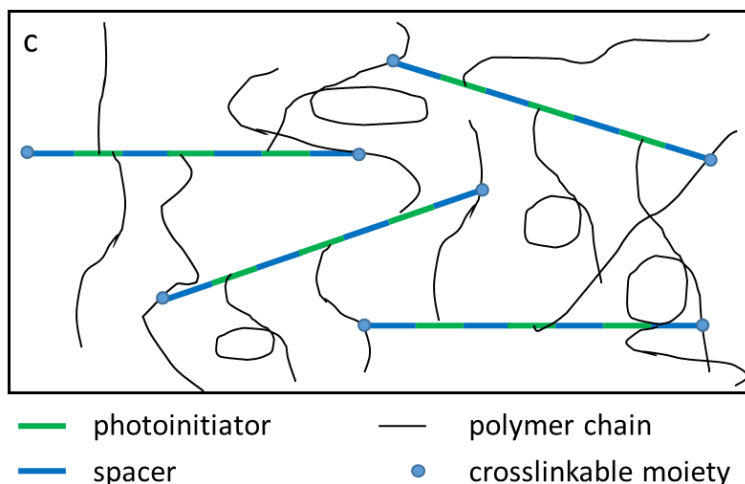


Figure 102: Immobilization via molecular weight and crosslinking

As a reference system serves a commercial Type II photoinitiator like benzophenone, which's majority stays unreacted in the polymer matrix (d), therefore can migrate out over time. Only a few molecules are able to initiate the polymerization, therefore covalently bond themselves to the network (Figure 103).

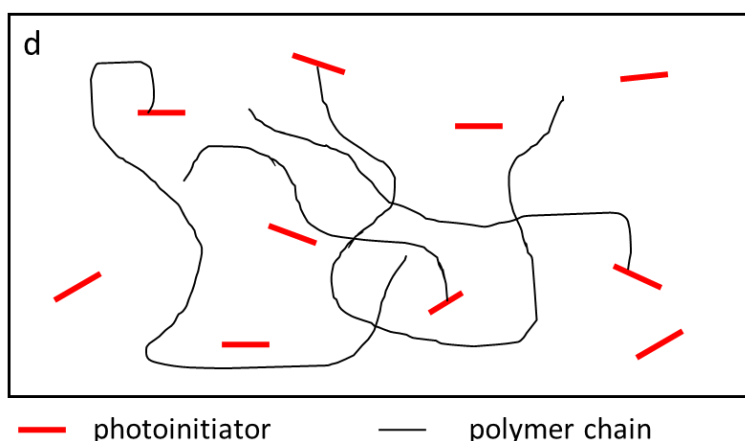


Figure 103: Reference system with e.g. benzophenone

### Polymerizable $\alpha$ -Ketoglutaric Acid-based Initiators (a)

The first approach focuses on low molecular weight  $\alpha$ -ketoglutaric acid-based di-esters, which do not exceed 500 g/mol to guarantee high mobility and movement on a molecular level in the polymerizing formulation and therefore an increased reactivity compared to the rather immobilized polyester chains from the first approach. To permanently crosslink those di-esters additional to the radical polymerization starting center at the carbonyl next to the ester, polymerizable endgroups, like methacrylates, are attached to the initiator molecule (Figure 104).

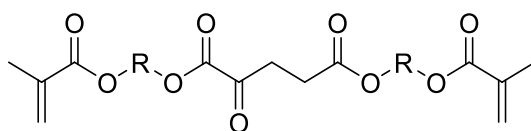


Figure 104:  $\alpha$ -Ketoglutaric acid-based di-ester with methacrylate endgroups ( $R = \text{aliphatic spacer}$ )

This kind of initiator contains up to four possible points, where monomers can interact, during the radical polymerization. One or two radical starting centers, depending if it is inter- or intramolecular hydrogen abstraction, and 2 crosslinkable endgroups. A highly crosslinked network can be achieved via the addition of this photoinitiator to a monomer formulation. The hydrogen abstraction is more likely to happen intermolecular, but the intramolecular case (dashed arrow) could also be obtained (Figure 105).

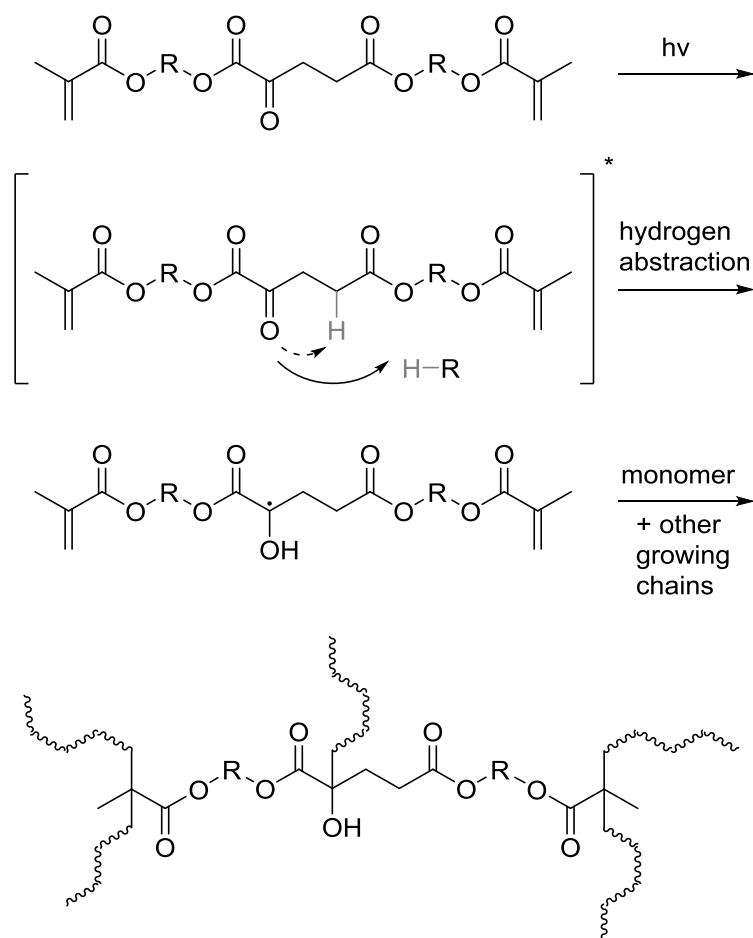


Figure 105: Polymerizable  $\alpha$ -ketoglutaric acid-based di-ester photoinitiator

### Macromolecular $\alpha$ -Ketoglutaric Acid-based Initiators (b)

To achieve a compound, which is capable of staying in the cured polymer matrix after UV-exposure. A molecular weight of above 500 g/mol leads to low migration, while exceeding 1000 g/mol is basically migration-free<sup>34</sup>, therefore polyesters based on  $\alpha$ -ketoglutaric acid were selected to weigh around 3000, 5000 and 10000 g/mol to ensure low migration. Also the effects of the polyester chain length are studied in terms of reactivity and migration capability (Figure 106).

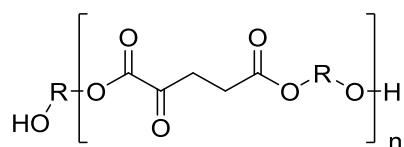


Figure 106:  $\alpha$ -Ketoglutaric acid-based polyester chain (R = aliphatic spacer)

In theory this concept is generating “grafting from” polymer networks, due to the photoinitiator in the backbone, which acts as a starting point for a further propagating polymer chains. The hydrogen abstraction can be inter- or intra-molecular, favoring the first process over the second in polar environment.<sup>39</sup> The result is a highly branched polymer chain, which is not able to migrate anywhere in the cured polymer network (Figure 107)

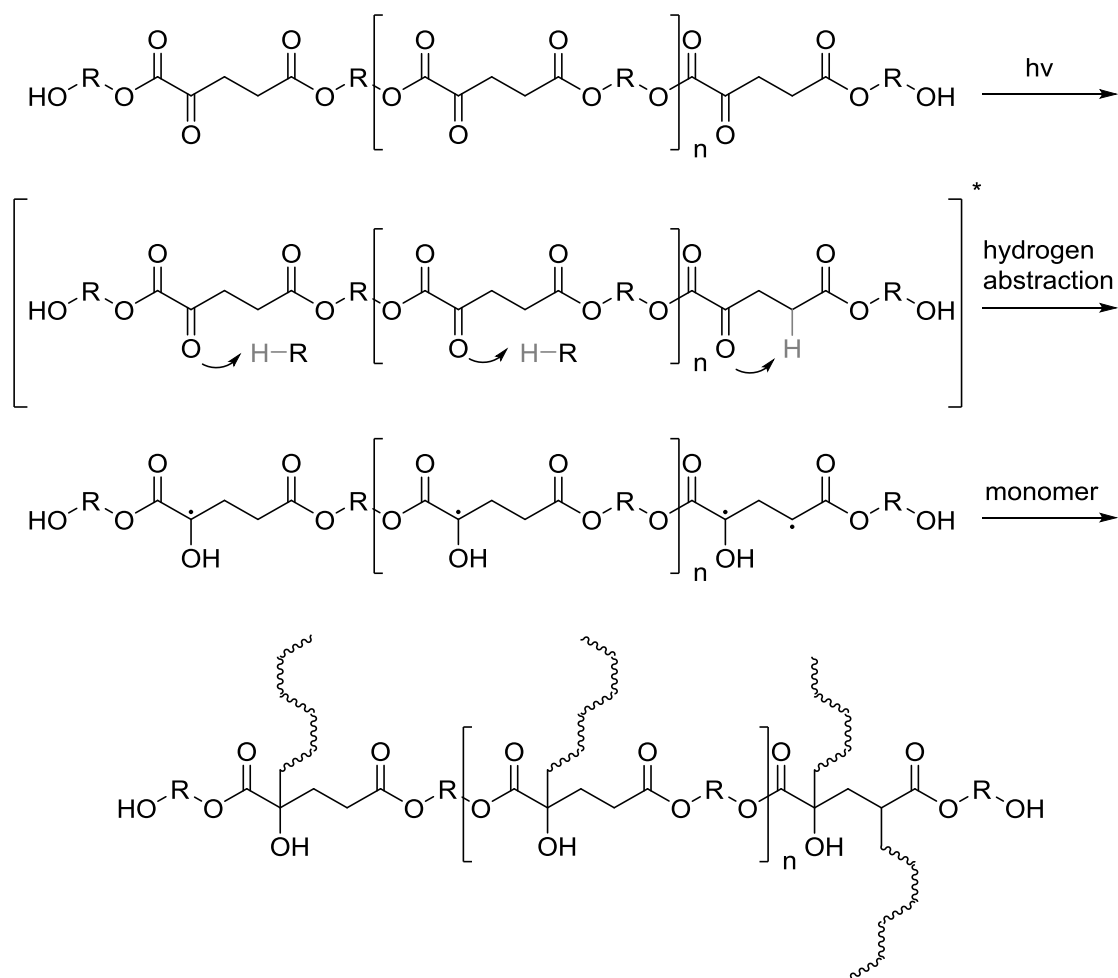


Figure 107: “Grafting from” mechanism of  $\alpha$ -ketoglutaric acid-based polyester photoinitiators

### Polymerizable, Macromolecular $\alpha$ -Ketoglutaric Acid-based Initiators (c)

Thirdly, there is a concept, which combines the two previous ones. A macromolecular photoinitiating polyester chain based on  $\alpha$ -ketoglutaric acid and a diol, containing polymerizable endgroups like methacrylates, is the result of this combination. Molecular weights of 3000, 5000 and 10000 g/mol are aimed, like in the first approach. This initiators are capable to generate, during irradiation, many initiating radicals and are therefore immobilized

in the polymer network via their sheer molecular weight, branches growing from the polyester chain and the crosslinkable endgroups (Figure 108).

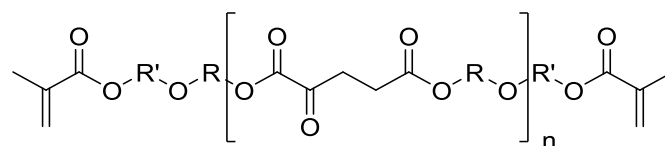


Figure 108:  $\alpha$ -Ketoglutaric acid-based polyester chain with crosslinkable endgroups ( $R, R' =$  aliphatic spacers)

The advantage of these macromolecular initiators to the “grafting from” only concept is, that there are additional crosslinkings via the polymerizable methacrylates. Therefore immobilization of the photoinitiator should be increased much more. If there is a need to immobilize an already very low migration macromolecular photoinitiator further via methacrylates will be investigated too, due to the increased synthetic expenditure. The initiation and crosslinking process of such a compound, based on  $\alpha$ -ketoglutaric acid, is illustrated in Figure 109.

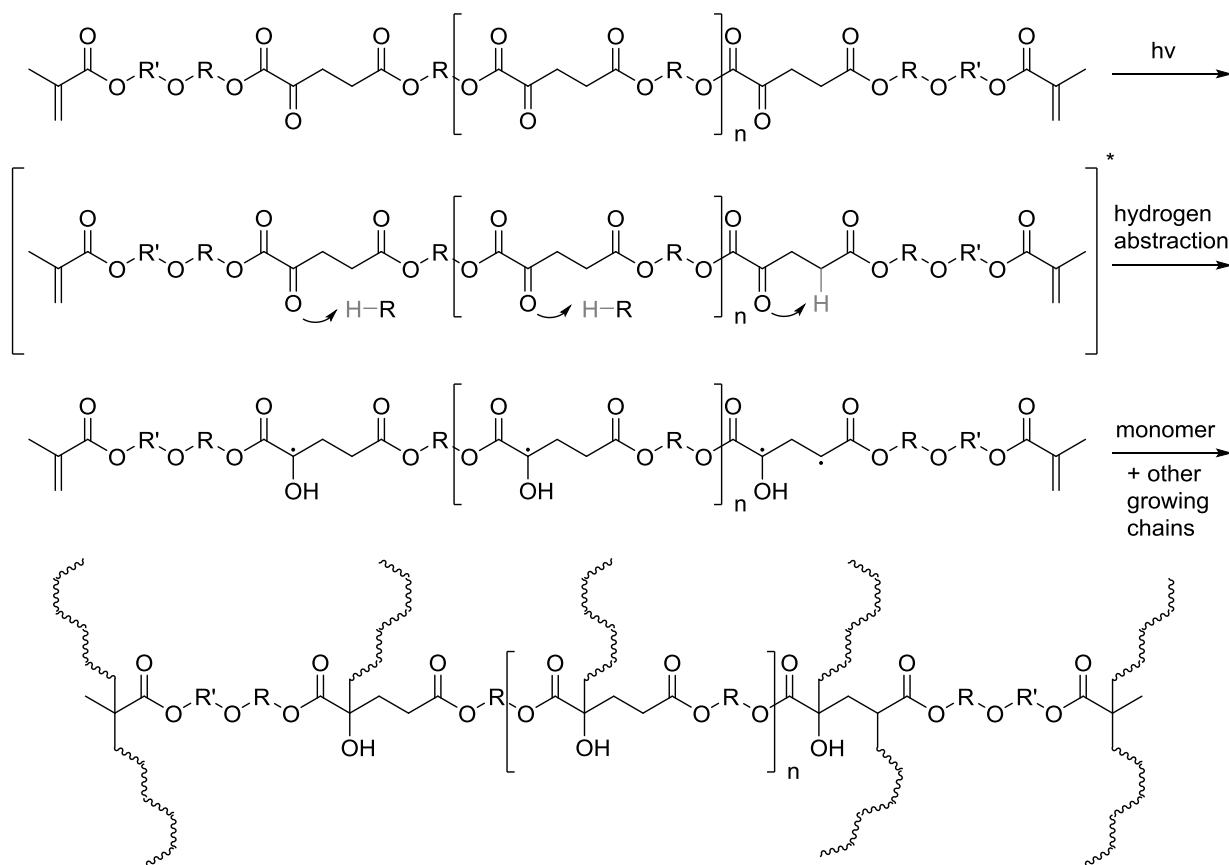


Figure 109: Polymerizable, macromolecular  $\alpha$ -ketoglutaric acid-based polyester photoinitiator



#### 5.4.1. Dynamic Mechanical Thermal Analysis

The selection of compounds and the preparation of the formulations was done in chapter 5.3. To determine the mechanical properties of the samples, for an instance glass transition temperature or storage modulus at elevated temperatures and at room temperature, a dynamic mechanical thermal analysis (DMTA) measurement was performed. Therefore samples with a specific geometry had to be manufactured, based on the Miramer formulations. To achieve those specific shapes, molds designed for DMTA experiments were filled with the liquid formulations and cured in an UV-oven with no wavelength filter, as a realistically procedure used by industry. The exposure to the UV-light was limited to 300 s per side, resulting in a total irradiation time of 600 s. The now solidified samples were grounded into shape to conduct the measurement. The temperature range was defined from -100 °C to 200 °C to monitor the mechanical properties over a broad application area, and the oscillating clamping tool was set to 1 Hz at an amplitude of 1%, illustrated in Figure 110.

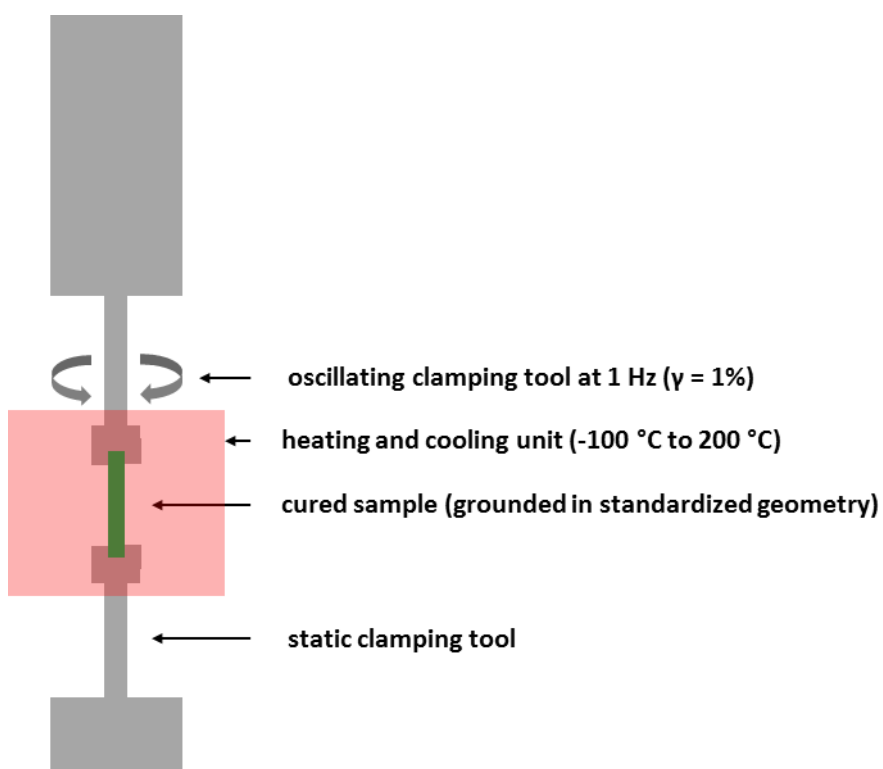


Figure 110: Schematic illustration of the DMTA measurement

This device monitored the loss modulus, storage modulus and the dissipation factor  $\tan\Delta$  over the temperature and therefore could evaluate the glass transition temperature  $T_g$  of a material. Also the storage modulus could be defined for certain points in the temperature scale, such as the modulus at 25 °C or at 150-160 °C, which corresponds to the rubbery state of this material. Two exemplary measurement curves are illustrated in Figure 111 and Figure 112.

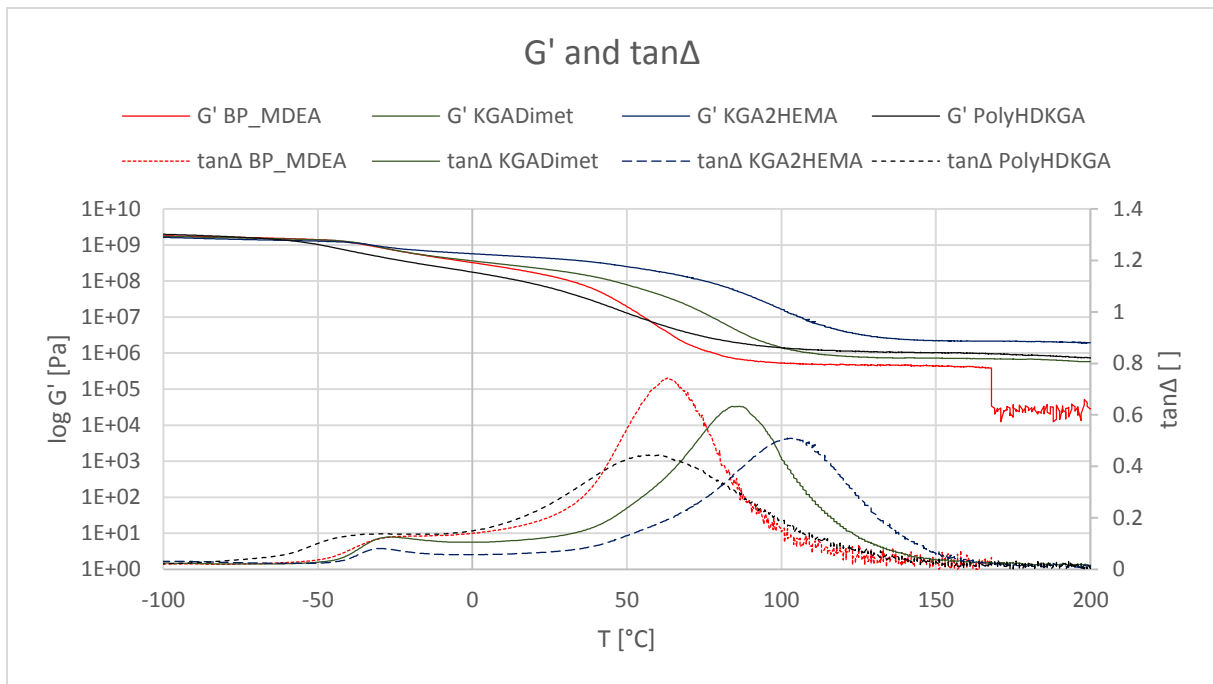


Figure 111: Storage modulus  $G'$  and dissipation factor  $\tan\Delta$ , evaluated via DMTA measurement

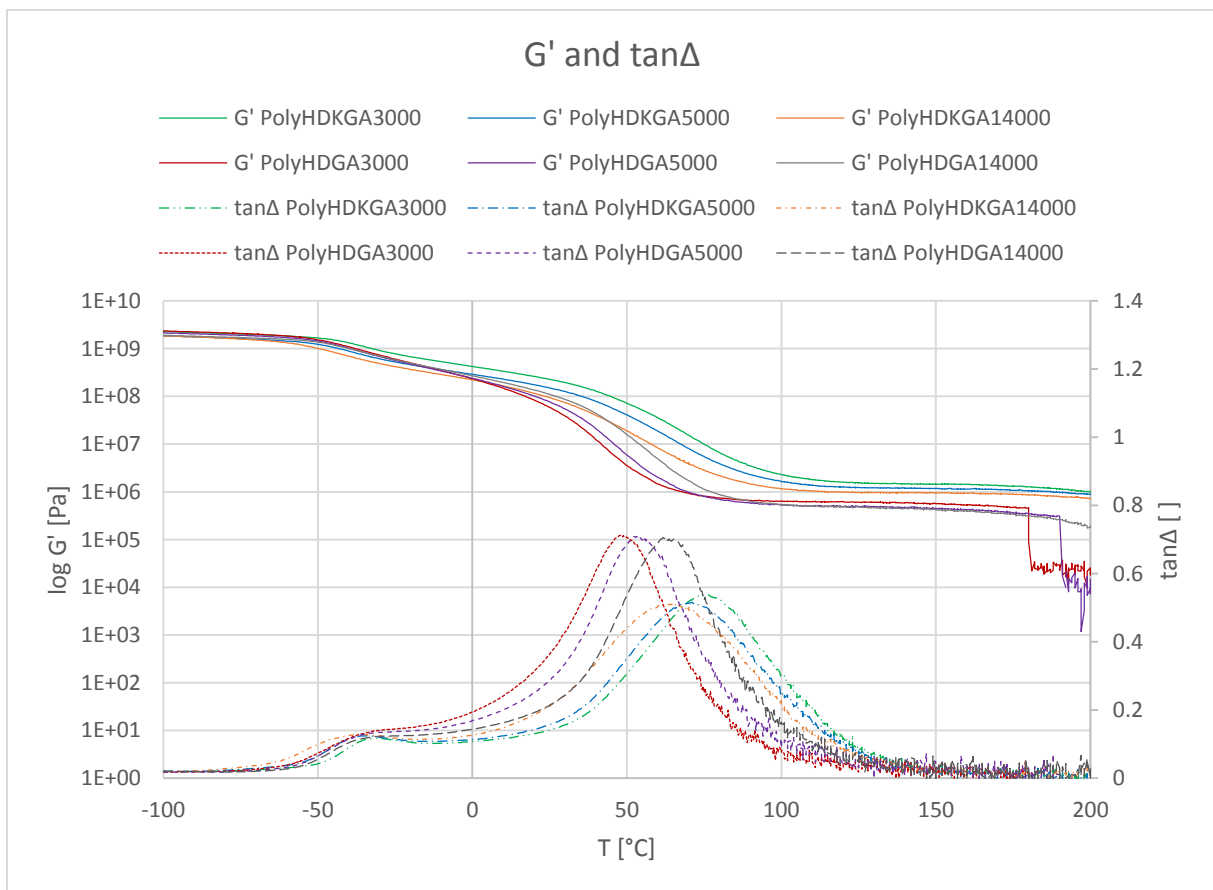


Figure 112: Storage modulus  $G'$  and dissipation factor  $\tan\Delta$ , evaluated via DMTA measurement

The glass transition temperature was defined as the maximum  $\tan\Delta$  during a measurement. Narrow peaks represent a homogeneous distribution of the polymer chains. If the sample

broke during the measurement, at this certain temperature a jump in the storage modulus like the BP\_MDEA system in Figure 111 at around 170 °C can be seen.

### Small molecules, polymerizable and polymeric Photoinitiators

At first, the experiments were conducted with the reference system benzophenone-MDEA, the dimethylester of the  $\alpha$ -ketoglutaric acid, the polymerizable initiator KGA2HEMA and the macromolecular initiator PolyHDKGA.

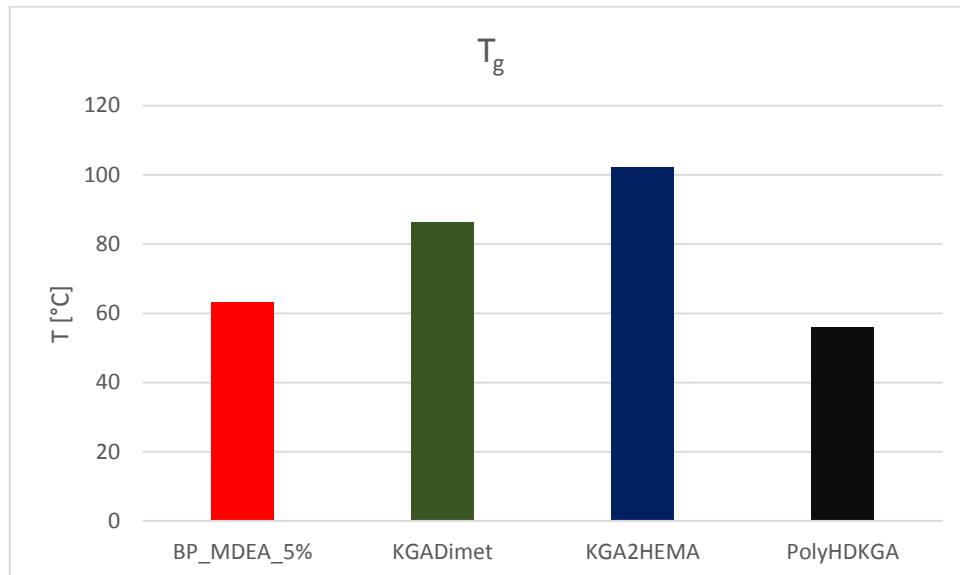


Figure 113: Glass transition temperature

The glass transition temperature, shown in Figure 113, is amongst other things correlated to the crosslinking density in the resulting polymer network, achieved by a photoinitiator. The reference system reached a  $T_g$  of 63 °C and with the increase of crosslinks this temperature raised. KGADimet, an initiator with up to two starting points for radical polymerization is already 20 °C higher in  $T_g$ , while KGA2HEMA exceeded the 100 °C mark with the same starting points for polymerization, but two additional possible crosslinks at the end of the molecule. PolyHDKGA, which is a flexible polyester with some radical starting point distributed along its chain, decreased the glass transition temperature by 7 °C compared to BP\_MDEA, and therefore acts as a softener in the material.

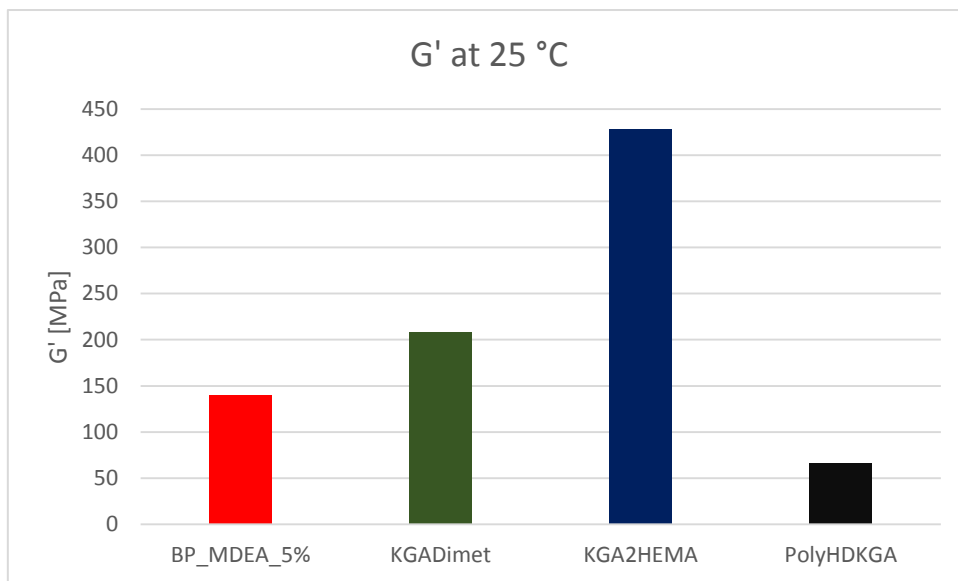


Figure 114: Storage modulus at room temperature (25°C)

As illustrated in Figure 114, the storage modulus at room temperature was around 150 MPa for the BP\_MDEA system. KGADimet increased this value to 200 MPa and the KGA2HEMA even reached above 400 MPa. Only PolyHDKGA as a softener decreased the modulus to approximately 66 MPa.

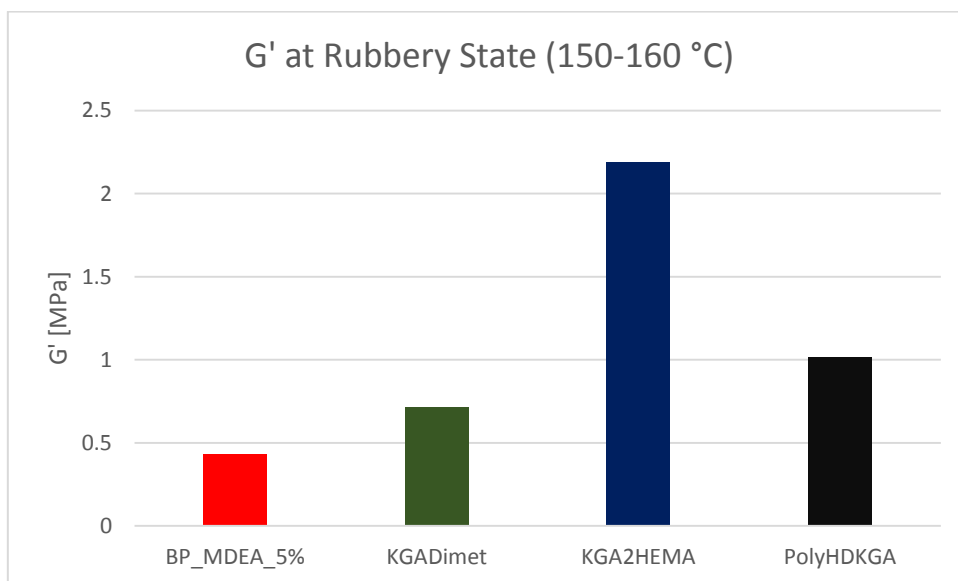


Figure 115: Storage modulus at rubbery state (150-160 °C)

If the storage modulus is considered at elevated temperatures (Figure 115), at the monomers rubbery state, the reference system fell below 0.5 MPa. The denser the crosslinking of the network, the higher the resulting modulus at 150-160 °C. KGADimet, which only provided up to two starting points for radical polymerization, had less crosslinking density compared to PolyHDKGA, which's modulus ended up at approximately 1 MPa. The macromolecular initiator may act as a softener in terms of  $T_g$ , but the branched and high molecular weight polyester containing networks achieved an elevated storage modulus at the rubbery state. KGA2HEMA

outperforms all other sample by the factor of two to four, due to its polymerizable photoinitiator, which could build up dense polymer networks.

### Polymerizable, polymeric Photoinitiators

After the first series of measurements, the  $\alpha$ -ketoglutaric acid and glutaric acid-based macromolecular, crosslinkable polyesters in three different molecular weights were tested.

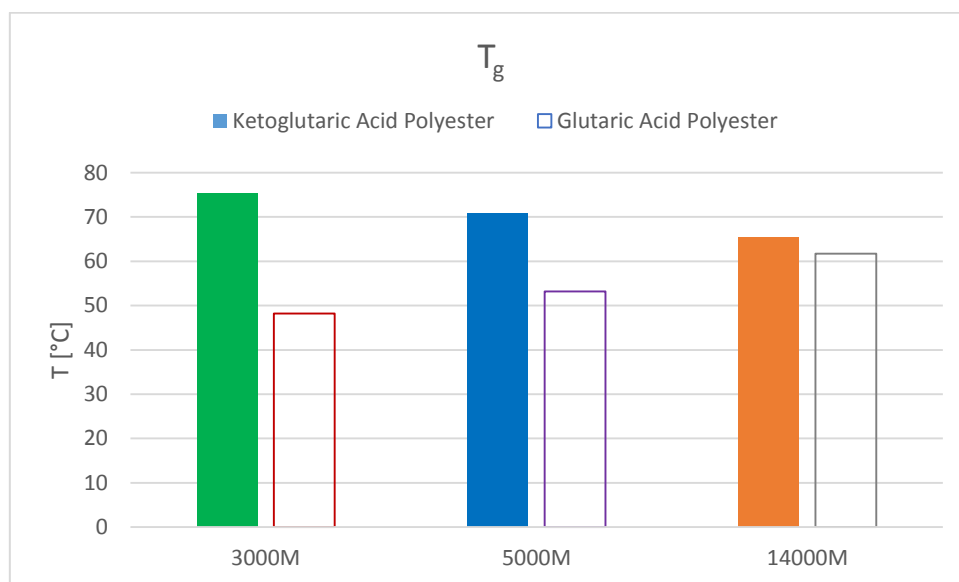


Figure 116: Glass transition temperature for PolyHD(K)GA-M products

Glass transition temperatures (Figure 116) for the  $\alpha$ -ketoglutaric acid-based polyesters were depending on the molecular weight. The smaller a crosslinkable polyester chain, the more crosslinks were possible and the initiators in the backbone also create many branches. Therefore the 3000 g/mol initiator achieved the highest  $T_g$  at around 75 °C, while the 14000 g/mol polyester was only slightly above the reference system, at 65 °C. This trend reverses for the glutaric acid-based polyesters with crosslinkable moieties and could only be explained with the formulation preparation excerpt, shown in Table 32 (underlined values). Due to the fact, that the additive was calculated in molar ratios, based on the repetitive unit in the polyester (Figure 39), the shorter the chains get, the more molecular weight is added by the two IPDI-HEMA endgroups. This resulted in an increased weight used for the formulation compared to the longer chain polyesters, where this endgroup did not make that much difference, due to the already high molecular weight by the chain itself.

Table 32: Excerpt of the preparation of the formulations containing glutaric acid-based polyesters as additives; POLYESTER-2 = 3000 g/mol; POLYESTER-3 = 5100 g/mol; POLYESTER-4 = 13600 g/mol

sample	additive [mg]	initiator [mg]	monomer [mg]	co-Initiator [mg]	inhibitor [mg]
PolyHDGA_3000M	871	600	<u>10136</u>	392	6
PolyHDGA_5000M	782	600	<u>10226</u>	392	6
PolyHDGA_14000M	741	600	<u>10267</u>	392	6

The result of this calculation was an increased amount of monomer in the formulations with longer polyester chains. Therefore the main component of Miramer, the  $T_g$  increasing isobornylacrylate (IBA) was in higher percentages present, resulting in elevated glass transition temperatures for high molecular weight glutaric acid-based polyesters.

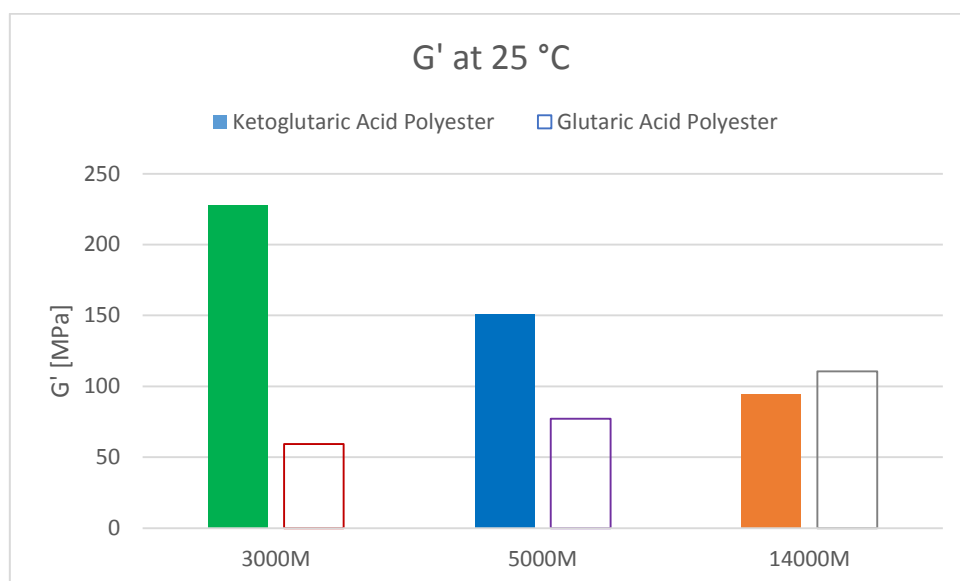


Figure 117: Storage modulus at room temperature (25 °C) for PolyHD(K)GA-M products

The storage modulus at room temperature (Figure 117) was as expected, with the highest value achieved by PolyHDKGA\_3000M, at around 230 MPa. The higher the molecular weight, the lower the modulus at 25 °C, due to the decrease of possible crosslinks in the  $\alpha$ -ketoglutaric acid polyester system. For the glutaric acid-based macromolecular, crosslinkable polyesters, this trend reversed. Approximately 60 MPa were achieved by the 3000 g/mol and up to 111 MPa by the 14000 g/mol additive.

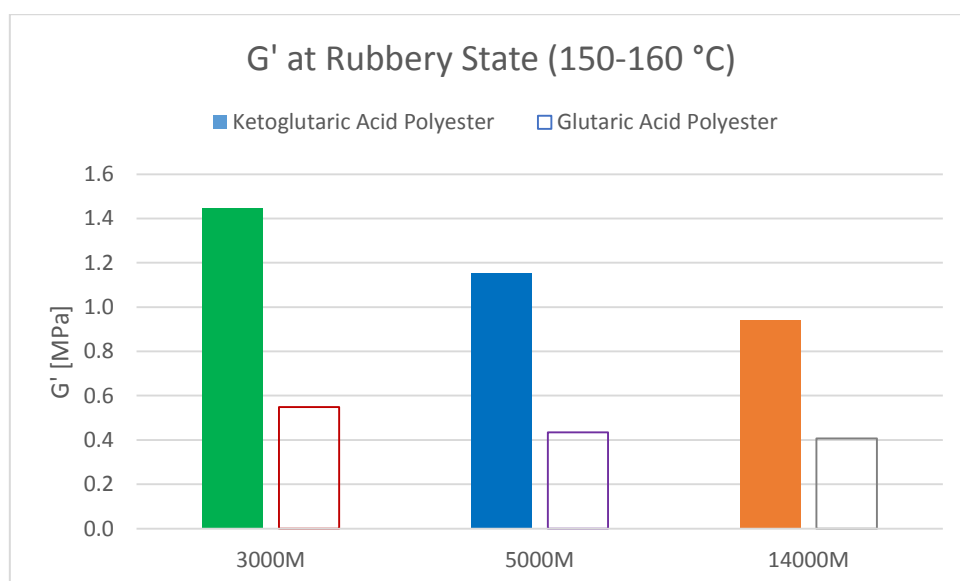


Figure 118: Storage modulus at rubbery state (150-160 °C) for PolyHD(K)GA-M products

Now the  $G'$  at the rubbery state was considered in Figure 118. The storage modulus at these temperatures depends strongly on the crosslinking density, as well as intermolecular forces, such as hydrogen bonding. As expected the crosslinking and hydrogen bonding was much more present in the 300 g/mol polyesters, with a trend to lower moduli for the 5000 and 14000 g/mol samples for both,  $\alpha$ -ketoglutaric acid and glutaric acid-based systems. This also proves, that the crosslinking of the networks were indeed increased for the smaller glutaric acid-based additives.

Overall the  $\alpha$ -ketoester-based photoinitiators performed better than BM\_MDEA samples during the DMTA experiments. Resulting in higher glass transition temperatures and increased storage moduli at 25 °C and 150-160 °C. Especially KGA2HEMA delivered up to four times the modulus of the reference system at the rubbery state and an increase of the glass transition temperature to above 100 °C.

#### 5.4.2. Tensile Tests

The selection of compounds and the preparation of the formulations was done in chapter 5.3. To get even more information about the mechanical properties and network architectures of all samples, after the DMTA study, tensile tests were performed. Therefore samples with a specific geometry had to be manufactured. To achieve those specific shapes, molds designed for tensile tests (ISO 527-2, 5b) were filled with the liquid formulations and cured in an UV-oven with no wavelength filter. The exposure to the UV-light was limited to 300 s per side, resulting in a total irradiation time of 600 s. The now solidified samples were grounded into shape to conduct the measurement. The samples were clamped in two static tools and afterwards the applied force was increased over time, until the sample broke in half. A schematic drawing of a tensile test is illustrated in Figure 119.

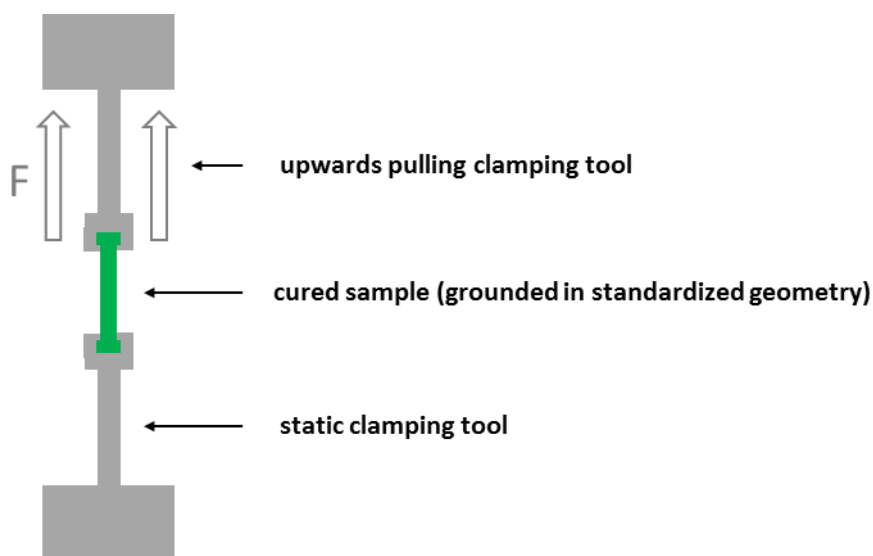


Figure 119: Schematic illustration of the tensile tests

This device evaluates the stress applied to the sample on the y-axis the strain on the x-axis. The resulted stress-strain curve includes information, like the yield strength, where the

applied stress achieves its maximum before the break, and the elongation at break, which describes the maximum elongation of the sample, before the sample snapped. At least triplicates were tested, to ensure reproducibility. One exemplary curve per sample is shown in Figure 120 and Figure 121.

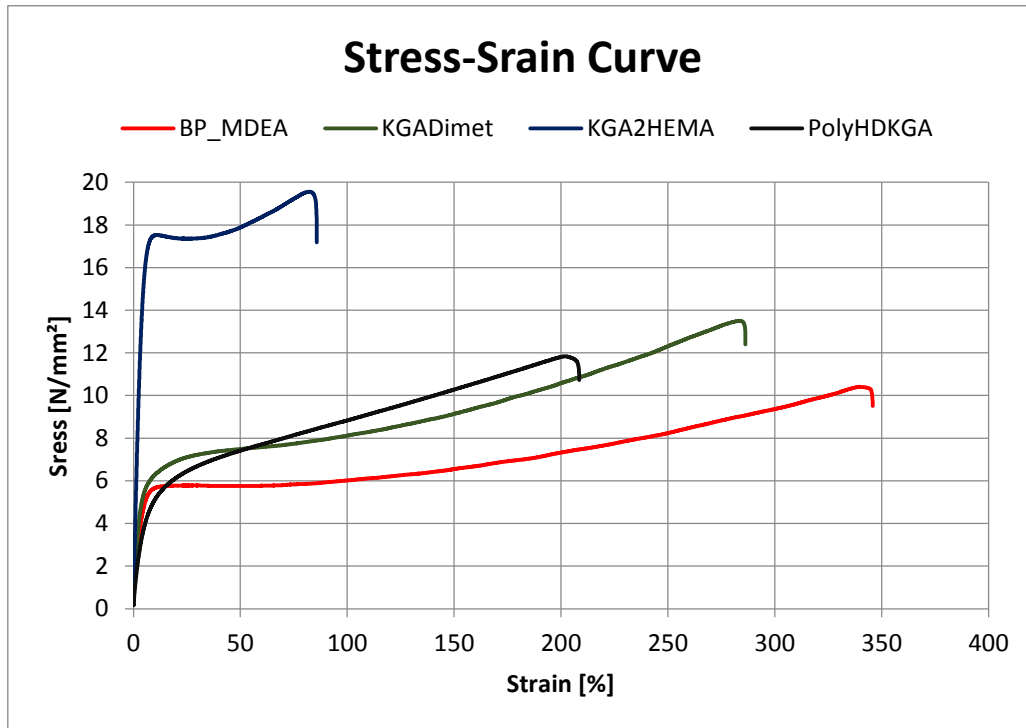


Figure 120: Stress-strain curve

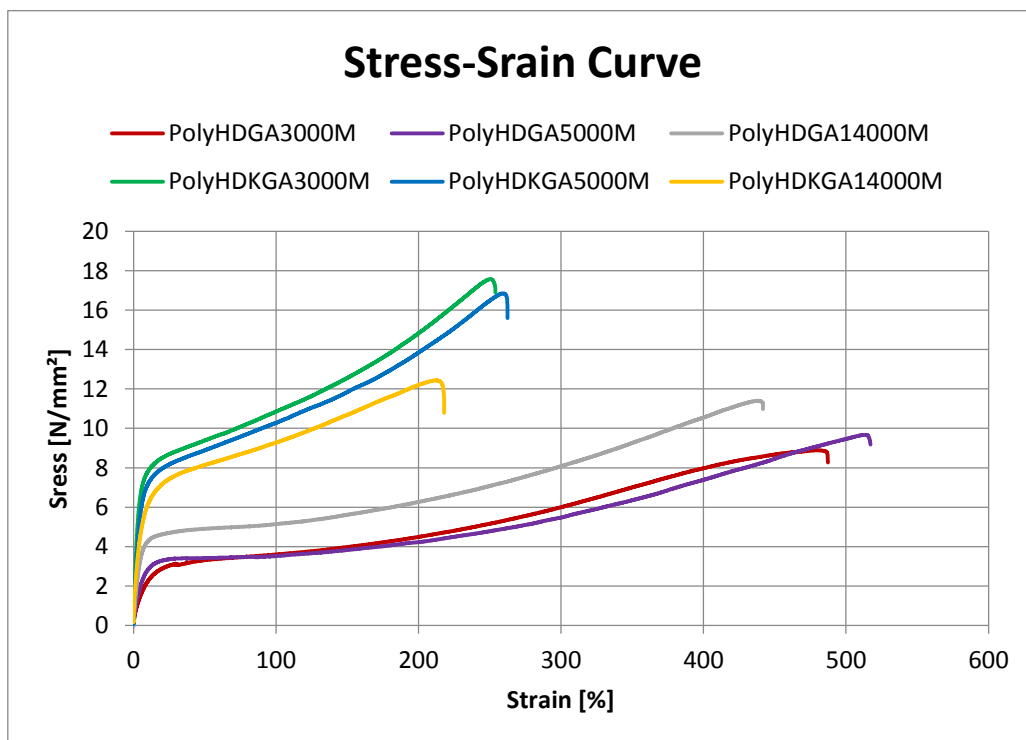


Figure 121: Stress-strain curve of the glutaric acid and  $\alpha$ -ketoglutaric acid-based, polymerizable polyesters



### Small molecules, polymerizable and polymeric Photoinitiators

Firstly, the reference system BP\_MDEA, the KGADimet, the polymerizable initiator KGA2HMA and the macromolecular initiator based on  $\alpha$ -ketoglutaric acid were measured.

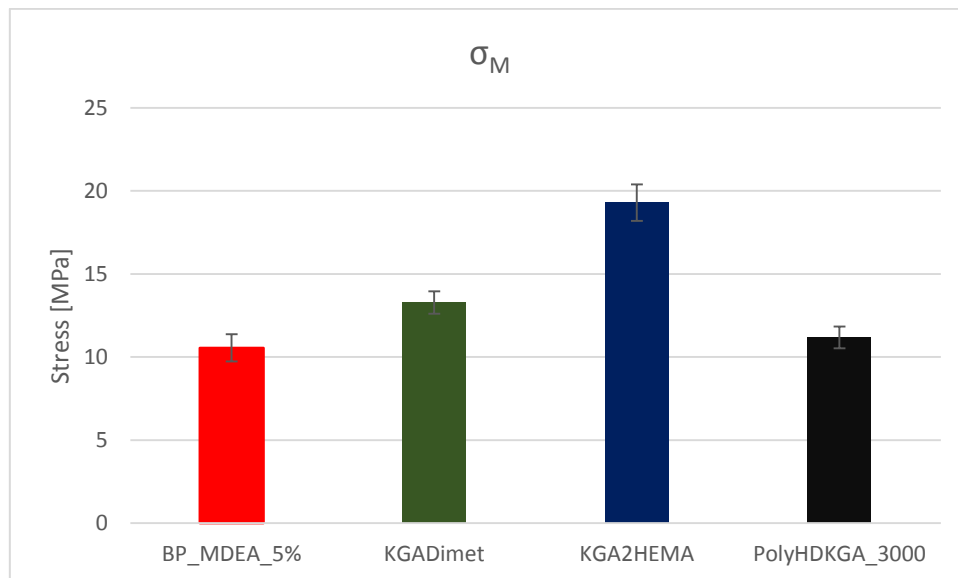


Figure 122: Yield strength

The maximum stress a sample could resist, was around 20 MPa for the densely crosslinked network achieved by the polymerizable KGA2HEMA. Only half of this yield strength was possible for the reference system and the polymeric PolyHDKGA. KGADimet reached values up to 13 MPa (Figure 122).

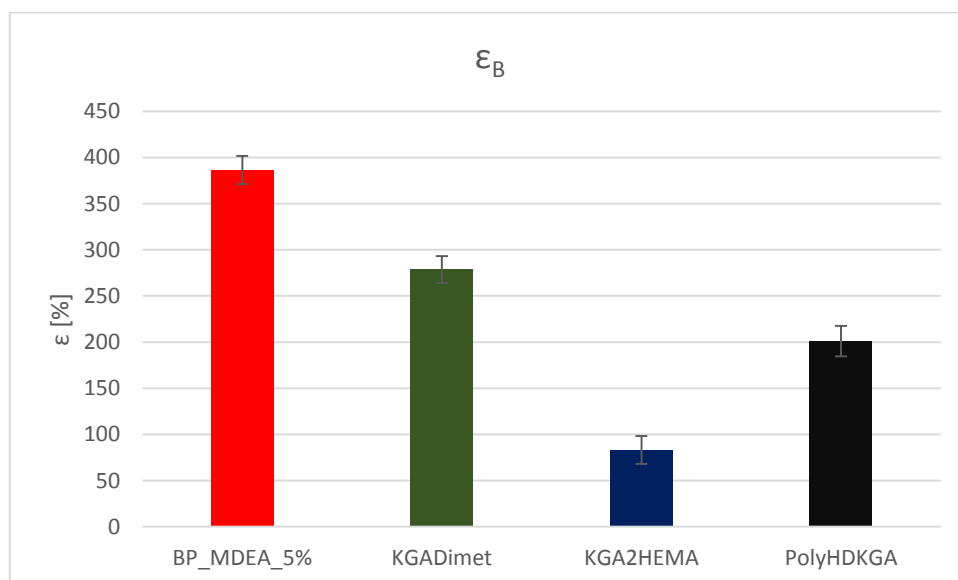


Figure 123: Elongation at break

BP\_MDEA elongated 3.8 times its length before it broke in half. Due to the introduction of more crosslinks with the  $\alpha$ -ketoglutaric acid-based initiators, their elongation at break decreases. The lowest  $\epsilon_B$  was provided by the KGA2HEMA samples (Figure 123).

## Polymerizable, polymeric Photoinitiators

The second series of experiments was conducted with all the different molecular weight crosslinkable polyesters, based on  $\alpha$ -ketoglutaric acid and glutaric acid.

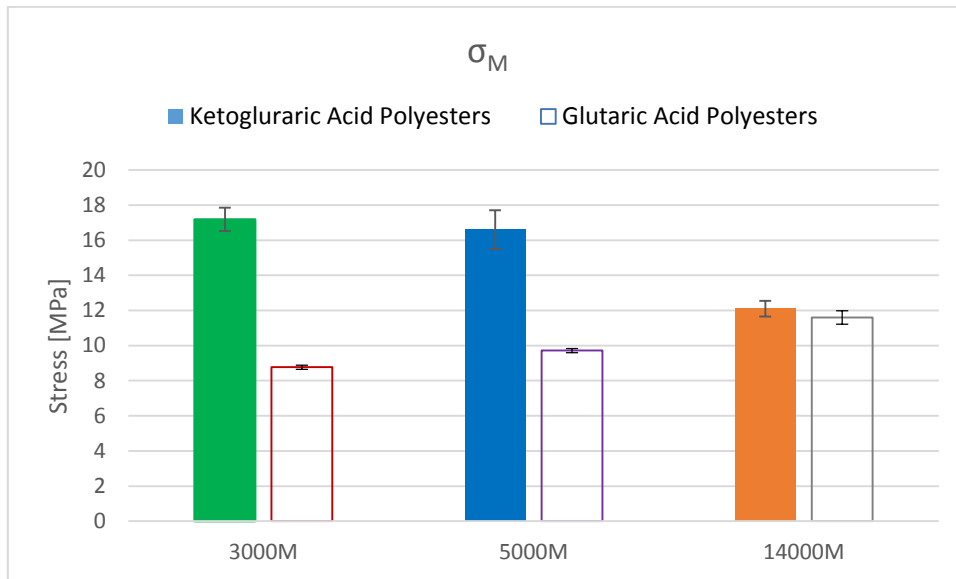


Figure 124: Yield strength for PolyHD(K)GA-M products

For the  $\alpha$ -ketoglutaric acid-based macromolecular, crosslinkable initiators the yield strength was increased with the amount of network links introduced by the photoinitiators. The lower the molecular weight, the more crosslinks added in the material and therefore a resulted increase in yield strength. An increase of molecular weight of the glutaric acid-based polyesters, resulted in an increase of the maximum resistance to applied stress (Figure 124).

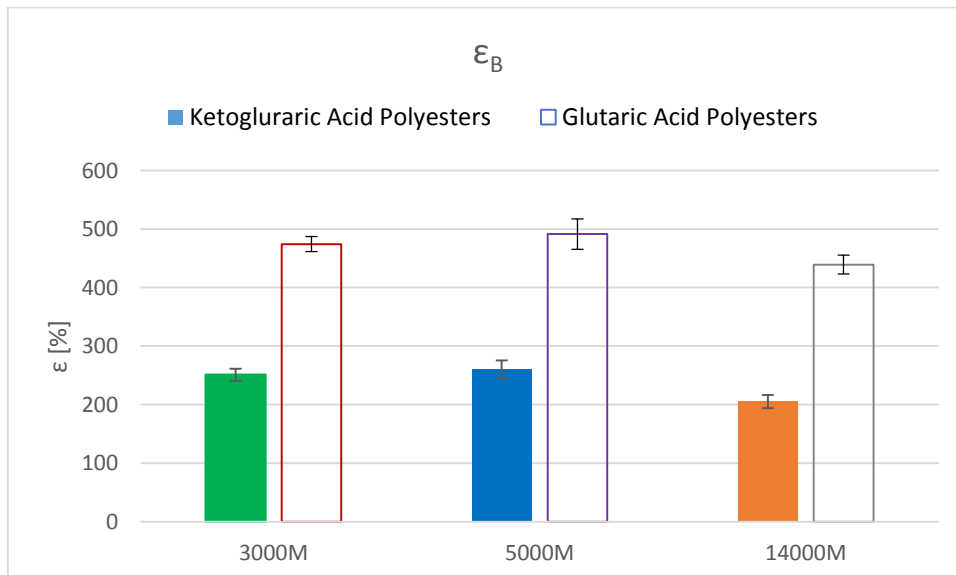


Figure 125: Elongation at break for PolyHD(K)GA-M products

To compare the elongations at break (Figure 125) for the glutaric acid with the reference system before, the data in Figure 125 had shown a general increase. 50% for the high 14000 g/mol polyester and around 100% for the 5000 and 3000 g/mol molecules. Miramer consist

out of 40 wt% 30000 g/mol diacrylate, which is responsible for the good  $\epsilon_B$ . By the addition of more non initiating dimethacrylates, this value increased significantly. The  $\alpha$ -ketoglutaric acid-based polymers had similar elongations at break as the PolyHDKGA in previous experiments at around 200 to 260%.

Overall there were a wide variety of elongations at break, achieved by the  $\alpha$ -ketoglutaric acid-based initiators. Also the storage modulus could be increased for every sample compared to BP\_MDEA, reaching up to nearly 20 MPa for the KGA2HEMA system, by remaining an elongation of 80% at break. The PolyHDKGA-M products performed much better compared to their photo-unreactive counterparts in terms of  $G'$  and  $G'_{150-160\text{ }^\circ\text{C}}$ , due to the increased crosslinking density.

#### 5.4.3. Charpy Impact Tests

In terms of mechanical properties, this was the last test conducted. Samples with a specific geometry had to be made. To achieve those specific shapes, molds designed for charpy impact tests (DIN 53435:2018-09) were filled with the liquid formulations and cured in an UV-oven with no wavelength filter. The exposure to the UV-light was limited to 300 s per side, resulting in a total irradiation time of 600 s. The now solidified samples were grounded into shape to conduct the measurement. Now all samples were put onto the device, the 10 kg hammer was set in place to afterwards hit the sample body, as soon as it was released, to break the sample in half. A schematic drawing of a charpy impact experimental setup is illustrated in Figure 126.

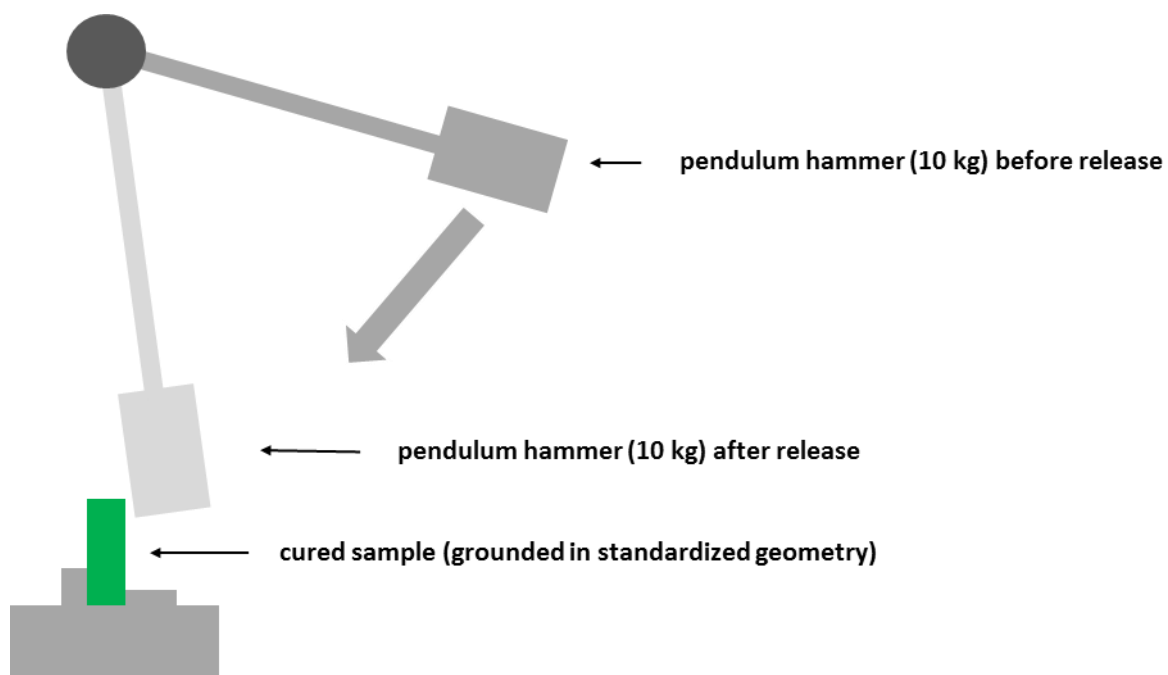


Figure 126: Schematic illustration of a charpy impact test device

Unfortunately the charpy impact tests were not successful. None of the samples broke in half during these experiments. The only observation was a slight bending of the sample geometry. Just for interest, even multiple hits by the 10 kg hammer could not result in a break of a single sample.

## 5.5. Leaching Tests

Limit migration out of cured polymer networks was a major objective. To quantify the amount of not covalently bonded initiator molecules in a cured material, leaching tests were performed with every sample from the photorheometry (reactivity tests 5.2 and mechanical tests 5.4). The idea behind this concept was an even distributed sample, 200  $\mu\text{m}$  thick. Another advantage of using the photorheometer samples was, that the conversion of each sample is already determined, therefore this factor could be included in the interpretation of the results. Using a punch, a 1 cm in diameter, circular shape was punched out of the cured sample foil (Figure 127).

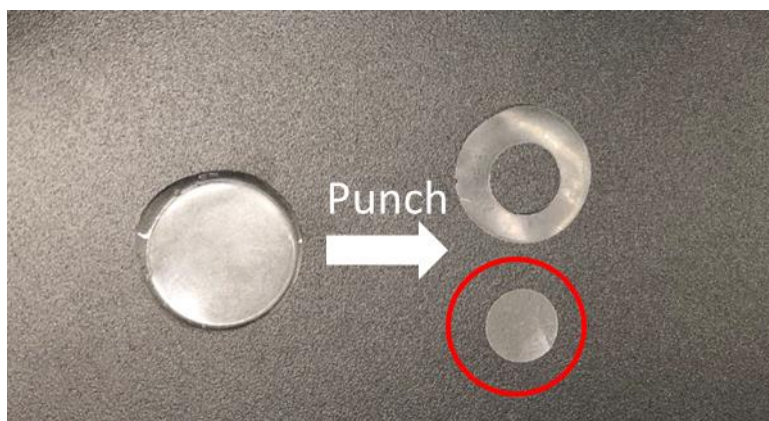


Figure 127: Cured sample foil from previous photorheometer tests, stamped into a specific, circular geometry

Afterwards the samples weight was determined, and was put into a closed penicillin flask with 5 mL of a commercial industrial used solvent, methyl tert-butylether (MTBE). In this solvent, the polymer network swelled with the MTBE and therefore releasing its small, non-covalently bond photoproducts and unreacted monomer. After a total time of 6 days, the tests were stopped. The samples were weighed again, to determine their solvent uptake and after this procedure put into an oven at 80  $^{\circ}\text{C}$  at reduced pressure for 6 days. Then the dry samples were weighed to calculate the weight difference, which correlates with the leachability. The more weight is loss during this process, the more compounds are able to migrated out of the cured polymer material. At least triplicates were measured to ensure a low deviation.

### Miramer Formulations

First the Miramer-based samples from the reactivity tests were analyzed. After the 6 days, the material was completely swollen with the methyl tert-butylether.

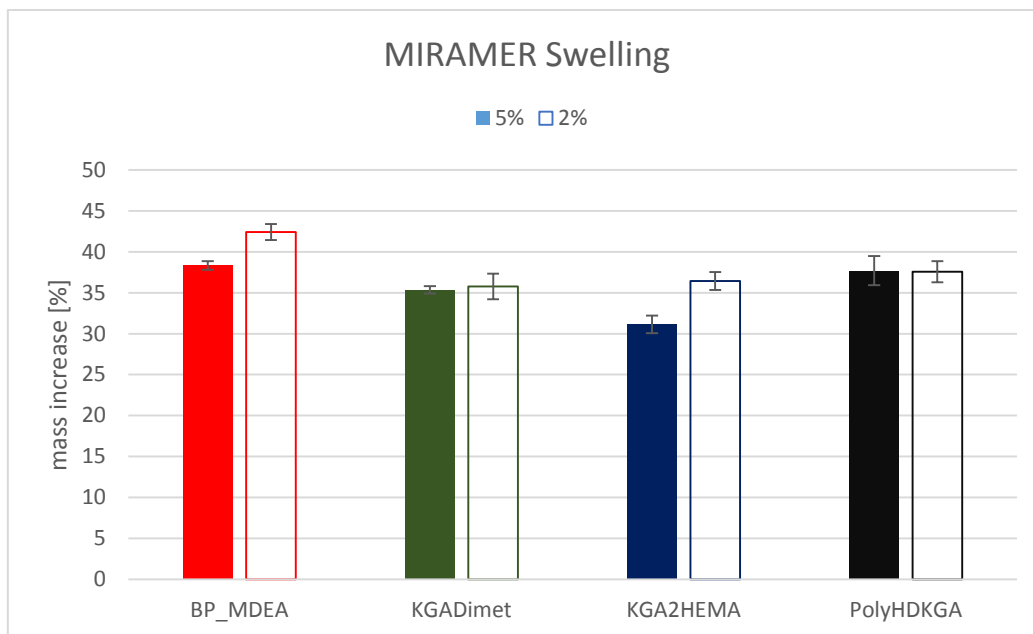


Figure 128: Mass increase of the samples compared to their original weight after 6 days in MTBE

The increases in their mass is shown in Figure 128. The highest percentage for the 5% samples was reached by the reference system and the macromolecular photoinitiator PolyHDKGA. At a mass increase around 35% and 31%, the KGADimet and polymerizable KGA2HEMA were the samples with the lowest swellability. This could be explained due to the increased crosslinking probability of the KGA2HEMA molecule and therefore less solvent, which could penetrate the polymer network. Overall percentages between approximately 30 and 40% were achieved by all samples, which results in a highly swollen network. Under these intentionally extreme conditions every non reacted monomer, photoinitiator or additive should leach out. The 2% samples' behavior was similar.

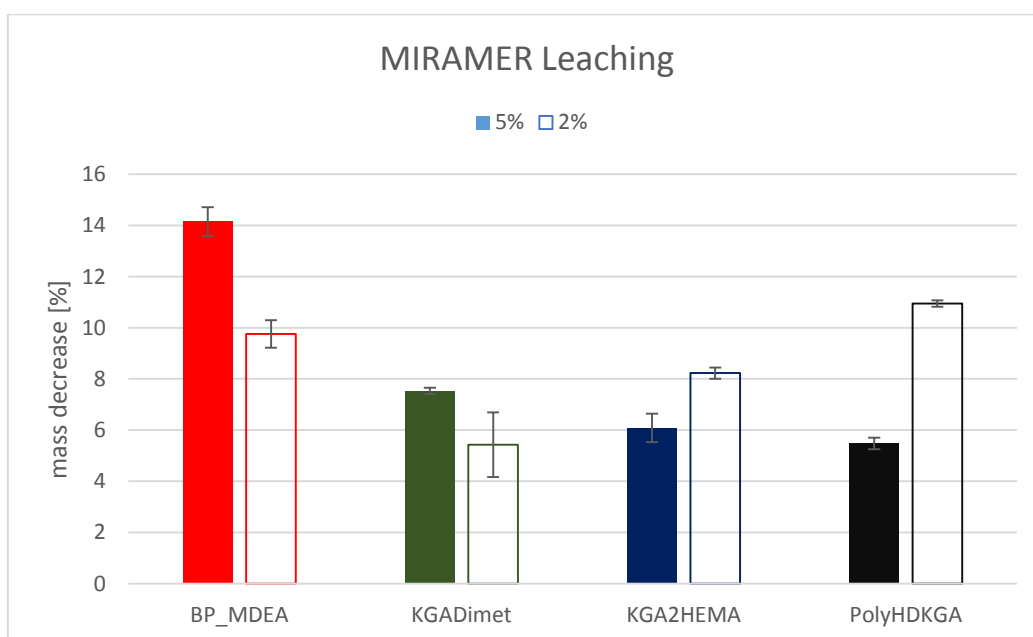


Figure 129: Mass decrease of the samples compared to their original weight after 6 days of drying

As illustrated in Figure 129, the leaching tests went well for the  $\alpha$ -ketoglutaric acid-based initiators. Considering the 5% samples, BP\_MDEA recorded a mass loss at around 14%, while for the small molecule KGADimet and polymerizable KGA2HEMA the mass decreases were around 8%. This result was due to the more efficient crosslinking of the photoinitiators into the polymer network. With up to three crosslinkable points in the KGA2HEMA, it was likely to covalently bond to the material. Only PolyHDKGA was below 6%, which can be explained by the macromolecular initiator, which is immobilized very well. Interestingly the conversion of the macromolecular PolyHDKGA was as low as for the polymerizable initiator in the 2% formulations, but less of the PolyHDKGA migrated out of the polymer network. Overall the ketoesters performed better than the 2 or 5% reference system, with the exception 2% PolyHDKGA sample, which achieved only very low conversion.

### TEGDMA Formulations

The next series of tests was performed in the monomer TEGDMA, due to the incompatibility of the PolyISOKGA polyesters with the Miramer.

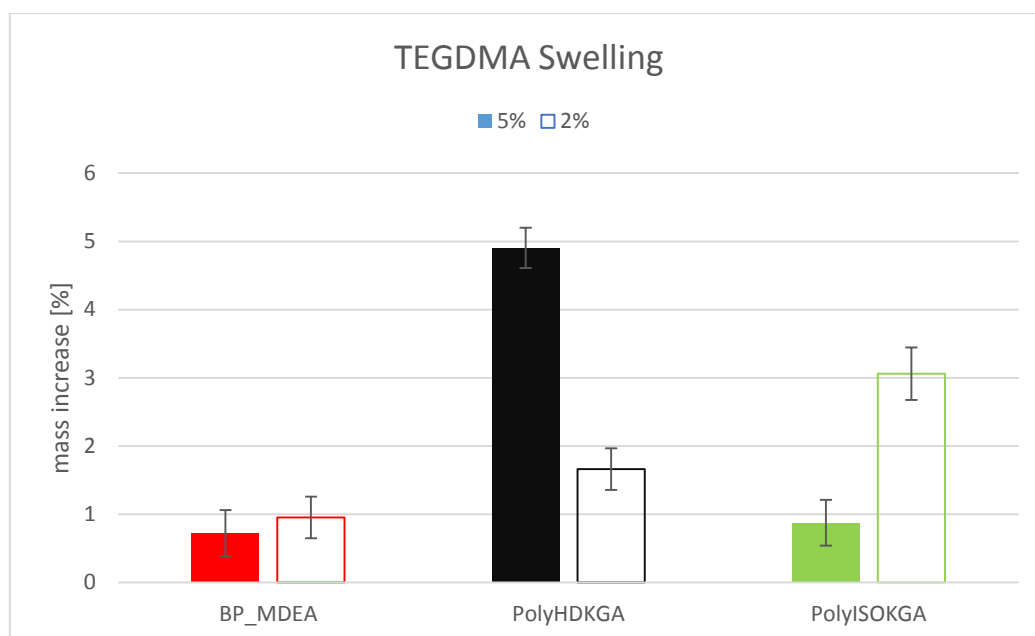


Figure 130: Mass increase of the samples compared to their original weight after 6 days in MTBE

In Figure 130 the mass increases of the samples are illustrated. The highest swellability was determined in the polymeric PolyHDKGA sample at around 5%, followed by the polymeric PolyISOKGA and the BP\_MDEA samples at below 1%. Interestingly, the PolyHDKGA is very affine to the MTBE and the resulting network was very wide, due to its increased solvent uptake during the tests. PolyISOKGA was comparable with BP\_MDEA, but the 2% formulation took up more solvent due to less conversion.

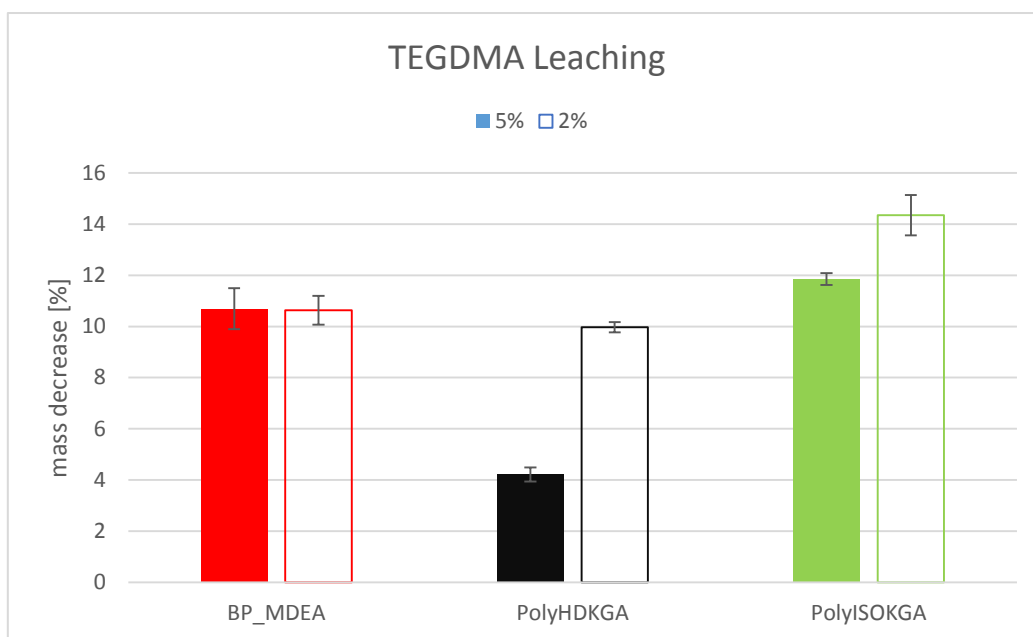


Figure 131: Mass decrease of the samples compared to their original weight after 6 days of drying

The leaching test results for the TEGDAM monomer are shown in Figure 131. The reference system lost around 10% in mass for both concentration of initiator. Below this threshold is the PolyHDKGA initiator, which only lost less than half of the percentage of BP\_MDEA. The 2% sample of the polymeric PolyHDKGA and the polymeric PolyISOKGA samples had shown lower DBC's in the photorheometer experiments, therefore increased leaching. This could be explained due to the long immobilized chains in the polymer network, which could not migrate out efficiently. For the PolyISOKGA, which resulted in the lowest double bond conversion, this mass decreases were above the reference system at 12 to 14%.

### HPLC Analysis

To investigate the compounds, which leached out of the polymer samples, a HPLC study was carried out. Concentrations with around 5 mg/mL were selected for this analysis. An equivalent of the leaching solution was transferred into a vial and measured at the HPLC with a mobile phase containing an acetonitrile and water mixture. The light absorption was recorded on 5 different, preset wavelength, but for our purpose, only the 254 nm detection was important. As illustrated in Figure 132, firstly all educts, which were thought to possibly leach out, were measured in their pure form.

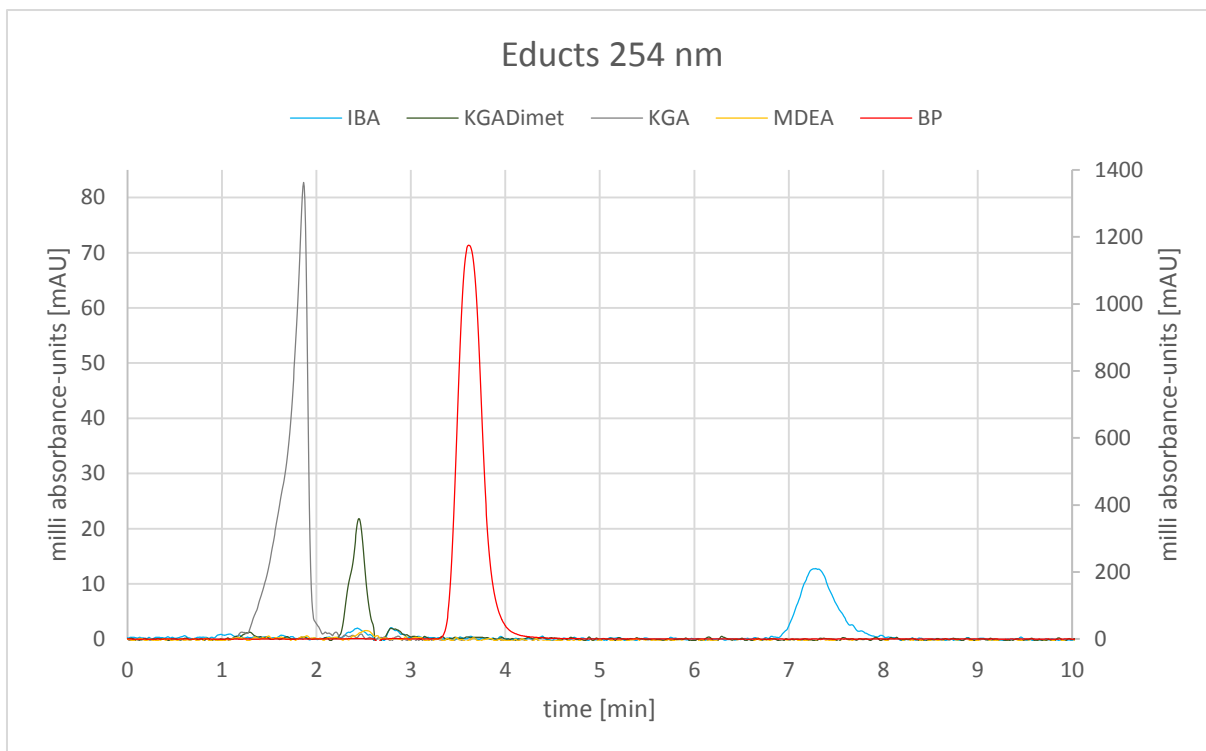


Figure 132: Retention times of isobornylacrylate (IBA),  $\alpha$ -ketoglutaric acid diethylester (KGADimet),  $\alpha$ -ketoglutaric acid (KGA), methyl diethanolamine (MDEA) and benzophenone (BP; second y-axis)

MDEA had shown no absorption behavior at 254 nm. The retention times of the educts now were compared to the leaching solutions of the materials. Therefore it was possible to argue, which compound leached out of a cured sample.

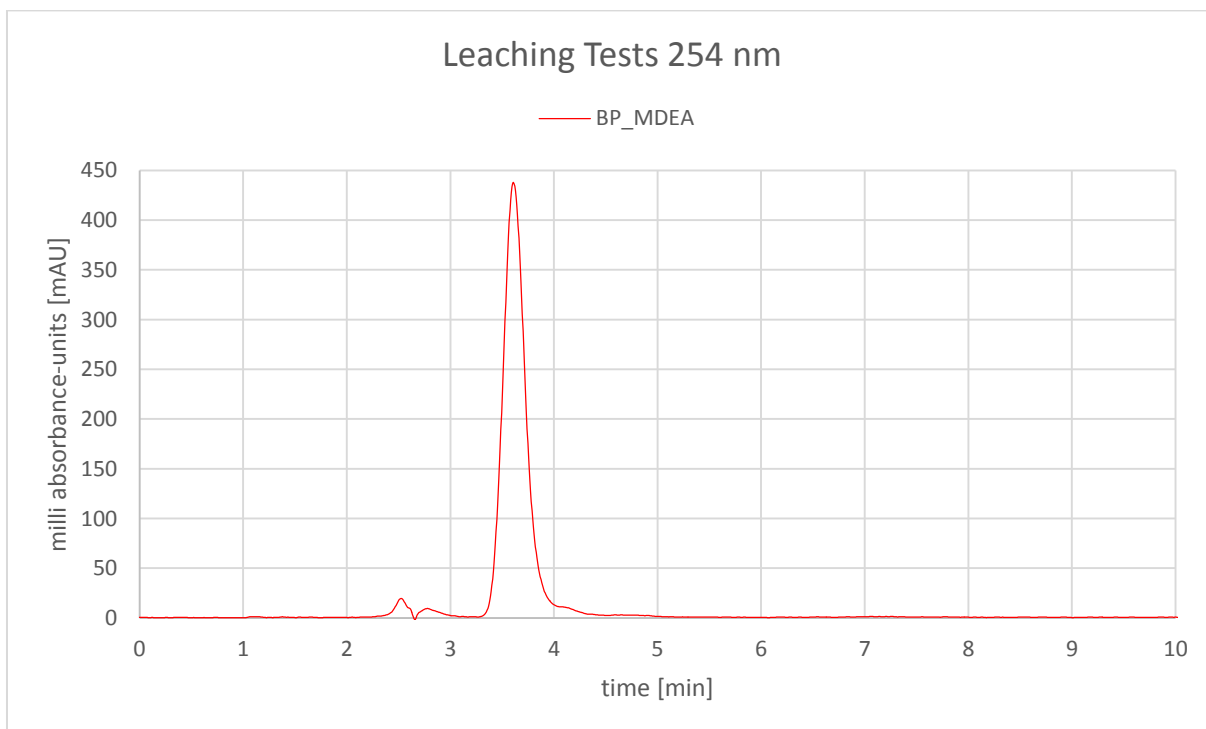


Figure 133: Leaching solution of cured sample: BP\_MDEA



The reference material definitely leached a major amount of benzophenone ( $t_R = 3.6$  min) and non-reacted isobornyl acrylate ( $t_R = 7.3$  min). Due to the high absorbance of benzophenone in Figure 133, the absorbance value of isobornyl acrylate is minor.

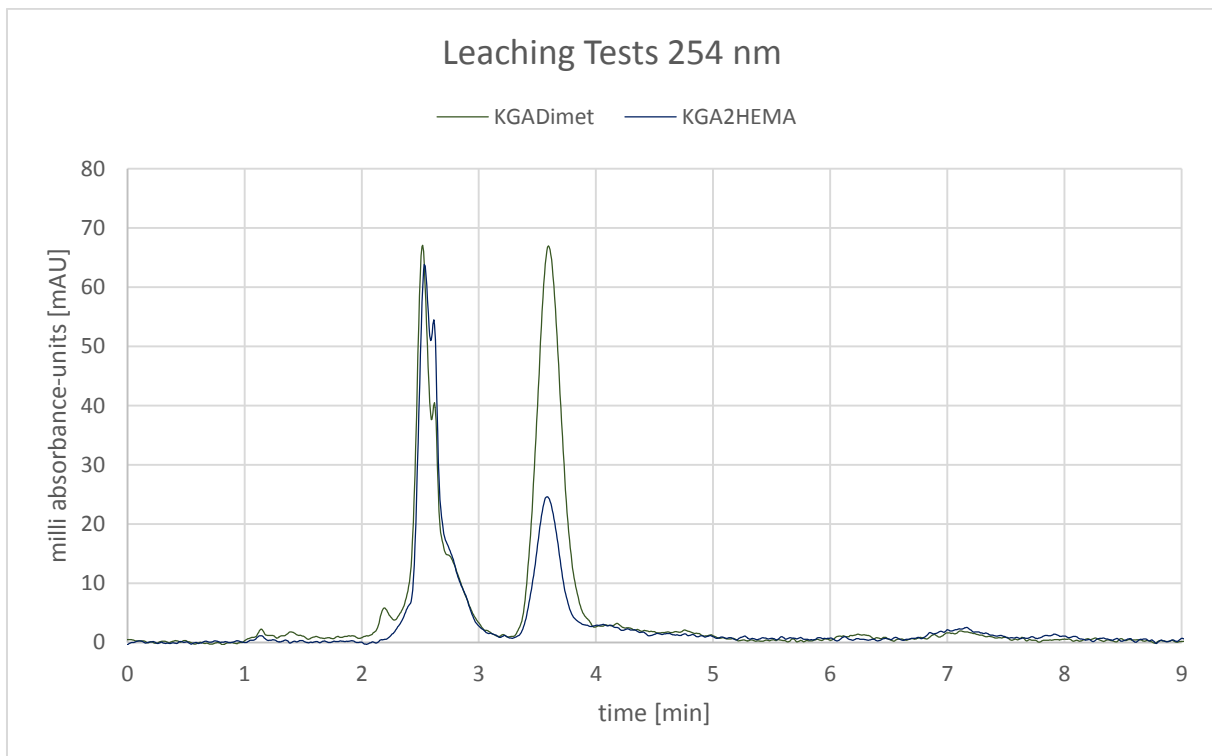


Figure 134: Leaching solution of cured sample: KGADimet and KGA2HEMA

In Figure 134 obviously the  $\alpha$ -ketoglutaric acid esters leached out a bit ( $t_R = 2.5$  min) and also some unreacted isobornylacrylate ( $t_R = 7.3$  min). The strange observation were traces of benzophenone in the solutions, but after further investigation it was safe to say, that after the first Photorheometer measurements of BP\_MDEA samples on a polar polyethylene tape, some of the benzophenone migrated into the tape. After measuring the second series of experiments, the benzophenone diffused back into the tested KGADimet formulation, placed on the same tape. The third series of measurements, KGA2HEMA samples, contained much less benzophenone.

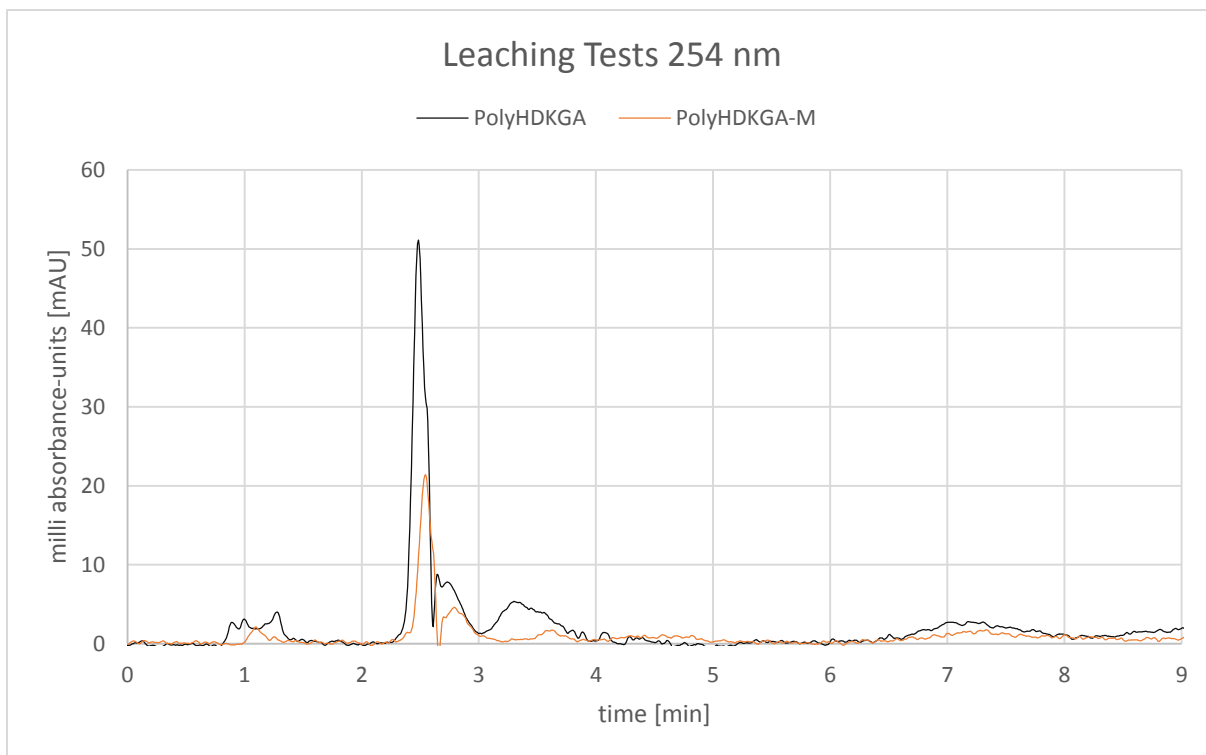


Figure 135: Leaching solution of cured sample: PolyHDKGA and PolyHDKGA\_062M

The polymeric initiator samples, shown in Figure 135, lead to a leaching solution containing  $\alpha$ -ketoglutaric acid esters ( $t_R = 2.5$  min) and unreacted isobornyl acrylate ( $t_R = 7.3$  min). Unlike in the KGADimet and KGA2HEMA samples, no benzophenone was contaminating the formulations during the measurement.

#### Small molecules, polymerizable and polymeric Photoinitiators

After finishing the test series with the samples from the reactivity tests, the second series was analyzed. This time, the samples from the mechanical tests, containing additional phenothiazine as inhibitor, were put into the solvent for leaching tests. The reference system, KGADimet, the polymerizable KGA2HEMA and the macromolecular PolyHDKGA, were measured first.

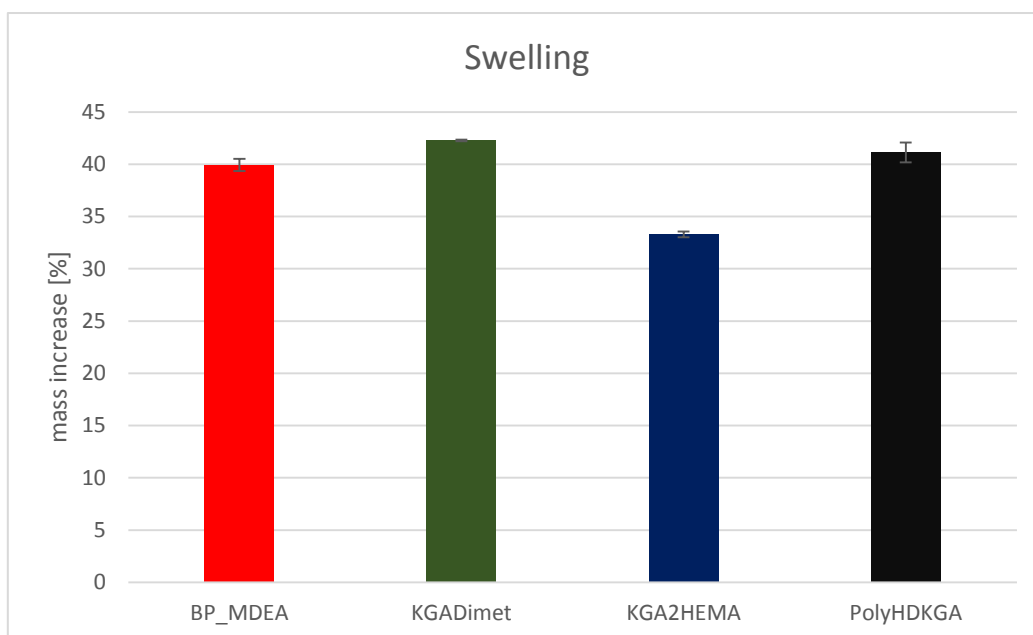


Figure 136: Mass increase of the samples compared to their original weight after 6 days in MTBE

The swelling was for all samples approximately the same, at around 40%, with the exception of the polymerizable KGA2HEMA, which's polymer network was densely crosslinked, therefore decreased the amount of solvent it could uptake to 33% (Figure 136).

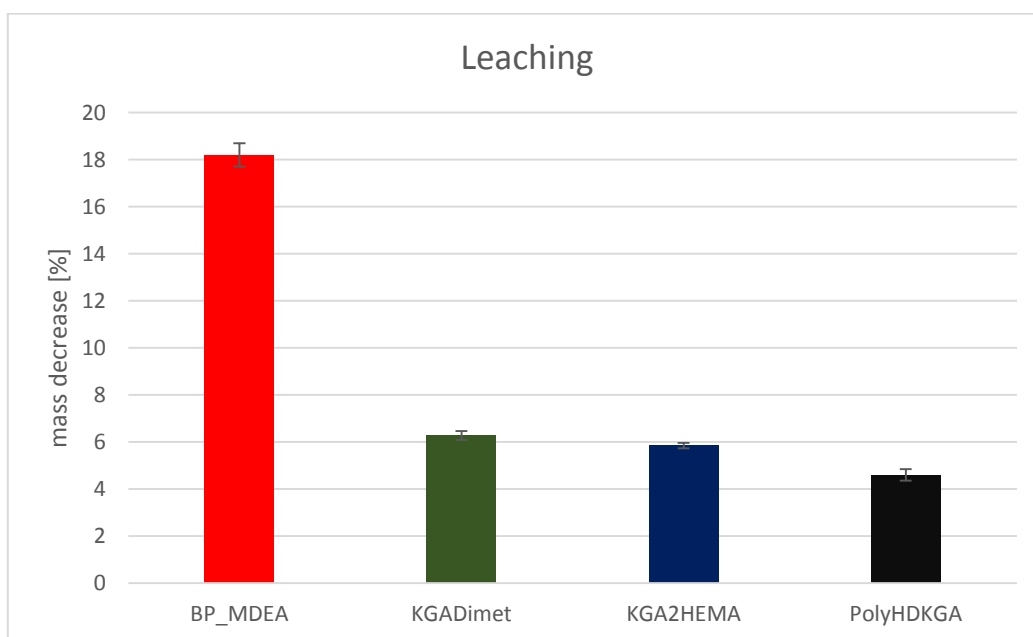


Figure 137: Mass decrease of the samples compared to their original weight after 6 days of drying

The leachability (Figure 137), was the highest for the reference system. Above 18% of its mass was leached out and dissolved by the MTBE. All  $\alpha$ -ketoglutaric acid-based initiators performed much better, with mass losses for the small molecule KGADimet and the polymerizable KGA2HEMA at approximately 6% and the macromolecular initiator even reached around 4% mass loss, due to its immobilization in the cured polymer matrix.

## Polymerizable, polymeric Photoinitiators

The second series contained the  $\alpha$ -ketoglutaric acid and glutaric acid-based polyesters with the crosslinkable methacrylate endgroups.

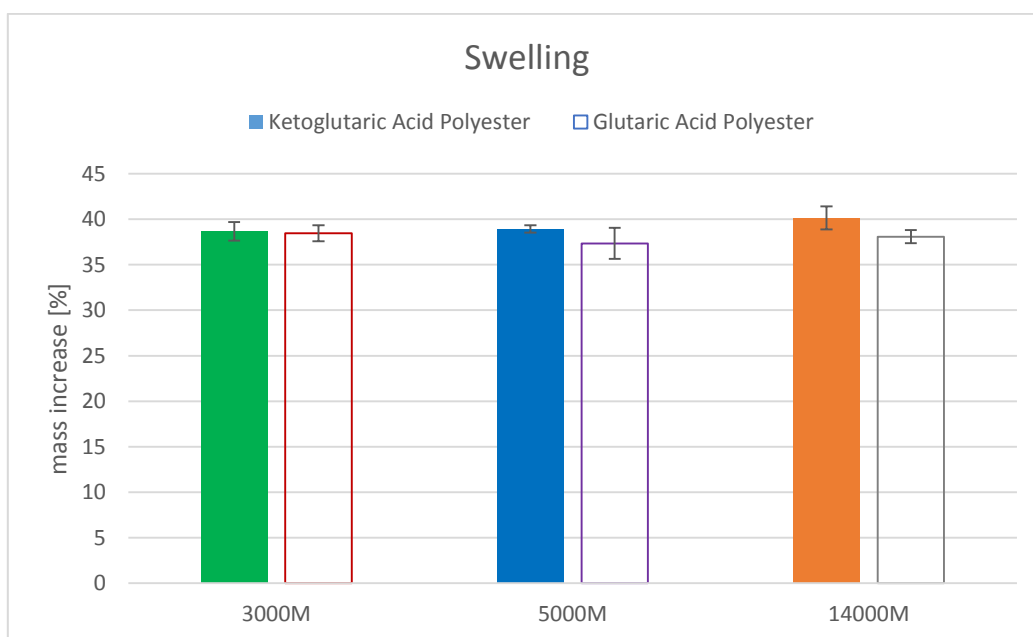


Figure 138: Mass increase of the samples compared to their original weight after 6 days in MTBE for PolyHD(K)GA products

In terms of swellability, all samples measured were in the range of 37-40% mass increase, therefore ideal conditions to compare those systems in the leaching tests (Figure 138).

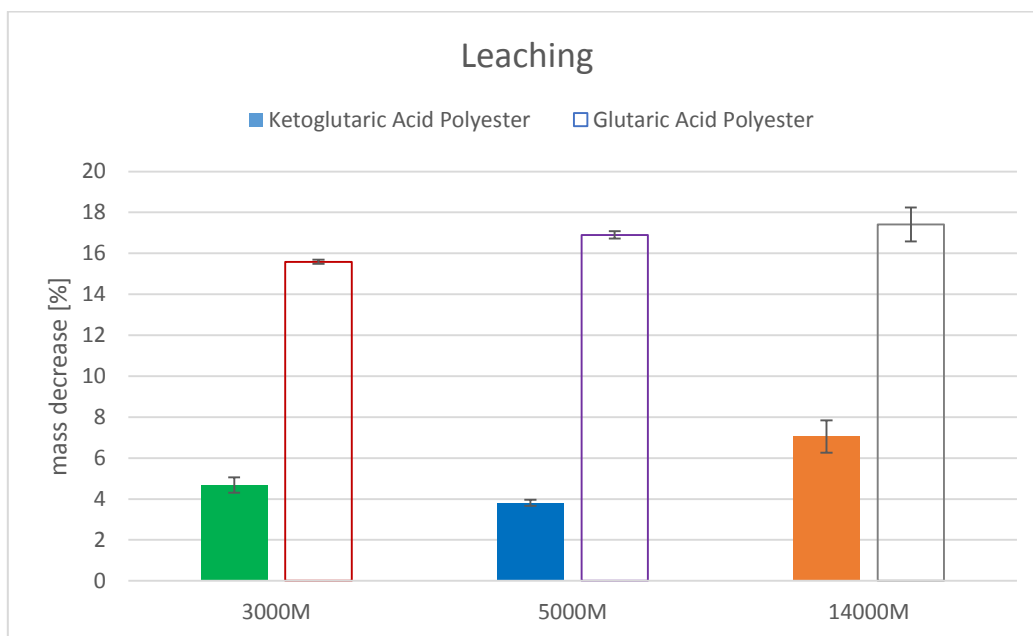


Figure 139: Mass decrease of the samples compared to their original weight after 6 days of drying for PolyHD(K)GA products

As shown in Figure 139, the glutaric acid-based polyesters, which also contained the benzophenone-MDEA system as an initiator, lost at least double the amount of mass, compared to the  $\alpha$ -ketoglutaric acid-based ones. The best performance delivered the 5000

g/mol followed by the 3000 g/mol  $\alpha$ -ketoglutaric acid-based macromolecular photoinitiator. Only the largest one, at 14000 g/mol, suffered a mass decrease of 7%, due to its over 10% lower conversion compared to all other samples in Figure 139, determined by photorheology.

Overall the samples, generated in the photorheometry experiments of the mechanical tests, performed better, most likely due to the 100 s increased UV-light irradiation. The only exception was the reference system, which lost 2% more of its initial weight. Due to the results provided by the leaching tests, a major objective of this thesis was achieved. The ketoester-based photoinitiators shown much lower weight decrease after 6 days of exposure to MTBE.

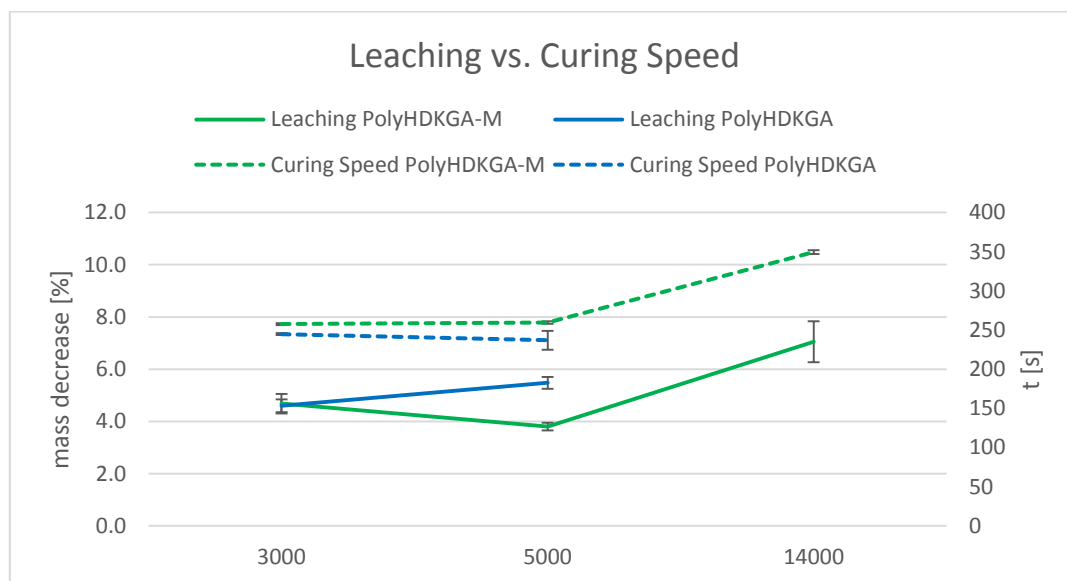


Figure 140: Leaching vs. curing speed ( $t_{95\%}$  values from the photorheology experiments)

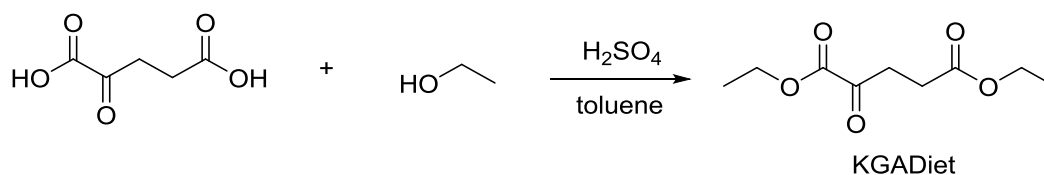
As illustrated in Figure 140, the leachability of the samples was compared to the curing speed. The result was a minimum at mass decrease for the PolyHDKGA\_5000M product and a lower time to reach the  $t_{95\%}$  value for the 3000 and 5000 g/mol modified polyester. Therefore the best choice for this system was the PolyHDKGA\_5000M, due to the lowest leachability and simultaneously high reactivity compared to the PolyHDKGA\_14000M. Considering the unmodified hydroxyl-terminated polyesters, the PolyHDKGA\_3000 shown less leaching compared to its 5000 g/mol equivalent. The lower compatibility with the polar Miramer matrix could explain the increased coil formation and a masking of some initiators in the polymer chain, therefore resulting in less total conversion and more leaching. Also the reactivity of the system, containing PolyHDKGA's, decreased compared to their endgroup modified counterparts.

## EXPERIMENTAL PART

### 1. Optimization of the Esterification Reaction

#### 1.1. Synthesis of $\alpha$ -Ketoglutaric Acid Di(m)ethylester [KGADi(m)et]

##### 1.1.1. $\alpha$ -Ketoglutaric Acid Diethylester [KGADiet]



To achieve the compound KGADiet, a synthesis similar to Roscales S. work<sup>46</sup> was performed. At first  $\alpha$ -ketoglutaric acid was recrystallized in acetone. Then 1 eq. (3.66 g, 25 mmol) of  $\alpha$ -ketoglutaric acid were added into a 250 mL three-necked round bottom flask with a cooler and a septum. Then 0.3 eq. (0.4 ml, 7.5 mmol) of sulfuric acid were added as the catalyst and the whole mixture was stirred and heated up. The oil bath was set to 100 °C and after 24 h of refluxing the reaction was finished. Reaction progress was controlled via TLC (PE:EE = 5:1; R<sub>f</sub>: 0.36). The remaining ethanol in the reaction mixture was evaporated in a rotary evaporator. To the residue 50 ml of deionized water were added and the pH value was set to approximately 7 with 1 N KOH. The aqueous phase was extracted with 3 x 100 ml ethyl acetate and the combined organic layers were dried over Na<sub>2</sub>SO<sub>4</sub>. The organic phase was evaporated on a rotary evaporator and the crude yield was 4.19 g (83%). Then the product was flushed through a silica gel column (214 g) via MPLC (PE:EE = 9:1). There were three products detected via a UV-detector (245 nm) and associated via TLC. Then the fractions with R<sub>f</sub> of 0.36 (PE:EE = 5:1) were combined and the solvent was evaporated. The yield of  $\alpha$ -ketoglutaric acid diethylester was 1.77 g (35%). The product is a clear colorless oil and was stored at -18 °C.

#### Analytatics:

**TLC (PE:EE = 5:1):** R<sub>f</sub>: 0.36

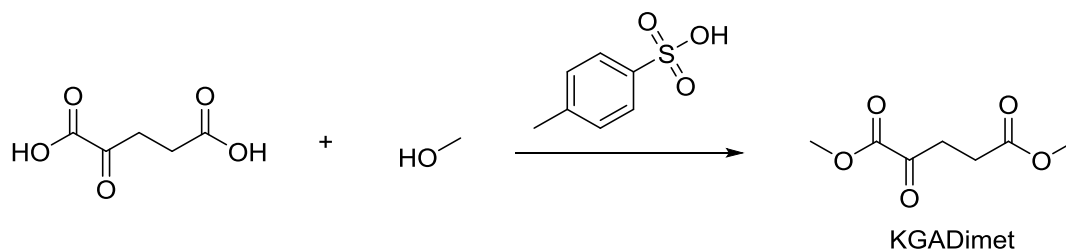
**<sup>1</sup>H-NMR (400 MHz, CDCl<sub>3</sub>):** 4.32 (q, J<sub>HH</sub> = 7.2 Hz, 2H, CO-CO-O-CH<sub>2</sub>), 4.13 (q, J<sub>HH</sub> = 7.20 Hz, 2H, CO-O-CH<sub>2</sub>), 3.14 (t, J<sub>HH</sub> = 6.6 Hz, 2H, CO-CO-CH<sub>2</sub>), 2.65 (t, J<sub>HH</sub> = 6.6 Hz, 2H, CO-CH<sub>2</sub>), 1.36 (t, J<sub>HH</sub> = 7 Hz, 3H, CO-CO-O-CH<sub>2</sub>-CH<sub>3</sub>), 1.24 (t, J<sub>HH</sub> = 7 Hz, 3H, CO-O-CH<sub>2</sub>-CH<sub>3</sub>)

**<sup>13</sup>C-NMR (400 MHz, CDCl<sub>3</sub>):** 192.8 (CO-CO-CH<sub>2</sub>), 172.0 (CO-CH<sub>2</sub>), 160.6 (CO-CO-CH<sub>2</sub>), 62.6 (CO-CO-O-CH<sub>2</sub>), 60.9 (CO-O-CH<sub>2</sub>), 34.2 (CO-CO-CH<sub>2</sub>), 27.8 (CO-CH<sub>2</sub>), 14.2 (CO-CO-O-CH<sub>2</sub>-CH<sub>3</sub>), 14.0 (CO-O-CH<sub>2</sub>-CH<sub>3</sub>)

**GC-MS:** 202.99 [M+H], 129.94 [M+H,-(CO-O-CH<sub>2</sub>-CH<sub>3</sub>)], 128.95 [M-(CO-O-CH<sub>2</sub>-CH<sub>3</sub>)], 101.99 [M+H,-(CO-CO-O-CH<sub>2</sub>-CH<sub>3</sub>)], 101.00 [M-CO-CO-O-CH<sub>2</sub>-CH<sub>3</sub>], 74.11 [M+H,-(CO-CH<sub>2</sub>-CH<sub>2</sub>-CO-O-

CH<sub>2</sub>-CH<sub>3</sub>], 73.14 [M-(CO-CH<sub>2</sub>-CH<sub>2</sub>-CO-O-CH<sub>2</sub>-CH<sub>3</sub>)], 55.13 [M+H,-(O-CH<sub>2</sub>-CH<sub>3</sub>),-(CH<sub>2</sub>-CH<sub>2</sub>-CO-O-CH<sub>2</sub>-CH<sub>3</sub>)]

### 1.1.2. $\alpha$ -Ketoglutaric Acid Dimethylester [KGADimet]



For the synthesis of KGADimet according to the book Polymer Synthesis,<sup>46</sup> first  $\alpha$ -ketoglutaric acid was recrystallized in acetone and the para-toluolsulfonic acid was recrystallized in chloroform. Then 1 eq. (29.16 g, 200 mmol) of the pure  $\alpha$ -ketoglutaric acid, 0.01 eq. (214.8 mg, 1.1 mmol) of para-toluolsulfonic acid were added into a 500 ml one-neck round bottom flask. Then 350 ml of absolute methanol were added, the flask was connected to a cooler and the oil bath was set to 80 °C. The reaction progress was checked via NMR and after 20 h, 15.46 g of anhydrous sodium sulfate were added to bind the formed water. After a total reaction time of 24 h the reaction was stopped and the mixture was cooled down to room temperature. The solvent was removed at the rotary evaporator. Then an oil bath was set to 120 °C and the residue was distilled in vacuum (BP: 0.05 mbar, 88-89 °C). The product (28.34 g, 81%) was a colorless, transparent oil, which was stored at -18 °C.

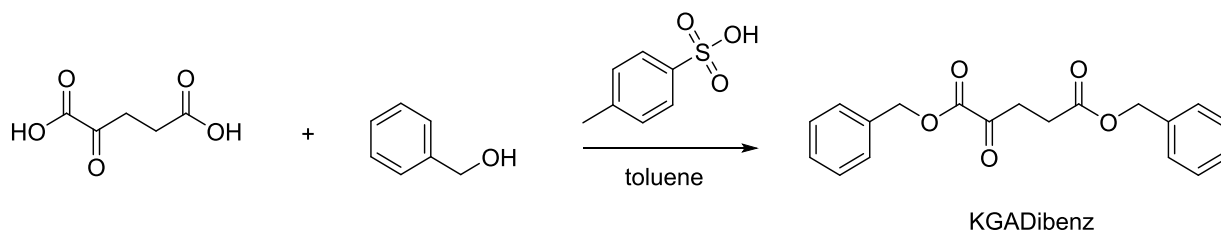
#### Analytatics:

<sup>1</sup>H-NMR (400 MHz, CDCl<sub>3</sub>): 3.88 (s, 3H, CO-CO-CH<sub>3</sub>), 3.68 (s, 3H, CO-CH<sub>3</sub>), 3.16 (t, JHH = 6.6 Hz, 2H, CO-CO-CH<sub>2</sub>), 2.68 (t, JHH = 6.6 Hz, 2H, CO-CH<sub>2</sub>)

<sup>13</sup>C-NMR (400 MHz, CDCl<sub>3</sub>): 192.2 (C=O-CO-O-CH<sub>3</sub>), 172.4 (C=O-O-CH<sub>3</sub>), 160.9 (CO-CO-O-CH<sub>3</sub>), 53.1 (CO-CO-O-CH<sub>3</sub>), 52.0 (CO-O-CH<sub>3</sub>), 34.2 (CO-CO-CH<sub>2</sub>), 27.4 (CO-CH<sub>2</sub>)

GC-MS: 175.15 [M+H], 143.04 [M-(O-CH<sub>3</sub>)], 116.15 [M+H,-(CO-O-CH<sub>3</sub>)], 115.11, [M-(CO-O-CH<sub>3</sub>)], 88.22 [M+H,-(CO-CO-O-CH<sub>3</sub>)], 87.17 [M-(CO-CO-O-CH<sub>3</sub>)], 59.17 [M-(CH<sub>2</sub>-CH<sub>2</sub>-CO-CO-O-CH<sub>3</sub>)], 55.18 [M-H,-2x (CO-O-CH<sub>3</sub>)]

### 1.2. Synthesis of $\alpha$ -Ketoglutaric Acid Dibenzylester [KGADibenz]



For the synthesis of KGADibenz similar to the work of Roscales S. and Joly G. D.,<sup>46,47</sup> first  $\alpha$ -ketoglutaric acid was recrystallized in acetone and the para-toluolsulfonic acid was recrystallized in chloroform. Then 1 eq. (2.44 g, 16.7 mmol) of the pure  $\alpha$ -ketoglutaric acid, 2

eq. (3.61 g, 33.4 mmol) of benzyl alcohol and 0.045 eq. (128.8 mg, 0.8 mmol) of para-toluolsulfonic acid were added into a 100 ml one-neck round bottom flask. Then 50 ml of absolute toluene were added and the flask was connected to a Dean Stark apparatus. The reaction mixture was refluxed for 18 h and the oil bath was set to 150 °C. After 18 h of reaction time the progress was checked by TLC (PE:EE = 5:1,  $R_f$ : 0.45). After that, the reaction mixture was cooled down to room temperature, the solvent was evaporated at the rotary evaporator and then 20 ml of saturated NaHCO<sub>3</sub> solution were added. Then the aqueous phase was extracted three times with ethyl acetate and the combined organic layers were dried over NaSO<sub>4</sub>. The resulting dry organic phase was evaporated at the rotary evaporator. The crude yield was 5.35 g (98%). Then the product was flushed through a silica gel column (435 g) via MPLC (PE:EE = 9:1). There were two products detected via a UV-detector (354 nm) and associated via TLC. Then the fractions with  $R_f$  of 0.45 (PE:EE = 5:1) were combined and the solvent was evaporated. The yield of  $\alpha$ -ketoglutaric acid dibenzylester was 3.52 g (65%). The product is a clear colorless oil and was stored at -18 °C.

#### Analytatics:

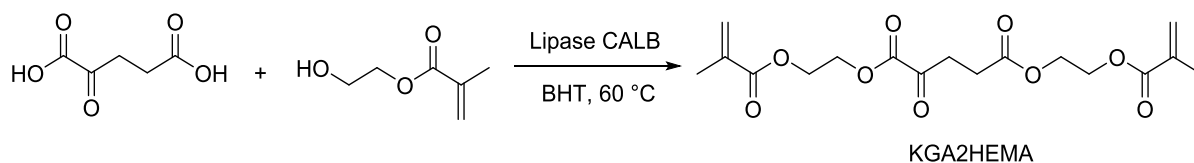
TLC (PE:EE = 5:1):  $R_f$ : 0.45

<sup>1</sup>H-NMR (400 MHz, CDCl<sub>3</sub>): 7.43-7.31 (m, 10H, Ar-H), 5.29 (s, 2H, CO-CO-O-CH<sub>2</sub>), 5.13 (s, 2H, CO-O-CH<sub>2</sub>), 3.19 (t,  $J_{HH} = 6.6$  Hz, 2H, CO-CO-CH<sub>2</sub>), 2.72 (t,  $J_{HH} = 6.6$  Hz, 2H, CO-CH<sub>2</sub>)

<sup>13</sup>C-NMR (400 MHz, CDCl<sub>3</sub>): 192.2 (CO-CO-CH<sub>2</sub>), 171.8 (CO-CH<sub>2</sub>), 160.3 (CO-CO-CH<sub>2</sub>), 135.6 (CO-CO-O-CH<sub>2</sub>-C), 134.4 (CO-O-CH<sub>2</sub>-C), 128.9-128.3 (Ar-CH) 68.1 (CO-CO-O-CH<sub>2</sub>), 66.8 (CO-O-CH<sub>2</sub>), 34.3 (CO-CO-CH<sub>2</sub>), 27.7 (CO-CH<sub>2</sub>)



## 2. Synthesis of Polymerizable Photoinitiators [KGA2HEMA]



The KGA2HEMA was synthesized similar to the work of Douka A. and Kumar A.<sup>51, 52</sup> At first  $\alpha$ -ketoglutaric acid was recrystallized in acetone. Then 1 eq. (3.95 g, 27 mmol) of the pure  $\alpha$ -ketoglutaric acid, 2eq. (7.34 g, 54 mmol) of 2-hydroxymethylmethacrylate and 1 wt% (113.8 mg) of Lipase acrylic resin from *Candida Antarctica* (<5.000 U/g) were added into a 50 ml two-necked round bottom flask equipped with an argon balloon. The reaction mixture was stirred under inert atmosphere and the oil bath was set to 60 °C. The reaction progress was checked via NMR and TLC (PE:EE = 8:2;  $R_f$ : 0.66). After 90 h of reaction time 100 mbar of vacuum were applied for 2 min to shift the equilibrium due to some formed water. Then the pressure was raised to 900 mbar. This process was repeated every 24 h. After a total reaction time of 306 h the mixture was diluted with 10 ml (PE:EE = 50:50) and was purified by MPLC (PE:EE = 75:15; gradient to 60:40). A 435 g silica gel column was used to separate the products and they were detected via a UV-detector (354 nm). The fractions were associated with the product via TLC ( $R_f$ : 0.66) were combined, BHT was added and the solvent was evaporated at the rotary evaporator at 280 mbar (air was sucked into the flask through a Teflon tube to provide enough oxygen for the inhibitor). Then the rest of the solvent was removed by a high vacuum pump at 0.5 mbar for 10 min. The product (3.15 g, 31%) was a colorless, transparent oil, which was stored at -18 °C.

### Analytcs:

TLC (PE:EE = 8:2):  $R_f$ : 0.66

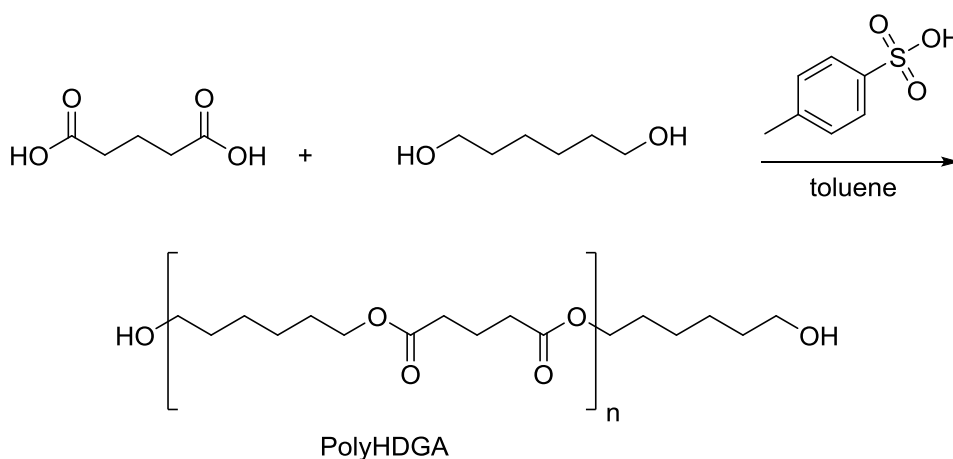
<sup>1</sup>H-NMR (400 MHz, acetone-d<sub>6</sub>): 6.05 (s, 2H, 2  $\underline{\text{CHH}}$ ), 5.62-5.59 (m, 2H, 2  $\underline{\text{CHH}}$ ), 4.54-4.48 (m, 2H, CO-CO-O- $\underline{\text{CH}_2}$ ), 4.43-4.38 (m, 2H, CH<sub>2</sub>-CH<sub>2</sub>-CO-O- $\underline{\text{CH}_2}$ ), 4.30 (s, 4H, CH<sub>2</sub>- $\underline{\text{CH}_2}$ -O-CO-C(CH<sub>2</sub>)-CH<sub>3</sub>), 3.15 (t,  $J_{\text{HH}} = 6.6$  Hz, 2H, CO-CO- $\underline{\text{CH}_2}$ ), 2.63 (t,  $J_{\text{HH}} = 6.6$  Hz, 2H, CO- $\underline{\text{CH}_2}$ ), 1.87 (t,  $J_{\text{HH}} = 1.2$  Hz, 6H, 2  $\underline{\text{CH}_3}$ )

<sup>13</sup>C-NMR (400 MHz, CDCl<sub>3</sub>): 191.9 (CO- $\underline{\text{CO}}$ -CH<sub>2</sub>), 171.8 ( $\underline{\text{CO}}$ -CH<sub>2</sub>), 160.2 ( $\underline{\text{CO}}$ -CO-CH<sub>2</sub>), 135.9 (CO-CO-O-CH<sub>2</sub>-CH<sub>2</sub>-O- $\underline{\text{CO}}$ ), 135.7 (CO-O-CH<sub>2</sub>-CH<sub>2</sub>-O- $\underline{\text{CO}}$ ), 126.4 (2C, CO- $\underline{\text{C}}$ -CH<sub>2</sub>), 126.1 (2C, CO-C- $\underline{\text{CH}_2}$ ), 64.0 (CH<sub>2</sub>-CO-CO-O-CH<sub>2</sub>- $\underline{\text{CH}_2}$ ), 22.6 (CO-CO- $\underline{\text{CH}_2}$ ), 62.5 (CH<sub>2</sub>-CO-O-CH<sub>2</sub>- $\underline{\text{CH}_2}$ ), 61.8 (CO- $\underline{\text{CH}_2}$ ), 34.2 (CO-CO- $\underline{\text{CH}_2}$ ), 27.5 (CO- $\underline{\text{CH}_2}$ ), 18.3 (CO-CO-O-CH<sub>2</sub>-CH<sub>2</sub>-O-CO-C- $\underline{\text{CH}_3}$ ), 18.2 (CO-O-CH<sub>2</sub>-CH<sub>2</sub>-O-CO-C- $\underline{\text{CH}_3}$ )

### 3. Synthesis of Macromolecular Photoinitiators

#### 3.1. Synthesis of Glutaric Acid-based Polyesters [Poly(HD/ISO)GA]

##### Glutaric Acid Hexanediol Polyester [PolyHDGA]



To achieve the polymeric PolyHDGA, a synthesis according to the book Polymer Synthesis<sup>46</sup> was performed. At first all educts were purified via recrystallization. The para-toluolsulfonic acid was recrystallized in chloroform and hexanediol in diethyl ether. Then 1 eq. of the glutaric acid, a suitable amount of pure hexanediol, depending on the aimed molecular weight, and 0.0025 eq. of para-toluolsulfonic acid were added into a 250 mL one-necked-round bottom flask, which was attached to a Dean-Stark Apparatus. Then absolute toluene was added. The oil bath was set to 125 °C and the mixture was magnetically stirred. The reaction progress was checked via acid value. After a total reaction time of 50 h, the product was precipitated in 3000 mL of cold petrol ether. Then the polyester was dissolved in 150 mL of distilled acetone and precipitated in 2 x 1500 mL of deionized water. The result was a white polymer, which was further dried in vacuum, yielding between 64 and 83% of PolyHDGA (Table 33).

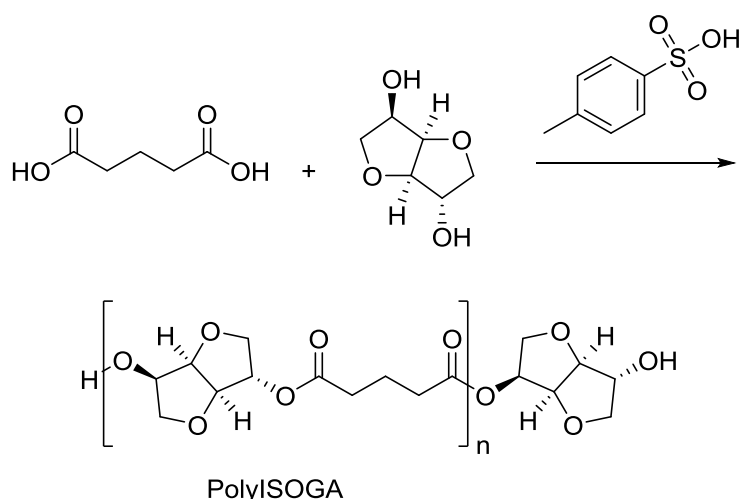
Table 33: Ratios of the glutaric acid, hexanediol and the catalyst (para-toluolsulfonic acid); amount of solvent used; resulting yields

Product	Diacid [mmol]	Diacid [g]	Diol [mmol]	Diol [g]	Catalyst [mmol]	Catalyst [mg]	Toluene [mL]	Yield [g]	Yield [%]
POLYESTER-1	80	10.56	81	9.54	0.2	31.1	30	13.18	77
POLYESTER-2	80	10.56	88	10.39	0.2	33.2	60	13.78	77
POLYESTER-3	80	10.56	84	9.92	0.2	33.2	90	14.59	83
POLYESTER-4	80	10.56	82	9.64	0.2	36.9	150	11.04	64

##### Analytics:

<sup>1</sup>H-NMR of POLYESTER-1 (400 MHz, CDCl<sub>3</sub>): 4.17 (t, JHH = 6.6 Hz, 56H, 14x O-CH<sub>2</sub>-CH<sub>2</sub>-CH<sub>2</sub>-CH<sub>2</sub>-CH<sub>2</sub>-CH<sub>2</sub>-O), 3.46 (q, JHH = 6.8 Hz, 4H, 2x CH<sub>2</sub>-OH), 2.42 (t, JHH = 7.3 Hz, 56H, 14x CO-CH<sub>2</sub>-CH<sub>2</sub>-CH<sub>2</sub>-CO), 2.17-2.10 (m, 27H, 14x CO-CH<sub>2</sub>-CH<sub>2</sub>-CH<sub>2</sub>-CO), 1.62-1.55 (m, 56H, 14x O-CH<sub>2</sub>-CH<sub>2</sub>-CH<sub>2</sub>-CH<sub>2</sub>-CH<sub>2</sub>-CH<sub>2</sub>-O), 1.32-1.26 (m, 56H, 14x O-CH<sub>2</sub>-CH<sub>2</sub>-CH<sub>2</sub>-CH<sub>2</sub>-CH<sub>2</sub>-CH<sub>2</sub>-O)

## Glutaric Acid Isosorbide Polyester [PolyISOGA]



For the synthesis of PolyISOGA, a procedure similar to the work of Noordover B. A. J.<sup>53</sup> was executed. At first all educts were purified via recrystallization. The para-toluolsulfonic acid was recrystallized in chloroform and isosorbide in isopropanol. Then 1 eq. of the glutaric acid, a suitable amount of pure isosorbide, depending on the aimed molecular weight, and 0.006 eq. of para-toluolsulfonic acid were added into a 100 mL three-necked-round bottom flask, which was attached to a mechanical stirrer (150 rpm), a distillation apparatus and a valve. The oil bath was set to 150 °C, a continuous stream of argon gas was applied via the valve for the first hour to help the formed water reach the distillation apparatus. The reaction progress was checked via acid value (Table 35). After 24 h, 20 mbar of vacuum were applied. After a total of 52 h the acid value indicated full conversion and therefore the reaction was stopped. 80 mL of acetonitrile were added to dissolve the viscous polyester in the flask. The polymer was then precipitated in 1700 mL of diethyl ether, which was further dried in vacuum. Yielding between 69 and 80% PolyISOGA as brownish polyesters (Table 34).

Table 34: Ratios of the glutaric acid, isosorbide and the catalyst (para-toluolsulfonic acid); amount of solvent used; resulting yields

Product	Diacid [mmol]	Diacid [g]	Diol [mmol]	Diol [g]	Catalyst [mmol]	Catalyst [mg]	Yield [g]	Yield [%]
POLYESTER-5	100	13.20	105	15.35	0.6	104.2	19.11	78
POLYESTER-6	100	13.20	110	16.08	0.6	105.9	20.14	80
POLYESTER-7	100	13.20	121	17.69	0.6	107.4	18.43	69

## Analytics:

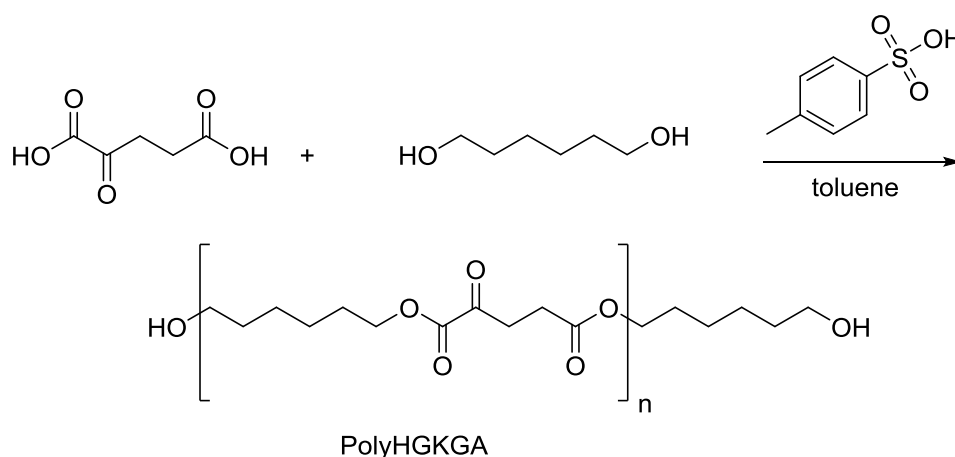
Table 35: Calculation of the acid value for POLYESTER-5 with a blank value of 0.050 mL in acetonitrile and a KOH concentration of 0.1649 mol/l

Reaction Time [h]	KOH [mL]	m <sub>sample</sub> [mg]	Acid Value [mgKOH/g]
1	11.146	461.5	222.4
23	3.552	238.1	136.1
31	0.940	261.0	31.5
48	0.310	297.5	8.1
52	0.078	316.8	0.8

<sup>1</sup>H-NMR of POLYESTER-7 (600 MHz, DMSO): 5.14-4.97 (m, 26H, 13x CH-CH<sub>2</sub>-CH<sub>2</sub>-CH), 4.84-4.62 & 4.41-4.35 (m, 26H, 13x CH<sub>2</sub>-CH-CH-CH<sub>2</sub>), 4.16-4.07 (m, 2H, 2x CH<sub>2</sub>-CH-OH), 4.08-4.01 (m, 2H, 2x OH), 3.85-3.74 & 3.42-3.23 (m, 52H, 13x CH<sub>2</sub>-O-CH-CH-CH<sub>2</sub>), 2.46-2.28 (m, 48H, 12x CO-CH<sub>2</sub>-CH<sub>2</sub>-CH<sub>2</sub>-CO), 1.89-1.67 (m, 24H, 12x CO-CH<sub>2</sub>-CH<sub>2</sub>-CH<sub>2</sub>-CO)

### 3.2. Synthesis of $\alpha$ -Ketoglutaric Acid-based Polyesters [Poly(HD/ISO)KGA]

#### $\alpha$ -Ketoglutaric Acid Hexanediol Polyester [PolyHDKGA]



To achieve the polymeric PolyHDKGA, a synthesis according to the book Polymer Synthesis<sup>46</sup> was performed. At first all educts were purified via recrystallization. The para-toluolsulfonic acid was recrystallized in chloroform, hexanediol in diethyl ether and the  $\alpha$ -ketoglutaric acid in acetone. Then 1 eq. of the pure  $\alpha$ -ketoglutaric acid, a suitable amount of pure hexanediol, depending on the aimed molecular weight, and 0.0025 eq. of para-toluolsulfonic acid were added into a 250 mL one-necked-round bottom flask, which was attached to a Dean-Stark Apparatus. Then absolute toluene was added. The oil bath was set to 125 °C and the mixture was magnetically stirred. The reaction progress was checked via NMR. After a total reaction time of 24 h, the mixture was precipitated in 2500 mL of cold petrol ether. The result was a white, slightly yellowish polymer, which was further dried in the vacuum. Afterwards the product was melted and dissolved in 2 x 75 mL of distilled acetone. Then the polyester was precipitated in 2 x 1800 mL of cold deionized water via a dropping funnel (~1.5 drops per

second). The result was a white polymer, which was further dried in vacuum, yielding between 50 and 92% of PolyHDKGA (Table 36).

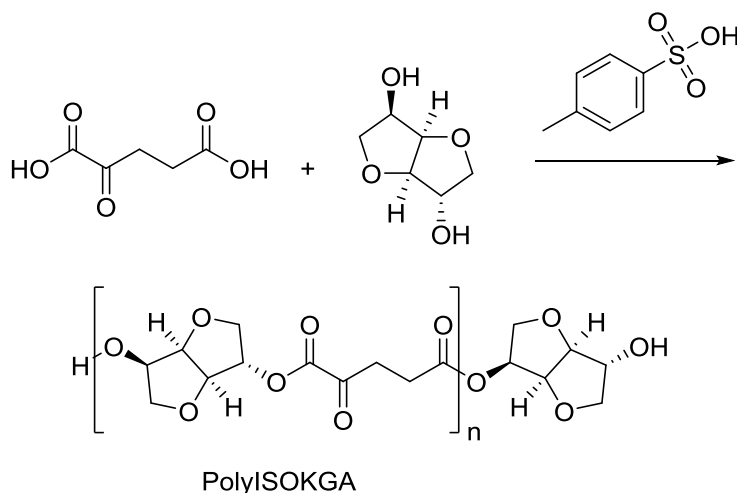
Table 36: Ratios of the  $\alpha$ -ketoglutaric acid, hexanediol and the catalyst (para-toluolsulfonic acid); amount of solvent used; resulting yields

Product	Diacid [mmol]	Diacid [g]	Diol [mmol]	Diol [g]	Catalyst [mmol]	Catalyst [mg]	Toluene [mL]	Yield [g]	Yield [%]
POLYESTER-9	80	11.68	88	9.54	0.2	34.7	60	15.57	82
POLYESTER-10	80	11.68	84	9.92	0.2	35.8	60	17.19	92
POLYESTER-8	80	11.68	81	9.54	0.2	33.1	150	9.24	50
POLYESTER-11	80	11.68	84	9.92	0.2	38.1	120	9.92	53
POLYESTER-12	80	11.68	83	9.83	0.2	36.5	120	11.01	59

#### Analytics:

$^1\text{H-NMR}$  of POLYESTER-12 (400 MHz,  $\text{CDCl}_3$ ): 4.26 (t,  $J_{\text{HH}} = 6.6$  Hz, 40 H, 20x  $\text{CO-CO-O-CH}_2\text{-CH}_2\text{-CH}_2\text{-CH}_2\text{-CH}_2\text{-O}$ ), 4.08 (t,  $J_{\text{HH}} = 6.6$  Hz, 40 H, 20x  $\text{CO-CO-O-CH}_2\text{-CH}_2\text{-CH}_2\text{-CH}_2\text{-CH}_2\text{-O}$ ), 3.65 (t,  $J_{\text{HH}} = 6.6$  Hz, 4H, 2x  $\text{CH}_2\text{-OH}$ ), 3.15 (t,  $J_{\text{HH}} = 6.6$  Hz, 40H, 20x  $\text{O-CO-CO-CH}_2$ ), 2.67 (t,  $J_{\text{HH}} = 6.6$  Hz, 40H, 20x  $\text{O-CO-CH}_2$ ), 1.78-1.72 (m, 40H, 20x  $\text{CO-CO-O-CH}_2\text{-CH}_2\text{-CH}_2\text{-CH}_2\text{-CH}_2\text{-O}$ ), 1.68-1.60 (m, 40H, 20x  $\text{CO-CO-O-CH}_2\text{-CH}_2\text{-CH}_2\text{-CH}_2\text{-O}$ ), 1.45-1.36 (m, 80H, 20x  $\text{O-CH}_2\text{-CH}_2\text{-CH}_2\text{-CH}_2\text{-O}$ )

#### $\alpha$ -Ketoglutaric Acid Isosorbide Polyester [PolyISOKGA]



For the synthesis of PolyISOGA, a procedure similar to the work of Noordover B. A. J.<sup>53</sup> was executed. At first all educts were purified via recrystallization. The para-toluolsulfonic acid was recrystallized in chloroform, isosorbide in isopropanol and the  $\alpha$ -ketoglutaric acid in acetone. Then 1 eq. of the  $\alpha$ -ketoglutaric acid, a suitable amount of pure isosorbide, depending on the aimed molecular weight, and 0.0025/0.006 eq. of para-toluolsulfonic acid were added into a 100 mL three-necked-round bottom flask, which was attached to a mechanical stirrer (150 rpm), a distillation apparatus and a valve. The oil bath was set to 150 °C, a continuous stream of argon gas was applied via the valve for the first hour to help the formed water reach the

distillation apparatus. The reaction progress was checked via NMR. 21 h later, 20 mbar of vacuum were applied for 4 h. After a total reaction time of 25 h the viscous, orange polymer was diluted with 80 mL of distilled acetonitrile and precipitated in 1500 mL of diethyl ether. The orange-yellowish polyester was further dried in vacuum. The dried product was then dissolved in distilled acetone. There a phase separation, with an upper yellowish phase and a brown phase on the bottom of the beaker, occurred. 1500 mL of diethyl ether were used to precipitate the upper phase and the polymer was further dried in vacuum. 12 to 51% yield as a yellowish polyester were achieved via this reaction (Table 37).

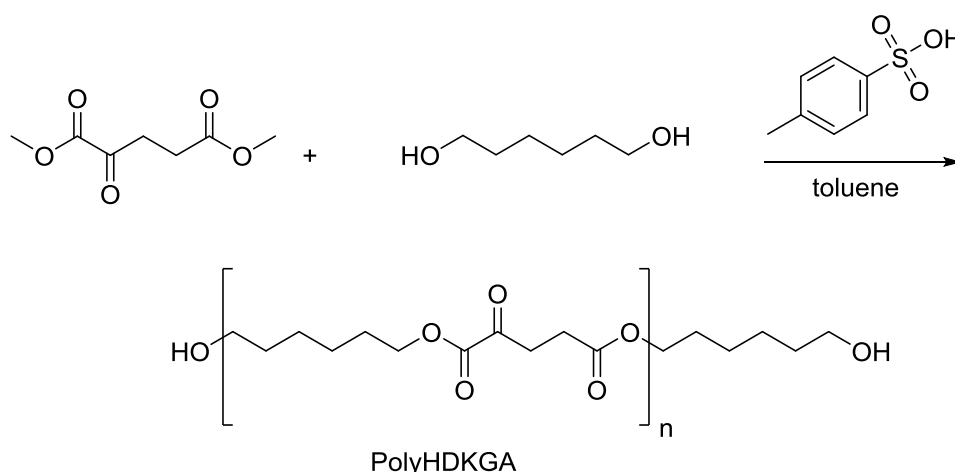
Table 37: Ratios of the  $\alpha$ -ketoglutaric acid, isosorbide and the catalyst (para-toluolsulfonic acid); amount of solvent used; resulting yields

Product	Diacid [mmol]	Diacid [g]	Diol [mmol]	Diol [g]	Catalyst [mmol]	Catalyst [mg]	Yield [g]	Yield [%]
POLYESTER-14	80	11.68	84	12.28	0.2	38.0	5.61	27
POLYESTER-15	80	11.68	88	12.86	0.2	34.6	10.96	51
POLYESTER-16	80	11.68	81	11.89	0.2	34.2	9.34	45
POLYESTER-14A	100	14.60	105	15.35	0.6	107.4	7.79	30
POLYESTER-17	100	14.60	102	14.91	0.6	104.0	3.59	14
POLYESTER-16A	100	14.06	101	14.67	0.6	106.2	3.13	12

#### Analytics:

$^1\text{H-NMR}$  of POLYESTER-15 (600 MHz, DMSO): 5.34-4.92 (m, 20H, 10x  $\text{CH-CH-CH-CH}$ ), 4.92-4.37 (m, 20H, 10x  $\text{CH-CH-CH-CH}$ ), 4.17-4.10 (m, 2H, 2x  $\text{CH}_2\text{-CH-OH}$ ), 4.10-4.02 (m, 2H, 2x  $\text{OH}$ ) 3.94-3.73 & 3.48-3.21 (m, 40H, 10x  $\text{CH}_2\text{-O-CH-CH-CH}_2$ ), 3.21-2.89 (m, 18H, 9x  $\text{CO-CO-CH}_2$ ), 2.79-2.54 (m, 18H, 9x  $\text{CO-CO-CH}_2\text{-CH}_2$ )

### $\alpha$ -Ketoglutaric Acid Dimethylester Hexanediol Polyester [PolyHDKGA]



For the synthesis of PolyHDKGA by a transesterification, a procedure according to the book *Polymer Synthesis*<sup>46</sup> was performed. At first hexanediol was recrystallized in diethyl ether and the para-toluolsulfonic acid was recrystallized in chloroform. Then 1 eq. (5.50 g, 30 mmol) of the  $\alpha$ -ketoglutaric acid dimethylester, 1.05 eq. (3.73 g, 32 mmol) of the pure hexanediol and 0.0045 eq. (23.6 mg, 0.15 mmol) were added into a 100 ml three-necked-round bottom flask, which was attached to a micro distillation bridge. Then 40 ml of absolute toluene were added. The oil bath was set to 80 °C and the mixture was magnetically stirred. The reaction progress was checked via NMR and after 2 h a reduced pressure of 850 mbar was applied. The second pressure reduction was after 46 h to 600 mbar and 5 ml of absolute toluene were added. After a total reaction time of 118 h, 10 ml of toluene were added to the mixture and the product was precipitated in 800 ml of cold diethyl ether. The result was a white, slightly yellowish viscous fluid, which was further dried in vacuum. Afterwards the polymer was dissolved in 30 ml of distilled acetone and reprecipitated in 500 ml of diethyl ether at room temperature. The polymer was a viscous solid after the second drying process. The NMR measurement had shown, that there is still hexanediol in the polymer. So the product was dissolved in 30 ml of distilled acetone and was precipitated in deionized water at room temperature. After the third drying process the product was a white sticky polymer. 3.95 g (39%) of the product were achieved.

#### Analytics:

<sup>1</sup>H-NMR (400 MHz, CDCl<sub>3</sub>): 4.26 (t, JHH = 6.6 Hz, 40 H, 20x CO-CO-O-CH<sub>2</sub>-CH<sub>2</sub>-CH<sub>2</sub>-CH<sub>2</sub>-CH<sub>2</sub>-O), 4.08 (t, JHH = 6.6 Hz, 40 H, 20x CO-CO-O-CH<sub>2</sub>-CH<sub>2</sub>-CH<sub>2</sub>-CH<sub>2</sub>-CH<sub>2</sub>-CH<sub>2</sub>-O), 3.65 (t, JHH = 6.6 Hz, 4H, 2x CH<sub>2</sub>-OH), 3.15 (t, JHH = 6.6 Hz, 40H, 20x O-CO-CO-CH<sub>2</sub>), 2.67 (t, JHH = 6.6 Hz, 40H, 20x O-CO-CH<sub>2</sub>), 1.78-1.72 (m, 40H, 20x CO-CO-O-CH<sub>2</sub>-CH<sub>2</sub>-CH<sub>2</sub>-CH<sub>2</sub>-CH<sub>2</sub>-O), 1.68-1.60 (m, 40H, 20x CO-CO-O-CH<sub>2</sub>-CH<sub>2</sub>-CH<sub>2</sub>-CH<sub>2</sub>-CH<sub>2</sub>-O), 1.45-1.36 (m, 80H, 20x O-CH<sub>2</sub>-CH<sub>2</sub>-CH<sub>2</sub>-CH<sub>2</sub>-CH<sub>2</sub>-O)

### 3.3. Molecular Weight Determination of the Polyesters

#### 3.3.1. Acid Value Determination

To determine the acid value during the reaction and of the final product a sample with a mass about 300 mg was weighed into a 100 mL Erlenmeyer flask at the analytic scale and then after adding 50 mL of acetone it was titrated with KOH. Also a blank value was measured (50 mL of pure acetone were titrated without a sample dissolved). The titration was continued until the solutions color changed from colorless to pink and to indicate this point, phenolphthalein was used as an indicator.<sup>46</sup>

The concentration of the potassium hydroxide solution was calculated first (Equation 6).

*Equation 6: Calculation of the concentration of the titer<sup>61</sup>*

$$c_{titer} \left[ \frac{\text{mol}}{\text{L}} \right] = \frac{m_{acid}}{M_{acid} * V_{base}}$$

$m_{acid}$  ... mass of potassium hydrogen phthalate [g]

$M_{acid}$  ... molecular weight of potassium hydrogen phthalate [g/mol]

$V_{base}$  ... volume used of potassium hydroxide solution in methanol [L]

The potassium hydroxide solution in methanol was made out of 5.61 g KOH and filled up to the 1 l mark with methanol. To determine the exact concentration (Equation 6) of the KOH solution a solution of 1.0243 g potassium hydrogen phthalate ( $M = 204.22 \text{ g/mol}$ ) in 250 mL deionized water was made. Then 25 mL of this solution were titrated with the unknown KOH solution to calculate the exact concentration:

$$c_{KOH} = \frac{0.10243 \text{ g}}{204.22 \text{ g/mol} * 0.003042 \text{ l}} = \mathbf{0.16488 \text{ mol/l}}$$

With the thus obtained titer concentration the acid value of the samples could be calculated as shown in Equation 7.

*Equation 7: Calculation of the acid value of the samples<sup>46</sup>*

$$AV \left[ \frac{\text{mgKOH}}{\text{g}} \right] = \frac{(V_{base} - V_{blank}) * c_{titer} * M_{base}}{m_{sample}}$$

$V_{base}$  ... volume used of potassium hydroxide solution in methanol for the sample [L]

$V_{blank}$  ... volume used of potassium hydroxide solution in methanol for the blank value [L]

$c_{titer}$  ... concentration of the titer [mol/L]

$M_{base}$  ... molecular weight of potassium hydroxide [g/mol]

$m_{sample}$  ... mass of sample used [mg]

The theoretical acid value was also determined to further calculate the conversion (Equation 8).



Equation 8: Calculation of the theoretical acid value<sup>46, 62</sup>

$$AV_{th} \left[ \frac{mgKOH}{g} \right] = \frac{\frac{m_{acid}}{M_{acid}} * n}{m_{total} * M_{base}} * 1000$$

$m_{acid}$  ... mass of acid weighed in [g]

$M_{acid}$  ... molecular weight of the acid [g/mol]

$n$  ... number of acid groups in the molecule [ ]

$m_{total}$  ... total mass of educts weighed in [g]

$M_{base}$  ... molecular weight of potassium hydroxide [g/mol]

Now the conversion can be calculated by referring the measured acid value to the theoretical acid value (Equation 9).

Equation 9: Calculation of the conversion using acid values

$$p [\%] = \left( 1 - \frac{AV}{AV_{th}} \right) * 100$$

$AV$  ... acid value of the measured sample [mgKOH/g]

$AV_{th}$  ... theoretical acid value calculated [mgKOH/g]

If the reaction mixture contained solvent, it was calculated which amount [mg] of educts are dissolved in which amount [mL] of solvent and as a sample 0.6 mL of the reaction mixture were taken, 50 mL of acetone were added and the sample was titrated with KOH. This assumption was as accurate as evaporation of the solvent, weighing of the residue and further calculating of the acid value via titration.

### 3.3.2. Hydroxyl Value Determination

The exact concentration of the 1 N potassium hydroxide solution in methanol was determined via titration of potassium hydrogen phthalate and calculated via Equation 6. The corrected hydroxyl value was evaluated via Equation 10.

Equation 10: Calculation of the corrected hydroxyl value of the samples<sup>46</sup>

$$corr. OHV \left[ \frac{mgKOH}{g} \right] = \frac{M_{base} * N_{base} * (V_{base} - V_{blank})}{m_{sample}} + AV$$

$M_{base}$  ... molecular weight of potassium hydroxide [g/mol]

$N_{base}$  ... normality of the potassium hydroxide solution [mol/L]

$V_{base}$  ... volume used of potassium hydroxide solution in methanol for the sample [L]

$V_{blank}$  ... volume used of potassium hydroxide solution in methanol for the blank value [L]

$m_{sample}$  ... mass of the sample used [mg]

$AV$  ... acid value of the sample [mgKOH/g]

Now the absolute molecular weight of a polyester can be calculated via the corrected hydroxyl value and the acid value, shown in Equation 11.

Equation 11: Calculation of the molecular weight of the polyesters

$$M_n \left[ \frac{g}{mol} \right] = \frac{M_{base} * z}{OHV + AV}$$

$M_{base}$  ... molecular weight of potassium hydroxide [g/mol]

$z$  ... number of terminal hydroxyl groups in the polyester [ ]

$AV$  ... acid value of the sample [mgKOH/g]

$OHV$  ... corrected hydroxyl value of the sample [mgKOH/g]

#### 3.3.2.1. Reaction with Acetic Anhydride and Titration

At first, a sample with a weight about 1 g was taken, put into a penicillin vial, dissolved in 10 mL of absolute pyridine, sealed and set under argon atmosphere. Then 3 mL of a premade acetylation reagent (30 g acetic anhydride and 70 g absolute pyridine) were added into the vial. Then the reaction mixture was heated to 110 °C for 70 minutes. To quench the reaction, 5 mL of deionized water were added and finally the resulting solution titrated with 1 N potassium hydroxide solution ( $f = 0.8997$ ) in methanol against phenolphthalein from colorless to pink. Two blanks were treated equally.<sup>54</sup>

#### 3.3.2.2. Reaction with Acetic Acid and Titration

A sample with the weight of approximately 1 g was put into a penicillin vial and dissolved in 20 mL of distilled acetone. Then an acetylation solution was prepared, containing 30 mL ethyl acetate, 1.5 mL acetic acid and 66.8 mg para-toluolsulfonic acid. The mixture was now sealed, stirred of 45 minutes at 50 °C and after the reaction time, quenched with 10 mL of a solution out of 60 mL pyridine and 40 mL deionized water. After that, the mixture was titrated with 1 N potassium hydroxide solution ( $f = 0.8997$ ), using phenolphthalein as an indicator, from colorless to pink. Two blank samples were treated equally.<sup>46</sup>

#### 3.3.3. Gel Permeation Chromatography

The samples were dissolved in absolute THF with 250 ppm BHT as inhibitor, achieving a concentration of 3 mg/mL. Before the GPC measurement, the dissolved polyesters were filtrated by a syringe filter to avoid insoluble parts of the polyester entering the column.

#### 3.3.4. <sup>1</sup>H-NMR Determination

To evaluate the molecular weight of the different polyesters via NMR, the samples were dissolved in deuterated chloroform for all hexanediol containing polymers and in DMSO for all isosorbide containing polymers. The  $CH_x$  group next to the hydroxyl endgroups in the molecule is referred to one or two  $CH_2$  peaks to calculate the average degree of polymerization and therefore the molecular weight  $M_n$ . The integrated region in the spectra for the evaluation of the molecular weights is shown in Table 38.

Table 38: Regions [ppm] for integration in the spectrum to determine the molecular weight; for all hexanediol containing polyesters a 400 MHz NMR was measured, and for the isosorbide-based ones a 600 MHz NMR

Polyester Sample	CH <sub>x</sub> [ppm]	CH <sub>2</sub> ref.1 [ppm]	CH <sub>2</sub> ref.2 [ppm]
<b>α-Ketoglutaric Acid Hexanediol</b>	3.71-3.60 (CH <sub>2</sub> )	4.31-4.22 (1xCH <sub>2</sub> )	4.13-4.04 (1xCH <sub>2</sub> )
<b>Glutaric Acid Hexanediol</b>	3.42-3.28 (CH <sub>2</sub> )	4.16-3.95 (2xCH <sub>2</sub> )	2.10-1.96 (1xCH <sub>2</sub> )
<b>α-Ketoglutaric Acid Isosorbide</b>	4.17-4.10 (CH)	3.07-2.92 (1xCH <sub>2</sub> )	2.60-2.44 (1xCH <sub>2</sub> )
<b>Glutaric Acid Isosorbide</b>	4.15-4.08 (CH)	2.45-2.30 (2xCH <sub>2</sub> )	1.86-1.68 (1xCH <sub>2</sub> )

### 3.3.5. <sup>31</sup>P-NMR Determination

Firstly about 50 mg of sample were weighted into a sealable 5 mL vial and dissolved in 300 μL of absolute DMF. Then 5 mg of N-hydroxy-5-norbornene-2,3-dicarboximide as the internal standard were added. Then the vial was set under argon atmosphere and sealed. Using a pipette, 100 μL of 2-chloro-1,3,2-dioxaphospholane and 100 μL of absolute pyridine and 600 μL of deuterated chloroform were added by quickly removing the lid of the vial, while setting the surroundings of the vial and the dioxaphospholane-bottle under argon atmosphere via a upside down funnel, connected with a argon gas outlet. After stirring this mixture for 10 minutes intensively at a vortex, a quantitatively evaluable <sup>31</sup>P-NMR was measured immediately.<sup>55</sup> The exact values for the weights are shown in Table 39.

Table 39: Weights and OHV calculation with the <sup>31</sup>P-NMR method; J describes the area of the integral

sample	internal standard [mg]	m <sub>sample</sub> [mg]	J <sub>sample</sub> [ ]	OHV [mmol/g]	OHV <sub>theory</sub> [mmol/g]
<b>polyTHF2900</b>	5.28	52.67	1.33	0.75	0.80
<b>α-ketoglutaric acid</b>	5.08	50.75	26.42	14.76	15.83
<b>hexanediol</b>	5.71	56.76	23.54	13.22	9.51
<b>isosorbide</b>	5.71	56.76	30.04	16.87	20.05
<b>glutaric acid 0 min</b>	5.79	57.56	28.05	15.75	16.35
<b>glutaric acid 30 min</b>	5.25	53.06	32.01	17.68	20.22

### 3.3.6. Reaction with Phenyl Isocyanate and Titration

To determine the isocyanate value of a polymer, approximately 0.3 g of sample were dissolved in 6 mL of absolute DMF in a penicillin vial. Then 5 mL of a 1 N solution of phenyl isocyanate in absolute toluene (5.956 g in 50 mL absolute toluene) were added into the vial, followed by sealing it for the reaction at 98 °C for 40 minutes. Afterwards the mixture was quenched with 5 mL of a 2 N dibutylamine solution in toluene (12.924 g in 50 mL absolute toluene) and 15 minutes later, 50 mL of isopropanol were added. Two blanks were treated equally. Then the samples and the blanks were titrated with a 0.1 hydrochloric acid from blue to green to a yellow end point, using bromocresol green as an indicator.<sup>56</sup> The polyTHF and the one α-ketoglutaric acid-based polyester is listed in Table 40.

The hydrochloric acid solution in deionized water was made out of 8.5 mL of concentrated HCl and filled to the 1 l mark with deionized water. Then 1 g of sodium carbonate (M = 105.99 g/mol) were diluted in 250 mL of deionized water. 25 mL of this solution were titrated with the established hydrochloric acid solution. The exact concentration was calculated via Equation 12.

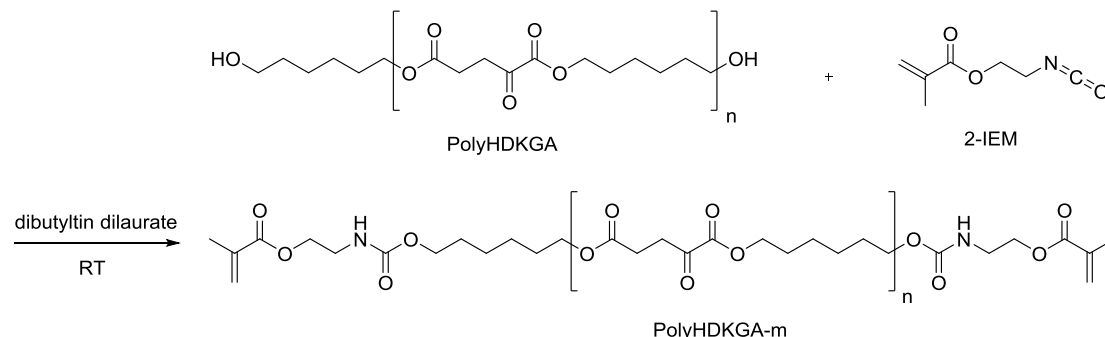
$$c_{HCl} = \frac{0.1 \text{ g} * 2}{105.99 \text{ g/mol} * 0.017025 \text{ l}} = \mathbf{0.1108 \text{ mol/l}}$$

Table 40: NCO value determination of one polyester and polyTHF with a blank value of 78.250 ml (0.1108 mol/l HCl)

sample	HCl [ml]	m <sub>sample</sub> [g]	NCO [%]
polyTHF2800_1	80.130	0.3060	0.029
polyTHF2800_2	80.320	0.3049	0.032
POLYESTER-12_1	79.320	0.3060	0.016
POLYESTER-12_2	79.182	0.2550	0.017

## 4. Synthesis of Macromolecular, Polymerizable Photoinitiators

### 4.1. $\alpha$ -Ketoglutaric Acid Hexanediol Polyester with 2-IEM Endgroup [PolyHDKGA-m]



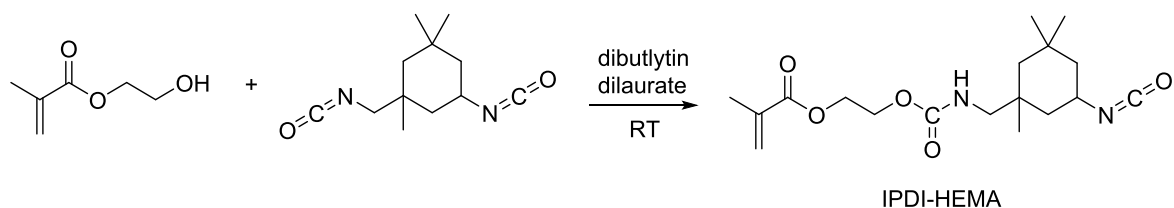
For the synthesis of PolyHDKGA-m, similar to the work of Ashraf S. M.,<sup>58</sup> the polyesters (ketoglutaric acid and 1,6-hexanediol) molecular weight was determined by GPC (4888 g/mol) and hydroxyl group determination via NMR (4905 g/mol). An average of 4900 g/mol was taken to further calculate the amount of 2-isocyanatoethyl methacrylate. 1 eq. (0.98 g, 0.2 mmol) of the polyester, 2 drops of and 20 ml of dibutyltin dilaurate and absolute toluene were added into a 50 ml three necked round bottom flask with a magnetic stir bar. Then the apparatus was flushed with argon gas and equipped with an argon balloon. Then 2.05 eq. (0.6 ml, 0.4mmol) of the 2-isocyanatoethyl methacrylate were added dropwise to the reaction mixture. The mixture was stirred for 14 h and then quenched with 5 ml of methanol. Then 20 ml of distilled acetone were added and the polyester was precipitated in 300 ml of cold diethyl ether. The white polymer product was dried in vacuum with a resulting yield of 0.36 g (34%).

#### Analytics:

$^1\text{H-NMR}$  (400 MHz,  $\text{CHCl}_3$ ): 6.12 (s, 2H, 2x O-CO-C-CH $\underline{\text{H}}$ ), 5.59 (s, 2H, 2x O-CO-C-CH $\underline{\text{H}}$ ), 5.34 (s, 2H, 2x O-CO-N $\underline{\text{H}}$ ), 4.26 (t, J $\underline{\text{H}}$ H = 6.6 Hz, 80 H, 40x CO-CO-O-CH $\underline{2}$ -CH $\underline{2}$ -CH $\underline{2}$ -CH $\underline{2}$ -CH $\underline{2}$ -CH $\underline{2}$ -O), 4.15 (t, 4H, J $\underline{\text{H}}$ H = 6.4 Hz, 2x NH-CH $\underline{2}$ -CH $\underline{2}$ ), 4.08 (t, J $\underline{\text{H}}$ H = 6.6 Hz, 80 H, 40x CO-CO-O-CH $\underline{2}$ -CH $\underline{2}$ -CH $\underline{2}$ -CH $\underline{2}$ -CH $\underline{2}$ -O), 3.65 (t, J $\underline{\text{H}}$ H = 6.4 Hz, 4H, 2x NH-CH $\underline{2}$ -CH $\underline{2}$ ), 3.15 (t, J $\underline{\text{H}}$ H = 6.6 Hz, 80H, 40x O-CO-CO-CH $\underline{2}$ ), 2.67 (t, J $\underline{\text{H}}$ H = 6.6 Hz, 80H, 40x O-CO-CH $\underline{2}$ ), 1.95 (s, 6H, 2x CH $\underline{3}$ ) 1.78-1.72 (m, 80H, 40x CO-CO-O-CH $\underline{2}$ -CH $\underline{2}$ -CH $\underline{2}$ -CH $\underline{2}$ -CH $\underline{2}$ -O), 1.68-1.60 (m, 80H, 40x CO-CO-O-CH $\underline{2}$ -CH $\underline{2}$ -CH $\underline{2}$ -CH $\underline{2}$ -CH $\underline{2}$ -O), 1.45-1.36 (m, 160H, 40x O-CH $\underline{2}$ -CH $\underline{2}$ -CH $\underline{2}$ -CH $\underline{2}$ -CH $\underline{2}$ -O)

## 4.2. Synthesis of Polyesters with the IPDI-HEMA Endgroup

### 4.2.1. Synthesis of the IPDI-HEMA Endgroup [IPDI-HEMA]



To achieve the IPDI-HEMA endgroup, an approach according to Ogg C. L.<sup>59</sup> was executed. At first an oil bath was set to 80 °C and 2-hydroxymethylmethacrylate was distilled (58-59 °C, 0.05 mbar). Then an oil bath was set to 110 °C and isophorone diisocyanate was also freshly distilled (101-102 °C, 0.02 mbar). Now 1 eq. (26.68 g, 120 mmol) of isophorone diisocyanate and 1 eq. (15.62, 120 mmol) of 2-hydroxyethyl methacrylate (stabilized with 250 ppm BHT) were weighed into a 50 mL one-neck round bottom flask equipped with a valve. After flushing the flask with argon, an argon balloon was attached to the valve and the oil bath was set to 60-70 °C. Reaction progress was monitored via ATR-IR spectroscopy. After 23.5 h two drops of dibutyltin dilaurate was added to the mixture and 3.5 h later the ATR-IR spectra did not change anymore. The reaction was now finished and cooled down to room temperature and stirred overnight. NCO-value titration indicated 98.3% conversion (Table 41) and a yield of 41.90 g of the IPDI-HEMA endgroup (99%).

#### Analytics

<sup>1</sup>H-NMR (400 MHz, CDCl<sub>3</sub>): 6.12 (s, 1H, O-CO-C-CH<sub>H</sub>), 5.59 (s, 1H, O-CO-C-CH<sub>H</sub>), 4.78 & 4.55 (s, 1H, CH-NH; CH<sub>2</sub>-NH), 4.32-4.31 (m, 4H, O-CH<sub>2</sub>-CH<sub>2</sub>-O), 3.84-2.88 (m, 3H, NH-CH<sub>2</sub>; NH-CH), 1.95 (s, 3H, HHC=C-CH<sub>3</sub>), 1.85-1.14 (m, 4H, NH-CH-(CH<sub>2</sub>)<sub>2</sub>), 1.10-0.87 (m, 11H, NH-CH<sub>2</sub>-C-CH<sub>2</sub>-C-(CH<sub>3</sub>)<sub>2</sub>; C-(CH<sub>3</sub>)<sub>2</sub>; NH-CH<sub>2</sub>-C-CH<sub>3</sub>)

<sup>13</sup>C-NMR (400 MHz, CDCl<sub>3</sub>): 167.4 (O-CO-C), 156.6 (O-CO-NH), 136.2 (CO-C=C), 126.2 (CO-C=C), 122.1 (N=C=O), 63.0 (CO-O-CH<sub>2</sub>), 62.5 (CO-O-CH<sub>2</sub>-CH<sub>2</sub>), 48.7 (CH-N=C=O), 48.2 (NH-CH<sub>2</sub>-C-CH<sub>2</sub>-C), 46.7 (NH-CH<sub>2</sub>), 41.7 (CH<sup>2</sup>-CH-N=C=O), 36.7 (NH-CH<sub>2</sub>-C-CH<sub>2</sub>-CH), 35.0 ((CH<sub>3</sub>)<sub>2</sub>-C), 32.0 ((CH<sub>3</sub>)<sub>2</sub>-C), 31.8 (CH<sub>3</sub>-C), 27.7 (CH<sub>3</sub>-C), 23.5 (CH<sub>3</sub>-C=C)

Table 41: Calculation of the isocyanate value with a blank value of 13.017 mL and an HCl concentration of 1.945 mol/l

HCl [mL]	m <sub>sample</sub> [g]	NCO [%]	Conversion [%]
12.200	0.50240	12.1	98.4
12.093	0.60077	12.3	97.2
12.207	0.56909	12.2	97.9
12.272	0.54836	11.9	99.8

To determine the isocyanate value, approximately 0.5 g of sample were weighed into an Erlenmeyer flask and dissolved in 25 mL of absolute toluene. Afterwards 25 mL of a 1 N solution of n-dibutylamine (12.92 g in 100 mL toluene) were added and the mixture was stirred

for 15 minutes at room temperature. Then bromophenol blue and 50 mL of isopropanol were added as an indicator and the mixture was titrated with 2 N hydrochloric acid to a yellow end point. Three blanks were treated equally.<sup>60</sup> The concentration of the hydrochloric acid ( $f = 0.9725$ ) was calculated via Equation 12.

*Equation 12: Calculation of the concentration of the titer<sup>61</sup>*

$$c_{titer} \left[ \frac{mol}{l} \right] = \frac{m_{acid}}{M_{acid} * V_{base}}$$

$m_{acid}$  ... mass of potassium hydrogen phthalate [g]

$M_{acid}$  ... molecular weight of potassium hydrogen phthalate [g/mol]

$V_{base}$  ... volume used of potassium hydroxide solution in methanol [L]

The isocyanate value was calculated via Equation 13.

*Equation 13: Calculation of the NCO value<sup>60</sup>*

$$NCO [\%] = \frac{(V_{blank} - V_{acid}) * c_{titer} * M_{NCO}}{m_{sample}} * 100$$

$V_{acid}$  ... volume used of hydrochloric acid solution in deionized water for the sample [L]

$V_{blank}$  ... volume used of hydrochloric acid solution in deionized water for the blank value [L]

$c_{titer}$  ... concentration of the titer [mol/L]

$M_{NCO}$  ... molecular weight of one isocyanate group [g/mol]

$m_{sample}$  ... mass of sample used [g]

The theoretical isocyanate value was determined via Equation 14.

*Equation 14: Calculation of the theoretical NCO value*

$$NCO_{th} [\%] = \frac{M_{product}}{M_{NCO}} * 100$$

$M_{product}$  ... molecular weight of the aimed product [g/mol]

$M_{NCO}$  ... molecular weight of one isocyanate group [g/mol]

The conversion can be calculated via dividing the theoretical by the actual isocyanate value shown in Equation 15.

*Equation 15: Calculation of the conversion*

$$p [\%] = \frac{NCO_{th}}{NCO} * 100$$

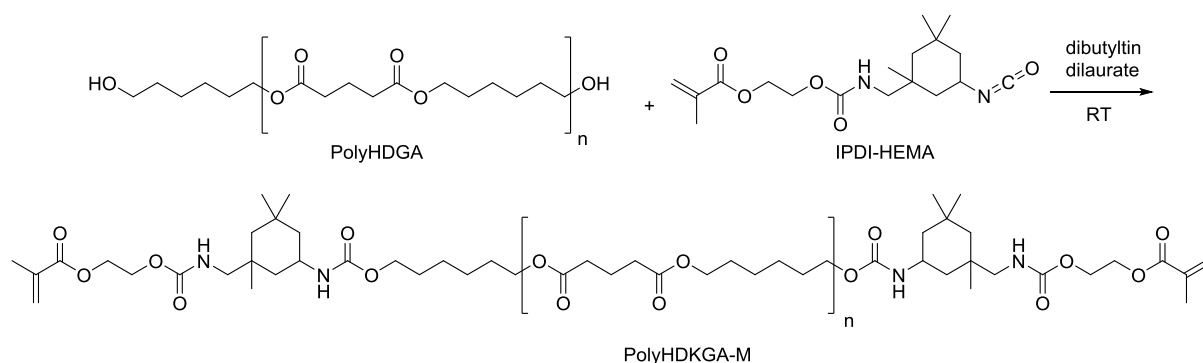
$NCO_{th}$  ... theoretical isocyanate value [%]

$NCO$  ... isocyanate value [%]

## 4.2.2. Synthesis of the Polyesters

### 4.2.2.1. Glutaric Acid-based Polyesters with IPDI-HEMA Endgroup [Poly(HD/ISO)GA]

#### Glutaric Acid Hexanediol Polyester with IPDI-HEMA Endgroup [PolyHDGA-M]



According to the work of Ashraf S. M.,<sup>58</sup> the PolyHDGA-M polyesters were synthesized. At first the polyesters molecular weight was determined by GPC and NMR to further calculate the amount of the isocyanate endgroup. 1 eq. of the polyester, 2.20 eq. of the isocyanate endgroup, 2 drops of dibutyltin dilaurate, absolute dichloro methane, and 200 ppm phenothiazine (0.8 mg), as an anaerobe inhibitor, were added into a 150 mL one necked round bottom flask with a magnetic stir bar. Then the apparatus was flushed with argon gas and equipped with an argon balloon. The mixture was stirred for 24 h at room temperature and finally the solvent was evaporated at the rotary evaporator. Afterwards the residue was washed with petrol ether (2x 100 mL) and after the petrol ether was removed via decantation, the polymer products (PolyHDGA) were dried in vacuum with resulting yields of 81% to 99% of white, viscous or solid, depending on the molecular weight, polyesters (Table 42).

Table 42: Ratios of the polyester and the IPDI-HEMA endgroup; amount of solvent used; resulting yields

Product	Polyester [mmol]	Polyester [g]	IPDI-HEMA [mmol]	IPDI-HEMA [g]	Dichloromethane [mL]	Yield [g]	Yield [%]
POLYESTER-2-1	1.7	5.00	3.7	1.30	50	4.98	81
POLYESTER-3-1	1	5.00	2.2	0.79	50	5.16	90
POLYESTER-4-1	0.5	5.00	1.2	0.40	150	5.31	99

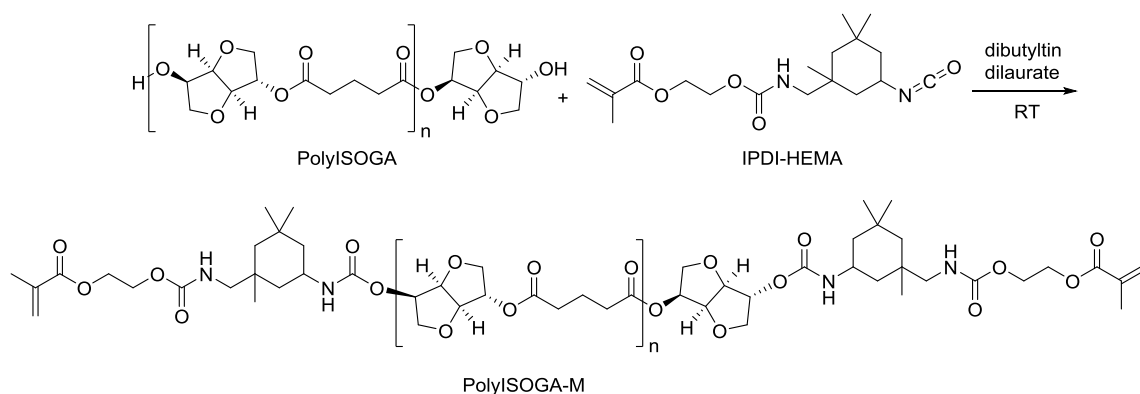
#### Analytcs

<sup>1</sup>H-NMR POLYESTER-3-1 (400 MHz, CDCl<sub>3</sub>): 6.12 (s, 2H, 2x O-CO-C-CHH), 5.59 (s, 2H, 2x O-CO-C-CHH), 5.02-4.73 (m, 2H, CH<sub>2</sub>-NH), 4.61-4.46 (m, 2H, CH-NH), 4.32-4.31 (m, 8H, 2x O-CH<sub>2</sub>-CH<sub>2</sub>-O), 4.06 (t, J<sub>HH</sub> = 6.6 Hz, 92H, 23x O-CH<sub>2</sub>-CH<sub>2</sub>-CH<sub>2</sub>-CH<sub>2</sub>-CH<sub>2</sub>-O), 3.84-2.88 (m, 3H, NH-CH<sub>2</sub>; NH-CH), 3.65 (t, J<sub>HH</sub> = 6.4 Hz, 4H, 2x CH-NH-CO-O-CH<sub>2</sub>), 2.37 (t, J<sub>HH</sub> = 6.6 Hz, 92 H, 23x CO-CH<sub>2</sub>-CH<sub>2</sub>-CH<sub>2</sub>-CO), 1.95 (s, 6H, 2x CH<sub>3</sub>) 1.95-1.91 (m, 46H, 23x CO-CH<sub>2</sub>-CH<sub>2</sub>-CH<sub>2</sub>-CO), 1.67-1.57 (m, 92H, 23x O-CH<sub>2</sub>-CH<sub>2</sub>-CH<sub>2</sub>-CH<sub>2</sub>-CH<sub>2</sub>-O), 1.44-1.32 (m, 92H, 23x O-CH<sub>2</sub>-CH<sub>2</sub>-CH<sub>2</sub>-CH<sub>2</sub>-CH<sub>2</sub>-O).



CH<sub>2</sub>-O), 1.85-1.14 (m, 4H, NH-CH-(CH<sub>2</sub>)<sub>2</sub>), 1.10-0.87 (m, 11H, NH-CH<sub>2</sub>-C-CH<sub>2</sub>-C-(CH<sub>3</sub>)<sub>2</sub>; C-(CH<sub>3</sub>)<sub>2</sub>; NH-CH<sub>2</sub>-C-CH<sub>3</sub>)

### Glutaric Acid Isosorbide Polyester with IPDI-HEMA Endgroup [PolyISOGA-M]



According to the work of Ashraf S. M.,<sup>58</sup> and analogous to the PolyHDGA-M, the PolyISOGA-M polyesters were synthesized. A resulting yield of 3.22 g (81%) of PolyISOGA-M as a brownish polyester was achieved.

The polyester was divided into three parts, weighed into penicillin vials and diluted in 10 mL of distilled acetone. Then, another 250 ppm of phenothiazine were added to achieve a total amount of 500 ppm of anaerobe inhibitor in the stock solutions. The concentrations of these solutions were calculated and illustrated in Table 43 for further tests, where exact quantities of the polyesters were needed.

Table 43: Stock solutions of the polyesters and their concentrations

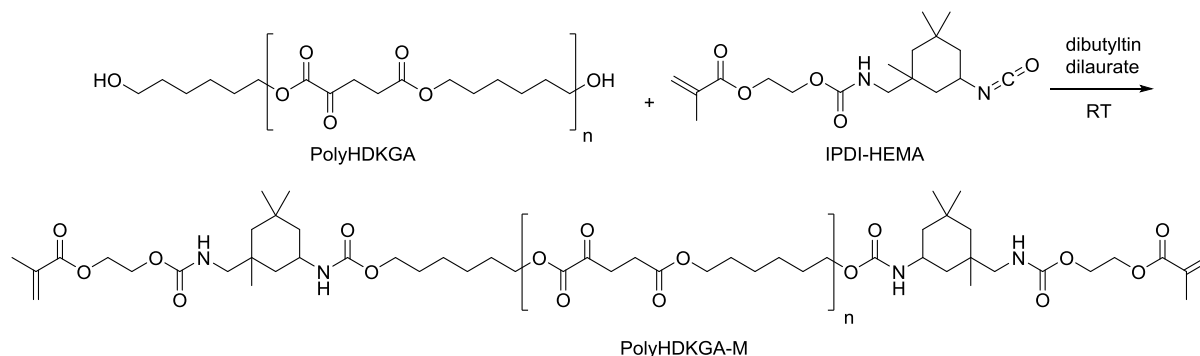
Polyester	m <sub>sample</sub> [g]	c <sub>sample</sub> [mg/mL]
<b>POLYESTER-15-1A</b>	1.1256	112.6
<b>POLYESTER-15-1B</b>	1.1588	115.9
<b>POLYESTER-15-1C</b>	1.0598	106.0

### Analysis

<sup>1</sup>H-NMR POLYESTER-15-1 (400 MHz, DMSO): 6.07 (s, 2H, 2x O-CO-C-CH<sub>H</sub>), 5.77-5.69 (m, 2H, 2x O-CO-C-CH<sub>H</sub>) 5.36-5.05 (m, 20H, 10x CH-CH<sub>H</sub>-CH<sub>H</sub>), 4.99-4.41 (m, 24H, 10x CH<sub>H</sub>-CH-CH-CH<sub>H</sub>; 2x CH-NH; 2x CH<sub>2</sub>-NH) 4.26-4.16 (m, 8H, 2x CO-CH<sub>2</sub>-CH<sub>2</sub>-CO) 4.14-4.01 (m, 2H, 2x CH<sub>2</sub>-CH-OH), 3.94-3.73 (m, 36H, 7.5x CH<sub>2</sub>-O-CH-CH-CH<sub>2</sub>; 2x NH-CH<sub>2</sub>; 2x NH-CH) 3.48-3.21 (m, 10H, 2.5x CH<sub>2</sub>-O-CH-CH-CH<sub>2</sub>), 3.24-2.97 (m, 18H, 9x CO-CO-CH<sub>2</sub>), 2.70-2.60 (m, 18H, 9x CO-CO-CH<sub>2</sub>-CH<sub>2</sub>) 1.94 (s, 6H, 2x HHC=C-CH<sub>3</sub>) 1.87-1.32 (m, 8H, 2x NH-CH-(CH<sub>2</sub>)<sub>2</sub>), 1.09-0.94 (m, 22H, 2x NH-CH<sub>2</sub>-C-CH<sub>2</sub>-C-(CH<sub>3</sub>)<sub>2</sub>; 2x C-(CH<sub>3</sub>)<sub>2</sub>; 2x NH-CH<sub>2</sub>-C-CH<sub>3</sub>)

4.2.2.2.  $\alpha$ -Ketoglutaric Acid-based Polyesters with IPDI-HEMA Endgroups  
[Poly(HD/ISO)KGA]

$\alpha$ -Ketoglutaric Acid Hexanediol Polyester with IPDI-HEMA Endgroup [PolyHDKGA-M]



According to the work of Ashraf S. M.,<sup>58</sup> and analogous to the PolyHDGA-M, the PolyISOGA-M polyesters were synthesized. The polymer products were dried in vacuum with resulting yields of 93% to 96% of yellowish polyesters (Table 44).

Table 44: Ratios of the polyester and the IPDI-HEMA endgroup; amount of solvent used; resulting yields

Product	Polyester [mmol]	Polyester [g]	IPDI-HEMA [mmol]	IPDI-HEMA [g]	Dichloromethane [mL]	Yield [g]	Yield [%]
POLYESTER-9-2	1	3.00	2.05	0.71	50	3.55	96
POLYESTER-8-2	0.3	3.00	0.63	0.23	50	3.01	94
POLYESTER-12-2	0.6	3.00	1.31	0.46	50	3.22	93

The product polyesters were divided into three parts, weighed into penicillin vials and diluted in 10 mL of distilled acetone. Then, another 250 ppm of phenothiazine were added to achieve a total amount of 500 ppm of anaerobe inhibitor in the stock solutions. The concentrations of these solutions were calculated and illustrated in Table 45 for further tests, where exact quantities of the polyesters were needed.

Table 45: Stock solutions of the polyesters and their concentrations

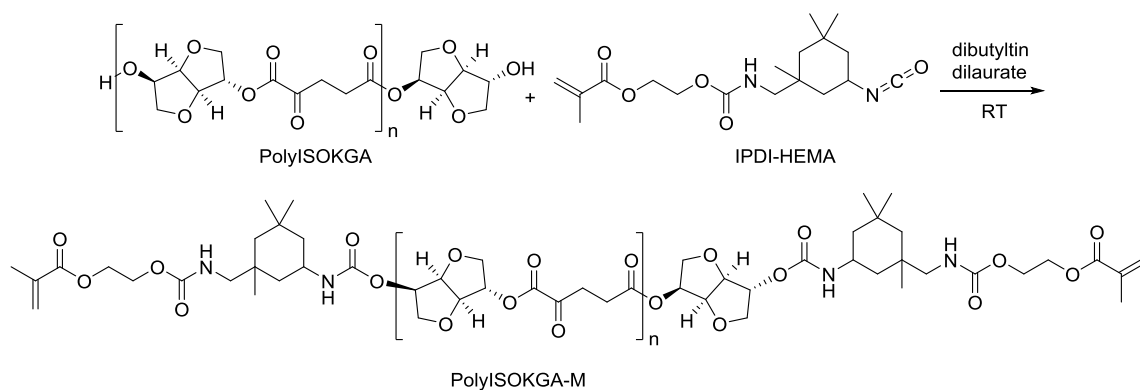
Polyester	$m_{\text{sample}}$ [g]	$c_{\text{sample}}$ [mg/mL]
POLYESTER-9-2A	1.3024	130.2
POLYESTER-9-2B	1.4428	144.3
POLYESTER-9-2C	1.3616	136.2
POLYESTER-8-2A	1.3727	137.3
POLYESTER-8-2B	1.2957	129.6
POLYESTER-8-2C	1.1894	118.9
POLYESTER-12-2A	1.0721	107.2

Polyester	m <sub>sample</sub> [g]	c <sub>sample</sub> [mg/mL]
POLYESTER-12-2B	0.9806	98.1
POLYESTER-12-2C	1.1242	112.4

### Analysis

**<sup>1</sup>H-NMR POLYESTER-12-2 (400 MHz, CDCl<sub>3</sub>):** 6.12 (s, 2H, 2x O-CO-C-CHH), 5.59 (s, 2H, 2x O-CO-C-CHH), 5.02-4.73 (m, 2H, CH<sub>2</sub>-NH), 4.61-4.46 (m, 2H, CH-NH), 4.32-4.31 (m, 8H, 2x O-CH<sub>2</sub>-CH<sub>2</sub>-O), 4.26 (t, JHH = 6.6 Hz, 44H, 22x CO-CO-O-CH<sub>2</sub>-CH<sub>2</sub>-CH<sub>2</sub>-CH<sub>2</sub>-CH<sub>2</sub>-O), 4.08 (t, JHH = 6.6 Hz, 44 H, 22x CO-CO-O-CH<sub>2</sub>-CH<sub>2</sub>-CH<sub>2</sub>-CH<sub>2</sub>-CH<sub>2</sub>-CH<sub>2</sub>-O), 3.84-2.88 (m, 3H, NH-CH<sub>2</sub>; NH-CH), 3.65 (t, JHH = 6.4 Hz, 4H, 2x CH-NH-CO-O-CH<sub>2</sub>), 3.15 (t, JHH = 6.6 Hz, 44H, 22x O-CO-CO-CH<sub>2</sub>), 2.67 (t, JHH = 6.6 Hz, 44H, 22x O-CO-CH<sub>2</sub>), 2.37 (t, JHH = 6.6 Hz, 92 H, 23x CO-CH<sub>2</sub>-CH<sub>2</sub>-CH<sub>2</sub>-CO), 1.95 (s, 6H, 2x CH<sub>3</sub>) 1.95-1.91 (m, 46H, 23x CO-CH<sub>2</sub>-CH<sub>2</sub>-CH<sub>2</sub>-CO), 1.78-1.72 (m, 44H, 22x CO-CO-O-CH<sub>2</sub>-CH<sub>2</sub>-CH<sub>2</sub>-CH<sub>2</sub>-CH<sub>2</sub>-O), 1.68-1.60 (m, 44H, 22x CO-CO-O-CH<sub>2</sub>-CH<sub>2</sub>-CH<sub>2</sub>-CH<sub>2</sub>-CH<sub>2</sub>-O), 1.45-1.36 (m, 88H, 22x O-CH<sub>2</sub>-CH<sub>2</sub>-CH<sub>2</sub>-CH<sub>2</sub>-CH<sub>2</sub>-O), 1.85-1.14 (m, 4H, NH-CH-(CH<sub>2</sub>)<sub>2</sub>), 1.10-0.87 (m, 11H, NH-CH<sub>2</sub>-C-CH<sub>2</sub>-C-(CH<sub>3</sub>)<sub>2</sub>; C-(CH<sub>3</sub>)<sub>2</sub>; NH-CH<sub>2</sub>-C-CH<sub>3</sub>)

### α-Ketoglutaric Acid Isosorbide Polyester with IPDI-HEMA Endgroup [PolyISOGKA-M]



According to the work of Ashraf S. M.,<sup>58</sup> and analogous to the PolyHDGA-M, the PolyISOGKA-M polyesters were synthesized. The polymer product was dried in vacuum with a resulting yield of 3.34 g (88%) as a brownish polyester.

### Analysis

**<sup>1</sup>H-NMR POLYESTER-7-1 (400 MHz, DMSO):** 6.03 (s, 2H, 2x O-CO-C-CHH), 5.69 (s, 2H, 2x O-CO-C-CHH) 5.20-4.89 (m, 26H, 13x CH-CH-CH-CH), 4.89-4.36 (m, 26 H, 13x CH-CH-CH-CH), 4.36-4.26 (m, 4H, 2x CH-NH; 2x CH<sub>2</sub>-NH) 4.26-4.17 (m, 8H, 2x CO-CH<sub>2</sub>-CH<sub>2</sub>-CO) 4.16-4.08 (m, 2H, 2x CH<sub>2</sub>-CH-OH), 3.87-3.71 (m, 45H, 9.75x CH<sub>2</sub>-O-CH-CH-CH<sub>2</sub>; 3x NH-CH<sub>2</sub>; 3x NH-CH) 3.39-3.31 (m, 13H, 3.25x CH<sub>2</sub>-O-CH-CH-CH<sub>2</sub>), 2.39-2.25 (m, 48H, 12x CO-CH<sub>2</sub>-CH<sub>2</sub>-CO), 1.88 (s, 6H, 2x HHC=C-CH<sub>3</sub>) 1.84-1.64 (m, 24H, 12x CO-CH<sub>2</sub>-CH<sub>2</sub>-CH<sub>2</sub>-CO) 1.60-1.27 (m, 8H, 2x NH-CH-(CH<sub>2</sub>)<sub>2</sub>), 1.04-0.86 (m, 22H, 2x NH-CH<sub>2</sub>-C-CH<sub>2</sub>-C-(CH<sub>3</sub>)<sub>2</sub>; 2x C-(CH<sub>3</sub>)<sub>2</sub>; 2x NH-CH<sub>2</sub>-C-CH<sub>3</sub>)

## 5. Analytics

### 5.1. UV-VIS Absorption

At first the samples were dissolved in absolute acetonitrile, achieving an aimed concentration of  $10^{-3}$  mol/L and transferred in 10 mm quartz cells for the UV-VIS experiments. At the photometer (scanning mode) wavelength from 250 to 450 nm at a slit width of 2 nm were measured (Table 46).

Table 46: initial data of the UV-VIS analysis with a volume of 0.003 L for all samples

sample	$A_{\max}$ (280-400 nm) [%]	$A_{\max}$ [nm]	$m_{\text{sample}}$ [mg]	c [mol/L]
<b>KGA</b>	0.52	332	14.5	0.033
<b>KGADimet</b>	0.60	324	15.4	0.029
<b>PolyISOKGA</b>	0.87	298	16.1	0.0024
<b>PolyHDKGA</b>	0.57	324	17.2	0.0012
<b>BP</b>	0.14	338	0.5	0.0010

### 5.2. Reactivity Tests

The first set of formulations contained 2 or 5 wt% of the photoinitiator benzophenone with an equimolar amount of MDEA in the monomers Miramer and TEGDMA. The photoinitiators based on  $\alpha$ -ketoglutaric acid were used in equimolar amounts (2 or 5 mol% based on benzophenone). Those formulations were then homogenized at a vortex for a few minutes to ensure homogeneous distribution in the very viscous Miramer. For the low viscosity monomer, TEGDMA, the mixtures were only vortexed a few seconds. All calculated masses of the components were weighed at the analytical scale and the exact values can be found in Table 47 and Table 48 for the Miramer-based formulations and in Table 49 and Table 50 for the TEGDMA-based formulations.

Table 47: 2% formulations in Miramer

<b>Miramer 2%</b>			
Formulation	Initiator [mg]	Monomer [mg]	Co-Initiator [mg]
<b>BP_MDEA</b>	60.04	3000.1	39.25
<b>KGADimet</b>	57.31	3000.4	-
<b>KGA2HEMA</b>	121.89	3000.0	-
<b>POLYESTER-9</b>	75.13	3000.0	-
<b>POLYESTER-15</b>	84.35	2999.7	-

Table 48: 5% formulations in Miramer

<b>Miramer 5%</b>			
<b>Formulation</b>	<b>Initiator [mg]</b>	<b>Monomer [mg]</b>	<b>Co-Initiator [mg]</b>
BP_MDEA	150.02	3000.0	98.08
KGADimet	143.30	3000.1	-
KGA2HEMA	304.68	3000.1	-
POLYESTER-9	187.92	3000.0	-
POLYESTER-15	210.95	2999.6	-

Table 49: 2% formulations in TEGDMA

<b>TEGDMA 2%</b>			
<b>Formulation</b>	<b>Initiator [mg]</b>	<b>Monomer [mg]</b>	<b>Co-Initiator [mg]</b>
BP_MDEA	20.04	999.8	13.10
POLYESTER-9	25.07	1000.0	-
POLYESTER-15	70.35	1000.7	-

Table 50: 5% formulations in TEGDMA

<b>TEGDMA 5%</b>			
<b>Formulation</b>	<b>Initiator [mg]</b>	<b>Monomer [mg]</b>	<b>Co-Initiator [mg]</b>
BP_MDEA	50.01	999.9	32.72
POLYESTER-9	62.38	1000.0	-
POLYESTER-15	28.18	1000.8	-

The photoinitiator for the formulations based on HDDA and 2M was 1 wt% ethyl pyruvate. Based on the molar amount of ethyl pyruvate the  $\alpha$ -ketoglutaric acid-based photoinitiators and the commercial type II photoinitiators Speedcure® BMS and BP were weighed in with co-initiator EDB. The ketoesters were also measured without EDB, shown in Table 51 for HDDA and in Table 52 for 2M.

Table 51: 1% formulations in HDDA

<b>Formulation</b>	<b>Initiator [mg]</b>	<b>Monomer [mg]</b>	<b>Co-Initiator [mg]</b>
EP	9.70	1011.4	-
KGADiet	17.66	997.3	-
KGA2HEMA_pure	32.48	1003.8	-
KGADiet_EDB	17.75	1000.7	16.73
KGA2HEMA_EDB	32.68	1001.8	16.45
KGADibenz	28.54	1002.8	-

Formulation	Initiator [mg]	Monomer [mg]	Co-Initiator [mg]
KGADibenz_EDB	28.26	1013.5	16.62
PolyHDKGA	42.03	1016.9	-
PolyHDKGA_EDB	40.61	994.6	16.53
BMS_EDB	26.22	1006.1	18.22
BP_EDB	15.69	996.6	16.65
EP_EDB	9.73	1006.6	16.65

Table 52: 1% formulations in 2M

Formulation	Initiator [mg]	Monomer [mg]	Co-Initiator [mg]
EP	10.17	999.1	-
KGADiet	17.69	1007.0	-
KGA2HEMA_pure	31.89	1006.4	-
KGADiet_EDB	17.15	1000.6	16.21
KGA2HEMA_EDB	32.26	1011.7	16.43
KGADibenz	27.30	1001.7	
KGADibenz_EDB	27.82	998.7	16.38
PolyHDKGA	40.69	1007.4	-
PolyHDKGA_EDB	41.19	1006.9	16.45
BMS_EDB	26.12	1003.2	16.96
BP_EDB	15.74	998.5	17.53
EP_EDB	9.76	1013.6	17.21

### Storage Stability Tests

All storage stability tests were carried out with the “mechanical tests” formulations. They simply were measured at the photorheometer again after a certain amount of time, to compare their remaining reactivity. These samples were stored at -18 °C in the dark before their measurement. The data is shown in Table 53.

Table 53: Measurements after 2 and 4 weeks at the photorheometer

weeks	sample	$t_g$ [s]	DBC at $t_g$ [%]	DBC [%]	$t_{95\%}$ [s]	$F_N$ [N]	$G'_{max}$ [kPa]	$G''_{max}$ [kPa]
1	PolyHDKGA_3000M	79.0	69.7	92.4	257.7	-17.3	842	228
	PolyHDKGA_5000M	73.5	67.5	93.5	259.5	-16.0	758	196
2	PolyHDKGA_3000M	85	68	94.2	252	-10.37	821	243
4	PolyHDKGA_5000M	76	60.0	95.7	246	-16.9	857	229

### 5.2.1. Photo Differential Scanning Calorimetry

To investigate the reactivity of each initiator, Photo-DSC measurements were conducted. The prepared formulations were weighed in  $12 \pm 1$  mg portions into small aluminum crucibles with a pipette. The crucible then was transported via the auto sampler into the measuring chamber. There was also a second crucible, the empty reference. The polymerization was induced by UV light with the wavelength of 320 to 500 nm and  $1 \text{ W / cm}^2$  at the end of the light guide. The exothermic of the polymerization was recorded over time. The polymerization was carried out isothermally at  $25^\circ \text{C}$ . The samples were exposed for 300 seconds. 3 determinations were made per formulation. Figure 141 shows an example of the exothermic during the DSC measurement.

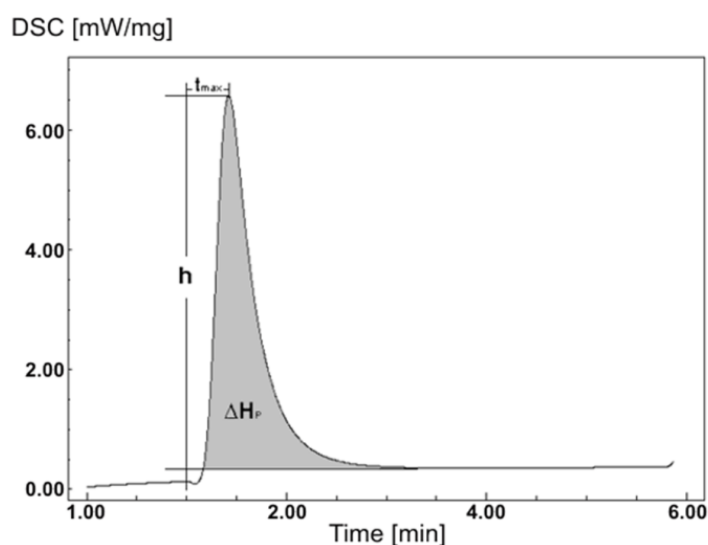


Figure 141: Time course of the exothermic during the polymerization<sup>63</sup>

The time to the highest exothermic is called  $t_{\text{max}}$ . In the time-resolved DSC spectrum, this corresponds to that point in time at which the peak height  $h$  achieved its maximum. This value then subtracted for 5 seconds as this time corresponds to the internal delay of the measuring device. Peak height  $h$ , correlates directly with the DSC [mW/mg] and the rate of polymerization  $R_p$ , higher values resulted in higher reactivity of the measured system. To determine the time in which 95% of the conversion was achieved ( $t_{95\%}$ ), the peak area  $\Delta H_p$  (heat of polymerization) was integrated to cover 95% of the area between the integration limits.

The double bond conversions (DBC) for Miramer and TEGDMA were determined via Equation 16 and the  $R_p$  was calculated via Equation 17. The theoretical heats of polymerization and the monomer densities were taken from

Table 54. Since KGA2HEMA is a non-commercial monomer, common values for similar molecular weight dimethacrylates were assumed and the density was determined using a 1 mL pycnometer.

Table 54: Theoretical heats of polymerization ( $H_{p,0}$ ) and densities ( $\rho$ ) of the monomers

Sample	$H_{p,0}$ [J/mol]	$H_{p,0}$ [J/g]	$\rho$ [g/l]
Miramer <sup>64</sup>	112700	234	1019
TEGDMA <sup>65</sup>	116935	299.45	1110
HDDA <sup>64</sup>	161000	711	1010
2M <sup>66</sup>	116935	299.45	1043
KGA2HEMA <sup>67</sup>	123000	332	1073

Equation 16: Calculation of the DBC<sup>68</sup>

$$DBC [\%] = \frac{\Delta H_p}{\Delta H_{p,0}} * 100$$

$\Delta H_p$  ... heat of polymerization of the sample [J/g]

$\Delta H_{p,0}$  ... theoretical heat of polymerization [J/g]

Equation 17: Calculation of the rate of polymerization<sup>69</sup>

$$R_p \left[ \frac{mmol}{l * s} \right] = \frac{DSC * \rho}{H_{p,0} * 1000}$$

DSC ... corresponds to the heat produced per mass unit of sample [mW/mg]

P ... density of the monomer [g/L]

$\Delta H_{p,0}$  ... theoretical heat of polymerization [J/g]

The full data of this experiment is illustrated in the attachment for TEGDMA (Table 57), Miramer (Table 58), 2M (Table 60) and HDDA (Table 58). All exact weighing are illustrated in Table 59 and Table 62.

### 5.2.2. Photorheometer Measurements

Approximately 150  $\mu$ L of the sample was put onto the glass plate, onto which a polyethylene tape was stick on to remove the sample easier after the measurement, via a pipette. The gap between the measurement stamp and the polyethylene tape was set to 200  $\mu$ m. After the viscosity measurement over 60 s (1 Hz oscillation and 1% amplitude), the NIR beam started to record the double bond conversion via comparing the integral of the (meth)acrylate band (6240 to 6100  $cm^{-1}$ ) and 5 s later the UV-lamp was switched on for 250 s (TEGDMA) or 400 s (Miramer). The irradiation was limited to 320 to 500 nm wavelength using a filter and the intensity was set to 20 mW/cm<sup>2</sup> at the glass plate. After the curing procedure, the samples were kept for the future leaching and swelling tests.

The full data of these measurements can be found in the attachment (Table 63 for TEGDMA and Table 64 for Miramer)

### 5.3. Photorheometer Measurements of the selected Initiators

The formulations contained 5 wt% of the photoinitiator benzophenone with an equimolar amount of MDEA and 500 ppm phenothiazine as the inhibitor in the monomer Miramer. The photoinitiators based on  $\alpha$ -ketoglutaric acid were used in equimolar amounts (5 mol% based on benzophenone). Those formulations were then homogenized at a vortex for a few minutes



to ensure homogeneous distribution in the very viscous Miramer. All calculated masses of the components were weighed at the analytical scale (Table 55).

Table 55: 5% formulations with inhibitor in Miramer

formulation	additive [mg]	initiator [mg]	monomer [mg]	co-initiator [mg]	inhibitor [mg]
BP_MDEA	-	600.2	11010.4	342.4	5.9
KGADimet	-	286.8	5716.1	-	3.0
KGA2HEMA	-	609.7	5392.0	-	3.0
PolyHDKGA_3000M	-	928.0	11078.6	-	4.0
PolyHDGA_3000M	871.3	600.0	10131.0	392.3	6.0
PolyHDKGA_5000M	-	857.4	11144.8	-	3.9
PolyHDGA_6500M	781.9	599.7	10224.1	392.2	5.9
PolyHDKGA_14000M	-	789.4	11219.4	-	4.0
PolyHDGA_14000M	741.0	600.1	10264.9	392.4	6.0

The full data of these measurements can be found in the attachment (Table 66).

## 5.4. Mechanical Tests

### 5.4.1. Dynamic Mechanical Thermal Analysis

First, samples with a specific geometry (width = 5 mm; thickness = 2.5 mm; height = 40 mm) were manufactured in a silicone mold after irradiating the liquid formulation with UV-light. This medium pressure mercury lamp based UV-oven had no wavelength filter applied and the exposure was 300 s per side within a distance of 10 cm, resulting in a total irradiation time of 600 s. Afterwards the samples were ground into shape with a tolerance of  $\pm 0.25$  mm along one dimension (Table 67). These samples were clamped into the clamping tools of the device and tightened with a screw. The measurement was performed under 1 Hz oscillation at 1% amplitude, heating from -100 °C to 200 °C (Table 56).

Table 56: DMTA measurement data

sample	$\tan\Delta_{\max}$ [°C]	FWHM [°C]	$G'_{\max}$ [MPa]	$G''_{\max}$ [MPa]	$G'_{25^\circ\text{C}}$ [MPa]	$G'_r$ [MPa]
BP_MDEA_5%	63.3	40.5	1820	105	140	0.4
KGADimet	86.4	48.3	1770	107	208	0.7
KGA2HEMA	102.0	54.1	1660	76	428	2.2
PolyHDKGA	56.1	74.4	2000	104	656	1.0
PolyHDKGA_3000M	75.3	56.7	2300	125	228	1.4
PolyHDKGA_5000M	70.9	58.0	1850	103	151	1.2
PolyHDKGA_14000M	65.4	64.2	1860	101	95	0.9
PolyHDGA_3000M	48.2	45.1	2370	129	59	0.5
PolyHDGA_5000M	53.2	43.1	2180	117	77	0.4
PolyHDGA_14000M	61.7	43.0	1910	105	111	0.4

#### 5.4.2. Tensile Tests

The tensile tests were performed with sample sizes of 2.5 mm x 2.5 mm across the thin path of the sample and a length of 35 mm (ISO 527-2, 5b). The liquid formulations were cured in an UV-oven with no wavelength filter attached at 320 to 500 nm for 300 s per side, which was a total resulting time of 600 s. Those samples were ground into shape with an accuracy of  $\pm 0.25$  mm. Now the samples were clamped into the device and the tightening screws were strongly fixed to hold the sample in place during the measurement. There was an increasing force applied to the samples, until they broke in half. The exact dimensions of the sample and the measurement data is listed in the attachment (Table 68).

#### 5.4.3. Charpy Impact Tests

Liquid formulations were put into a silicone mold with a specific geometry (length = 15 mm; width = 10 mm; height = 5 mm) according to the norm DIN 53435:2018-09. Afterwards the samples were cured with an UV-oven with no wavelength filter attached at 320 to 500 nm for 300 s per side, which was a total resulting time of 600 s. Those samples were ground into shape with an accuracy of  $\pm 0.25$  mm. Using a 10 kg hammer to break the samples in half, they just bent a little bit, resulting in no break for all of them.

#### 5.5. Leaching Tests

Already cured and punched out samples (approximately 30 mg) from the photorheometer tests were used for the swellability and leachability experiments. They were weighed at the analytical scale and afterwards put into penicillin vials containing 5 mL of methyl tert-butylether (MTBE) for 6 days. The vials were sealed and swirled once a day. Then the samples were taken out and after the removal of the solvent with a paper towel, they were weighed again. This process was carried out in around 30 s to stay reproducible and comparable, due to the fast evaporation of solvent, which was in the polymer network. Later the samples were put into an oven at 80 °C under reduced pressure (100 mbar) for 6 days to completely dry. As their weight did not change any more, they were weighed the last time at the analytical scale. The raw data is shown in the attachment in Table 65 for the reactivity tests and in Table 69 for the mechanical tests.

#### HPLC Analysis

The MTBE-based solutions from the leaching tests were transferred via a syringe attached to a filter into a HPLC-vial (1.5 mL) and measured with an acetonitrile to water ratio of 58:42.

## CONCLUSION

The aim of this thesis was the synthesis and testing of biocompatible  $\alpha$ -ketoesters as photoinitiators for radical polymerization. Furthermore these compounds should not migrate out of the cured material. Therefore three basic concepts were developed and their efficiency in specific areas compared among themselves afterwards. The first approach should be the limitation of the migration via covalent bonding to the polymer network. This could be achieved with the introduction of polymerizable endgroups, such as methacrylates. Secondly, macromolecular polyesters had to be obtained. Their migration and diffusion is strongly limited due to their sheer size. The last concept was the combination of the first two concepts. A polymeric, polymerizable molecule was aimed to get very low migration out of the cured material. All three approaches focused very low migration and good mechanical properties, while remaining high reactivity compared to a commercial reference system.

A variety of  $\alpha$ -ketoglutaric acid-based biocompatible UV-photoinitiators could be obtained. They can be divided into four categories, small initiators as reference molecules and the aimed macromolecular initiators, polymerizable initiators and polymeric, crosslinkable initiators. After analyzing their absorption behavior, it was clear, that  $\alpha$ -ketoesters were in the same range as commercial Type II photoinitiators, used in a wide range in industry. Due to those similarities, the reactivity and efficiency of the  $\alpha$ -ketoesters, as well as the mechanical properties of the resulting photopolymer networks were compared with such a commercial, benzophenone based Type II systems, based on benzophenone in combination with methyldiethanolamine.

Firstly, the reactivity of the synthesized  $\alpha$ -ketoesters was determined. Starting with a diacrylate, HDDA and a dimethacrylate mixture, 2M as monomers. A series of photo-DSC experiments were performed. The results were promising, due to the high reactivity in diacrylate and dimethacrylate systems. In terms of rate of polymerization, most  $\alpha$ -ketoesters outperformed the benzophenone-amine system by 50% and more in HDDA and in 2M even by a factor of above two for the diethylester of the  $\alpha$ -ketoglutaric acid. To cover 95% of the total double bond conversion, or in other words the speed to finish the majority of the polymerization is an important dimension for industry, therefore knowing the irradiation time and the related cost factor. In terms of  $t_{95\%}$ , all  $\alpha$ -ketoesters, with the exception of the macromolecular polyester outperformed the benzophenone-amine reference.

In the industrial monomer Miramer<sup>®</sup> UA5216 the reactivity tests went not as well as for the smaller difunctional monomers tested before. In this case, the rate of polymerization and the  $t_{95\%}$  value were only better for the small molecules based on  $\alpha$ -ketoglutaric acid. The polymerizable and macromolecular ones performed slightly worse compared to the reference system. Macromolecular polyesters had shown decreased reactivity due their size and resulting immobility in the formulation and during polymerization. A similar problem faced the polymerizable initiator, due to the co-polymerization during the growing network,

therefore the immobilization via covalent bonds. In both scenarios the photoinitiator was much less mobile and the formed radicals could not diffuse as easy as the small  $\alpha$ -ketoesters or the reference Type II initiators.

The advantage of those polymerizable or macromolecular photoinitiators was their low migration. After a swelling of above 35% for every material tested, significantly less leached out of the cured samples after exposure to an industrial widespread solvent, MTBE, after six days. Approximately half of the mass loss due to leaching was achieved by the  $\alpha$ -ketoesters compared to the benzophenone-amine samples. One major drawback, the lower conversion and therefore increased leaching of the uncured acrylates, which are more toxic than the photoproducts of  $\alpha$ -ketoesters, was present. Overall the curing with lower molecular weight  $\alpha$ -ketoesters would be advantageous in terms of avoidance of toxic migration components, like acrylates, due to their high conversions achieved during curing.

Considering Miramer® as an industrial scale monomer with good mechanical properties, samples were manufactured for mechanical tests. The cured specimens with specific geometries, necessary for every experiment, were produced on the base of storage stable, inhibited formulations. With all  $\alpha$ -ketoesters, except the material softening polyester based on  $\alpha$ -ketoglutaric acid and the flexible hexanediol, increased glass transition temperatures up to 40 °C were achieved. The best result was generated by the polymerizable  $\alpha$ -ketoglutaric acid derivative, which measured a  $T_g$  above 100 °C. Also the crosslinking density in the resulting networks was increased for all components tested, compared to the reference system. This property was affecting the storage modulus at room temperature and the rubbery state, increasing it up to a factor of 4 by the polymerizable KGA2HEMA.

Also the tensile strength was increased by the network architecture, created by the different  $\alpha$ -ketoesters tested. Depending on the application a wide variety of elongations at break and maximum stresses applied could be achieved. Entirely better properties were obtained in samples, containing  $\alpha$ -ketoesters as photoinitiators. Unfortunately the monomer was unsuitable for charpy impact tests, therefore they were skipped. The leaching tests of the sample foils achieved great results in terms of mass decrease. Compared to the benzophenone-amine system, which recorded a mass loss of 18%, all  $\alpha$ -ketoesters tested measured 6% and less, depending if their molecular weight is low or if they are polymeric.

## MATERIALS AND METHODS

- 1. Chemicals:** If not otherwise mentioned, all commercially available reagents were used in a quality common for organic synthesis and used without further purification. All solvents were distilled before their usage. Dry solvents have been dried according to standard literature.<sup>70</sup>
- 2. TLC:** Thin-layer-chromatography was done on aluminum TLC-plates from Merck (silica gel 60, F<sub>254</sub>).
- 3. Orange-light Laboratory:** All lamps in this special for photoinitiators design laboratory were Osram lumilux with light color 62. In addition to those lamps, all windows were sealed with Asmetec metolight SF-UV-filters (type ASR-SF-LY5) foils to prevent the samples from UV-light exposure. All wavelength below 520 nm are therefore blocked completely inside this room.
- 4. GC-MS:** The gaschromatography measurement with mass spectrometer coupling was performed on a Trace GC Ultra with a BGB-5 column (l = 30 m) from the company Thermo Scientific. This device is equipped with an auto sampler (AS 3000) and the ion trap ITQ 1100. The data was processed with the software Xcalibur Qual Browser in the version 2.0.7.
- 5. RT-NIR Photorheometer:** All measurements at the Modular Compact MCR 302 WESP from Anton Paar were irradiated with the EXFO Omnicure 2000 (calibrated with an Omnicure R2000 radiometer. Intensity was set to 25 mW/cm<sup>2</sup> at the glass plate; wavelength filtered to 320-500 nm) in combination with a glass fiber filled double-core light guide (3 mm fiber diameter), exposing the sample to UV-light from two sides below the glass plate. Simultaneously a FT-NIR-device (Vertex 80) from the company Bruker monitored the conversion of the samples. OPUS in the version 7.0 was used to process the data.
- 6. DMTA:** Dynamic mechanical thermal analysis was conducted on a Physica MCR 301 from Anton Paar with the additional heating and cooling unit (CTD 450), which is responsible for the temperature gradient during the measurement. RheoPlus v3.40 was used for analyzing the graphs.
- 7. NMR:** NMR spectra were recorded on a Bruker Avance at 400 MHz for <sup>1</sup>H and 100 MHz for <sup>13</sup>C and 162 MHz for <sup>31</sup>P. For some polyesters, the Bruker Avance at 600 MHz for <sup>1</sup>H was selected. The signals were always referenced on the used NMR-solvent with a deuterium grade of at least 99.5%:

<sup>1</sup>H: CDCl<sub>3</sub>: 7.26 ppm, DMSO-d<sub>6</sub>: 2.50 ppm

<sup>13</sup>C: CDCl<sub>3</sub>: 77.16 ppm, DMSO-d<sub>6</sub>: 39.52 ppm

The chemical shifts were reported in ppm (s = singlet, d = doublet, t = triplet, q = quartet, m = multiplet). Analysis of the spectra was performed with the program TopSpin v 2.1 by Bruker.

- 8. Photo-DSC:** Photo-DSC studies were performed on a Photo-DSC 204 F1 from Netsch equipped with an auto sampler. The UV-light source (EXFO Omnicure 2000: calibrated with an Omnicure R2000 radiometer. Intensity was set to 1 W/cm<sup>2</sup> at the end of the light guide; wavelength filtered to 320-500 nm) was used in combination with a glass fiber filled double-core light guide (3 mm fiber diameter). The measurements were conducted under nitrogen atmosphere (20 mL/min). Proteus - Thermal Analysis in version 5.2.1 from Netsch was used for processing the data. For all samples 25  $\mu$ L aluminum crucibles were used.
- 9. GPC:** GPC measurements were performed on a Malvern VISCOTEK TDA system equipped with a VISCOTEK SEC MALS 9 light scattering detector, a Viscotek TDA 305-021 RI+Visc detector, and a UV Detector Module 2550 for TDA 305. Samples were prepared as syringe-filtered 3 mg/mL THF-solutions spiked with 0.5 mg/mL butylhydroxytoluol (BHT) as flow marker. Separation was conducted through three consecutive PSS SDC columns (100 Å, 1000 Å, and 100000 Å) using THF as solvent at a flow rate of 0.8 ml/min.

Standard conventional calibration was done with polystyrene standards (PSS) between 470000 and 44000 g/mol. In case of triple detection, calibration was performed with a 105 kDa PS standard from Malvern, and the dn/dc ratio was determined via defined concentration and peak integral of the RI signal. OmniSEC v05.12.461 from Malvern was used to process the data.

- 10. Tensile Test:** All samples were measured on a Zwick Z050 tensile testing machine equipped with a 1 kN load sensor. Crosshead speed was 5 mm min<sup>-1</sup> and the software used for analyzing the data was TestXpert II.
- 11. Charpy Impact Test:** Were performed on a Karl Frank GmbH Dynstat device, Type 573 using 10 kg hammer.
- 12. Titration Device:** The titrations were carried out on a 736 GP Titrino device from Metrohm, equipped with a 703 Ti Stand.
- 13. HPLC:** The analysis was made with a modular HP Agilent 1100 device, equipped with a HP photodiode array detector and a quaternary gradient pump. For the separation an OUT LipoMare C<sub>18</sub> (105 Å; 5  $\mu$ m, 150 x 4 mm) reversed phase column was used at a flow rate of 0.7 ml/min (ACN:H<sub>2</sub>O = 58:42). The device was equipped with an auto sampler and the software ChemStation for LC 3D systems from Agilent Technologies (vB03.02-SR2 [341]).
- 14. ATR-IR:** FTIR-ATR was measured on a Spectrum 65 FTIR-ATR spectroscope from Perkin-Elmer. For the analysis of the results the software Spectrum from PerkinElmer in version 10.03.07 was used.
- 15. UV-Oven:** Was an Uvitron International INTELLI-RAY 600, equipped with a medium pressure mercury broadband UV-lamp and a distance to the samples of 10 cm (600 W; UV-A: 125 mW/cm<sup>2</sup>; Vis: 125 mW/cm<sup>2</sup>).

- 16. MPLC:** The medium pressure liquid chromatography was carried out with a Büchi MPLC-system equipped with the control unit (C-620), fraction collector (C-660) and UV-photometer (6-35). Merck silica gel 60 (0.040-0.063 mm) was used as solid phase.
- 17. Autoclave:** The high pressure stainless steel (1.4571) reactor BR-40 (max. 203 °C; 200 bar) from Berghof had a PTFE-inlet with a volume of 25 mL. Parameter display and settings were provided by the Berghof BTC-3000 control unit.
- 18. UV-VIS Spectrometer:** For the UV-Vis experiments samples were dissolved in pure acetonitrile and measured in 10 mm quartz cells on a Lambda 750 UV-Vis photometer (scanning mode) from 250 to 450 nm at a slit width of 2 nm. The software Spectrum from PerkinElmer v10.03.07 was used to process the data.

## ABBREVIATIONS

<b>UV</b>	<b>ultraviolet</b>
<b>wt%</b>	weight percent
<b>PI</b>	photoinitiator
<b>nm</b>	nanometer
<b>g</b>	gram
<b>mol</b>	mole
<b>%</b>	percent
<b>eq.</b>	equivalent
<b>°C</b>	degree Celsius
<b>h</b>	hours
<b>min</b>	minutes
<b>bar</b>	bar
<b>EDB</b>	N,N'-dimethylpyridin-4-amine
<b>NMR</b>	nuclear magnetic resonance
<b>BHT</b>	butyl hydroxytoluene
<b>HEMA</b>	2-hydroxyethyl methacrylate
<b>IPDI</b>	isophorone diisocyanate
<b>mg</b>	milligram
<b>mol%</b>	mole percent
<b>DCM</b>	dichloro methane
<b>POLYESTER-1-4</b>	glutaric acid hexanediol-based polyester (PolyHDGA)
<b>POLYESTER-8-12</b>	$\alpha$ -ketoglutaric acid hexanediol-based polyester (PolyHDKGA)
<b>POLYESTER-14-17</b>	glutaric acid isosorbide-based polyester (PolyISOGA)
<b>POLYESTER-5-7</b>	$\alpha$ -ketoglutaric acid isosorbide-based polyester (PolyISOKGA)
<b>RTXXX-M</b>	endgroup modified polyesters
<b>THF</b>	tetrahydrofuran
<b>DMF</b>	dimethylformamide
<b>M<sub>n</sub></b>	number average molecular mass
<b>M<sub>w</sub></b>	mass average molecular mass
<b>VIS</b>	visible light
<b>KGA</b>	$\alpha$ -ketoglutaric acid
<b>KGADimet</b>	$\alpha$ -ketoglutaric acid dimethylester
<b>KGADiet</b>	$\alpha$ -ketoglutaric acid diethylester
<b>KGADibenz</b>	$\alpha$ -ketoglutaric acid dibenzylester
<b>KGA2HEMA</b>	$\alpha$ -ketoglutaric acid di-2-hydroxyethyl methacrylate
<b>MDEA</b>	methyl diethanolamine
<b>W</b>	watt



<b>cm</b>	centimeter
<b>cm<sup>2</sup></b>	square centimeter
<b>s</b>	seconds
<b>t<sub>max</sub></b>	time to polymerization maximum
<b>DSC</b>	differential scanning calorimetry
<b>DBC</b>	double bond conversion
<b>t<sub>95%</sub></b>	time to cover 95% of the DBC
<b>R<sub>p</sub></b>	rate of polymerization
<b>t<sub>g</sub></b>	time to gelpoint
<b>F<sub>N</sub></b>	normal force
<b>N</b>	newton
<b>t</b>	time
<b>MTBE</b>	methyl tert-butylether
<b>ppm</b>	parts per million
<b>μm</b>	micrometer
<b>Hz</b>	hertz
<b>mW</b>	milliwatt
<b>NIR</b>	near infrared
<b>μL</b>	microliter
<b>mL</b>	milliliter
<b>L</b>	liter
<b>G'</b>	storage modulus
<b>G''</b>	loss modulus
<b>log</b>	logarithm to the base of 10
<b>tanΔ</b>	dissipation factor
<b>T<sub>g</sub></b>	glass transition temperature
<b>Pa</b>	pascal
<b>kPa</b>	kilopascal
<b>MPa</b>	megapascal
<b>kg</b>	kilogram
<b>PE</b>	petrol ether
<b>EE</b>	ethyl acetate
<b>RT</b>	room temperature
<b>m</b>	mass
<b>c</b>	concentration
<b>J</b>	coupling constant
<b>PTFE</b>	polytetraflouroethene
<b>2-IEM</b>	2-isocyonatoethyl methacrylate

## SUPPLEMENTING INFORMATION

Table 57: Photo-DSC data for the formulations based on TEGDMA

sample	t <sub>max</sub> [s]	DSC [mW/mg]	t <sub>95%</sub> [s]	Area% [J/g]	R <sub>p</sub> [mmol/l*s]	DBC [%]
PolyHDKGA_5%_1	22.3	11.6	79.7	244.4	110.1	81.6
PolyHDKGA_5%_2	20.8	11.5	77.2	244.4	109.2	81.6
PolyHDKGA_5%_3	20.8	11.5	75.1	242.3	109.2	80.9
PolyHDKGA_2%_1	26.0	9.5	99.1	239.5	90.2	80.0
PolyHDKGA_2%_4	27.9	9.4	101.2	234.9	89.2	78.4
PolyHDKGA_2%_3	25.5	9.6	107.2	237.5	91.1	79.3
PolyISOKGA_5%_1	26.9	9.5	122.5	245.2	90.2	81.9
PolyISOKGA_5%_2	27.4	9.9	117.0	249.1	94.0	83.2
PolyISOKGA_5%_3	27.2	9.7	121.9	250.2	92.1	83.6
PolyISOKGA_2%_1	30.3	8.5	129.4	238.2	80.7	79.5
PolyISOKGA_2%_2	29.9	8.6	113.3	230.8	81.6	77.1
PolyISOKGA_2%_3	30.1	8.6	121.1	238.8	81.6	79.7
BP_MDEA_5%_1	70.7	2.0	179.9	202.7	19.0	67.7
BP_MDEA_5%_2	69.6	2.1	177.0	207.7	19.9	69.4
BP_MDEA_5%_3	69.6	2.1	183.3	214.2	19.9	71.5
BP_MDEA_2%_1	96.6	1.7	193.4	193.9	16.1	64.8
BP_MDEA_2%_2	96.7	1.7	187.9	188.8	16.1	63.0
BP_MDEA_2%_3	95.7	1.7	186.2	189.6	15.9	63.3

Table 58: Photo-DSC data for the formulations based on Miramer

sample	t <sub>max</sub> [s]	DSC [mW/mg]	t <sub>95%</sub> [s]	Area% [J/g]	R <sub>p</sub> [mmol/l*s]	DBC [%]
PolyHDKGA_5%_1	16.5	6.6	82.0	202.6	59.7	86.6
PolyHDKGA_5%_2	15.0	6.4	95.0	193.5	57.9	82.7
PolyHDKGA_5%_3	16.4	6.7	80.3	205.9	60.6	88.0
PolyHDKGA_2%_1	18.7	5.5	105.2	201.8	49.7	86.2
PolyHDKGA_2%_2	20.0	5.1	115.5	202.9	46.1	86.7
PolyHDKGA_2%_3	17.5	6.0	92.2	190.4	54.3	81.4
PolyISOKGA_5%_1	56.3	1.2	201.6	124.9	10.9	53.4
PolyISOKGA_5%_2	59.6	1.2	201.0	126.5	10.9	54.1
PolyISOKGA_5%_3	52.1	1.4	194.9	134.1	12.7	57.3
PolyISOKGA_2%_1	77.2	0.8	221.0	92.9	7.2	39.7
PolyISOKGA_2%_2	67.3	1.0	217.8	113.3	9.0	48.4
PolyISOKGA_2%_3	57.0	1.1	205.1	116.8	9.9	49.9

BP_MDEA_5%_1	7.7	8.0	57.3	168.8	72.3	72.1
BP_MDEA_5%_2	7.0	8.5	75.9	171.7	76.9	73.4
BP_MDEA_5%_3	7.2	7.5	75.3	173.2	67.8	74.0
BP_MDEA_2%_1	8.4	7.1	57.3	161.4	64.2	69.0
BP_MDEA_2%_2	9.9	6.1	69.4	164.4	55.2	70.2
BP_MDEA_2%_3	8.9	6.7	72.8	165.9	60.6	70.9
KGA_Dimet_5%_1	10.9	9.1	43.6	193.4	82.3	82.6
KGA_Dimet_5%_2	10.7	9.2	44.7	196.5	83.2	84.0
KGA_Dimet_5%_3	10.3	9.7	44.7	199.3	87.7	85.2
KGA_Dimet_2%_1	11.4	8.9	44.1	193.7	80.5	82.8
KGA_Dimet_2%_2	13.5	7.2	57.7	186.1	65.1	79.5
KGA_Dimet_2%_3	12.1	8.0	51.6	189.4	72.3	80.9
KGA_2HMEA_5%_1	12.6	6.8	81.6	197.2	61.5	84.3
KGA_2HMEA_5%_2	15.0	6.4	96.2	193.5	57.9	82.7
KGA_2HMEA_5%_3	14.5	6.9	78.3	190.7	62.4	81.5
KGA_2HMEA_2%_1	16.0	4.4	143.0	188.5	39.8	80.5
KGA_2HMEA_2%_2	21.1	2.5	153.7	161.5	22.6	69.0
KGA_2HMEA_2%_3	22.6	3.0	158.7	154.7	27.1	66.1

Table 59: Weights of the samples measured via photo-DSC based on TEGDMA and Miramer

TEGDMA		Miramer	
sample	weighing [mg]	sample	weighing [mg]
PolyHDKGA_5%_1	12.77	PolyHDKGA_5%_1	12.23
PolyHDKGA_5%_2	12.05	PolyHDKGA_5%_2	11.99
PolyHDKGA_5%_3	12.24	PolyHDKGA_5%_3	11.41
PolyHDKGA_2%_1	13.00	PolyHDKGA_2%_1	10.06
PolyHDKGA_2%_2	12.13	PolyHDKGA_2%_2	11.77
PolyHDKGA_2%_3	10.45	PolyHDKGA_2%_3	11.93
PolyISOKGA_5%_1	10.66	PolyISOKGA_5%_1	12.70
PolyISOKGA_5%_2	13.00	PolyISOKGA_5%_2	11.60
PolyISOKGA_5%_3	12.56	PolyISOKGA_5%_3	10.00
PolyISOKGA_2%_1	11.68	PolyISOKGA_2%_1	11.45
PolyISOKGA_2%_2	11.66	PolyISOKGA_2%_2	12.88
PolyISOKGA_2%_3	12.56	PolyISOKGA_2%_3	11.36
BP_MDEA_5%_1	11.46	BP_MDEA_5%_1	10.33
BP_MDEA_5%_2	11.28	BP_MDEA_5%_2	10.21
BP_MDEA_5%_3	12.81	BP_MDEA_5%_3	13.01
BP_MDEA_2%_1	12.00	BP_MDEA_2%_1	10.21
BP_MDEA_2%_2	12.90	BP_MDEA_2%_2	12.99
BP_MDEA_2%_3	12.61	BP_MDEA_2%_3	11.25

		KGA_Dimet_5%_1	12.91
		KGA_Dimet_5%_2	12.51
		KGA_Dimet_5%_3	11.39
		KGA_Dimet_2%_1	11.65
		KGA_Dimet_2%_2	11.31
		KGA_Dimet_2%_3	11.26
		KGA_2HMEA_5%_1	12.82
		KGA_2HMEA_5%_2	12.74
		KGA_2HMEA_5%_3	12.97
		KGA_2HMEA_2%_1	12.85
		KGA_2HMEA_2%_2	13.00
		KGA_2HMEA_2%_3	12.47

Table 60: Photo-DSC data for the formulations based on HDDA

sample	tmax [s]	DSC [mW/mg]	t95% [s]	Area% [J/g]	Rp [mmol/l*s]	DBC [%]
EP_4	9.1	28.8	62.8	468.6	180.7	65.9
EP_2	9.3	28.2	65.2	467.4	176.9	65.7
EP_3	9.7	28.3	65.9	423.8	177.5	59.6
RTA001_1	10.1	25.4	62.5	453.9	159.3	63.8
RTA001_2	10.2	24.5	64.5	455.5	153.7	64.1
RTA001_3	10.0	25.5	61.0	465.2	160.0	65.4
RTA010_1	12.3	26.0	69.4	473.3	163.1	66.6
RTA010_2	12.3	25.2	65.1	427	158.1	60.1
RTA010_3	12.4	25.4	67.9	430.8	159.3	60.6
RTA001_EDB_1	9.2	28.9	56.7	451.4	181.3	63.5
RTA001_EDB_2	9.1	29.9	52.9	456.3	187.6	64.2
RTA001_EDB_3	9.3	29.4	60.4	459.2	184.4	64.6
RTA010_EDB_1	11.6	29.5	54.2	427.5	185.1	60.1
RTA010_EDB_2	11.5	30.3	53.8	433.3	190.1	60.9
RTA010_EDB_3	11.7	29.6	51.3	428.4	185.7	60.3
RTA002_1	9.1	27.1	65.7	460.6	170.0	64.8
RTA002_2	9.4	26.8	61.0	460.0	168.1	64.7
RTA002_3	9.2	27.5	59.5	464.5	172.5	65.3
RTA002_EDB_1	9.2	27.4	55.8	441.9	171.9	62.2
RTA002_EDB_2	9.4	26.8	56.3	439.4	168.1	61.8
RTA002_EDB_3	9.4	26.8	61.2	444.4	168.1	62.5
POLYESTER-12_1	9.8	22.4	76.1	431	140.5	60.6
POLYESTER-12_2	8.6	25.1	66.7	431.6	157.5	60.7

POLYESTER-12_3	9.3	23.8	71.9	443.4	149.3	62.4
POLYESTER-12_EDB_1	9.2	24.1	59.7	424	151.2	59.6
POLYESTER-12_EDB_2	9.3	23.8	57.5	419.6	149.3	59.0
POLYESTER-12_EDB_3	9.4	19.4	57.2	368.1	121.7	51.8
BMS_EDB_1	7.6	24.9	52.8	476.2	156.2	67.0
BMS_EDB_2	7.5	24.6	45.9	459.3	154.3	64.6
BMS_EDB_3	8	25.9	45.3	474.5	162.5	66.7
BP_EDB_1	12	14.1	66.9	476.9	88.5	67.1
BP_EDB_2	11.4	14.1	70.2	474.9	88.5	66.8
BP_EDB_3	11.6	14.1	64.7	473.8	88.5	66.6
EP_EDB_1	7.7	34.9	40.8	452	218.9	63.6
EP_EDB_2	7.7	33.1	42	448	207.6	63.0
EP_EDB_3	7.8	33	42.3	448	207.0	63.0

Table 61: Photo-DSC data for the formulations based on 2M

sample	tmax [s]	DSC [mW/mg]	t95% [s]	Area% [J/g]	Rp [mmol/l*s]	DBC [%]
EP_1	25.2	3.8	125.2	142.5	33.9	47.6
EP_2	23.4	4.2	125.5	147.2	37.5	49.2
EP_3	26.9	3.8	127.2	142.8	33.9	47.7
RTA001_1	18.4	5.4	110.2	158.1	48.2	52.8
RTA001_2	18.4	5.5	123.7	164.1	49.1	54.8
RTA001_3	18.9	5.9	114.0	176.9	52.6	59.1
RTA010_1	19.7	5.0	133.1	149.3	44.6	49.9
RTA010_2	19.5	4.8	90.1	138.5	42.8	46.3
RTA010_3	19.1	4.8	128.6	142.9	42.8	47.7
RTA001_EDB_1	12.6	7.5	92.1	174.4	66.9	58.2
RTA001_EDB_2	18.1	5.6	80.1	137.8	49.9	46.0
RTA001_EDB_3	12.1	7.4	83.0	166.9	66.0	55.7
RTA010_EDB_1	14.4	6.2	88.3	150.2	55.3	50.2
RTA010_EDB_2	14.4	6.1	91.2	149.1	54.4	49.8
RTA010_EDB_3	14.8	6.7	99.8	167.5	59.8	55.9
RTA002_1	16.6	6.0	86.6	154.6	53.5	51.6
RTA002_4	17.5	5.9	91.4	155.5	52.6	51.9
RTA002_3	22.4	5.3	136.4	164.0	47.3	54.8
RTA002_EDB_1	13.3	7.1	88.3	164.4	63.3	54.9
RTA002_EDB_2	13.3	7.1	84.3	160.4	63.3	53.6

RTA002_EDB_3	13.6	7.1	90.2	166.2	63.3	55.5
POLYESTER-12_1	23.1	2.9	119.0	123.0	25.9	41.1
POLYESTER-12_2	25.2	2.8	126.2	125.5	25.0	41.9
POLYESTER-12_3	23.5	2.9	120.6	123.8	25.9	41.3
POLYESTER-12_EDB_1	17.7	4.7	92.0	138.7	41.9	46.3
POLYESTER-12_EDB_2	17.2	5.4	90.5	152.2	48.2	50.8
POLYESTER-12_EDB_3	17.7	5.3	97.6	154.3	47.3	51.5
BMS_EDB_1	10.8	5.1	90.4	164.6	45.5	55.0
BMS_EDB_2	11.4	5.1	98.0	169.5	45.5	56.6
BMS_EDB_3	11.1	5.1	100.2	168.1	45.5	56.1
BP_EDB_1	18.2	2.3	143.5	146.4	20.5	48.9
BP_EDB_2	19.1	2.2	142.0	143.2	19.6	47.8
BP_EDB_3	19.9	2.2	147.2	145.8	19.6	48.7
EP_EDB_1	12.6	7.7	72.6	179.0	68.7	59.8
EP_EDB_2	13.2	7.6	79.4	170.0	67.8	56.8
EP_EDB_3	13.1	7.5	65.0	162.0	66.9	54.1

Table 62: Weights of the samples measured via photo-DSC based on HDDA and 2M

HDDA		2M	
sample	weighing [mg]	sample	weighing [mg]
EP_1	11.93	EP_1	10.06
EP_2	11.62	EP_2	10.52
EP_3	11.48	EP_3	11.79
Speedcure73_1	11.63	Speedcure73_1	11.74
Speedcure73_2	11.43	Speedcure73_2	11.87
Speedcure73_3	11.54	Speedcure73_3	10.37
RTA001_1	11.67	RTA001_1	11.49
RTA001_2	11.64	RTA001_2	11.62
RTA001_3	11.63	RTA001_3	12.20
RTA010_1	11.68	RTA010_1	11.82
RTA010_2	11.70	RTA010_2	11.08
RTA010_3	11.51	RTA010_3	10.76
RTA001_DMAB_1	11.64	RTA001_DMAB_1	10.39
RTA001_DMAB_2	11.65	RTA001_DMAB_2	11.98
RTA001_DMAB_3	11.73	RTA001_DMAB_3	11.50
RTA010_DMAB_1	11.31	RTA010_DMAB_1	11.21
RTA010_DMAB_2	11.31	RTA010_DMAB_2	10.60

RTA010_DMAB_3	11.83	RTA010_DMAB_3	10.64
RTA002_1	11.47	RTA002_1	10.96
RTA002_2	11.88	RTA002_2	11.70
RTA002_3	11.50	RTA002_3	10.95
RTA002_DMAB_1	11.55	RTA002_DMAB_1	10.45
RTA002_DMAB_2	11.95	RTA002_DMAB_2	11.12
RTA002_DMAB_3	11.91	RTA002_DMAB_3	11.93
POLYESTER-12_1	11.28	POLYESTER-12_1	10.29
POLYESTER-12_2	10.37	POLYESTER-12_2	11.99
POLYESTER-12_3	11.65	POLYESTER-12_3	10.47
POLYESTER-12_EDB_1	11.99	POLYESTER-12_EDB_1	10.23
POLYESTER-12_EDB_2	12.33	POLYESTER-12_EDB_2	11.73
POLYESTER-12_EDB_3	11.71	POLYESTER-12_EDB_3	12.17
BMS_EDB_1	10.99	BMS_EDB_1	10.27
BMS_EDB_2	11.44	BMS_EDB_2	11.74
BMS_EDB_3	11.23	BMS_EDB_3	11.04
BP_EDB_1	11.51	BP_EDB_1	10.51
BP_EDB_2	10.97	BP_EDB_2	10.65
BP_EDB_3	11.07	BP_EDB_3	11.05
EP_EDB_1	11.67	EP_EDB_1	10.11
EP_EDB_2	11.47	EP_EDB_2	11.79
EP_EDB_3	11.20	EP_EDB_3	11.38

Table 63: Reactivity tests photo rheology data for the formulations based on TEGDMA

sample	$t_g$ [s]	DBC at $t_g$ [%]	DBC [%]	$t_{95\%}$ [s]	$F_N$ [N]	$G'_{max}$ [kPa]	$G''_{max}$ [kPa]
<b>BP_MDEA_5%</b>	29.6	10	83.6	162	-32.1	887.6	210.1
	31.8	12	82.2	173	-32.4	877.6	208.4
	31.6	9	82.2	172	-32.9	872.8	206.7
<b>BP_MDEA_2%</b>	31.6	6	74.2	256	-32.6	809.0	190.7
	31.8	6	74.4	255	-33.3	808.1	190.8
	31.2	7	74.9	254	-32.8	797.1	186.9
<b>PolyHD_KGA_5%</b>	30.2	8	79.0	122	-36.2	810.6	190.0
	30.6	5	79.1	122	-35.6	786.1	181.2
	34.4	5	79.4	119	-33.9	795.9	182.8
<b>PolyHD_KGA_2%</b>	91.0	34	73.4	158	-32.7	723.5	163.4
	98.0	41	73.7	158	-33.3	713.3	156.8
	93.0	35	73.5	157	-31.6	712.2	156.8
	88.0	32	73.5	160	-31.2	720.2	158.4
<b>PolyISO_KGA_5%</b>	63.0	9	71.9	163	-27.9	619.7	156.1

	69.0	12	72.3	163	-26.8	654.0	139.5
	63.0	8	70.8	166	-24.3	637.9	137.9
PolyISO_KGA_2%	100.0	16	68.9	184	-21.1	472.3	97.0
	101.0	14	69.1	184	-21.7	485.3	101.3
	108.0	16	69.6	185	-21.7	478.9	96.2
	97.0	15	69.6	172	-22.5	504.7	103.6

Table 64: Reactivity tests photo rheology data for the formulations based on MIRAMER

sample	$t_g$ [s]	DBC at $t_g$ [%]	DBC [%]	$t_{95\%}$ [s]	$F_N$ [N]	$G'_{max}$ [kPa]	$G''_{max}$ [kPa]
BP_MDEA_5%	9.8	35	93.9	83	-14.2	769.7	215.5
	10.0	34	93.1	76	-13.4	771.2	193.7
	9.6	35	93.5	80	-13.4	816.7	211.6
BP_MDEA_2%	13.6	30	88.5	114	-13.6	851.7	219.9
	11.8	26	87.8	108	-13.1	869.0	230.6
	10.6	26	90.5	106	-14.9	870.4	235.8
PolyHD_KGA_5%	68.0	33	91.6	220	-16.0	836.1	216.8
	70.0	34	91.6	245	-17.0	866.9	217.9
	79.0	25	91.4	246	-17.0	855.1	212.9
PolyHD_KGA_2%	224.0	50	87.7	349	-12.5	544.6	228.4
	212.0	47	87.4	344	-12.3	579.7	218.4
	172.0	40	86.9	339	-12.8	291.7	176.6
PolyISO_KGA_5%	-	-	-	-	-	-	-
PolyISO_KGA_2%	-	-	-	-	-	-	-
KGA_Dimethyl_5%	30.0	36	97.0	86	-18.9	761.8	189.5
	29.6	38	96.9	88	-19.7	803.1	197.3
	30.4	37	96.9	89	-18.0	845.9	206.7
KGA_Dimethyl_2%	51.0	44	97.0	132	-18.9	761.8	189.5
	52.0	40	96.9	141	-19.7	803.1	197.3
KGA_2HEMA_5%	24.6	23	91.7	181	-20.8	867.6	213.9
	25.6	26	91.9	176	-20.3	846.9	209.9
KGA_2HEMA_2%	127.0	71	86.6	195	-18.9	522.7	212.5
	125.0	70	86.6	206	-19.4	585.9	228.1
	134.0	68	85.1	212	-18.6	452.5	200.1

Table 65: Raw data of the swelling and leaching tests (reactivity tests)

sample	number	dry mass before [mg]	swelled [mg]	dry mass after [mg]	swelling [%]	leaching [%]
--------	--------	----------------------	--------------	---------------------	--------------	--------------



<b>MIRA_KGA_2HEMA_2%</b>	1	29.16	47	26.87	38.0	8.5
	2	30.16	47	27.93	35.8	8.0
	3	29.66	46	27.42	35.5	8.2
<b>TEGDMA_PolyHDKGA_2%</b>	4	29.94	30.56	27.28	2.0	9.8
	5	30.12	30.68	27.43	1.8	9.8
	6	30.22	30.59	27.42	1.2	10.2
	7	31.09	31.59	28.23	1.6	10.1
<b>TEGDMA_PolyISOKGA_5%</b>	8	31.33	31.63	28.03	0.9	11.8
	9	30.74	31.02	27.41	0.9	12.1
	10	30.49	30.89	27.34	1.3	11.5
	11	31	31.11	27.69	0.4	12.0
<b>TEGDMA_PolyHDKGA_5%</b>	12	29.92	31.34	28.75	4.5	4.1
	13	30.4	31.87	29.04	4.6	4.7
	14	30.41	32.07	29.21	5.2	4.1
	15	29.67	31.32	28.56	5.3	3.9
	16	29.49	31.02	28.26	4.9	4.4
<b>TEGDMA_BP_2%</b>	17	29.95	30.11	26.89	0.5	11.4
	18	29.99	30.37	27.26	1.3	10.0
	19	29.45	29.77	26.65	1.1	10.5
<b>MIRA_BP_2%</b>	20	25.96	46	23.73	43.6	9.4
	21	26.6	45	24.03	40.9	10.7
	22	27.06	47	24.71	42.4	9.5
	23	27.48	48	25.11	42.8	9.4
<b>MIRA_BP_5%</b>	24	27.68	45	24.37	38.5	13.6
	25	26.82	43	23.54	37.6	13.9
	26	26.27	43	22.86	38.9	14.9
<b>TEGDMA_PolyISOKGA_2%</b>	27	30.93	31.69	26.78	2.4	15.5
	28	31.32	32.29	27.43	3.0	14.2
	29	31.48	32.47	27.38	3.0	15.0
	30	31.66	32.74	27.82	3.3	13.8
	31	31.49	32.65	27.79	3.6	13.3
<b>TEGDMA_BP_5%</b>	32	29.4	29.72	26.29	1.1	11.8
	33	30.14	30.22	27.36	0.3	10.2
	34	30.1	30.35	27.34	0.8	10.1
<b>MIRA_KGA_DIM_5%</b>	35	31.48	49	29.29	35.8	7.5
	36	31.56	49	29.38	35.6	7.4
	37	31.33	48	29.09	34.7	7.7
<b>MIRA_KGA_2HEMA_5%</b>	38	31.03	46	29.23	32.5	6.2
	39	30.12	43	28.22	30.0	6.7
	40	30.4	44	28.85	30.9	5.4

<b>MIRA_PolyHDKGA_2%</b>	41	30.32	50	27.34	39.4	10.9
	42	30.93	50	27.92	38.1	10.8
	43	30.7	48	27.63	36.0	11.1
	44	30.99	49	27.92	36.8	11.0
<b>MIRA_KGA_DIM_2%</b>	45	30.46	49	29.30	37.8	4.0
	46	30.99	48	28.95	35.4	7.0
	47	32.31	49	30.69	34.1	5.3
<b>MIRA_PolyHDKGA_5%</b>	48	31.13	49	29.57	36.5	5.3
	49	31.8	50	30.18	36.4	5.4
	50	31.08	52	29.38	40.2	5.8

Table 66: Reactivity tests photo rheology data for the formulations based on Miramer

sample	$t_g$ [s]	DBC at $t_g$ [%]	DBC [%]	$t_{95\%}$ [s]	$F_N$ [N]	$G'_{max}$ [kPa]	$G''_{max}$ [kPa]
<b>BP_MDEA_5%</b>	11	38	93.2	85	-16.74	769.7	215.5
	10.8	36	93.5	94	-18.07	758.7	206
	11	35	93.9	107	-17.49	797.7	223.8
<b>PolyHDKGA</b>	68	30	93.5	245	-17.02	866.9	217.9
	71	32	93.3	243	-16.01	836.1	216.8
	79	31	93.5	246	-16.99	855.1	212.9
<b>PolyHDKGA_062M</b>	32	4	90.0	347	-11.39	575.8	197.8
	40	4	88.0	352	-14.56	551.5	180.3
	134	63	90.6	351	-12.62	597.6	194.6
<b>PolyHDKGA_068M</b>	74	38	93.7	261	-15.71	771.1	201.1
	73	35	93.3	258	-16.35	745.3	191
<b>PolyHDKGA_049M</b>	80	40	94.3	256	-17.39	843.7	225.6
	75	42	91.1	258	-17.8	840.6	229.3
	82	41	91.8	259	-16.71	843.3	229.5
<b>PolyHDGA_067M</b>	10.8	34	94.7	71	-16.26	724.9	193.5
	10.8	35	94.6	69	-16.34	737.1	195.3
	11	36	93.9	69	-15.52	774.5	217.4
<b>PolyHDGA_053M</b>	10	31	93.7	74	-16.92	679.7	196.3
	9.6	30	94.2	71	-16.03	701.2	202.5
	10	31	94.6	69	-16.41	707.9	204.3
<b>PolyHDGA_050M</b>	8	25	92.7	69	-19.12	695.9	210.9
	8.8	25	92.4	69	-17.11	673.3	205.4
	8.2	26	92.6	68	-17.01	658.5	198.5
<b>KGADimet</b>	36.4	39	94.9	119	-17.37	912.9	235.6
	37.6	33	94.8	123	-16.92	836.2	209.5
	37.4	34	93.5	118	-19.15	844.2	209.4

KGA2HEMA	25	27	91.7	180	-20.76	867.6	213.9
	25.8	23	91.9	178	-20.5	845.9	207.9

Table 67: Dimensions of the DMTA samples

sample	width [mm]	thickness [mm]	height [mm]
BP_MDEA_5%	5.01	2.32	40
PolyHDKGA	4.98	2.19	40
PolyHDKGA_3000M	5.09	2.36	40
PolyHDKGA_5000M	5.11	2.17	40
PolyHDKGA_14000M	5.07	2.32	40
PolyHDGA_3000M	4.76	2.63	40
PolyHDGA_5000M	4.83	2.42	40
PolyHDGA_14000M	4.99	2.42	40
KGADimet	5.17	2.61	40
KGA2HEMA	5.27	2.24	40

Table 68: Measurement data of the tensile tests

sample	$E_t$ [Mpa]	$\sigma_M$ [MPa]	$\epsilon_M$ [%]	$\sigma_B$ [Mpa]	$\epsilon_B$ [%]	h [mm]	b [mm]	$A_0$ mm <sup>2</sup>
BP_MDEA	148.8	9.6	392.2	9.1	396.4	2.60	2.28	5.93
	168.4	11.6	394.6	11.3	398.3	2.22	2.17	4.82
	162.4	10.4	360.2	9.5	365.0	2.18	2.22	4.84
PolyHDKGA	136.9	10.7	180.5	8.9	185.9	2.66	2.15	5.72
	124.8	11.8	217.2	10.9	221.2	2.30	2.11	4.85
	135.0	11.8	202.3	10.7	208.5	2.31	2.14	4.94
	140.9	10.3	183.1	9.5	188.6	2.28	2.17	4.95
050M	71.1	8.9	479.5	8.3	487.2	2.45	2.21	5.41
	90.4	8.7	455.4	8.2	461.4	2.28	2.20	5.02
053M	97.7	9.7	513.6	9.2	517.1	2.36	2.19	5.17
	106.6	9.6	551.0	9.2	558.2	2.39	2.27	5.43
	111.4	9.9	461.1	9.4	465.6	2.26	2.26	5.11
067M	134.2	12.2	447.4	12.0	450.3	2.21	2.14	4.73
	130.0	11.5	451.9	10.9	459.2	2.35	2.16	5.08
	142.7	11.9	429.9	11.7	432.8	2.17	2.14	4.64
	140.7	11.1	408.6	10.4	412.5	2.15	2.18	4.69
	136.6	11.4	438.0	11.0	441.8	2.37	2.17	5.14
046M	225.6	17.6	259.5	16.7	261.6	2.56	2.26	5.79
	229.6	16.0	231.4	14.6	234.2	2.56	2.28	5.84
	241.8	17.6	250.6	16.9	254.0	2.50	2.13	5.33
	230.7	17.5	253.4	16.8	254.2	2.08	2.21	4.60
068M	210.7	15.7	242.9	14.5	245.5	2.25	2.30	5.18
	228.3	15.1	237.7	14.2	240.8	2.37	2.20	5.21

	206.0	16.9	259.1	15.6	262.4	2.33	2.19	5.10
	206.4	17.0	276.1	16.4	278.2	2.18	2.23	4.86
	226.7	18.3	271.3	17.1	274.6	2.32	2.11	4.90
<b>062M</b>	177.9	12.4	212.4	10.8	218.1	2.23	2.32	5.17
	196.7	12.2	189.1	11.2	195.3	2.09	2.22	4.64
	189.7	11.3	185.4	9.8	193.4	2.27	2.24	5.08
	190.9	12.4	206.9	10.8	214.5	2.17	2.22	4.82
<b>KGADimet</b>	215.7	12.4	251.9	11.5	255.8	2.33	2.31	5.38
	215.2	13.9	291.3	13.7	294.0	2.11	2.29	4.83
	214.4	13.5	283.5	12.4	286.2	2.21	2.22	4.91
<b>KGA2HEMA</b>	471.5	19.6	82.2	17.2	85.7	2.41	2.43	5.86
	468.4	20.2	89.6	19.3	92.0	2.31	2.42	5.59
	461.9	18.7	73.8	17.5	76.5	2.43	2.56	6.22
	459.5	18.7	75.6	16.8	78.4	2.35	2.49	5.85

Table 69: Raw data of the swelling and leaching tests (mechanical tests)

sample	number	dry mass before [mg]	swelled [mg]	dry mass after [mg]	swelling [%]	leaching [%]
<b>MIRA_PolyHDKGA049M</b>	1	30.55	51	29.04	40.1	5.2
	2	31.55	51	30.19	38.1	4.5
	3	29.86	48	28.62	37.8	4.3
<b>MIRA_PolyHDGA050M</b>	4	26.64	43	23.02	38.0	15.7
	5	27.15	45	23.5	39.7	15.5
	6	26.82	43	23.22	37.6	15.5
<b>MIRA_PolyHDGA053M</b>	7	28.08	45	24.01	37.6	17.0
	8	27.24	42	23.35	35.1	16.7
	9	27.32	45	23.33	39.3	17.1
<b>MIRA_PolyHDKGA062M</b>	10	27.8	45	25.95	38.2	7.1
	11	27.79	47	26.04	40.9	6.7
	12	28.6	49	26.85	41.6	6.5
	13	28.71	49	26.92	41.4	6.6
	14	28.85	48	27.08	39.9	6.5
	15	14.05	23	12.92	38.9	8.7
<b>MIRA_PolyHDGA067M</b>	19	28.28	45	23.91	37.2	18.3
	20	27.82	45	23.64	38.2	17.7
	21	26.26	43	22.58	38.9	16.3
<b>MIRA_PolyHDKGA068M</b>	22	28.88	47	27.86	38.6	3.7
	23	28.25	46	27.16	38.6	4.0
	24	28.66	47	27.59	39.0	3.9
	25	29.61	49	28.56	39.6	3.7
<b>MIRA_BP_MDEA_5%</b>	26	13.88	23	11.75	39.7	18.1
	27	29.03	49	24.68	40.8	17.6
	28	27.88	46	23.46	39.4	18.8

<b>MIRA_PolyHDKGA_5%</b>	29	29.78	50	28.49	40.4	4.5
	30	31.07	54	29.78	42.5	4.3
	31	31.55	53	30.07	40.5	4.9
<b>MIRA_KGA_Dimet</b>	32	26.52	46	24.91	42.3	6.5
	33	27.18	47	25.56	42.2	6.3
	34	27.7	48	26.13	42.3	6.0
<b>MIRA_KGA_2HEMA</b>	35	28.84	43	27.28	32.9	5.7
	36	29.88	45	28.24	33.6	5.8
	37	29.33	44	27.67	33.3	6.0

## REFERENCES

1. Lago, M. A.; de Quiros, A. R. B.; Sendon, R.; Bustos, J.; Nieto, M. T.; Paseiro, P. *Food Addit Contam A* **2015**, 32, (5), 779-798.
2. Nakagawa, Y.; Tayama, K. *Arch Toxicol* **2002**, 76, (12), 727-731.
3. Brock, T.; Groteklaes, M.; Mischke, P., *European Coatings Handbook*. Vincentz: 2000.
4. <http://www.paint.org/industry/history.cfm>. **2019**.
5. Myers, R. R. *J Macromol Sci Chem* **1981**, A 15, (6), 1133-1149.
6. Bett, S. J.; Dworjany, P. A.; Garnett, J. L. *J Oil Colour Chem As* **1990**, 73, (11), 446-453.
7. Allen, N. S.; Edge, M. *J Oil Colour Chem As* **1990**, 73, (11), 438.
8. Nesvadba, P. *Encyclopedia of Radicals in Chemistry, Biology and Materials* **2012**, 1.
9. Fouassier, J.-P., *Photoinitiation, Photopolymerization, and Photocuring: Fundamentals and Applications*. Hanser: 1995.
10. L., F. J.-. *British Dental Journal volume 186* **1999**, 384.
11. Crivello, J. V.; Reichmanis, E. *Chem Mater* **2014**, 26, (1), 533-548.
12. <http://www.northsearesins.com/resin.html>. **2019**.
13. Murphy, J., *Additives for Plastics Handbook*. Elsevier Science: 2001.
14. R., K.; G., B.; G., R. *Farbe und Lack* **1980**, 224-230.
15. Fouassier, J. P., *Photochemistry and UV Curing: New Trends 2006*. Research Signpost: 2006.
16. F., K. J. *Radiation Curing* **1974**, 2-17.
17. L., O. C. *Journal of Radiation Curing* **1976**, 3.
18. S., D. R.; P., O. S. *Jorunal of the Chemical Society Chemical Communications* **1974**, 209-210.
19. Bonamy, A.; Fouassier, J. P.; Lougnot, D. J.; Green, P. N. *J Polym Sci Pol Lett* **1982**, 20, (6), 315-320.
20. Su, W. F., *Principles of Polymer Design and Synthesis*. Springer Berlin Heidelberg: 2013.
21. Crivello, J. V.; Dietliker, K.; Bradley, G., *Photoinitiators for Free Radical Cationic & Anionic Photopolymerisation*. Wiley: 1999.
22. McConnell, H. J. *Chem. Phys.* **1952**, 20.
23. [https://www.shsu.edu/chm\\_tgc/chemilumdir/JABLONSKI.html](https://www.shsu.edu/chm_tgc/chemilumdir/JABLONSKI.html). **2019**.
24. <http://micro.magnet.fsu.edu/primer/java/jablonski/lightandcolor/index.html>. **2019**.
25. Fouassier, J. P.; RABEK, J. F., *Radiation Curing in Polymer Science and Technology*. Springer Netherlands: 1993.
26. Andrzejewska, E.; Zych-Tomkowiak, D.; Andrzejewski, M.; Hug, G. L.; Marciniak, B. *Macromolecules* **2006**, 39, (11), 3777-3785.

27. Becker, H. G. O., *Einführung in die Photochemie*. Thieme: 1983.
28. Cohen, S. G.; Parola, A.; Parsons, G. H. *Chem Rev* **1973**, 73, (2), 141-161.
29. Kilambi, H.; Reddy, S. K.; Schneidewind, L.; Lee, T. Y.; Stansbury, J. W.; Bowman, C. N. *Macromolecules* **2007**, 40, (17), 6112-6118.
30. Gruber, H. F. *Prog Polym Sci* **1992**, 17, (6), 953-1044.
31. Liu, R. Z.; Mabury, S. A. *Environ Sci Technol* **2018**, 52, (17), 10089-10096.
32. EFSA. *EFSA Journal* **2005**, 293.
33. IACR. **2013**, 284-304.
34. Green, W. A., *Industrial Photoinitiators: A Technical Guide*. Taylor & Francis: 2010.
35. Zapka, W., *Handbook of Industrial Inkjet Printing: A Full System Approach*. Wiley: 2018.
36. Fouassier, J. P.; Lalevée, J., *Photoinitiators for Polymer Synthesis: Scope, Reactivity, and Efficiency*. Wiley: 2013.
37. Bishop, C., *Vacuum Deposition onto Webs, Films and Foils*. Elsevier Science: 2011.
38. Gauss, P.; Knaack, P.; Liska, R. *ESPS Mullhouse conference poster 2018*.
39. Davidson, R. S.; Goodwin, D.; Deviolet, P. F. *Tetrahedron Lett* **1981**, 22, (26), 2485-2486.
40. Murov, S. L.; Carmichael, I.; Hug, G. L., *Handbook of Photochemistry, Second Edition*. Taylor & Francis: 1993.
41. Bergfeld, W. F.; Belsito, D. V.; Carlton, W. W.; Klaassen, C. D.; Schroeter, A. L.; Shank, R. C.; Slaga, T. J.; Panel, C. I. R. E. *Int J Toxicol* **1998**, 17.
42. Glöckner, P., *Radiation Curing*. Elsevier Science: 2009.
43. Lowenstein, J. M., *Methods in Enzymology*. Academic Press: 1960.
44. <http://iqriosity.blogspot.com/2014/05/molecular-weight-control-in-step-growth.html>. **2019**.
45. Cowie, J. M. G., *Polymers: Chemistry and Physics of Modern Materials, 2nd Edition*. Taylor & Francis: 1991.
46. Braun, D.; Cherdrón, H.; Ritter, H., *Polymer Synthesis: Theory and Practice: Fundamentals, Methods, Experiments ; with 31 Tables*. Springer: 2001.
47. Roscales, S.; Ortega, A.; Martín-Aragón, S.; Bermejo-Bescos, P.; Csaky, A. G. *Eur J Org Chem* **2012**, (27), 5398-5405.
48. Guoliang, C. *Patent; Synthesis method of hydroxyethyl acrylate* **2013**, 1-4.
49. Joly, G. D.; Krepski, L. R.; Gaddam, B. N.; Abuelyaman, A. S.; Craig, B. D.; Dunbar, T. D.; Cao, C.; Oxman, J. D.; Falsafi, A.; Moser, W. H.; Bui, H. T. *U. S. Patent* **2011**, 1-35.
50. Neises, B.; Steglich, W. *Angew Chem Int Edit* **1978**, 17, (7), 522-524.
51. Douka, A.; Vouyiouka, S.; Papaspyridi, L.-M.; Papaspyrides, C. D. *Prog Polym Sci* **2018**, 79, 1-25.
52. Kumar, A.; Gross, R. A. *Biomacromolecules* **2000**, 1, (1), 133-138.

53. Noordover, B. A. J.; van Staalduinen, V. G.; Duchateau, R.; Koning, C. E.; van Benthem, R. A. T. M.; Mak, M.; Heise, A.; Frissen, A. E.; van Haveren, J. *Biomacromolecules* **2006**, *7*, (12), 3406-3416.
54. Ogg, C. L.; Porter, W. L.; Willits, C. O. *Ind Eng Chem* **1945**, *17*, (6), 394-397.
55. Pu, Y. Q.; Cao, S. L.; Ragauskas, A. J. *Energ Environ Sci* **2011**, *4*, (9), 3154-3166.
56. Reed, D. H.; Critchfield, F. E.; Elder, D. K. *Anal Chem* **1963**, *35*, (4), 571.
57. Blagbrough, I. S.; Mackenzie, N. E.; Ortiz, C.; Scott, A. I. *Tetrahedron Lett* **1986**, *27*, (11), 1251-1254.
58. Muller, I. A.; Kratz, F.; Jung, M.; Warnecke, A. *Tetrahedron Lett* **2010**, *51*, (33), 4371-4374.
59. Dufour, P.; Oldring, P. K. T.; Allen, N. S., *Chemistry and Technology of UV & EB Formulation for Coatings, Inks & Paints: Photoinitiators for free radical and cationic polymerisation*. SITA Technology: 1991.
60. [http://www.astm.org/cgi-bin/resolver.cgi?D2572-97\(2010\)](http://www.astm.org/cgi-bin/resolver.cgi?D2572-97(2010)). **2010**.
61. Grubitsch, H.; Willard, H. H.; Furman, N. H., *Grundlagen der quantitativen Analyse: Theorie und Praxis*. Springer Vienna: 2013.
62. Ashraf, S. M., *A Laboratory Manual of Polymers*. I.K. International Publishing House Pvt. Limited: 2008.
63. Dworak, C. *Biomedical Engineering - Frontiers and Challenges* **2011**, 143-156.
64. Brandrup, J.; Immergut, E. H.; Grulke, E. A., *Polymer Handbook, 4th Edition*. Wiley: 2004.
65. Gorsche, C.; Griesser, M.; Gescheidt, G.; Moszner, N.; Liska, R. *Macromolecules* **2014**, *47*, (21), 7327-7336.
66. Dworak, C.; Kopeinig, S.; Hoffmann, H.; Liska, R. *J Polym Sci Pol Chem* **2009**, *47*, (2), 392-403.
67. Huang, C. W.; Sun, Y. M.; Huang, W. F. *J Polym Sci Pol Chem* **1997**, *35*, (10), 1873-1889.
68. Menczel, J. D.; Prime, R. B., *Thermal Analysis of Polymers: Fundamentals and Applications*. Wiley: 2014.
69. Flory, P. J., *Principles of Polymer Chemistry*. Cornell University Press: 1953.
70. Armarego, W. L. F.; Chai, C., *Purification of Laboratory Chemicals*. Elsevier Science: 2009.